Performance modelling for product development of advanced window systems

Appelfeld, David

Publication date:
2012

Document Version
Publisher's PDF, also known as Version of record

Performance modelling for product development of advanced window systems

David Appelfeld

PhD Thesis

Department of Civil Engineering

2012

DTU Civil Engineering Report R-267 (UK)
May 2012

DTU Civil Engineering
Department of Civil Engineering

Performance Modelling for Product Development of Advanced Window Systems

David Appelfeld

Ph.D. Thesis

Department of Civil Engineering
Technical University of Denmark

2012

Supervisors:

Professor Svend Svendsen, DTU Civil Engineering, Denmark
Associate Professor Toke Rammer Nielsen, DTU Civil Engineering, Denmark

Assesment Committee:

Ph.D. Bengt Hellström, Lund University, Sweden
Ph.D. Karsten Duer, Velux A/S, Denmark
Professor Carsten Rode, DTU Civil Engineering, Denmark

Performance Modelling for Product Development of Advanced Window Systems

Printed by DTU-Tryk
Department of Civil Engineering
Technical University of Denmark
ISBN: 9788778773500
ISSN: 1601-2917
Report: BYG R-267

Preface

This doctoral thesis is submitted as a partial fulfilment of the requirements for the Danish Ph.D. degree. The first part introduces the research topic, presents and discuses the results and findings. The second part is a collection of articles based on the research, which contain fundamental aspects of the work and present the work in details from a scientific point of view.

"To get something you never had, you have to do something you've never done." - Unknown

Lyngby, the 31th May 2012

David Appelfeld

Acknowledgements

I want to express my sincere and deep thanks to everyone who have helped me during this research.

Foremost, I would like to thank my supervisor Professor Svend Svendsen and my co-supervisor Associate Professor Toke Rammer Nielsen for their guidance and discussion during the years as well as for giving me the opportunity to become a Ph.D.

I would also like to thank to all my colleagues at DTU Civil Engineering, Section of Building Physics and Services, for the very friendly and beneficial working environment.

My special thanks goes to Eleanor Lee, Andrew McNeil and Jacob Jonsson for all their help, guidance and inspiration during my external stay as a guest researcher at the Lawrence Berkeley National Laboratories.

At the end, I would especially like to thank my parents, girlfriend and friends for supporting me during the working.

Grants

This research was supported partially by grants from Danish Energy Agency and by Technical University of Denmark, Department of Civil Engineering.

Abstract

The research presented in this doctoral thesis shows how the product development (PD) of Complex Fenestration Systems (CFSs) can be facilitated by computer-based analysis to improve the energy efficiency of fenestration systems as well as to improve the indoor environment.
The first chapter defines the hypothesis and objectives of the thesis, which is followed by an extended introduction and background. The third chapter briefly suggests the PD framework which is suitable for CFSs. The fourth and fifth chapter refer to the detailed performance modelling of thermal properties (chapter 4) and optical properties (chapter 5) of CFSs. The last chapter concludes the thesis and the individual investigations.
It is complicated to holistically evaluate the performance of a prototyped system, since simulation programs evaluate standardised products such as aluminium venetian blinds. State-of-the-art tools and methods,which can address interrelated performance parameters of CFS, are sought. It is possible to evaluate such systems by measurements, however the high cost and complexity of the measurements are limiting factors. The studies in this thesis confirmed that the results from the performance measurements of CFSs can be interpreted by simulations and hence simulations can be used for the performance analysis of new CFSs. An advanced simulation model must be often developed and needs to be validated by measurements before the model can be reused. The validation of simulations against the measurements proved the reliability of the simulations. The described procedures can be used at the initial stages of the PD to foresee the consequences of the innovation, and aim at the development by an iterative testing to meet the requirements.
It was demonstrated that by improving the fenestration system, the overall building energy demand can be reduced by optimizing lighting, heating and cooling. The indoor environment quality can be improved by careful shading strategy and maximizing the use of daylight. The recent developments of the building simulation programmes enabled to perform annual, dynamic and climate based energy evaluation of CFSs.

The case study of development of a window frame made of glass fibre reinforced polyester (GFRP) demonstrated that this composite material is suitable for window frames. A window with positive net energy gain (NEG) and a slim window frame was developed, by a combination of a low thermal transmittance and high load capacity of the material. Furthermore, the ventilated window, which uses the glazing cavity for ventilating the outside air that is supplied to the room, was investigated. By this concept some of the heat loss of the window can be regained by preheating the supplied air and thus increase the net energy gain of the window. However, the usage of the window for such a purpose is limited by the low heat recovery efficiency, which drops with the increase of the airflow. The heat balance of the ventilated window varies significantly from the heat balance of standard window. The theoretical heat balance of the ventilated window was defined in the study.
In this thesis, properties of several shading systems were investigated including an analysis of the visual comfort. The simulations of daylight, lighting demand and glare were accomplished by ray tracing simulations in the software Radiance. The results from these investigations demonstrated that the performance of unique shading systems can be simulated, such as micro structural shading or light redirecting systems. It was illustrated that an advanced analysis is needed to evaluate a CFS, a simple evaluation, e.g. $g - value$ or $U_w - value$, would not provide sufficient knowledge about the new properties. Bi-directional description of the optical properties of the shading system was used for investigation of lighting conditions and glare as well as NEG under different incident angles.
The overall conclusion of the thesis is that it is possible to develop and optimize any CFS with the help of computer performance modelling. The PD methods can clearly identify the objectives of the investigation and set out the appropriate way to achieve the optimal solution.

Resumé

Forskningen der præsenteres i denne ph.d.-afhandling viser, hvordan produktudvikling PD af komplekse vinduessystemer CFSs kan faciliteres af edb-baserede analyser for at forbedre energieffektiviteten af vinduessystemer, samt til at forbedre indeklimaet.
Det første kapitel definerer hypotesen og målet med afhandlingen, som efterfølges af en udvidet introduktion og baggrund. Det tredje kapitel foreslår, i korte træk, et produktudviklingsforløb der er egnet til CFSs. Det fjerde og femte kapitel refererer til detaljeret modellering af termiske egenskaber (kapitel 4) og optiske egenskaber (kapitel 5) af CFSs. Det sidste kapitel konkluderer afhandlingen og de enkelte undersøgelser. Det er kompliceret at udføre en holistisk vurdering af ydeevnen af prototyper, da simuleringsprogrammer evaluerer standardiserede produkter såsom alu-persienner. State-of-the-art værktøjer og metoder, som kan adressere interaktionen mellem forskellige ydelsesparametre, er undersøgt. Det er muligt at vurdere prototyper ved målinger, men den høje omkostning og kompleksitet af målingerne er begrænsende faktorer. Undersøgelserne i denne afhandling bekræftede, at resultaterne fra målingerne af ydeevne kan fortolkes ved simuleringer, og dermed kan simuleringer bruges til at udføre analyser af ydeevne for nye CFSs. En avanceret simuleringsmodel skal ofte udvikles og valideres ved målinger, før modellen kan genbruges. Valideringen af simuleringer mod målingerne viste pålideligheden af simuleringer. De beskrevne procedurer kan anvendes på de indledende stadier af PD til at forudse konsekvenserne af innovative tiltag og sigter mod en iterativ udviklingsproces indtil de opstillede krav er opfyldte. Det blev påvist, at ved at forbedre vinduessystemet, kan det samlede energibehov for bygninger reduceres ved at optimere dagslys, varme og afkøling. Indeklimaets kvalitet kan forbedres ved en omhyggelig solafskærmningsstrategi og ved at maksimere brugen af dagslys. Den seneste udvikling i bygningssimuleringsprogrammer gjorde det muligt at udføre en årlig, dynamisk og klimabaseret energiberegning for CFSs.
Casestudiet om udviklingen af en vinduesramme fremstillet af glasfiberarmeret polyester GFRP viste, at dette kompositmateriale er egnet til vinduesram-

mer. Et vindue med positivt energitilskud NEG og en slank vinduesramme blev udviklet ved en kombination af en lav termisk transmission og høj materialestyrke. Endvidere blev et ventileret vindue, hvor udeluft tilføres efter at have passeret det ene glashulrum, undersøgt. Ved dette koncept kan en del af varmetabet af vinduet genvindes til forvarmning af luft som tilføres og dermed øge nettoenergigevinster af vinduet. Imidlertid er brugen af vinduet til et sådant formål begrånset af varmegenvindingseffektivitet i ventilationssystemet, som falder med forøgelsen af luftstrømmen. Varmebalancen for det ventilerede vindue adskiller sig betydeligt fra varmebalancen for et standardvindue. Den teoretiske varmebalance for det ventilerede vindue blev defineret i undersøgelsen.

I denne afhandling blev egenskaber for flere solafskærmningssystemer undersøgt, herunder en analyse af den visuelle komfort. Simuleringerne af dagslys, lysbehov og blænding blev udført ved ray tracing simuleringer i softwaren Radiance. Resultaterne fra disse undersøgelser viste, at udførelsen af unikke solafskærmningssystemer kan simuleres, såsom mikro-strukturelle solafskærmninger eller lysdirigerende systemer. Det blev vist, at en avanceret analyse er nødvendig for at vurdere en CFS, en simpel evaluering som f.eks. *g-værdi* eller $U_w - værdi$, ikke vil give tilstrækkelig viden om de nye egenskaber. Bidirektionel beskrivelse af de optiske egenskaber af solafskærmningssystemet blev anvendt til undersøgelse af lysforhold og blænding samt NEG under forskellige indfaldsvinkler.

Den overordnede konklusion er, at det er muligt at udvikle og optimere ethvert CFS ved hjælp af edb-baseret modellering. PD metoderne kan klart identificere målene for undersøgelsen og fastsætte en passende måde at opnåden optimale løsning.

Contents

List of Figures

List of Tables

Acronyms

ASHRAE	American Society of Heating, Refrigeration and Air-Conditioning Engineers
BBM	Black-Box-Model
BSDF	bi-directional scattering function
CFD	Computational Fluid Dynamics
CFS	Complex Fenestration System
DA	daylight autonomy
DC	daylight coefficient
DF	daylight factor
DGP	Daylight Glare Probability
DOE	Department of Energy
EPBD	Energy Performance of Building Directive
GFRP	glass fibre reinforced polyester
GHB	Guarded Hot Box
HVAC	Heating, Ventilation, Air Conditioning
IA	incidence angle
IEA	International Energy Agency
IESNA	Illuminating Engineering Society of North America
ISI	Institute for Science Information

ISO	International Standard Organization
LBNL	Lawrence Berkeley National Laboratory
LPD	lighting power density
MSPSS	micro-structural perforated shading screen
NEG	net energy gain
NIR	near-infrared
PD	product development
SHGC	solar heat gain coefficient
TPM	three-phase method
TRY	test reference year
UDI	useful daylight illuminance
WPI	working plane illuminance

Nomenclature

%fancyhead

Symbol	Units	Description
A_f	m^2	Projected frame area
A_g	m^2	Projected visible glazing area
A_w	m^2	Projected window area
$U - value$	W/m^2K	Thermal transmittance
$U_f - value$	W/m^2K	Thermal transmittance of a window frame
$U_g - value$	W/m^2K	Thermal transmittance of a glazing
$U_w - value$	W/m^2K	Thermal transmittance of a single window
l_Ψ	m	Visible perimeter of glazing
Ψ	W/mK	Linear thermal transmittance due to combination of thermal effect of glazing, spacer and frame
$g - value$	$-$	Total solar transmittance
τ_{sol}	$-$	Solar Transmittance
τ_{vis}	$-$	Light Transmittance
τ_{sw}	$-$	Total solar energy transmittance of a window
τ_g	$-$	Solar energy transmittance of a glazing
τ_f	$-$	Solar energy transmittance of a frame
	$-$	Solar Transmittance of a frame
NEG	$kWh/(m^2year)$	Net energy gain
I	kWh/m^2	Coefficient for solar gains
D	kWh	Coefficient for heat loss
E	$kWh/(m^2year)$	Total primary energy demand of buildings
$U_{w,trans,ext}$	W/m^2K	Thermal transmittance of a ventilated window
$U_{w,vent}$	W/m^2K	Ventilation heat loss of window
$U_{w,trans}$	W/m^2K	Total thermal transmittance of a window in a ventilated window
$Q_{w,trans}$	W	Energy flux from indoor environment to window
$Q_{w,trans,ext}$	W	Energy flux from window to outdoor environment
$Q_{air,vent}$	W	Energy flux to heat up ventilated air to room temperature

$Q_{w,vent}$	W	Advective energy flux (energy transported by ventilated air)
A_w	m^2	Window area
h_{ci}	W/m^2K	Indoor convective heat transfer coefficient
h_{ce}	W/m^2K	Outdoor convective heat transfer coefficient
h_{ri}	W/m^2K	Indoor radiative heat transfer coefficient
h_{re}	W/m^2K	Outdoor radiative heat transfer coefficient
c_p	(J/kgK)	Specific heat capacity
ϕ	m^3/s	Volume flow
ρ	kg/m^3	Density
q_{sp}	W/m^2	Heat flow rate density of sample
ϕ_{in}	W	Corrected metering box heat input
ϕ_{sur}	W	Surround panel heat flow rate
ϕ_{edge}	W	Edge zone heat flow rate
T_{si}	$^\circ C$	Indoor surface temperature of a window
T_{sie}	$^\circ C$	Outdoor surface temperature of a window
$T_{gap,in}$	$^\circ C$	Air temperature in a window inlet valve
$T_{gap,out}$	$^\circ C$	Air temperature in a window outlet valve
T_{ni}	$^\circ C$	Interior environmental temperature
T_{ne}	$^\circ C$	Exterior environmental temperature
T_{vent}	K	Ventilation mean air temperature
W	m	Width
H	m	High
Δ	$-$	Uncertainty

Structure of thesis

About the thesis

This doctoral thesis consists of three parts. **Part I - Introduction and summary**, describes and discuses the background, methods, results with discussion and conclusion of the thesis. Part I is supported by and refer to **Part II - Appended papers** with research publications in the form of the 4 scientific articles published or submitted to Institute for Science Information (ISI) journals. **Part III - Appendix** contains supplementary documents, including additional research publications where the author was not the main author, and/or some of the results are already mentioned in the previous ISI publications. The results of the research are presented in the 4 main ISI papers. Their connection is illustrated in figure 1, consisting of three main parts, which are product development, thermal performance modelling and optical performance modelling. The product development is partly represented in every article. Article I and II focus on the thermal performance modelling of fenestrations and Article III and IV are oriented on the optical performance modelling of fenestrations. None of the parts are possible to separate from each other and thus thermal and optical performance modelling are partially mentioned in every article.

Thesis outline - Part I

The description of the motivation for the research in this thesis is presented in chapter 1, followed by introduction and background. This chapter also includes energy requirements, performance modelling methodology and terminology. Chapter 2 describes the product development methods for developing CFSs. Chapter 3 focuses on discussing the thermal performance modelling of CFSs and presents results from the investigations. Chapter 4 discuses optical performance modelling of CFSs and presents results of the investigations. The conclusions are given in chapter 5.

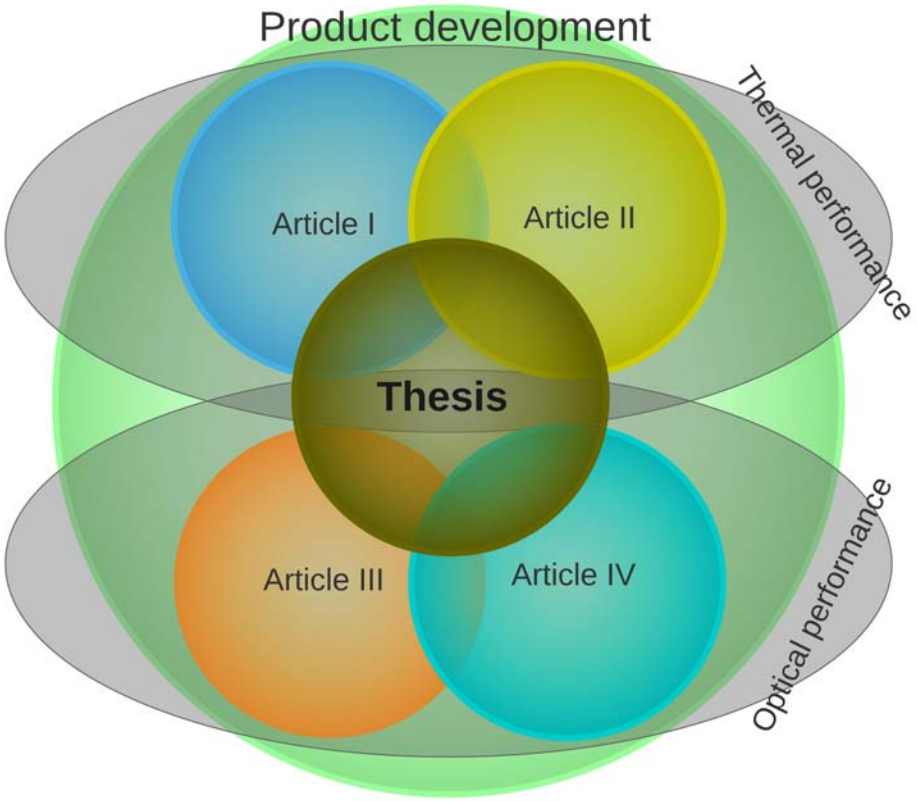

***Figure 1**: Visualization of the whole project structure.*

List of Publications

The ISI articles are listed below, including the abstracts:

Paper I
D. Appelfeld, C.S. Hansen & S. Svendsen, *"Development of a slim window frame made of glass fibre reinforced polyester"*, Published in: Energy & Buildings

Abstract
This paper presents the development of an energy efficient window frame made of a GFRP material. Three frame proposals were considered. The energy and structural performances of the frames were calculated and compared with wooden and aluminium reference frames. In order to estimate performances, detailed thermal calculations were performed in four successive steps including solar energy and light transmittance in addition to heat loss and supplemented with a simplified structural calculation of frame load capacity and deflection. Based on these calculations, we carried out an analysis of the potential energy savings of the frame. The calculations for a reference office building showed that the heating demand was considerably lower with a window made of GFRP than with the reference frames. It was found that GFRP is suitable for window frames, and windows made of this material are highly competitive in their contribution to the energy savings. A rational product development method was followed, and the process clearly identified the objectives of the investigation and set out the appropriate way to attain them. Using simple rational development methods, a well-defined and effective window was achieved smoothly and quickly, as is illustrated in the case study.

Paper II
D. Appelfeld & S. Svendsen, *"Experimental analysis of energy performance of a ventilated window for heat recovery under controlled conditions"*, Published in: Energy & Buildings

Abstract
A ventilated window in cold climates can be considered as a passive heat recovery system. This study carried out tests to determine the thermal transmittance of ventilated windows by using the Guarded Hot Box. By testing under defined boundary conditions, the investigation described the heat balance of the ventilated window and clarified the methodology for thermal performance evaluation. Comparison between windows with and without ventilation using

the window-room-ventilation heat balance revealed that a ventilated window can potentially contribute to energy savings. In addition, it was found that a significant part of preheating occurred through the window frames, which positively influenced the heat recovery of the window but increased the heat loss. Results also showed that increasing air flow decreased the recovery efficiency until the point when the additional thermal transmittance introduced by the ventilation was higher than the effect of heat recovery. Accordingly, the use of the ventilated windows might be most suitable for window unit with low ventilation rates. The results correlated with theoretical calculations in standards and software. However, the concept of a window thermal transmittance (U_w) value is not applicable for energy performance evaluation of ventilated window and requires deeper analysis.

Paper III

D. Appelfeld, A. McNeil & S. Svendsen, *"An hourly-based performance comparison of an integrated micro-structural perforated shading screen with standard shading systems"*, Published in: Energy & Buildings

Abstract

This article evaluates the performance of an integrated micro-structural perforated shading screen (MSPSS). Such a system maintains a visual connection with the outdoors while imitating the shading functionality of a venetian blind. Building energy consumption is strongly influenced by the solar gains and heat transfer through the transparent parts of the fenestration systems. MSPSS is angular-dependent shading device that provides an effective strategy in the control of daylight, solar gains and overheating through windows. The study focuses on using direct experimental methods to determine bi-directional transmittance properties of shading systems that are not included as standard shading options in readily available building performance simulation tools. The impact on the indoor environment, particularly temperature and daylight were investigated and compared to three other static complex fenestration systems. The bi-directional description of the systems was used throughout the article. The simulations were validated against outdoor measurements of solar and light transmittance.

Paper IV

D. Appelfeld, S. Svendsen, *"Performance of a daylight redirecting glass shading system"*, Submitted to: Lighting Research and Technology

Abstract

This paper evaluates the daylighting performance of a prototype external dy-

namic shading and light redirecting system. The demonstration project was carried out on a building with an open-space office. The prototype and original façades had the same orientation and surroundings. The research employs available simulation tools for the performance evaluation of the shading system. This was accompanied by measurements of the daylight conditions in the investigated space. The prototype system improved the daylighting conditions compared to the existing system. The visual aspects were kept, as the redirected daylight did not cause discomfort glare. By utilizing higher illuminance, it was possible to save 20% of the lighting energy. The thermal insulation of the fenestration was maintained, with slightly increased solar gains, without producing an excessive overheating.

The supplementary articles are listed below:

Paper V
A. McNeil, C.J. Jonsson, D. Appelfeld, G. Ward, & E.S. Lee, *"A validation of a ray-tracing tool used to generate bi-*directional scattering distribution functions for complex fenestration systems"*, Submitted to: Solar Energy,2012

Paper VI
D. Appelfeld, S. Svendsen & S. Traberg-Borup, *"Performance of a daylight redirecting glass shading system demonstration in an office building"*, Published in: Proceedings of Buildings Simulation

Part I

Introduction and summary

Chapter 1

Introduction and Background

During recent decades there has been an increased national and international focus on lowering the energy demands in buildings [1, 2]. Buildings currently account for 40% of the energy use in most countries, putting them among the largest energy end-use sectors. Therefore buildings hold great potential for cost-effective energy savings. [3]. The International Energy Agency (IEA) has identified the building sector as one of the most cost-effective sectors for reducing energy consumption, with estimated possible energy savings of 1509 million tonnes of oil equivalent (Mtoe) by 2050 [4]. Lighting represents almost 20% of global electricity consumption. This consumption is similar to the amount of electricity generated by nuclear power [5].The electrical lighting is often between 20-40% of used energy in commercial buildings [6]. An interest is growing among architects and consultants towards intelligent building components which can achieve buildings' energy effectiveness, complying with the strict energy codes and national emissions reduction goals [7, 8].

Contemporary commercial and institutional buildings have high internally-generated loads by people/lights/equipment and well-insulated envelopes, which cause low heating and high cooling loads [9], compared to residences which have relatively low internal loads vs. their envelope loads. The largest energy usage in buildings is attributed to heating, cooling and electrical lighting. Windows and façades together with shading systems influence all three and are one of the most crucial elements in the building envelops, which also influence indoor environment. Therefore the detailed evaluation of the interaction between façade performance, energy demand and the indoor environment needs to be carried out. By an optimization of window elements, energy consumed for heating, cooling and electric lighting can be reduced. The optimization strategies consider heating by increasing solar gains, cooling by providing solar protection and lighting by utilizing daylight[10]. All

the functions cannot be addressed by a traditional window. The traditional window has to be combined with a shading system, which all together can be described as a Complex Fenestration System (CFS). Since a significant portion of energy in buildings is devoted to lighting and ventilation for the indoor air quality, daylight and cooling have a large energy saving potential for advanced solar shading systems.
Today, a window is considered as energy-efficient if it has a low thermal transmittance, $U_w - value$. However, that is not sufficient to describe a window's energy performance as the evaluation has to address an interaction between window performance, energy demands and indoor environment. Another example of currently used evaluation parameter is a normal-incidence light transmittance which is not an accurate indicator for angularly dependant systems as they need an bi-directional description [11]. An angularly dependent system is every fenestration system which is not a simply continuous layer, such as pane of glass or coating.
The factors to consider are thermal transmittance, solar energy transmittance, visual transmittance, durability, shape, cost, influence on a building's energy consumption including supply of fresh air, artificial light savings by use of daylight, and the visual and thermal comfort of occupants. These performance parameters could be split into two categories, **thermal** and **optical** performance. The challenge is to evaluate those parameters in the interconnected context, since some of the functions are contradicting, e.g. increasing solar gains in winter while providing shading in summer [9]. The available simulation programs cannot easily evaluate unique CFSs using standardized methods, since they are mostly created to evaluate specific solutions. All those pre-requests and parameters indicate a necessity of comprehensive performance analysis of a CFS. The detailed evaluation can reveal the potentials of unique fenestration solutions. Moreover the detailed evaluation can speed up introduction of innovative solutions to the market by spreading awareness and better understanding of the complex properties.

1.1 Hypothesis and objectives

The central hypothesis of the thesis is that by using comprehensive modelling of thermal and optical performance of a CFS it is possible to develop a CFS which will serve several functions, fulfil new energy regulations, ensure comfortable thermal and visual indoor environment and form the basis for design of low-energy buildings in the future.

The aim of this project is to investigate and set product development methods for development of new advanced energy-effective window systems. These systems will work as a complex lighting system with improved energy performance with respect to heat loss, solar gain, solar shading, visual transmittance and ventilation.The complex lighting system is considered for both newly built low-energy buildings and refurbishment of existing buildings.

The main problem discussed in this thesis is the accessibility and accuracy of tools and methods to perform an adequate performance evaluation of newly developed fenestration technologies, i.e. windows, façades, shadings and their combinations. The focus is on the performance prediction by simulations, with respect to energy use and indoor climate. The objectives for the development of CFS is visualised in figure 1.1, including the description of the windows' multi-functionality.
The performance of several CFSs was tested and the simulations were validated against measurements as the simulations have to reflect the reality. The current complexity and inaccuracy of the evaluation is limiting the effective implementation of new solutions within the construction industry.
The limitations of the available simulation tools and testing methods can be overcome by performing state-of-the-art simulations.
The main motivation for this research is to establish procedures for generating information, which can be used during product development of CFSs or during an initial phase of building design. Performance simulations are used in the early stage of the building design to predict an impact of the given CFS on the overall performance of the building. The predictions are made in order to fulfil the given requirement by the legislation and client. Furthermore, the predictions are carried out for the performance optimization. The most difficult part is to describe the CFS's properties with a reasonable level of detail in order to see the impact of the changes and innovation. The current practise is that the solar and thermal properties are simplified and

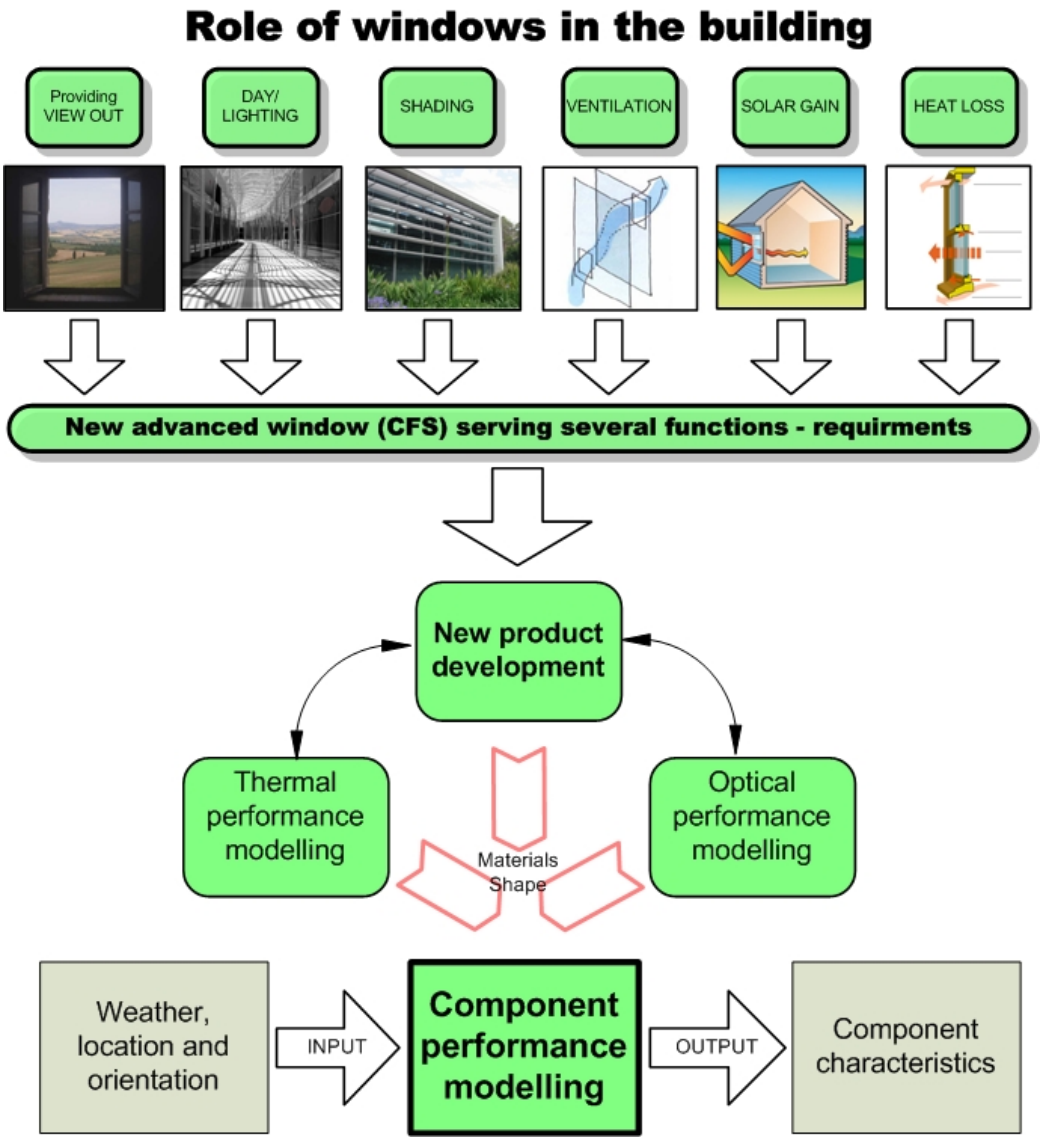

***Figure 1.1**: Schematic description of the objetive of the performance development of a CFS.*

notable assumptions are made. The material properties and system's geometry are often substituted by similar existing solutions, which in many cases remove the innovative element of the solution.

1.1.1 Limitations

The development and testing process presented in this thesis is not trying to be necessary simple and is dealing with the performance evaluation of CFSs from the scientific perspective. The purpose here is not to introduce a perfect CFS as there is none generically correct solution for all situations and each has different requirements. Therefore the thesis is suggesting the process how to analytically achieve the suitable solution.

1.2 Background

Windows are typically responsible for a large fraction of the heat loss in buildings as windows, especially window frames, have higher thermal transmittance than other parts of the building envelope. However, windows can contribute to the heating by solar gains[12]. Providing daylight is another main feature of the windows. Daylight is a preferable source of lighting by humans and has positive effect on the healthy environment and productivity [13]. Furthermore, by utilizing daylight the energy used for artificial light can be reduced [14].
Additionally, windows are mediators of a ventilation and air exchange in both old and new buildings. The thermal transmittance of façades was reduced in the past decades by introducing glazings with coating, sealed glazings and limiting heat loss by heat breaks in the frames. The window frames were improved by introducing new materials and designs of frames leading to highly insulated and high performance windows [15, 16]. In spite of those actions, windows are still large contributors of heat loss. However, the natural air exchange of the façade by the air leaking and air infiltration was significantly reduced. Regarding the standards for the total energy consumption of buildings; heating, cooling, ventilation, hot water and lighting have to be included [17]. Therefore additional ventilation, possibly with heat exchanger, has to be taken into account for the energy consumption as well as to ensure the quality of indoor environment [18, 19, 20].
An increased thermal resistance of building envelops can lower heating loads but also increase risk of overheating by capturing excessive solar gains, especially in office buildings. Additionally, the glazed areas in new office buildings are getting larger, which increases solar gains during the cold periods of year

and increases the working plane illuminance (WPI). However during warmer seasons the over-glazed areas can generate overheating and glare, and thus solar shading is necessary. Removing overheating by a mechanically cooling and ventilation is expensive and can negate the savings from solar gains in winter. This results in growing importance of the cooling loads [21, 22]. Therefore solar shading is an effective strategy to reduce overheating and diffuse direct sunlight to reduce the energy consumption. There are many shading systems and it is difficult to precisely describe the performance of a non-standardized solution, especially in overall context of building.

Transparent parts of building envelopes serve several functions [21]:

1. Provide enough light transmittance, and daylight utilization.
2. Thermal insulation to ensure health and comfortable indoor environment.
3. They should provide sufficient solar energy transmittance during cold months, to reduce heating demand.
4. They should prevent indoor space from overheating during warmer months by shading excessive solar gains.
5. The view to outside is desired and should be unobstructed and maintained.

1.3 Energy, Environment, Indoor Climate

The goals of the CFSs are to contribute to reduce the overall annual energy building consumption and eliminate the heat loss of buildings' envelops when the space is heated. The transparent parts of the CFSs is a source of a renewable energy in the form of solar energy. Furthermore, the CFSs provides the direct connection to outdoor, providing the view to outside and supply of fresh air by openable windows and thus contribute to a comfortable and healthy indoor climate.
The immediate goal of the CFS is to provide occupants with the cost effective and easy way to operate and maintain indoor spaces without a negative impact on health and comfort.

The sustainability of the CFS is ensured by focus on three main factors:

- **Energy** - CFS provides a positive contribution to the energy balance of buildings. It provides a thermal insulation and enables to obtain solar gains.

- **Environment** - Each building interacts with a surrounded environment. Therefore the performance of CFS is dependent on the surrounding conditions and the solution has to be focused on utilizing its location.

- **Indoor Climate** - Thermal and visual comfort of occupants ensures healthy and comfortable indoor climate by supply of daylight and fresh air.

All those aspects interact with each other. The diagram in figure 1.2 illustrates the interaction. Windows and transparent elements of a façade in general should positively contribute to the human health and well-being as the indoor environment can be influenced by them. Additionally, the transparent areas work as a source of renewable energy.
The building energy consumption in the relation to the CFS is heating, lighting and cooling, and they interact with each other, see figure 1.3. The heating is influenced by the solar gains through a fenestration. When the façade is extensively transparent it can provide large solar gains, which increase the risk of overheating and hereby influence the cooling loads. To remove the excessive heat, the energy to increase the ventilation air flow or cooling is needed to reduce the over heating. By the optimal use of the solar shading this energy can be reduced as the over heating can be avoided. When enough daylight is provided to reach the required level of WPI, then an artificial light can be turned off. This implicitly reduces the cooling loads as a lighting produces heat. On the other hand the low thermal transmittance of façade will increase the heating loads during the heating season as the solar gains will be smaller. Since a significant portion of energy in buildings is devoted to a lighting and ventilation, daylight and cooling have large energy saving potential.[23].

1.4 Product development of CFS

The development of fenestration system is a complex process as a holistic solution is often required. The transparent parts of building envelope, always serves several purposes, as mentioned in section 1.2 on page 8. Furthermore, fenestration influences the building energy. Firstly with the heat exchange to outdoor, thus *thermally*, and secondly with allowing light to penetrate indoor, thus *optically*. Both factors explicitly influence the indoor environment. The design and development process of CFS is not trivial task as it involves a web of interdependent variables [10]. Therefore, in this thesis a sequence of steps

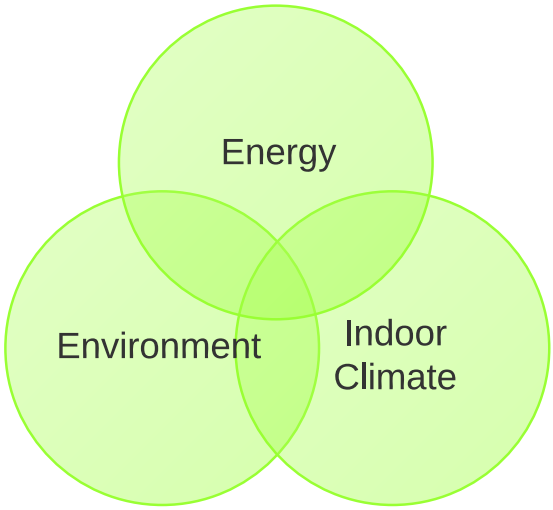

***Figure 1.2**: Interaction between three sustainable aspects of window/CFS*

is presented. First step is to identify the purpose and need of fenestration and second the quantification and qualification of the requirements is suggested. The whole process is discussed in section 2 on page 29 and in the papers in the Part II.

1.5 Performance simulations of CFS

There is usually a lack of information and knowledge in the early stage of design to understand the complexity of the interrelated performance indicators for an actual building. The building industry needs a comprehensive reference which describes both the fenestration design and the performance of such systems in a building [10].
The results from performance simulations can in many cases be hard to understand in the holistic context. In this thesis the framework for a design of high performance CFSs is suggested in order to facilitate the performance simulation usability. The CFS serves several functions which makes it difficult to decide what is a better solution in the overall context. E.g. the system can be good from one perspective, allowing lots of daylight and solar gains, but from another perspective can cause the risk of overheating. The suggested performance modelling is designed to reduce the energy consumption of buildings and to improve the quality of indoor environment.
Fenestration systems which incorporate innovative technologies are often not included in commonly used building performance simulation programs, e.g.

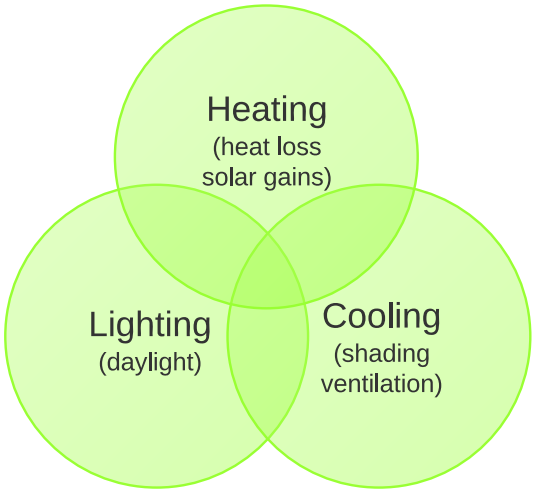

***Figure 1.3**: Interaction between three heating, cooling and lighting*

ESP-r [24], TRNSYS [25], EnergyPlus [26]. Therefore it may be difficult to predict the performance and further improve new and existing solutions. Moreover, designers and building owners can not fully indicate the advantages of those innovative solutions [27]. The conservative assumptions of performance are often made when evaluating the CFS's impact on a building. The inaccuracy of the current performance prediction limits introduction of innovative and advanced technologies to the market.
The current building simulation programs are mainly focused on the performance simulations of buildings with little detail on the performance of CFS. Those programs allow mainly to use only standardized and commonly used shading systems, however using new materials, shapes and concepts is limited. The recent development of ESP-r integrated a module to the program which allows to input information about state-of-the-art CFSs solutions [28]. By this approach any CFS can be used without modelling of the details within the program.
In the case of product development of the CFS it is important to move the focus from the building closer to the CFS. However it has to always stay in direct connection, as the building energy is influenced by the CFS.
The are several reasons to do performance simulation focused on a façade:

- Newly developed façades are often too complex for modelling in the building simulation programs. The lack of programs' capabilities often slow down the development of innovative and unique solutions. Ad-

ditionally, the market penetration would limb along as the designers would not be able to employ the new features.

- The accuracy plays a major importance as it is needed to know what is the performance of the real product. In some cases the improvement can not be discovered as the inaccuracy error can be the same or bigger than the performance improvement. This is especially a case when the performance depends on the new unique features of the system.
- In order to further develop new and high performance CFS solutions comparison and benchmarking against existing solutions has to be made.

1.5.1 Thermal performance modelling

The calculations of the thermal properties of CFS elements is important for estimating the heat loss through the fenestration. The energy performance can be evaluated on several levels, e.g. starting with the heat loss coefficient of a window frame and ending with a study of window's effect on the building energy consumption. It is recommended to perform multiple calculations starting with a simple evaluation and continuing to more comprehensive assessment to see the overall performance.

Thermal transmittance of window

The thermal transmittance of window $U_w - value$ is the basic indicator of the thermal properties of windows and façades. The standardised $U_w - value$ calculation method is described in the standard ISO 10077-2 [29]. There is several specifically aimed programs on the market for those calculations, e.g. Therm [30], WinIso [31] or Heat2 [32]. These programs can solve the conductive and convective heat transfer equations as well as they are using radiation models to calculated heat loss according to the standard ISO 15099 [33]. The standard calculation of the thermal transmittance of window, $U_w - value$ is prescribed in ISO 10077-2 and based on the thermal transmittance of glazing $U_g - value$, and frame $U_f - value$, and on the liner transmittance of the glazing edge Ψ [29, 34]. The $U_w - value$ of the whole window is obtained by eq. 1.1. The $U_f - value$ is calculated in the absence of a glazing, which is substituted by a highly insulated panel in order to eliminate the effect of the thermal bridge by the glazing edge and spacer. According to ISO 10077-2 the linear thermal transmittance of a glazing edge, or by other words spacer, has to be calculated. The edge effect is different for every combination of frame, spacer and glazing and it is necessary to calculate it

for each solution. For the calculation of Ψ, the spacer is replaced with a simplified shape with equivalent thermal conductivity [35].

$$U_w = \frac{U_g \times A_g + U_f \times A_f + \Psi \times l_\Psi}{A_w} \tag{1.1}$$

Thermal transmittance of ventilated window

In this research an experimental study of the ventilated window with a heat recovery was carried out, see appended paper II and chapter 3.2 for detailed information. The principle of the thermal transmittance of window, $U_w - value$, is not directly applicable for the ventilated window. The ventilated window can serve two additional purposes to a regular window. Firstly, providing supply of fresh air and secondly preheating ventilated air by recovering heat loss of the window. The schematic picture of the ventilated window is shown in figure 1.4. The thermal properties of the ventilated window depend on several parameters, among others the specimen itself, boundary conditions, direction of heat flux, temperature differences, and airflow.
The difference to a standard understanding of the thermal transmittance of window, $U_w - value$, is that the heat loss through the window is increased by introducing the airflow, which is partly reclaimed by the airflow. Since the ventilation changes the heat balance of the window/building and generates an additional heat loss by the ventilation, a different evaluation process had to be considered for the heat balance definition. Several studies provide models for specific examples and ideas to improve the performance of the ventilated windows, however the experimental results are rarely available [36, 37, 38]. An energy balance of the ventilated window was documented by several investigations, mainly theoretical and numerical [20, 39, 36, 40, 41].

Net energy gain of window

As the next step the net energy gain (NEG) method is used to calculate the effect of a window in the context of the heat losses and solar gains [12, 42]. There are various ways of assessing the energy performance of a window. But it is clearly insufficient to evaluate the window with the thermal transmittance only. To achieve the positive NEG, a large glazing, slim frames and glazing with high transmittance would be preferable as it will improve both the thermal transmittance and the solar gains [16, 15]. The NEG method is based on the window's solar gains minus the window's heat loss during a standard period, which is defined as the heating season depending on the outdoor air temperature. This takes into account the tilt and relative orientation of the window in the reference building [12]. The NEG can reveal

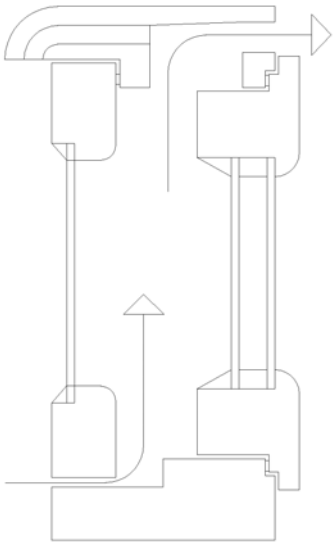

***Figure 1.4**: Schematic picture of the used ventilated window with airflow marked.*

that a window with a very low $U_w - value$ has lower NEG than a window with higher $U_w - value$.
For example, the window with $U_w - value$ of 1.27 W/m^2K ($U_f - value$ 1.33 W/m^2K) can have higher NEG than a window with $U_w - value$ 0.79 W/m^2K ($U_f - value$ 0.75 W/m^2K) [43, 15]. This resulted from the greater area of glazing in the case of the window with higher $U_w - value$, which means that the heat loss can be compensated by the extra solar gains. The NEG formula is described by eq. 1.2.

$$NEG = \tau_{sw} \times I - U_w \times D \tag{1.2}$$

where D is the coefficient for heat loss and I is the coefficient for solar gains. Both coefficients are dependent on a location and window orientation. For Denmark, I is 196.4 kWh/m^2 and D is 90.36 kKh [12]. This approach to an energy performance evaluation allows an easy and quick comparison of various windows.
The total solar energy transmittance of a window τ_{sw} is needed for the calculation of NEG and is combined from the solar energy transmittance of the glazing and frame, see 1.3 [33].

$$\tau_{sw} = \frac{\sum \tau_g \times A_g + \sum \tau_f \times A_f}{A_w} \tag{1.3}$$

Analysis of window impact on building energy use

The last step in the thermal energy performance assessment is a comprehensive evaluation of an effect of window on the energy consumption of building. An energy impact on an office building, domestic building and single cell office was evaluated in different parts of this thesis and the details are described in the appended papers.
Again, several different software were used for these analyses throughout the thesis:

- **iDbuild** is a building simulation tool for an evaluation of energy performance and indoor environment based on hourly weather data. The program is able to illustrate how performance parameters and combinations of them affect the energy performance, thermal indoor environment, air quality, and daylight conditions [44].
- **Be06**[1] calculations are performed in accordance with the procedure in the EU Directive on the energy performance of buildings and Danish Building Regulations [2, 1, 17]. The Be06 software calculates the needed energy supply to all types of buildings for room heating, ventilation, cooling, hot water and artificial lighting and is compared to the energy frame in the Building Regulations [45].
- **ESP-r** is an integrated energy modelling tool for simulating of the thermal, visual and acoustic performance of buildings and energy use associated with environmental control systems. The system is equipped to model heat, air, moisture and electrical power flows in an user determined resolution [46, 24]. ESP-r was mainly used for its ability to model the optical properties of CFSs without modelling the details of façade within the program [28]. The Black-Box-Model (BBM) within ESP-r provides such a feature [28].

It has been found that bi-directional information about fenestrations provide more accurate estimation of heating and cooling loads [47]. For this purpose the BBM with resolution of 5°of azimuth and altitude is suitable. The standard method of an evaluation, where only normal-incidence value of a transmittance is used, heating demand was overestimated up to 23% and that cooling demand was underestimated up to 99% according to study by Kuhn compare to using bi-directional information [48, 49].

[1]Program Be06 was replaced by the newer version of the program, Be10. However Be06 was the current version of the program when the research in appended paper I was carried out.

1.5.2 Optical performance modelling

In this chapter, the optical performance modelling background is introduced, including the used simulation techniques and methods within the thesis. The appended papers III and IV are mainly dealing with the optical performance and characterization of various newly developed and unique shading systems. Appended paper I touches the topic too, mainly by investigating NEG and solar transmittance of the developed window.
Almost every fenestration system provides some level of optical connection between interior and exterior. The connection is described by transmittance of the CFS which is dependent on the incidence angle and the solar radiation. The amount of solar energy transmitted through a window at a given time depend on location, orientation and system geometry. The program Radiance is used as a ray tracing software to perform daylighting and visual comfort investigations. Radiance is an accurate backward ray tracing Unix-based programme [50]. Radiance was validated by several research papers for similar purposes as investigated in this thesis [51, 52]. Furthermore, Window6 was used for generation the bi-directional scattering function (BSDF) matrices describing the transmittance of windows and CFSs [30]. The program iDbuild was mainly used for a calculation of energy performance, thermal indoor environment but also for daylighting conditions in an office [44]. Furthermore, by the program WIS directional transmittance of a glazing or CFS was calculated [53]. The programs Columen [54], Spectrum [55] or Caluwin [56] were used to calculate a visible and solar transmittance of various glazings.

Daylight

Visual comfort and use of daylight are central points for providing comfortable buildings with a healthy indoor environment[57]. The increased use of daylight and careful design of the lighted environment has the potential for both health benefits and increased safety and productivity [58]. The design with daylight in mind can provide comfortable indoor daylight conditions without excessive solar gains [59]. A careful design and using well defined fenestration solution provides enough daylight without increasing the size of an Heating, Ventilation, Air Conditioning (HVAC) system when compared to a windowless room. Such a design combines shading, glazing and façade orientation with a respect of its site and local climate. This can be achieved with active or passive daylighting design including glare control or light redirection. Both components of daylight (direct and diffuse daylight) are important because they determine indoor daylight conditions, similarly

to the cooling loads which are highly dependent on the direct sunlight [21].

Daylight simulations

The performance of any fenestration system varies during a year and is dependent on the sun position and sky distribution. Annual simulations provides useful information about a CFS and remove the drawback of standard static daylight simulations which focuses only on extreme conditions, e.g. 21^{st} of December. Furthermore annual simulations are more realistic because they use measured weather data over several years. In this thesis the test reference year (TRY) weather file for Copenhagen, Denmark was used [60]. Hourly weather data are used for the simulations as the resolution is sufficient and provides realistic results [61]. The daylight simulations are computer based calculations. The daylight simulations predict a situation according to the input which is mainly based on information about a building including interior description and sky conditions.
Annual daylight simulations are in the literature also referred to as dynamic daylighting simulations, which are conducted in the steps in agreement with three-phase method, which is explained in paragraph Three Phase Method on page 18 [62, 63].

1 Creating a sky model with irradiance/illuminance data.

2 Using time steps within the working hours.

3 Making a Radiance simulation for each time step and each sensor position or rendering, i.e. view, daylighting and transmission matrix combination.

4 Assess how many times the required designed working illuminance is satisfied (or partly satisfied).

5 Count how much artificial light is needed to add to satisfied minimal WPI.

Daylight evaluation matrices

The required working plane illuminance (WPI) is defined by several standards, and design recommendations. This chapter defines which thresholds are used for different daylight evaluation matrices. The annual evaluation is suitable for the performance modelling as the evaluation of a single scenario would not reflect the real daylighting performance of the CFS. Additionally the information about useful daylight conditions in an indoor environment

is more valuable than knowing the conditions during the extreme conditions only. The commonly used daylight factor (DF) does not use any of the above mentioned requirements as well as it does not quantify the redistribution of a direct light to provide diffuse illuminance. Furthermore, DF underestimated the daylight levels within the room for southern orientated rooms and overestimate the illuminance values for north facing rooms [64]. Instead of the DF, the useful daylight illuminance (UDI) and daylight autonomy (DA) is used in this thesis [65, 66, 52, 67, 57].
The **DA** is the percentage of hours satisfying the minimal designed WPI from the total number of working hours in a year [68]. The commonly used design WPI is between 300 - 500 lux.
The **UDI** matrix quantifies when daylight is perceived as useful for occupants or not. It is calculated as the percentage of the occupied working hours when the WPI is between the lower and upper threshold.
The different WPI levels are used within this thesis. They are based on the review of the following literature [66, 52, 69, 67, 70, 57, 71]:

- **100 lux** - Is considered as insufficient for performing tasks under daylighting conditions and it is the lower limit for UDI.
- **300 lux** - Is often considered as sufficient for performing working tasks.
- **500 lux** - Is described as minimal WPI for the office work and it is used as the threshold for DA analysis.
- **4500 lux** - 30% of people find the horizontal illuminance above the level too high and uncomfortable [71]. The upper limit is not clearly defined in literature and thus 4500 lux is used as the upper limit for UDI.

The midrange between 100 lux and 4500 lux is considered as usable for most of occupants. Some subjects may consider the values in this range as uncomfortable, however these values should not be considered as useless since every subject perceive an illuminance level differently [57, 71].

Three phase method

The three-phase method (TPM) is based on the daylight coefficient (DC) principle by which the annual daylight simulations can be performed effectively with a relatively low amount of computational resources [72]. The DC approach subdivides the sky into divisions and then the contributions from each division/direction are calculated independently, for more information see paragraph Bi-directional characteristics of CFS on page 21. The TPM

can generate both renderings and illuminance values. The renderings are mainly used for analysis of a visual comfort, e.g. glare, and the illuminance readings for a daylight distribution analysis. To calculate the annual illuminance on a working plane the TPM using Radiance was used throughout the thesis. The method calculates separately the effect of the sky, outdoor, indoor and fenestration, resulting in a vector with illuminance values $\boldsymbol{i}$ [63].

$$i = V \times T \times D \times s \tag{1.4}$$

Four matrices are generated and multiplied between each other according to eq. 1.4 [73, 63]. The Radiance program **rtcontrib** is used to generate the transmission results in the matrix form. The transmission of fenestration system matrix, **T** matrix, describes bi-directional transmission through a fenestration. In this thesis the bi-directional scattering function (BSDF) matrix is generated either by the Radiance tool genBSDF [27] or by Window6 [30] or it could also be measured by gonio-photometer [74, 75]. The exterior daylighting matrix, **D** matrix, describes the light transmission between sky and the fenestration and is divided into the 145 subdivisions [76]. The interior view matrix, **V** matrix, describes the lighting scene indoor and defines either point for illuminance readings or view for renderings. The sky vector **s** describes sky distribution by assigning luminance values to each patch representing the sky directions. The sky was divided into 2305 patches according to Reinhart's subdivision for detailed results [77].
The TPM approach reuses already generated matrices as some of them do not change over a year. E.g. when static shading is investigated then only one T-matrix is needed, as well as the exterior or interior does not change over a year. In many situations the sky is only changing variable as the luminance of sky is a time dependent variable which continuously change. Additionally, by changing only one of the matrices various aspects could be effectively investigated; different orientations by changing the daylighting matrix, location by changing sky vector, and different CFS by using different BSDF matrix [63].

Glare

Optimally CFSs should fulfil visual comfort, while providing sufficient daylight penetration. Those two features are in many cases contradicting as introducing higher illuminance levels by daylight can implicitly cause glare problems. The glare analysis is needed as the view to outside may include looking to the direct light [78]. Additionally an uncomfortable glare can reduce productivity. However, the perception of glare is often reduced, even under high glare index values, when working under daylighting conditions

[79]. The glare perception is dependent on a view direction and position, which is sometime called the visual zone [71, 80]. Therefore in each analysis a view have to be defined and preferably several different views. The Daylight Glare Probability (DGP) was selected as a glare index because it is based on the extensive human evaluation study [81, 82]. Furthermore, when glare is evaluated it is recommended to make an analysis during working hours, which are often set between 8:00 and 18:00. An enhanced simplified DGP calculation method is suitable for annual DGP analysis as it is possible to include the direct sunlight in the analysis [81]. Glare readings are made from rendered images in Radiance, because it is not possible to evaluate the discomfort glare just by the horizontal illuminance [57].

Electrical light savings by daylight

Apart of favouring daylight by people as a light source for visual task, the savings of electricity for artificial lighting are desired. Depending on the daylight-linked lighting control strategy the daylight can be utilized. Therefore a percentage of the working hours satisfying the daylighting conditions has to be accounted in order to evaluate these savings. The artificial light energy savings are equal to the lighting energy which can be substituted by daylight. This substitution is linear and thus idealized. The savings are compared to a situation when no daylight is utilized. The WPI for an office work required by the European standard CEN-EN 15251 is 500 lux and by Illuminating Engineering Society of North America (IESNA) is 300 lux [70, 83, 57]. However, there is not described a minimal lighting power density (LPD) to reach the required WPI. Standard EN 15193 prescribe the LPD of 15 W/m^2 as the basic and 25 W/m^2 as comprehensive requirement [84].
As the daylight illuminance decreases with a depth of space, more artificial light is needed in back of a room. It is suitable to split the evaluated space into few reasonably sized zones which can be evaluated individually. Then the minimal required WPI by daylight has to be fulfilled in the back of each zone, which means that the whole zone is lit sufficiently.
In this thesis three different daylight-linked lighting control strategies were used:

1 **On/off-control** controls the electric lighting within a zone. Lighting is switched off when the WPI is sufficient by daylight.

2 **Bi-level switching control**, half of the lamps in a zone is switched off when daylight fulfils at least half of the required WPI and is switched off when the WPI criteria is fully met.

3 **Continuous control**, the electrical lighting is linearly dimmed by amount equal to the available daylight, until minimal supplied output of 20% and then switched off when the criteria is met.

Bi-directional characteristics of CFS

The light transmittance related analysis, such as daylight, visual comfort or artificial light energy saving analysis is by a definition angular-depended. In the relation of CFS this dependency is strongly related to the outdoor illuminance conditions, time and indoor space distribution [74]. To have the information about both visual transmittance, T_{vis}, and solar transmittance, T_{sol}, accurate and detailed as possible the bi-directional scattering function (BSDF) provides necessary knowledge about the directional optical properties. By BSDF together with the knowledge of local conditions a fenestration design can be adjusted to maximise a performance utilization of CFS. The BSDF matrix consists eight matrices with information about front and back, visible and NIR, reflectance and transmittance of a CFS. By a BSDF it is possible to depict an outcoming light distribution for a given incidence direction [85]. The accessibility of this information can facilitate the development and optimization of CFS. The example of description of visible transmittance of the clear glazing by BSDF is shown in figure 1.5. The BSDF coordinates are translated to perpendicular XY coordinates with altitude and azimuth between 90°and -90°. From figure 1.5 it is easy to see how the transmittance varies with the incidence angle.

Furthermore, by using TPM and BSDF it is possible to perform inexpensive parametric studies by varying geometry or materials. The new software development of the program Radiance allows generating BSDF matrices, which describes transmittance dependent on an incidence angle (IA). The programme **genBSDF** was mainly used to generate the BSDF matrices in this thesis[27]. The programme genBSDF generates blocks of values which describe 145 Klems's incidence angles for one of 145 oppositely placed outgoing directions [76, 86] which is based on the Tregenza coordinates [87]. The 145 subdivisions describing 145 incidence angle is defined within the Task 21 of the International Energy Agency [88, 89]. The illustration of incoming and outgoing Klems directions is in figure 1.6. The tested models in this thesis were created according to the physical geometry and material properties, and the results were validated against the measurements. Again, all the analyses were carried out in several sequential steps with an increasing level of information to ensure the compactness of an analysis.

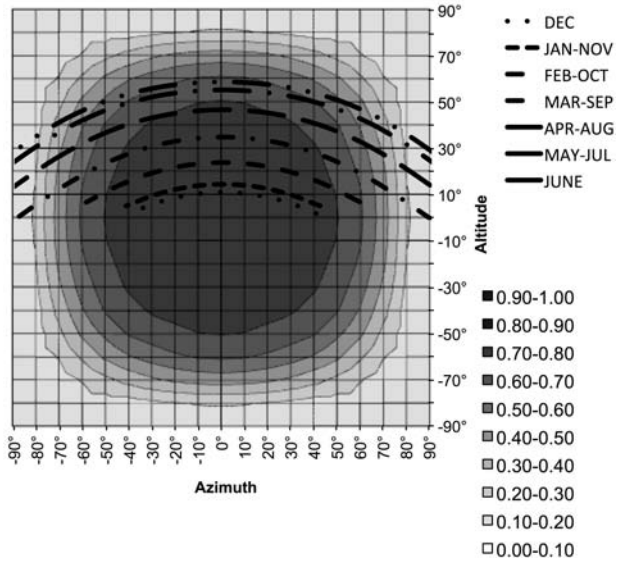

***Figure 1.5**: Example of BSDF for visible transmittance of clear glazing with solar path of Copenhagen*

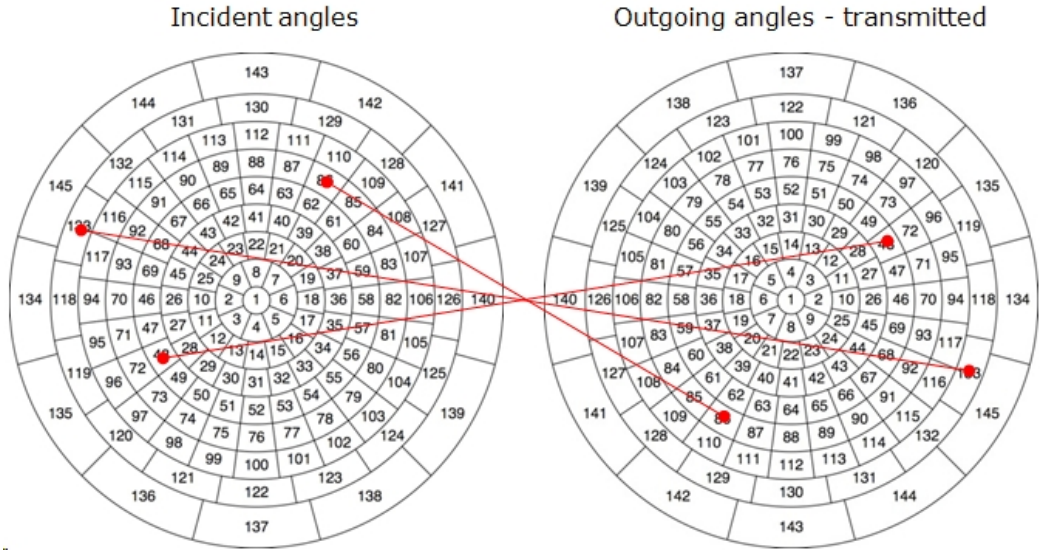

***Figure 1.6**: Angular projection of distribution of Klems angles over the hemispher*

1.6 Solar shading

The transparent parts of a fenestration can be considered as a light and energy source. By allowing daylight and a solar radiation to penetrate an indoor space, visual discomfort and overheating may occur. This is caused by an unobstructed and excessive radiation from the sun and sky. High solar transparency can cause a space overheating, especially in new office buildings as their heating loads are low. This is also valid for buildings in moderate climates, e.g. Denmark, as the cooling loads are significant contributor to the total energy consumption of buildings [90]. Modern buildings are thermally well-insulated, therefore the importance of shading the solar gains become important, especially on southern and east/west facing façades.
Those drawbacks can easily negate savings from the solar gains, which were achieved during winter as well as from the artificial light energy savings. Removing overheating by a mechanical cooling and ventilation is expensive, therefore southern orientated façades should be equipped with a solar shading to control both the thermal and visual comfort. The importance of the cooling loads is growing as the commercial buildings has typically a low heating gains and high cooling loads. Residential buildings have relatively low internal loads vs. their envelope loads [9]. On the other hand, properly shaded windows will have only little difference in the performance at any orientation, however the windows without the shading will have a big difference between orientations. A solar shading is an effective strategy to reduce overheating and diffuse the direct sunlight and consequently reduce the energy consumption [10]. In this thesis the investigated shading systems were designed to improve a visual comfort by reducing a visual discomfort from bright sky and direct view of the sun, as well as to maintain the daylight conditions. CFSs have in most of the cases several functions and thus detailed simulations of the systems have to be applied. The appended papers III and IV are dealing with the solar shadings which are multifunctional.

1.7 Energy requirements and consumption

In Denmark, the building code follows the the Energy Performance of Building Directive (EPBD) which specifies requirements on the total primary energy demand of buildings. The total energy demand includes heating, cooling, domestic hot water, ventilation and lighting (lighting only for offices, commercial and public buildings). The calculation formula for offices, commercial and public buildings is eq. 1.5a and for residential buildings and hotels is eq. 1.5b, where $\boldsymbol{A}$ is a heated floor area [1]. $\boldsymbol{E}$ is the maximum

***Table 1.1**: The energy gain requirments for windows*

	$kWh/(m^2year)$		
	Until Jan 2015	After Jan 2015	After Jan 2020
Vertical windows	-33	-17	0
Roof windows	-10	0	10

specific annual primary energy use in $kWh/(m^2year)$. Energy produced by renewable energy sources, such as a solar heating and solar electricity, is subtracted from the total.

$$E_{frame,offices} = 71.3 + \frac{1650}{A} \qquad [kWh/(m^2year)] \qquad (1.5a)$$

$$E_{frame,dwellings} = 52.5 + \frac{1650}{A} \qquad [kWh/(m^2year)] \qquad (1.5b)$$

Apart from the energy framework, which defines the minimal requirements, two classes for low-energy buildings are defined in BR10 [1]. The low-energy office buildings class for 2015 is defined in accordance with eq. 1.6a and for the residential buildings and hotels in 1.6b. The low-energy class 1 for 2020 for offices is defined as in eq. 1.6c and for dwelling buildings as in eq. 1.6d.

$$E_{frame2015,offices} = 41 + \frac{1000}{A} \qquad [kWh/(m^2year)] \qquad (1.6a)$$

$$E_{frame2015,dwellings} = 30 + \frac{1000}{A} \qquad [kWh/(m^2year)] \qquad (1.6b)$$

$$E_{frame2020,offices} = 25 \qquad [kWh/(m^2year)] \qquad (1.6c)$$

$$E_{frame2020,dwellings} = 20 \qquad [kWh/(m^2year)] \qquad (1.6d)$$

The Danish building code also defines the energy gain, E_{ref}, for the standard window size of 1.23 m $\times$ 1.48 m. The energy gain for the windows in the heating season until January 2015, after January 2015, and after January 2020 are defined in table 1.1. These design requirements have to be kept in mind for construction of any new building and for large renovations.
The visual comfort to reach the required WPI is defined in CEN-EN 15251 [70]. The limits of the LPD are defined in European standard EN 15193 [84], with 15 W/m^2 as the basic requirement and 25 W/m^2 as the comprehensive requirement in regards to the visual comfort.

1.8 Measurements

Measurements supplemented most of the research results from the simulations as it is important to combine measurements with simulations, especially in cases when the reference case for a comparison is not available. Measurements are necessary for the validation of numerical models used in this work. The validated simulated models by measurements can be used for performance assessment and thus the cost of measurements can be reduced or eliminated [48].
During this research the Guarded Hot Box (GHB) measurements were used to measure a thermal transmittance of windows. Furthermore to ensure reliability of simulated illuminance and irradiance photometric measurements by lux-meters and irradiance-meters were done.

1.8.1 Guarded Hot Box

Thermal transmittance of the ventilated window was measured by the adjusted GHB for measurements of the "dark $U_w - value$". The adjustments were made in order to provide an airflow through the glazing cavity and to be able to measure the properties of such a window. A window of standard size of 1.23 m × 1.48 m was placed between a cold and warm chamber in a measuring box with the constant temperature difference of 20 K. The steady-state conditions were maintained by an electrical heater in the measuring box. The input power defined the total heat flow through the specimen. The GHB was calibrated according to standards EN ISO 12567-1 and EN ISO 8990 [91, 92].

1.9 Test office

In this thesis four different test rooms or/and buildings were used for simulations.
In the appended paper I, a low-energy class 1 office building with 60 offices and a large glazed staircase space was used. The office building was simulated to investigate its energy use and an effect on the indoor environment with respect to the temperature and daylight. Furthermore a domestic building was simulated in accordance with the mandatory calculation procedure described in the EU Directive on the energy performance of buildings [2, 1, 17].
In the appended paper II a simplified mid-size room of 4 m × 5 m × 3 m, with an external wall of 15 m^2 and the total volume of 60 m^3 was used for assessment of the ventilated window under different scenarios. The scenarios with the building before and after renovation are used. The simple renova-

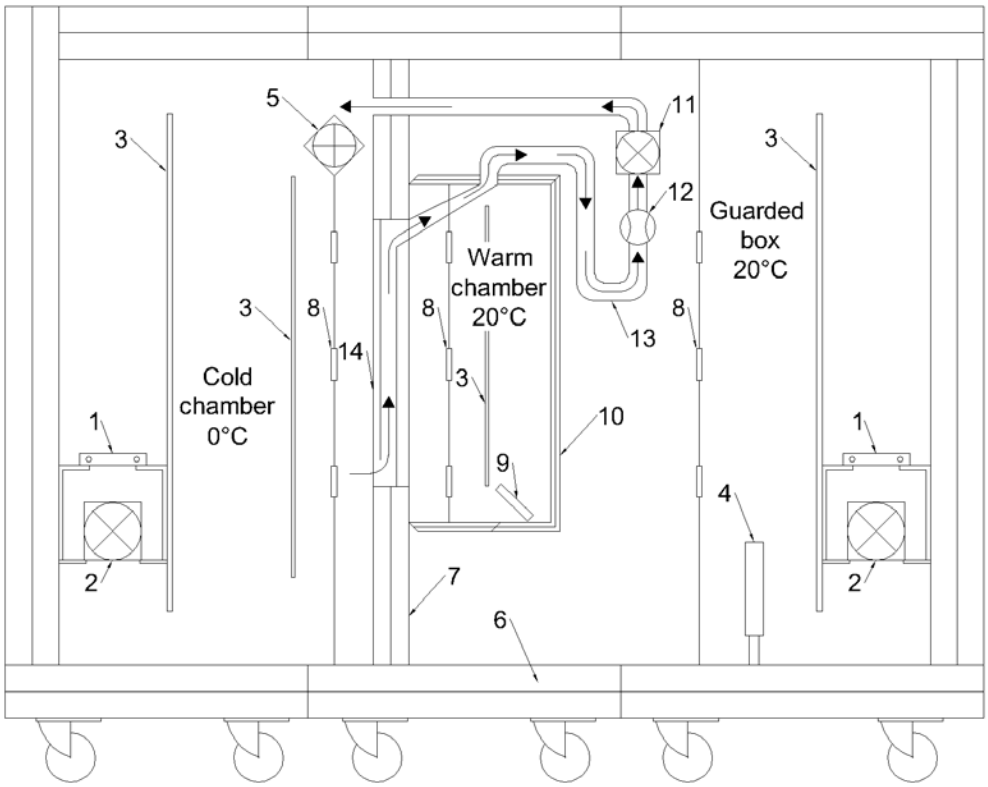

Figure 1.7*: Set-up of the GHB with air flow, and micro manometer. 1, cooling element; 2, fan; 3, baffle; 4, guarded box electrical heater; 5, cold side wind simulator; 6, sandwich element with polyurethane core; 7, surround panel wall from polystyrene foam (XPS) - 170 mm; 8, air temperature sensors; 9, electrical heater in metering box; 10, metering box wall from polystyrene; 11, fan with variable transformer; 12, micro manometer; 13, flexible sucking duct; 14, measured sample of size 1230 mm × 1480 mm (w × h).*

tion was by adding 10 cm of insulation on 70 cm brick wall. Furthermore the windows were changed from original with $U_w - value$ of 2.5 W/m^2K to 1 W/m^2K for traditional window and between 1.1 W/m^2K and 1.3 W/m^2K for the window with an integrated ventilation.
In the appended paper III a standard test office was used. The room model is based on the test office in IEA Task 27 in order to have standardized model [93]. The simulated model was a single office for three occupants with dimension of 3.5 m wide, 5.4 m deep, and 2.7 m high and with a large window. In the appended paper IV, the demonstration building equipped with a prototype of an external dynamic integrated shading and light redirecting system was used. The whole building has dimensions of 66 m $\times$ 28 m with the longer façade oriented 11°west of south. The investigated space in the existing building was approximately 9.5 m wide and 14 m deep with the ceiling height of 3.45 m. The building' and façade' layout allowed to preserve a reference space with the same orientation and similar layout as the investigated spaces.

Chapter 2

Product development of complex fenestration systems

This chapter focuses on how to evaluate Complex Fenestration Systems (CFSs) during a developed of new products. The aim of this chapter is not to present only one way of an evaluation but rather to form a perspective on how to define an evaluation process for specific solutions. This methodology is focused on how to evaluate performance of a CFS in an accurate, detailed and understandable way. The presented framework describes a product development methodology focused on thermal and optical modelling. The interaction between all three elements of the methodology is illustrated in figure 2.1. The objective and output of the thesis would lie in the intersection of the three circles in the figure.
Generally, a comparison of simulations and measurements can be considered as the only method which provides reasonable and accurate validation of simulations. During this research, results from simulations were validated by measurements of unique CFSs. The appended papers describe the testing methods of each investigation Therefore, a reference to the appended papers is used when detailed information is needed. However, the main principle results are presented in the thesis.
Indoor climate conditions, i.e. visual and thermal comfort, could be assessed by questionnaires. However, the physical measurement approach was chosen, as it is independent on a participation of large amount of tested objects, which could prolong the time needed for the evaluation.
This chapter is primarily focused on product development methodology. Furthermore, this chapter is follower by the second key area which focuses on **thermal performance** evaluation, described in chapter 3 and third key area with focus on **optical/visual performance** evaluation, presented in chapter 4.

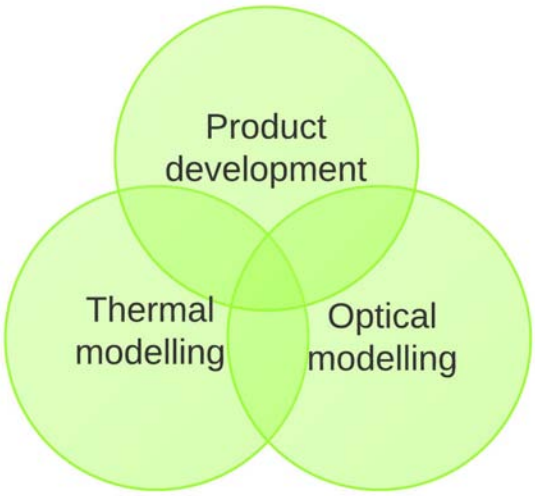

***Figure 2.1**: Schematic description of areas of methodology within the thesis.*

2.1 Product development method

There is a need for tools and methods in the development of CFSs to clearly and quickly understand the complexity of interrelated performance criteria. These tools help to generate knowledge in an early stage of building design about significance of the fenestration in the context of an actual building.
In this chapter, the reference procedure for a design of fenestration systems is suggested. The framework does not intend to be essentially simple despite the fact that it would be useful to have a simply defined succession of steps leading to the desired solution assessment.
The complexity is caused by a large number of interdependent criteria for the evaluation. The performance analysis should be carried out on several levels, with increasing level of detail, in order to increase the understanding of the overall performance. Starting with a single parameter assessment, e.g. the thermal transmittance of window $U_w - value$ and continuing towards an overall evaluation, a more holistic evaluation would be achieved.
The rational product development method suggested by Nigel Cross [94] is suitable for a product development in the building industry [15]. The main and general principle of the rational product development method is shown in figure 2.2. The process starts with identification of opportunities and

potentials within a project. The objective and problem specification defining the overall problem comes next. Based on requirements for solving the problem, sub-problems can be defined. Furthermore, several design alternatives are generated as sub-solutions, and they are evaluated by quantitative performance calculations. The performance calculations vary from project to project and some of them are depicted in the following paragraph 2.2. This evaluation approach allows selecting the final and the most appropriate solution.

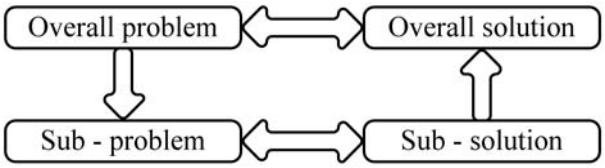

***Figure 2.2**: Skeleton of rational product development method.*

The objectives of product development (PD) can be clarified based on the defined opportunities. The problem objectives can be defined in several levels and their relationship and connections between the levels are explored. E.g. a well performing CFS can serve several purposes which are illustrated in the objective tree in figure 2.3. This figure shows how the objectives are clarified from the top level to the bottom level by asking the question "HOW" and the individual sub-objectives are fulfilled from the lower level to the top by asking the question "WHY".

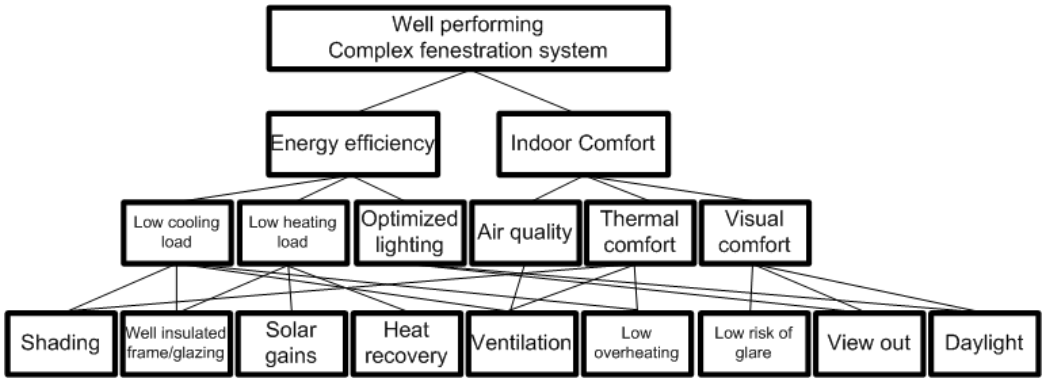

***Figure 2.3**: Example of hierarchical diagram of relationships between design objectives.*

2.2 Evaluation parameters

The solar gains and heat losses through windows have a large impact on the building cooling and heating loads. By providing a natural light, windows can reduce lighting electricity demand. By a proper selection of windows and shadings the heating and cooling loads can be reduced. The direct loads reduction has secondary impacts on reducing the operational cost and equipment downsizing [10].
A fenestration system can be evaluated by several different and interconnected parameters which introduce a large variability and complexity of the performance assessment. It is not possible to look at the façade by only simple indicators. Various parameters and criteria in the performance evaluation are necessary because windows do not work only as a construction blocking the heat losses or opening to the outside; therefore a combination of parameters has to be used. The overall design criteria for widows and CFSs in modern buildings can typically be:

- Energy use - heating, cooling and electrical lighting.
- Thermal comfort - overheating, ventilation.
- Visual comfort - daylight, glare and view.

All these criteria are dependent on each other and could be addressed in the context of following parameters:

- Façade orientation.
- Building location and external obstructions.
- Time and day of a year.
- Window size and position on façade.
- Shading geometry and position.
- Shading control strategy.
- Human factors - view direction, contrast, temperature.
- Material properties (glazing, shading, frames, etc.).

A building location specify climate conditions including the sun position and sky distribution, which is further dependent on the actual time and date as these conditions are time dependent. Another criterion is light transmittance T_{vis} and solar transmittance T_{sol} of a CFS, which is also related to the façade orientation and the building location [48]. By these parameters solar heat gain coefficient (SHGC) can be described, which is also referred to as total

solar energy transmittance, $g - value$. The $g - value$ is a single number value/factor by which the solar gains can be roughly estimated. The thermal transmittance of a window is one of the major energy performance characteristic defining the heat loss. There are also criterion, such as venting or air leakage of a window, which are considered when the window is used for venting and supply of fresh air.
This work focuses on determining an interconnection of all the parameters, which can be defined, by a performance matrix wh ich includes several criterion. The detailed description of the evaluation performance matrix is in the following paragraph 2.3.
There are many other relevant parameter to include in the performance evaluation, however the thermal, optical and comfort parameters are the most important for the performance analysis of a CFS with regard to energy consumption and indoor environment.

Main design evaluation parameters:

- **Total energy use**
  - Heating
  - Cooling
  - Electric lighting
  - Solar gains
- **Daylight**
- **View out**
- **Shading**
- **Visual comfort (e.g. glare)**
- **Thermal comfort (e.g. over heating)**

2.3 Framework

In figure 2.4 an example of a case with four solutions of CFSs and six variables is illustrated. This is a generic example used only for an illustration of the principle. Each axis represents one parameter, however each of the parameters can consist several sub-parameters, e.g energy can consist energy need for cooling and heating of a building. In other cases it can be only NEG [12]. The ranking scale is not fixed as the parameters have different units or can be evaluated differently. The most important is to be consistent

with each parameter for every solution, as only comparable results can be compared. Furthermore, this evaluation method is suitable for a relative and quantitative evaluation as each solution has to rank among other solutions.

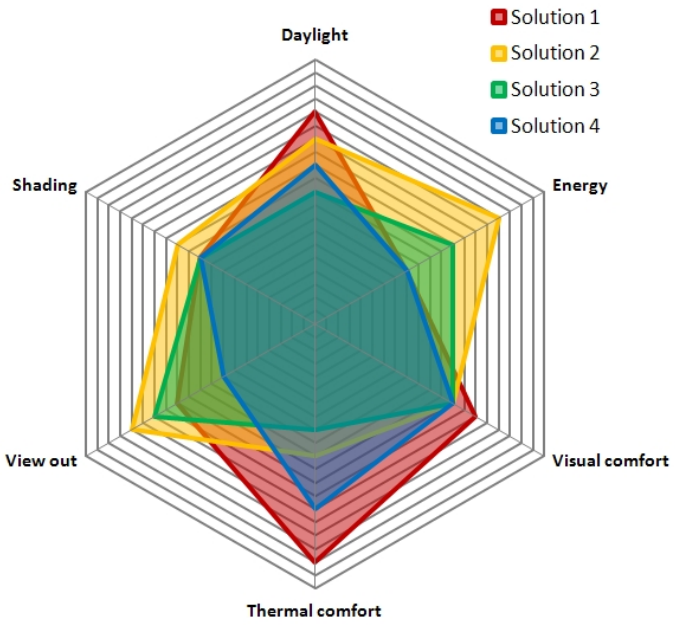

***Figure 2.4**: Example of an evaluation of several performance criteria by radar chart.*

Chapter 3

Optimization of thermal properties of fenestration components

The results from measurements and simulations of two different types of windows are presented and discussed in this chapter.
Firstly, the investigation of a window with a frame made of glass fibre reinforced polyester (GFRP) is presented. This study uses the rational product development method to structure and organize the development of the development of window frames. Three proposed frame designs are compared to each other and to two reference commercial frames. Additionally, an increased solar and light transmittance of façade by reducing the frame thickness is discussed. The detailed investigation is presented in an appended paper I.
Secondly, the experimental investigation of the ventilated window is presented and the theoretical definition of the heat balance of ventilated window is discussed, the detailed results are in an appended paper II.
Both studies are focused on thermal performance of windows, however the connection to the optical performance, presented in chapter 4 is discusses as there is a logical link between optical and thermal performance. The structure of both investigations is based on the methodology presented in chapter 2.1. It means that several parameters are evaluated and compared to a reference in order to quantify the results.
The main hypotheses of this chapter are:

1a By a suitable use of product development method is possible to develop an energy efficient window with a positive effect on an indoor environment.

1b Window frames made from a composite material can significantly improve the overall window performance.

2 Window with an integrated ventilation system can regain some of the heat loss from the window and thereby increase the window's net energy gain.

3.1 Slim window frame made of glass fibre reinforced polyester

This investigation is two fold. Firstly it aims to use the rational product development method to facilitate a development of an energy efficient window. Secondly, several designs of a window frame made from GFRP are suggested. The suggested frames are holistically evaluated by the simulations. The GFRP is used as the window industry is seeking new technologies and materials to further improve energy performance of windows. The thermal evaluation of the frames is split into 4 steps as described in 1.5.1. These are:

1 Thermal transmittance of the frame ($U_f - value$).

2 Thermal transmittance of the window ($U_w - value$).

3 Net energy gain of whole window.

4 Building energy demand.

Additionally, the load capacity and deformation of the frames were assessed against a wind load.
In order to focus on the evaluation of performance of the frames the other variables, such as the glazing, were maintained constant and unchanged throughout the investigation.

3.1.1 Identification of objectives

According to the rational product development method, the problem specification is necessary in order to define the evaluation process. It was identified that the calculations have to be focused on the detailed thermal performance evaluation of the frame. Furthermore, the solar energy gains have to be taken into account. Using triple glazing was a pre-request as well as the GFRP as the frame material. The objectives and their relationship were identified and the hierarchical tree diagram is in figure 3.1. The clarified objectives serve

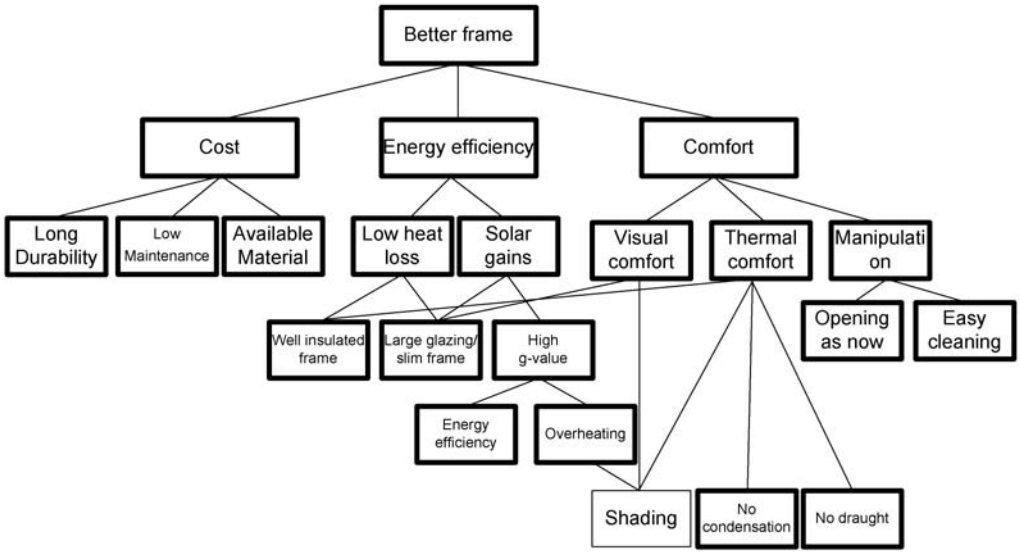

***Figure 3.1**: Hierarchical diagram of relationships between objectives for improved window frame.*

several purposes and are defined by user specifications and requirements, as well as by limitations of production and technologies. The identified specifications are listed in Table 3.1.
Based on the specifications, three frames made from GFRP, were suggested and are shown in figure 3.2. In this figure the two reference cases are shown as well. The frame width, thermal resistance of the frame, solar gains of the whole window, operability, easy maintenance and a gasket tightness are the parameters which determined the evaluation procedure. The description of the investigated frames is as following:

(a) **Reference Frame 1** is the traditional wooden window used in Danish houses with a single side-hung casement opening outwards.

(b) **Reference Frame 2** is a typical aluminium window, which is mostly used in office buildings but also in domestic buildings.

(c) **Alternative 1** is a sliding projecting window with top-hung casement opening outside. The window allows turning the outer surface to the interior for easy cleaning.

(d) **Alternatives 2a** is a tilt and turn window which opens inward. The window is equipped with a standard tilt and turn hinge.

(e) **Alternatives 2b** is a tilt and turn window which opens inward. The window is equipped with a special hinge that can be hidden in the

***Table 3.1**: Thermal and energy properties of evaluated frame alternatives.*

Specification-Window frame from GFRP		
Number	R or W*	Requirements
1	R	Using standard double or triple glazing
2	R	Glued glazing into the frame by silicon or epoxy resin
3	W	Frame visible high at the most 50mm
4	R	Sides of the frame connected by mechanical connections in the corners
5	W	Use same profiles for both triple and double glazed window
6	R	Wooden appearance from inside
7	W	The finishing of the frame has to be available in several colours
8	R	Manipulation by one hand
9	R	Easy operable and easy to clean
10	R	Slim hinges for placement into the frame
11	R	Hinges screwed directly into the wall
12	R	Water and air tight gasket between sash and frame - 2mm
13	R	Maximal deformation 1/300 of a window side length or max 8mm
14	R	Minimal strength of frame 300MPa
15	R	Net energy gain above -20kWh/m^2 per year for double glazed window
16	R	Net energy gain above 0kWh/m^2 per year for triple glazed window
17	R	Insulation in the wall has to be covered water-tight by the frame
18	R	Minimal thickness of profile wall 1.5mm

**R, requirements; W, wishes.*

casement frame and reduce the frame width compared to the alternative 2a by 12mm.

The proposed alternatives have to be evaluated, which is the last step within the PD method and decision process. This can be repeated several times in order to optimize the frame design.

3.1.2 Results and discussion

In this chapter the results of calculations are discussed. The energy and thermal performance evaluation is split into four consequence assessment steps and is followed by the load capacity analysis. In table 3.2 the basic results and characteristics for each frame are listed. This table is followed by more comprehensive results, presented in table 3.3.
The GFRP has several distinctive properties compared to typical materials used for window frames, such as aluminium, PVC or wood. The GFRP is eight times stronger than PVC and three and half times stronger than wood. The thermal conductivity of the GFRP is several times lower than of aluminium and similar to wood and PVC. For all the details see the appended paper I.

Thermal properties

The discussion is divided into four steps as defined above.

STEP 1 Starting with the thermal transmittance of window, $U_f - value$, the best performing frame is Reference 1 with the $U_f - value$ of 1.22 W/m^2K. The low value is achieved by low thermal conductivity of wood. The $U_f - value$ of the alternative frames 2a and 2b is a significantly higher compared to alternative 1, due to the large air cavity between window and sash frame, which is connected to the exterior. Unfortunately the cavity is necessary for a smooth window opening. The $U_f - value$ is not sufficient description of window energy performance as it evaluates only one element of window without a connection to the overall performance. With the lower $U_f - value$, the risk of condensation of the frame is higher. The temperature was calculate at the critical places and the condensation resistance factor was sufficiently high to prevent condensation for all alternatives.
STEP 2 The overall thermal transmittance of a window, $U_w - value$, was calculated for a window size of 1.23 m $\times$ 1.48 m. The major effect on overall window's $U_w - value$ had a portion of glazed area compare to the frame

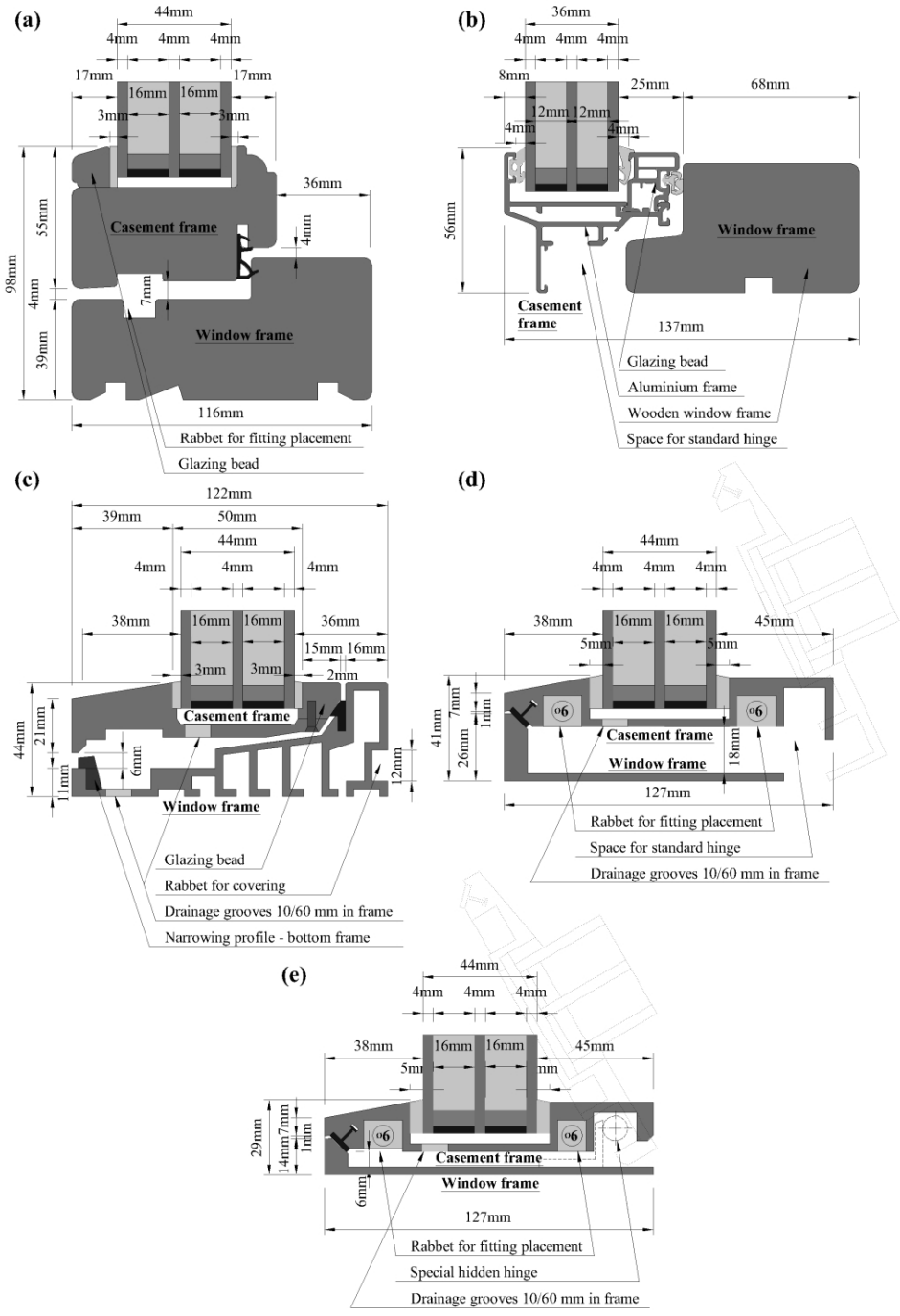

***Figure 3.2**: (a) Reference 1-wooden frame, (b) Reference 2-aluminium frame, (c) Alternative 1, (d) Alternative 2a, (e) Alternative 2b.*

***Table 3.2**: Window and frame properties of the evaluated alternatives.*

Window characteristics	Reference 1	Reference 2	Alternative 1
Width of frame $[mm]$	98	56	44
Linear transmittance-Ψ $[W/mK]$	0.034	0.053	0.032
g-Value glazing/window $[-]$	0.51/0.37	0.51/0.43	0.51/0.45
Light transmittance of glazing/window $[-]$	0.7/0.51	0.7/0.59	0.7/0.61
Frame area of window* [%]	27	16.1	12.7

Window characteristics	Alternative 2a	Alternative 2b
Width of frame $[mm]$	41	29
Linear transmittance-Ψ $[W/mK]$	0.031	0.032
g-Value glazing/window $[-]$	0.51/0.45	0.51/0.47
Light transmittance of glazing/window $[-]$	0.7/0.62	0.7/0.64
Frame area of window* [%]	11.8	8.4

* *The standard window size of 1.23 m × 1.48 m is used.*
NOTE: The values are not identical with table 5 in the appended paper I.

area. The traditional frames cover around 20% to 30% of the window area, while the proposed frames cover around 10%. The detailed numbers about the frame coverage are shown in the table 3.2. The $U_w - value$ for all the windows is between 0.85 W/m^2K and 0.79 W/m^2K, except for Reference 2, which has the $U_w - value$ 1.24 W/m^2K. The decrease of $U_w - value$ of the proposed frames was caused by substituting frame by glazing with a lower $U_g - value$. The additional effect of the larger glazed area is that the solar gains are linearly increased with the size of the transparent area. This is evaluated in next step by the NEG method.

STEP 3 The proposed windows all have positive NEG, which means that they become a net source of heat rather than a net sink of heat. Furthermore, the reference windows have a larger heat loss than solar gains. The larger glazed area created by a reduced frame width consequently increase a visible light transmittance which can improve an indoor daylight conditions. The improved performance is mainly a result of the slimmest frame, alternative 2b, which provides the highest NEG, 19.3 $kWh/(m^2year)$. This is an improvement by 23.2 $kWh/(m^2year)$ compared to Reference 1 and

by 47.9 $kWh/(m^2year)$ compared to Reference 2. Alternatives 1 and 2a provide also a high NEG performance which is 15.7 $kWh/(m^2year)$ and 11.2 $kWh/(m^2year)$ respectively.
STEP 4 The last and the most comprehensive evaluation is the simulation of whole building energy performance in iDbuild and Be06. The two cases are studied in depth. The first case is the total energy consumption of an office building (Case 1). The second case is the total energy consumption of a domestic building (Case 2). The total energy consumption includes heating, cooling, ventilation, hot water and lighting.
Case 1 The aluminium window frame is primarily used in office buildings and is used in the study as the reference frame. The best performing frame is Alternative 1 and 2b which reduced the total energy consumption in the reference building from 34.5 $kWh/(m^2year)$ to 28 $kWh/(m^2year)$. The increase in the overall performance is caused by using the slim frame made from GFRP, which increase the transparent part of window and reduce the total heat loss of the frame. Furthermore, the larger glazing area provides more visible light transmittance and therefore increases the daylight factor (DF) in the middle of the room from 5.4% (Reference 1) to 6.3% (Alternative 2b).
Case 2 The wooden window frame is primarily used in domestic buildings and is used in the study as the reference frame. Again, the frame Alternative 2b rank the best between all the proposed frames. By using this frame the heating energy can be reduced by 3.5 $kWh/(m^2year)$ compare to the wooden frame, Reference 1, and by 9.8 $kWh/(m^2year)$ compare to the aluminium frame, Reference 2. The total energy reduction of Alternative 2b and Alternative 1 is 0.8 $kWh/(m^2year)$ compare to the frame Reference 1.
The conclusion from the thermal and energy investigation of the different window frames is that the frame Alternative 2b has the best performance among the proposed solutions in the respect of the overall energy performance. Additionally, the DF in the office building was increased.

Structural performance

Three separate requirements to evaluate feasibility and the structural performance of the windows were used.

1. A maximum deformation limit in regards to an air tightness of the seal, where a serviceability state wind pressure was used.

2. A maximum deformation limit in regards to a failure of the glass. An ultimate limit state wind load was applied to the windows.

***Table 3.3**: Thermal and energy properties of evaluated frame alternatives.*

	Window characteristics	Reference 1	Reference 2	Alternative 1
1	$U_f - value$ (W/m^2K)	1.22	3.19	1.43
2	$U_w - value$ (W/m^2K)	0.85	1.24	0.79
3	NEG (kWh/m^2)	-3.9	-28.4	15.7
4	Building energy demand/heating			
	Case 1 (kWh/m^2)	29.5/11	34.5/15	28/9
	Case 2 (kWh/m^2)	67.7/61.1	74.9/67.4	66.9/58.1

	Window characteristics	Alternative 2a	Alternative 2b
1	$U_f - value$ (W/m^2K)	2.00	1.9
2	$U_w - value$ (W/m^2K)	0.85	0.8
3	NEG (kWh/m^2)	11.2	19.3
4	Building energy demand/heating		
	Case 1 (kWh/m^2)	29/10	28/9
	Case 2 (kWh/m^2)	67.8/58.9	66.9/57.6

3. A load capacity was used to check that the bending stresses in the frames due to movement did not exceed the strength of the material.

For a given side length it is possible to calculate the largest possible second side length using the above three requirements. Figure 3.3 illustrates an envelope of the results and the lines in the figure limit the boundaries for a maximal window size. As can be seen, the proposed alternatives provide a greater window size, which means that the design and the material properties of GFRP allow bigger windows to be built without risk of a wind failure.

3.1.3 Conclusion

From the results of the study it can be concluded that the best energy performing window was achieved by using a slim frame with low thermal transmittance combined with a large glazed area. This provided a higher solar gains, while the load capacity was maintained, therefore GFRP can be considered as competitor to other window frame materials. Savings of 6.5 $kWh/(m^2year)$ were reached in the office building with this frame, compared to the window with a traditional aluminium frame. Throughout the individual steps of the evaluation it was illustrated that the performance of windows has to be evaluated in the context of several parameters in order to

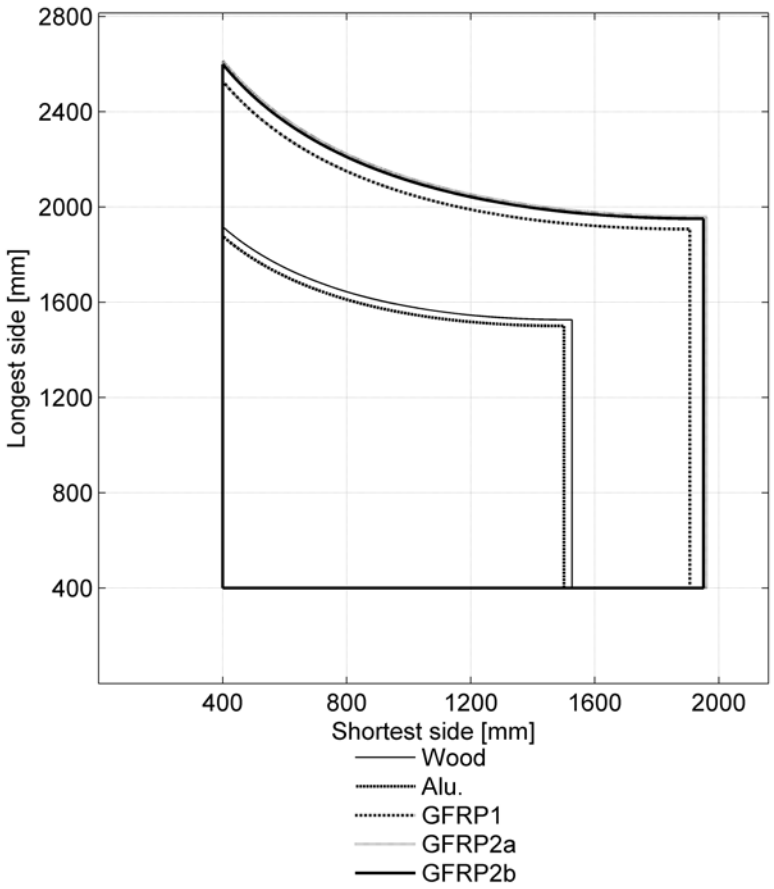

***Figure 3.3**: Envelope of possible window sizes for different frame types.*

get overall performance. The development process was facilitated by using the rational product development method.

3.1.4 Future work

The models with simplified radiation models in the frame cavities were used in this study and it would be useful to further investigate the thermal behavioural of frame cavities by more detailed models, e.g. by Computational Fluid Dynamics (CFD) modelling. Moreover, by enlarging the glazed areas by the slim frames, more solar gains were introduced, which may increase a risk of over heating. Therefore it would be useful to carry out further inves-

tigation, and optimize the window size in order to maximally benefit from higher solar gains.

3.2 Energy performance of a ventilated window

In this chapter the experimental study of a window with integrated ventilation is presented. Firstly, it was necessary to define the heat balance of a ventilated window as an airflow thorough an air cavity change a heat balance compared to the standard principle of $U_w - value$. Secondly, the measurements and results are described in this chapter. Thirdly, the chapter is concluded by the calculations of potential savings, illustrated on a case study which is comparing three different scenarios. The first case is a building before renovation with old windows. Second case is a building after renovation with new standard windows, and the third case is the same as the second but with a ventilated window instead.
The ventilated window would be most often used for renovations, when it is either difficult or expensive to use balanced mechanical ventilation with a heat exchanger. Renovated buildings are more air tight and air infiltration is significantly reduced compared to the situation before the renovation. As fresh air has to be supplied, exhaust ventilation is often used and the ventilated air has to be warmed up to the room temperature, therefore the ventilation heat loss is significant [20, 95, 19].
The results from this investigation have to be generically applicable. The effect of the ventilation itself was separated as well as boundary conditions were kept the same. The experimental work focused on quantifying of the regained heat loss of the window.

3.2.1 Heat balance

To be able to define the impact of a ventilated window on the energy consumption, the transmittance heat losses of the window and ventilation heat loss have to be distinguished. The effect of solar radiation was removed by measuring "dark U-value", which is driven by the temperature difference only and in this case was 20 K [39]. The basis of the theory for calculations and definition of the heat balance is based on the standard ISO 15099 [33] which is integrated within the program WIS [96, 97]. Furthermore, a study by Lau Markussen Raffnsoe was used to defining the heat balance [98].
As mentioned before thermal transmittance of window $U_w - value$ is not applicable for the calculation of heat transmittance of the ventilated window therefore $U_{w,trans}$ is used instead. $U_{w,trans}$ consists the heat loss from the window $U_{w,trans,ext}$ and the heat loss from the ventilation, $U_{w,vent}$. The $U_{w,vent}$ is equal to the energy needed to preheat the supplied air. $U_{w,trans}$ is generally

given in eq. 3.1e, and is defined in a way it can be calculated for window with or without ventilation air flow. The heat balance of the window/room is based on the combination of heat balances between an interior and window, between window and exterior, and for ventilation. The energy flux from the interior to the window $Q_{w,trans}$, energy flux between the exterior and the window $Q_{w,trans,ext}$, and energy carried by ventilated air $Q_{w,vent}$ is defined in eqs. 3.1b - 3.1d. By a combination of those equations, the total energy flux $Q_{w,trans}$ and total heat transmittance of the window can be defined as in eq. 3.1e, where $Q_{w,trans}$ is based on the energy fluxes, the area of the sample, and the environmental temperature difference. This concept is applicable for both windows, with or without ventilation.

$$Q_{w,trans} = Q_{w,trans,ext} + Q_{w,vent} \tag{3.1a}$$
$$Q_{w,trans} = (h_{ci} + h_{ri}) \times A_w \times (T_{ni} - T_{si}) \tag{3.1b}$$
$$Q_{w,trans,ext} = (h_{ce} + h_{re}) \times A_w \times (T_{se} - T_{ne}) \tag{3.1c}$$
$$Q_{w,vent} = \rho \times c_p \times \varphi \times (T_{gap,out} - T_{gap,in}) \tag{3.1d}$$
$$U_{w,trans} = \frac{Q_{w,trans,ext} + Q_{w,vent}}{A_w} \times (T_{ni} - T_{ne}) \tag{3.1e}$$

where, h is either convective *(c)* or radiative *(r)* heat transfer for outdoor *(e)* or indoor *(i)* surface. T_{ni} and T_{ne} is the temperature of interior and exterior environmental and T_{si} and T_{se} is the temperature of interior and exterior surface. $T_{gap,in}$ is the temperature of the air entering the glazing cavity and the temperature of preheated air, at the exhaust is $T_{gap.out}$.

3.2.2 Measurements

The aim of the measurements is to determine the heat recovery efficiency of the ventilated window under various airflows. The temperatures on the glazing surfaces and in the ventilated cavity were monitored, while the cold chamber in GHB had steady temperature of 0°C and the warm chamber was between 19°C and 19.5°C. It is illustrated in figure 3.4 that the temperatures decreased with the increase of the airflow. The increase was mainly caused by raising the surface heat transfer coefficient. The translation of the air speed to the airflow volume is; 1.3 l/s to 0.015 m/s and 8 l/s to 0.091 m/s. The mean air temperature in the ventilated cavity decreased steeper than the surface temperatures of the glazing. This is caused by increase of the ventilated air volume in the cavity and the surface heat flux through the glazing could not increase the air temperature equally. Thus, the mean air

temperature was approximating the mean temperature of the cavity surface closer to the exterior. By increasing the temperature difference over the glazing as shown in 3.4, it was validated that the airflow rate affects the increase of the heat flux through the glazing.
By monitoring the input of the electrical heater in the measuring box the heat flux through the sample was obtained. The total heat flux was between 35.8 W and 77.8 W which corresponds with the window without airflow and the window with airflow of 8 l/s respectively.

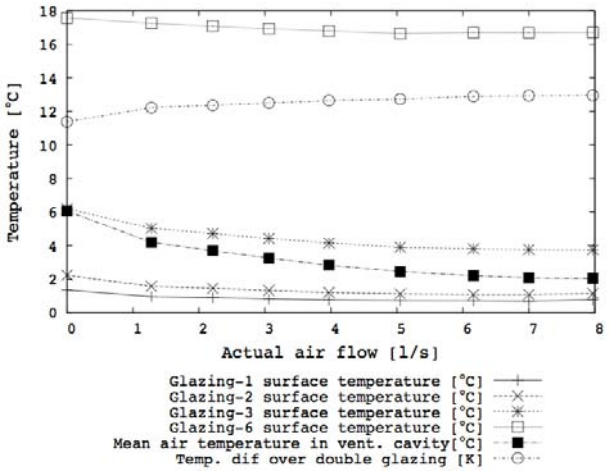

Figure 3.4*: Surface temperatures of glass on position 1, 2, 3 and 6 and air temperature in the ventilated cavity between the glass panes.*

3.2.3 Results and discussion

Heat recovery

By ventilated air some of the heat loss is regained and recovered. The heat exchange happens through the glazing's surfaces as well as within the ventilated valves in the frames. The temperatures in the inlet and outlet valve were monitored and the temperatures are shown in figure 3.5. The ventilated air was preheated in the inlet valve approximately by 3°C under the airflow of 1.3 *l/s* and by 1°C with air flow of 8 *l/s*. The air at the outlet raised by 8°C for the airflow of 1.3 l/s and 3.3°C for the airflow of 8 *l/s*. The temperature of preheated air in the outlet was used to define regained energy from the heat loss. Figure 3.6 shows that the regained heat energy varied between 12.9 W (7 W/m^2) and 34.2 W (18.2 W/m^2) for the airflow between 1.3 *l/s* and 8 *l/s* respectively.
The temperature difference in the frames increased which consequently caused

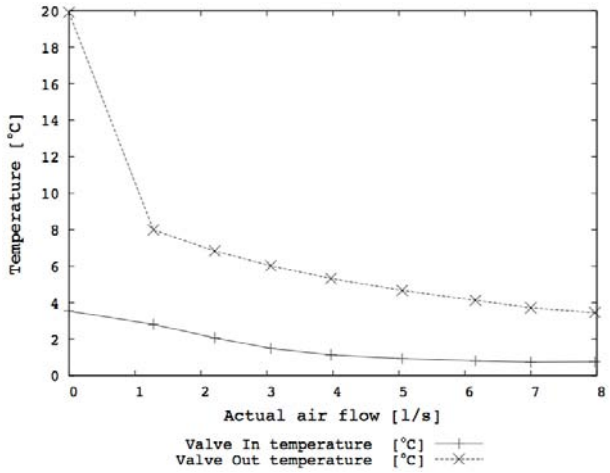

***Figure 3.5**: Air temperatures in the inlet and outlet valves.*

higher surface heat exchange coefficient. However, the thermal transmittance of the frames also increased to 1.8 W/m^2K for bottom frame, 2.3 W/m^2K top frame and 1.7 W/m^2K for side frames. The higher airflow increased the heat loss of the frames, which was partly regained but also transmitted to the exterior. Figure 3.7 shows a combination of the regained energy and the window's extra heat loss. The preheated energy by the ventilated air was calculated from eq. 3.1d and depend on the outlet temperature. The extra heat loss of the window was calculated as the difference between the heat loss of window without and with ventilation. This combination of heat losses shows that the energy recovery efficiency of the ventilated window lost its effect at the airflow around 6 *l/s*, see figure 3.7. This relationship shows that it is not valuable to increase an airflow rate because it increases the extra heat loss through the window which cannot be regained. This indicates that the lower airflow rates are more efficient for a heat recovery.

Case study

The case study and its evaluation was based on the heating up the required amount of ventilated air to the room temperature of 20°C, from the outdoor temperature of 0°C. The air preheating within the ventilated window was compared to a standard window combined with an exhaust ventilation. Different airflows through the window were defined by the number of used windows, each of standardized size of 1.48 m × 1.23 m. This means that the scenario with one window represented the airflow of 8 *l/s* , with two windows 4 *l/s* and with three windows 2.5 *l/s*. The rest of parameters were kept the same in order to investigate the preheating effect only.

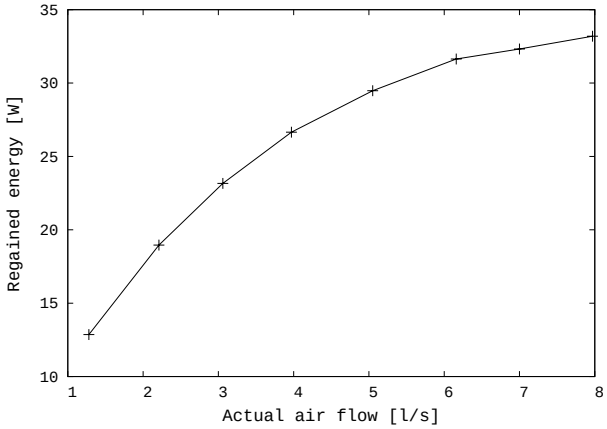

***Figure 3.6**: Amount of recovered heat by ventilated window.*

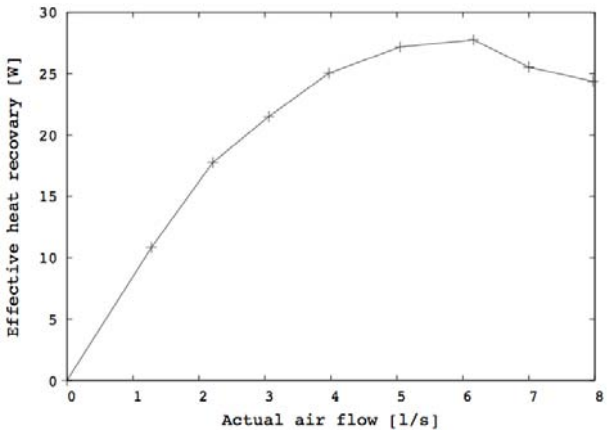

***Figure 3.7**: Effective heat recovery of the window.*

In total nine cases were calculated, based on three airflows and three scenarios which are:

1 The first scenario depicted the energy for heating a room in the building before the renovation.

2 The second scenario evaluated the room after renovation with standard new windows installed.

3 The third scenario is the same as the second scenario but with the ventilated windows installed.

The performance of windows is evaluated by $U_{w,trans}$. By comparing the heat loss by ventilation to the total energy heat loss it was found that after the building renovation the ventilation heat loss is around 1/2 of the total heat loss, compared to 1/4 before. Particularly the change was from 26.6% to 50.2%, from 24.8% to 47.6% and from 23.3% to 45.3% for the room with one, two and three windows installed. This illustrates how the ventilation heat loss becomes more significant part of the total energy demand of the heating after the building renovation.
When the ventilated air is preheated in the ventilated window, the air entering a room changed the temperature from 20 K to 16.5 K, 14.7 K and 13.5 K for scenario with one, two and three windows. This reduced the total energy demand of the room by 8.8%, 10.9% and 9.8% for the scenarios with one, two and three windows. The calculated energy savings were determined by using a ventilated air exchange of 0.5 h^{-1}. It was assumed that an air infiltration in the dwelling building was 0.5 h^{-1} before renovation and 0.07 h^{-1} after renovation when the building was air tightened and windows replaced. The savings just for the ventilation are 17.5%, 26.5% and 32.5% for the scenarios with one, two and three windows. From the total energy decrease it was found that the higher benefits occur in the scenario with two windows installed, which indicated that the optimization of the wall-window ratio was necessary as well as the heat recovery of the window decreased with higher airflows. Furthermore, lower airflow rates are preferable, because in most of cases several windows could be used for space ventilation as well as a higher airflow velocity from the window outlet could be uncomfortable and cause draught. The detailed results are presented in table 3.4, including the potential heating energy saving by each scenario.

3.2.4 Conclusion

By the experiment it was revealed that the ventilated air can be partly preheated in the ventilated window by recovering some of the heat loss of the

***Table 3.4**: Heat energy savings comparison for room with and without the ventilated window.*

Scenario 1	Before renovation		
	1 win	2 win	3 win
Heat loss by ventilation [W]	201.7	201.7	201.7
Heat loss by infiltration [W]	201.7	201.7	201.7
Heat loss by external wall [W]	263.6	227.2	190.8
Heat loss by window [W]	91.0	182.0	273.1
Total heat loss [W]	757.9	812.6	867.2
Ventilation vs. total [%]	26.6	24.8	23.3
Energy decrease by VW [%]	-	-	-
Scenario 2	After renovation		
	1 win	2 win	3 win
Heat loss by ventilation [W]	201.7	201.7	201.7
Heat loss by infiltration [W]	28.2	28.2	28.2
Heat loss by external wall [W]	131.8	113.6	95.4
Heat loss by window [W]	40.0	80.1	120.1
Total heat loss [W]	401.7	423.6	445.4
Ventilation vs. total [%]	50.2	47.6	45.3
Energy decrease by VW [%]	-	-	-
Scenario 3	After renovation + ventilated window		
	1 win	2 win	3 win
Heat loss by ventilation [W]	166.4	148.2	136.1
Heat loss by infiltration [W]	28.2	28.2	28.2
Heat loss by external wall [W]	131.8	113.6	95.4
Heat loss by window [W]	40.0	87.4	142.0
Total heat loss [W]	366.5	377.4	401.7
Ventilation vs. total [%]	45.4	39.3	33.9
Energy decrease by VW [%]	8.8	10.9	9.8

window. The heat exchange takes place in a glazing and in ventilated valves in the frame.s However, the heat exchange in the frames also introduced a higher heat loss through the frame and consequently caused an increase of the total thermal transmittance of the window. The heat recovery efficiency is strongly dependent on the airflow volume. The efficiency decrease with higher airflows, therefore the ventilated windows are more suitable for buildings where a low ventilation rate is required. For the investigated case the savings of the total energy demand were more than 10%. Addition the heat balance for the window-room-ventilation system was defined and can be used for comparison of traditional windows with ventilated windows.

3.2.5 Future work

Windows are always placed on exterior building envelops and exposed to the solar radiation. Therefore further investigation should be aimed to have realistic outdoor conditions, including the solar radiation. The solar energy absorbed in the glazing can be further used for preheating the ventilated air. The large glazing cavity used for the ventilation is optimal for placement of a solar shading, which can also absorb the solar energy and can significantly influence the heat balance of the ventilated window. This behavioural could be highly utilized during the summer when the ventilated air can be vented from outdoors to outdoors and remove extensive solar gains absorbed in the glazing and shading material. More detailed studies on absorbed solar energy and its removing by ventilation in the airflow window should be carried out.

Chapter 4

Utilizing of the optical properties of integrated shading systems

In this chapter, the results from measurements and simulations of two different and unique shading systems are presented and discussed. Firstly, an investigation of integrated micro-structural perforated shading screen (MSPSS) is presented, and the system is compared to three convectional shading systems, appended paper III. Secondly, the performance of a daylight redirecting glass shading system is discussed and presented, appended paper IV. The discussion is primarily focused on optical properties, however, the thermal performance is indivisible from an optical performance and therefore the investigation is connected to the previous chapter 3. The structure of both cases is based on the methodology presented in the chapter 2. It means that several parameters are evaluated and compared to a reference. The parameters are e.g. daylight, glare and visual comfort, lighting energy, energy performance and thermal comfort, etc. The main hypothesises of this chapter are:

1 A micro structural screen layer can be used as a shading system which does not block view to the outside, shade and reduce cooling loads. Furthermore the performance of such a system can be evaluated by simulation tools.

2 It is possible, by a careful design of the daylight redirecting glass shading system, to improve daylight conditions in the back of a room while the visual comfort and visual connection to the outside is maintained.

4.1 Performance modelling of micro-structural perforated shading screen

The system is made of an insulated double glazed unit with a low-e coating on the interior glass pane on the surface in the glazing cavity (glazing surface 3) and with the micro-structural perforated shading screen (MSPSS) on the opposite surface (glazing surface 2). The MSPSS is made from a stainless steel sheet with elliptical holes smaller than 1 mm. The holes are cut in a downward direction (when viewed from the inside) to reduce transmission from outdoor sources above the horizon, which are the sun and sky. An increased transmission for negative altitude compared to the normal incidence, when looking from inside, allows better view to the outside. The view through the MSPSS and the unobstructed view is presented in figure 4.1. The MSPSS combines solar and glare protection and provides direct view out. Some of the features are contradicting as well as the system is angularly dependent and asymmetrical. These are the reasons why this system was selected as the testing example as well as this system is not included in any building performance simulation program.

***Figure 4.1**: View through MSPSS (left), unobstructed view (right)*

To make sure that the simulations are reliable, measurements under outdoor conditions were carried out. The measurement procedure is presented in section 4.1.1. Furthermore, the MSPSS was compared to three other fenestration systems; clear double glazed window without shading, clear double glazed window with horizontal venetian blinds, and clear double glazed window with a semi-transparent roller shade. To have comparable results, all

conditions apart from changing the shading system were kept, e.g. the same glazing, and all the shading systems were placed in a glazing.
The reference case with a clear glazing was studied in order to demonstrate the effect of shading and glazing separately. A commonly used venetian blinds system was used because it has similar features as the MSPSS, e.g. provides shading and permits view out. A roller shade was used as a reference because it blocks solar gains and glare more efficiently than a semi-opened system, however it blocks the view to the outside.

4.1.1 Measurements and simulations

The outdoor measurements were performed during sunny days in June and July. The movable measuring rig is shown in figure 4.2, including the tested sample. The rig allowed to adjust the sample according to the sun position, and thus different incidence angles (IAs) could be measured in a relatively short time. Only IAs up to 60°could be measured as the size of the sample did not allowed to measure higher IAs.

***Figure 4.2**: Movable measurement test rig with sample mounted.*

The illuminance and irradiance sensors were placed behind the sample and on the side of the sample. By dividing these two measurements a relative light transmitted of the sample was calculated. The surroundings of the measurement location were neglected by using relative measurements and therefore

the obstacles did not introduced a large error to the results. By recording the time, sun position, total horizontal hemispherical diffuse illuminance and direct normal illuminance, it was possible to reproduce sky conditions by the simulations.
The program Radiance was used for the transmittance calculations, and daylight and glare analysis for all investigated CFSs. The results from Radiance were further used for calculation of an electrical lighting savings by utilizing of daylight. The BSDF matrices generated by the program genBSDF were combined with thermal transmittance calculations within the program Window6 in order to investigate NEG. The matrices were further used in ESP-r for the calculation of total energy demand of the tested office.

4.1.2 Results and discussion

In this section the results of the simulations of all four tested CFSs are presented and the measurements of the MSPSS are compared to the simulations. The evaluating criteria of the MSPSS were energy use, visual and thermal comfort. They were addressed in a context of a façade orientation, building location, time of a day and year, shading strategy, and human factors (view, comfort and temperature). As the performance of a shading system is dependent on the sky distribution, the annual performance evaluation was carried out. This required using bi-directional information of the light transmittance (T_{vis}) and the solar transmittance (T_{sol}) of the CFSs.

Validation of simulations

The comparison of the Radiance simulations and measurements is shown in figure 4.3. The comparisons of T_{vis} and T_{sol} correlated, which indicated that simulations can be used for the evaluation and that the results are reliable. The curves variation is between 0% to 4%, except the visible transmittance at the IA of 60°where the relative error is 18%. However the error is relative and is small when the absolute values are taken into account. Also, the position during the measurements could be slightly off as the position was in its maximum. The validation of the simulations of BSDF of CFS is important as it is a complex description as well as it is a relatively new approach. The measurements were not done in all the directional, however it was sufficient to vary IA in one direction.

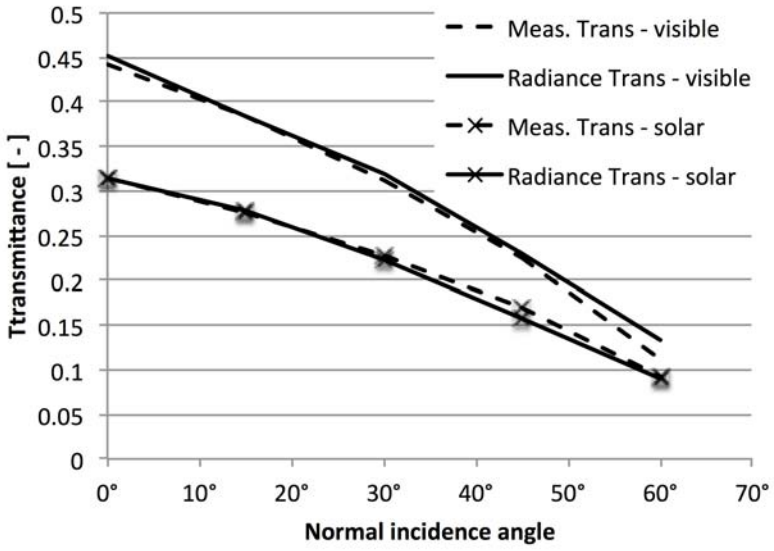

***Figure 4.3**: Validation of the Radiance simulation by measurements - comparison of the results.*

Bi-directional transmittance

The visualization of the visible transmittance, T_{vis}, for all the tested CFSs, is shown in figure 4.4. The graphs are independent on a location and orientation and consequently it is applicable for any situation. For that reason, the annual sun path for Copenhagen is added to the graphs. This adds a level of understanding of a location for a south oriented façade. By the combination of information about a bi-directional transmittance and location it is possible to see as the performance of angularly dependent CFS change during a year. For instance, during the winter when the sun altitude is low, more solar gains could be obtained as the transmittance is higher, while more effective solar shading is provided in the summer. The maximum transmittance of the MSPSS and venetian blinds was between 0.5 and 0.6, while for clear glazing it was up to 0.8. The glazing with the roller shade had high shading coefficient and the transmittance was as low as 0.2.

Daylight performance

The transparency of a fenestration influences a WPI and savings of an electrical lighting energy by daylight. The roller shade limits daylight penetration and thus significantly reduces the light energy savings. Incidence angle de-

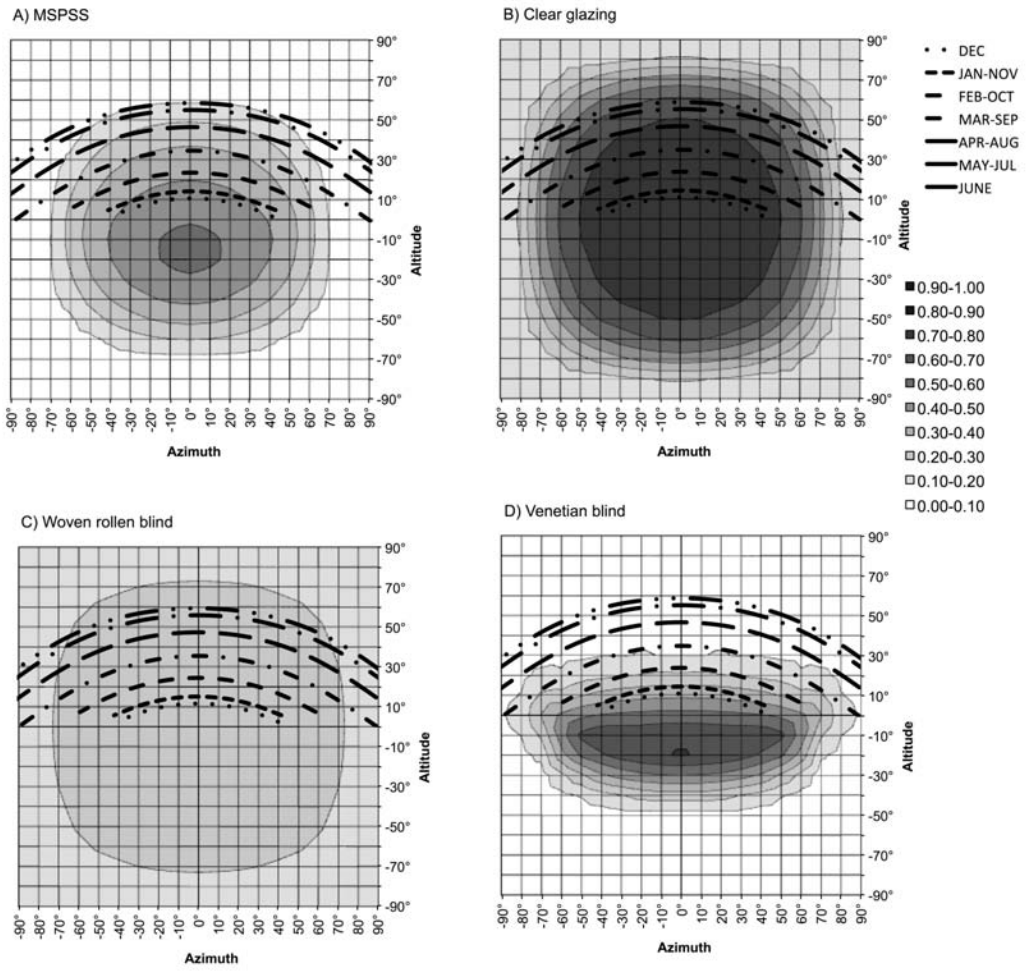

***Figure 4.4**: Visible transmittance of CFSs with solar path of Copenhagen.*

pendent shading systems, e.g. the MSPSS and venetian blind, have higher transmittance at the negative altitude than the normal incidence. This means that the systems block light radiation from the sky and increase the view to outside, as designed. The highest transmittance is around -15°of altitude, looking from inside.

The daylight autonomy (DA) was used for the evaluation of daylight in the single office space. Figure 4.5 shows DA for all four CFSs and indicates the percentage of a time during which a certain level of illuminance is reached. For example, the CFS with MSPSS had 80% of working hours exposed to at least 216 lux in the distance of 0.5 m from the façade. The solutions with a shading performed similarly with a slightly better performance with the MSPSS. In spite of the high WPI in the front of the room with clear glazing,

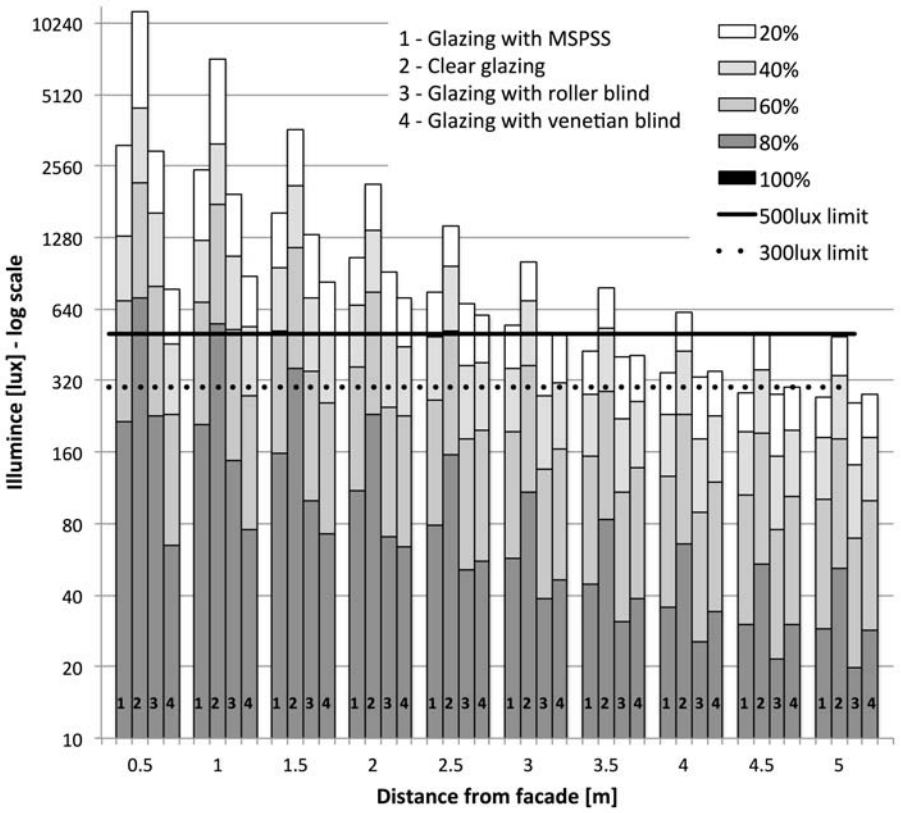

***Figure 4.5**: Daylight authonomy*

the high illuminance can not be utilazed. Additionally the high illuminance can cause a discountable glare and overheating as it reached 10 klux. Therefore other CFSs provide equivalent or better performance. In the back of the room the minimal WPI is not achieved with any solution.

Energy performance

As expected the solar transmittance follows the same pattern as the visible transmittance. The standard calculation of NEG is corrected in regards of the angular dependency, however it is simplified. Figure 4.6 illustrates the effect of IA on the NEG. The figure shows NEG separated for different orientations of each façade as well as the total NEG. As the NEG is primary oriented on the solar gains and does not value the shading efficiency, therefore the MSPSS performed the worst in regards of NEG. However, the shading should be used mainly for a south facing façade and potentially for a

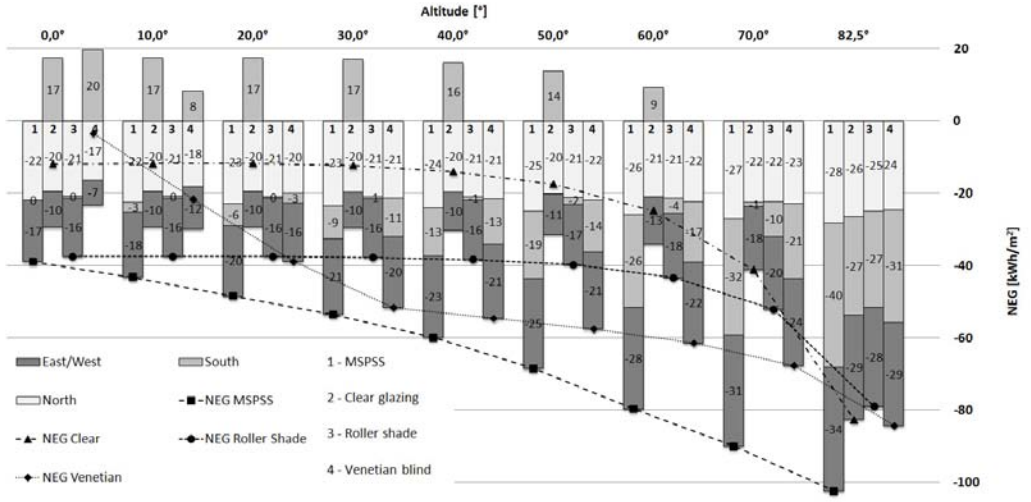

***Figure 4.6**: NEG for four different CFSs, split for different orientation and dependent on IA.*

east/west façade in order to reduce a risk of overheating during the summer. Therefore MSPSS perform well in regards of solar shading. The angularly dependent systems shade mainly under a high altitude, while the roller shade and clear glazing have relatively constant NEG.
The NEG method does not include cooling loads and thus more comprehensive analysis is required. The program ESP-r can handle BSDF matrix for any CFS. Table 4.1 contains the results for heating and cooling loads calculated in ESP-r. The calculations were done for three different locations with different geographical latitude as each location has different solar radiation. All the shading solutions (roller shade, MSPSS, venetian blinds) provided similar shading protection and reduced cooling loads by 20-30% compared to the window without the shading (clear glazing). However, the roller shade reduces a visibility and therefore an usage is limited as a view to outside is preferable by many users.

Glare analysis

The view connection with the outside and to the bright sky and the direct sunlight can cause discomfort glare. Glare protection is desired in addition to shading of solar radiation by Complex Fenestration System (CFS). The DGPs index was investigated in a single cell office with 3 different view positions, see figure 4.7. Different views are necessary for the analysis as glare is dependent on the light intensity and view direction. The annual glare assessment by the DGP index for every hour and for four different CFSs

***Table 4.1**: Energy loads for heating and cooling for all CFSs and investigated locations.*

Location	Energy performance ($kWh/m^2/year$)							
	MSPSS		Clear		Roller shade		Venetian blind	
	HL	CL	HL	CL	HL	CL	HL	CL
Copenhagen	8.5	22.5	6.6	30.4	9.0	22.8	9.3	20.3
Prague	12.3	24.4	10.5	30.4	12.7	24.3	13.2	23.2
Rome	0.0	63.5	0.0	78.1	0.0	63.9	0.1	59.4

Note: HL-heating loads; CL-cooling loads.

is shown in carpet plots in figure 4.8. The sky distribution was generated based on the weather data file for Copenhagen and thus the sky changed every hour. Each view in figure 4.7 had different conditions, which are as following.

- **View 1** was parallel along the window pointing to east and thus the higher DGP values occurred before noon.
- **View 2** faced to south-east and the higher DGP values were during afternoon.
- **View 3** was oriented toward to the window, south, and the higher DGP index was at noon.

The clear glazing does not provide any glare protection, because the direct sunlight is not blocked, and therefore the risk of discomfort glare is highest. The glare is present all year round for the clear glazing, which is not common for the shading systems which block some glare in different periods of the year. The roller shade blocks the view completely and blocks all glare for view 1 and view 3. However with the view 2 a glare occurred because the view position was close and oriented to the window as well as the roller shade was partly transparent. View 2 experienced most glare for all CFSs in general. By comparing the venetian blinds with MSPSS, the venetian blinds performed slightly better as the transmittance under higher IA is lower which is also possible to see from figure 4.4. From the investigation it is possible to see that for a visual comfort evaluation it is necessary to block direct sunlight, and that even with the completely closed roller shade visual discomfort and glare can occur.
The BSDF matrices provided useful information for all analyses compared to using only the normal-incidence values which would be otherwise similar for all the investigated CFSs.

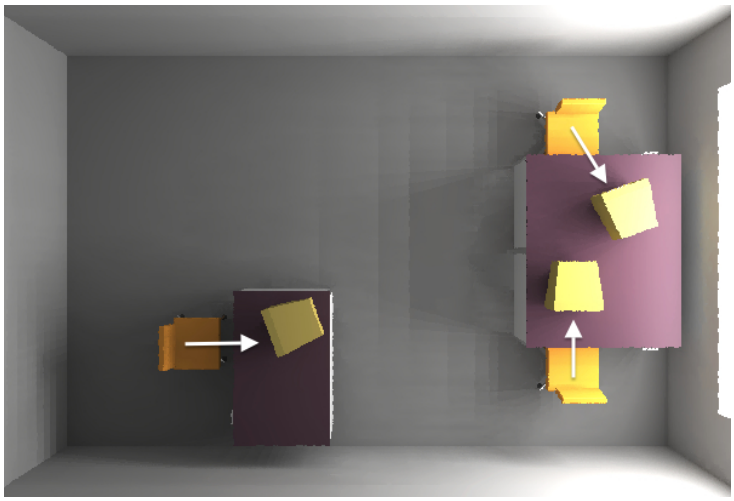

***Figure 4.7**: The plane view of the office with view directions.*

Lighting energy savings

As mentioned in the introduction, the utilization of daylight can provide large savings by reducing an artificial lighting energy. This investigation primary evaluates shading properties. However disproportional shading of visible light is unwanted. The on/off and bi-level lighting control strategy was used and was further described on page 20. The front lighting zone, closest to the façade, has the highest WPI and provides more savings compared to the back zone. In zone 1, closest to the façade the savings were up to 80% compared to the situation with light on all the time. In zone 1, it did not matter if the control was on/off or bi-level as the WPI was higher than the threshold most of the time. This is in a contrast to the back of the room where a significant part of the savings was achieved by using the bi-level control. In general, illuminance levels were lower in the back of the room. There is a minimal difference between shading solutions in the front zone, and most of the savings would be reached with clear glazing in the back zone. The clear glazing provided savings up to 55% while the other CFSs reached around 30% of savings with bi-level control. However, the savings by clear glazing are not significantly higher. It is also worthy to mention that most of the savings are during the winter, which is desired as there is a lack of daylight during this period of the year. More detailed information are presented in the appended paper III.

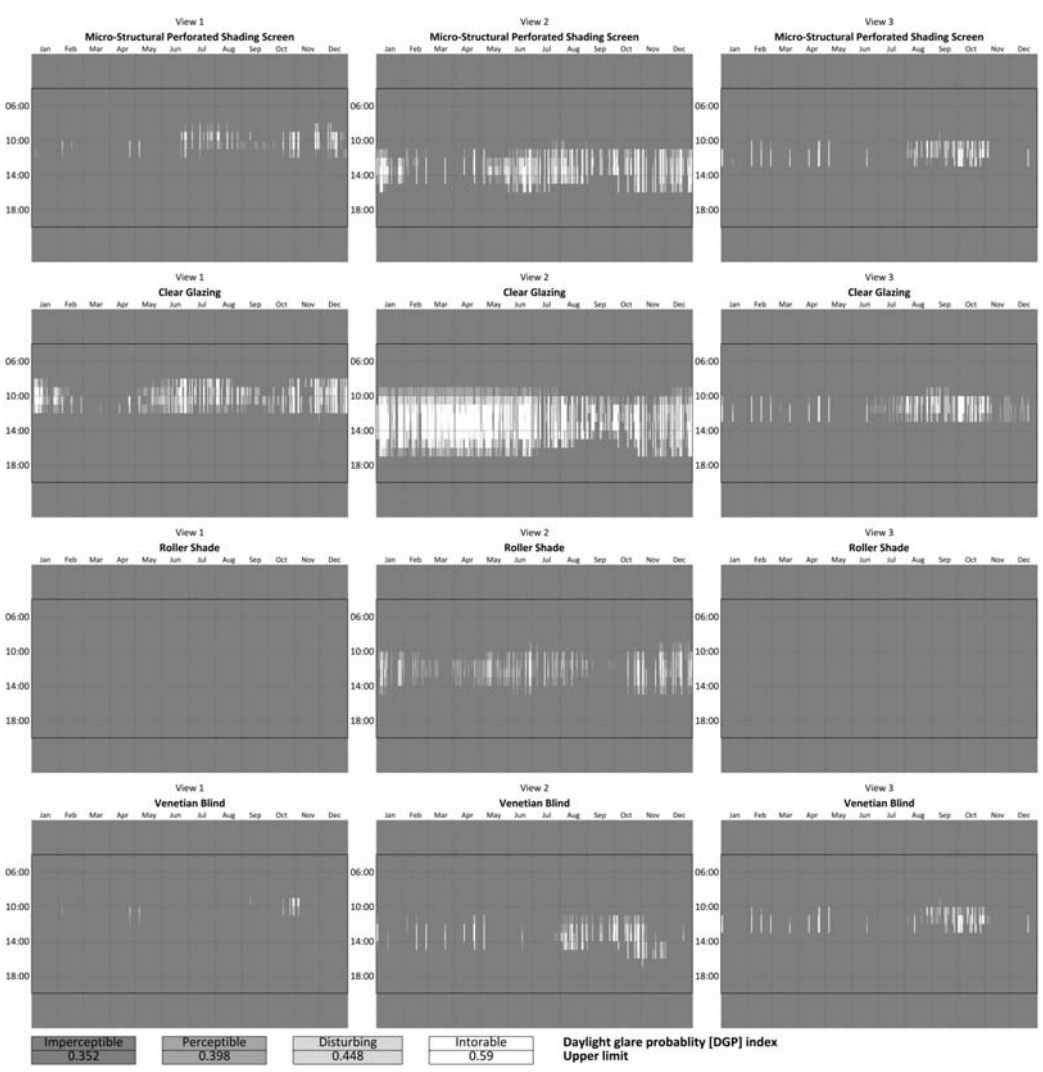

***Figure 4.8**: Annual plots of the DGP for three views and all CFS in the location of Copenhagen.*

4.1.3 Conclusion

The comparison of several interrelated parameters for four Complex Fenestration System (CFS) was carried out. The main focus was put on the evaluation an integrated micro-structural perforated shading screen (MSPSS). It was found that the angular dependent shading systems can be beneficial all year round. They provided daylight and solar gains while decreasing the risk of overheating during the summer when the sun's altitude is high. The visual comfort was evaluated by the Daylight Glare Probability (DGP) index, and it was demonstrated that the visual comfort depends on the blocking direct light as well as optimal positioning of the view direction.

4.1.4 Future work

The performance of angularly dependent CFSs is dependent on an incidence angle which is related to the time of a year and location. The performance of such a systems could be investigated for different locations and then the geometry could be optimized for a specific location.

4.2 Demonstration of redirecting glass shading system

The shading and daylight redirecting system is an exterior shading system made from highly reflective solar control glass. The experimental study was based on simulations and measurements which were carried out at the demonstration building. The investigated space was a deep open-office which lack natural light in the back of the room. The layout of the building, highlighted test and reference area, lighting control zones, building orientation, and position and direction of views for glare analysis are shown in figure 4.9. The evaluation of this shading system is based on several parameters as the system is multi-functional. The main functions are:

- Daylight transmittance and redirection, and daylight utilization.
- Sufficient solar energy transmittance during cold months.
- Preventing indoor space from overheating during warmer months by shading excessive solar radiation.
- The view to the outside should be unobstructed and maintained.

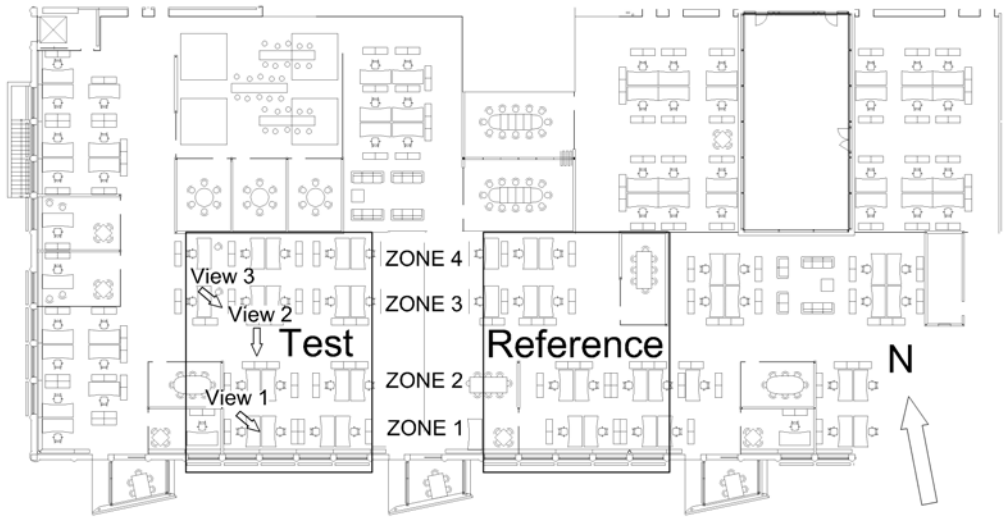

***Figure 4.9**: The layout of the building with open-space office and marked view directions and lighting zones position.*

The centre feature of this system is to increase the daylight illuminance in the indoor space and to reduce lighting energy by increased daylight utilization. Daylight utilization further depend on a daylight-linked lighting control strategy. The quality of a daylight lit space depends on several factors, e.g. luminance distribution and direction, as well as glare [65]. This CFS is based on the daylight redirection, therefore glare analysis and visual comfort is critical. Additionally, the thermal performance was analysed as the system can increase solar energy gains of the envelope.

4.2.1 Shading systems and shading strategy

This CFS is designed to increase the WPI in the back of the room, by redirecting daylight to the ceiling by the reflective surfaces. The design is based on previous studies by Laustsen and Iversen [99, 100]. By a high visible transparency and view through the glass, the system allows view to the outside. The shading effect is achieved by the highly reflective solar control glass which reflects the unwanted solar radiation back to the exterior when the system is in the shading mode.
The rotation of four upper redirecting lamellas is towards the façade (counterclockwise) when the shading is closing. This is different to the reference (original) shading system. The lower four lamellas are independently moved and can stay in the closed or opened position. The operation scheme for the system are shown in figure 4.10. The control strategy has two determiners. Firstly to redirect daylight during overcast or intermediate sky (redirecting position), and secondly to shade during sunny days (closed position). The best performing redirecting position is 30°rotated toward the façade and it was designed in order to avoid the reflections to the occupants' faces, see figure 4.10. 30°was based on the profile angle of the sun for the location of the building, and therefore the shading system can stay in this position all year round, except May and June when the position is 25°. The system has three possible positions:

- Redirecting position - 30°(25°), only for tested system and for four upper lamellas.
- Opened position - 0°, tested and reference system.
- Closed position - 90°, tested and reference system.

4.2.2 Results and discussion

All the shading system features are reflected in the analyses, which evaluate the multi functionality of the system from different perspectives as suggested

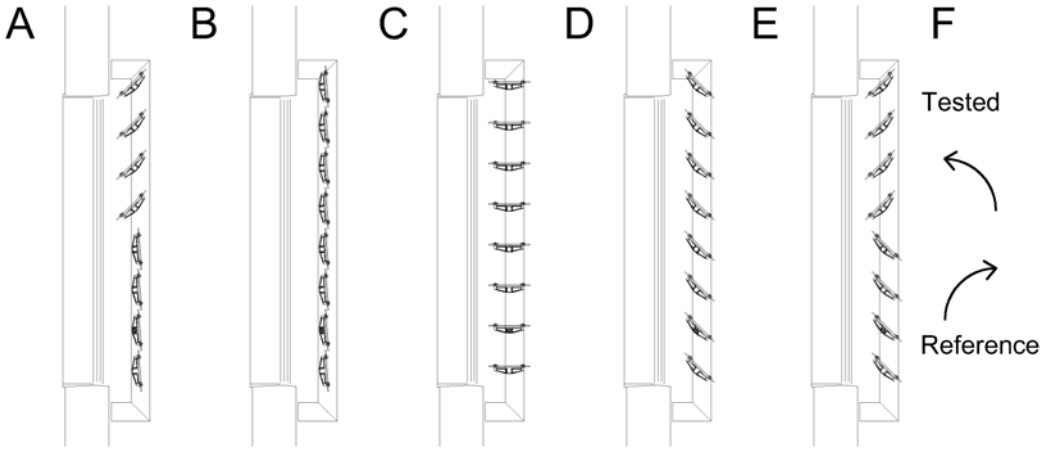

***Figure 4.10**: Illustration of the positions and rotations of the shading system.*
A) Tested system in redirecting position with closed lower 4 lamellas.
B) Whole shading system in the closed position.
C) Whole shading system in the opened position.
D) Reference shading system in the rotation of 45°.
E) Tested shading system in redirecting position with lower for lamellas in the rotation of 45°.
F) Rotation direction of tested and reference system from the opened position to the closed position.

in the paragraph 2.1. Again, the simulations are initially validated by measurements as the system is not included in any standard building performance simulation tool. The analyses consist of day(light) analysis, evaluation of glare and energy performance analysis.

Validation of simulations

The simulations were firstly validated against the measurements made at the demonstration building. The measurement and simulation sensors had free view to the window. The compared sensors for the illuminance were placed in the distance of 3.6 m from the window, which is approximately in the distance where the daylight conditions could be improved. The comparison is shown in figure 4.11. There is several discrepancies between measured and simulated results. The furniture in the open-space office was movable and could be misplaced during the measurements, as well as there was no control of the interior manual shading devices. These errors were kept in mind in order to

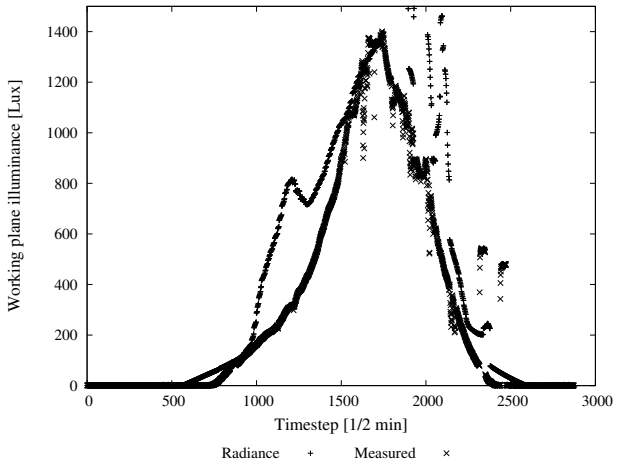

***Figure 4.11**: Validation of the Radiance model by measurements.*

minimize the error. Additionally, by using of a day without occupancy it was ensured that an artificial light was switched off. The curves in figure 4.11 are partially correlating. During the time period between 16:30 and 21:00 (time step 2000 and 2500) it was common for both curves that the data are scattered, which was probably caused by a reflection from surrounding surfaces. The peak in the morning in the simulations is not common with the measured data and this was probably caused by the unknown position of the internal shading or by blocking of the direct sunlight coming from a side of the sensor.

Daylight performance

The main feature, redirecting daylight to the ceiling and then further into the room is demonstrated in figure 4.12. From the figure it is possible to see that the illuminance on the ceiling, 3.4 m from the façade increased approximately by 500 lux, which increases utilization of daylight further in the room. As the increase of the illuminance was proved, the next step in the evaluation was to assess the daylighting conditions. The annual WPI was investigated by the Radiance calculations and three-phase method (TPM). The annual daylight autonomy (DA) was evaluated. Figure 4.13 shows DA for the new redirecting system with dynamic control. The original system is presented in figure 4.14. The illumiance of 500 lux in at least 50% of the time, moved from the distance of 3.2 m to 4.5 m into the room. The improvement of the daylight conditions is visible all over the depth of the investigated space. Furthermore, the room depth with at least 300 lux in 20% of the time was moved from 7.8 m to 10.2 m from the façade and covers most of the working

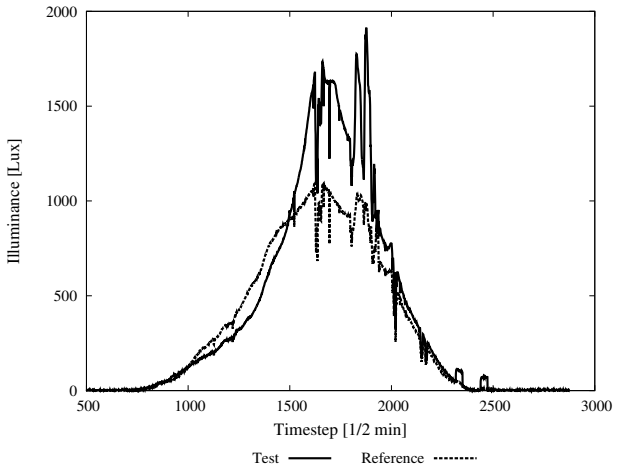

***Figure 4.12**: Comparison of measured illuminance under ceiling for test and reference area.*

area in the office. Thereby it can be stated that the tested system has higher illuminance more often and covers a larger area. Next used annual daylight

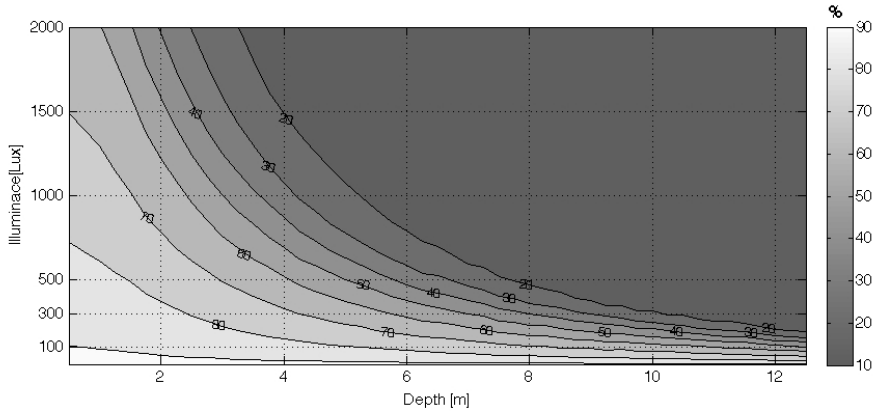

***Figure 4.13**: Daylight autonomy of the tested shading system with dynamically controlled position.*

evaluation matrix was useful daylight illuminance (UDI) which indicates useful range for the illuminance and justifies whether the illuminance is too high or too low. Once more the investigation is throughout the space and the results were split according to the different rotation positions of the system. The UDI value increased especially in the back of the room where the tested system provided 20% more UDI above 100 lux. All over the room UDI was improved. Near to the façade, approximately 1 m from the façade, the upper limit of UDI was exceeded more frequently. However, working places

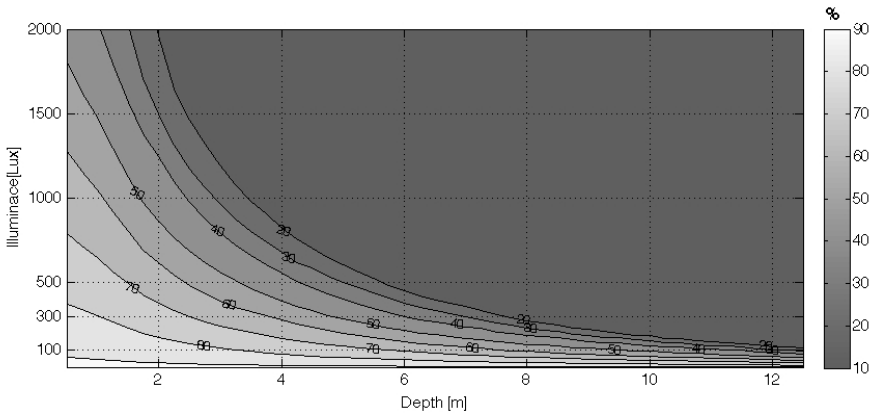

***Figure 4.14**: Daylight autonomy of the reference shading system in the closed position.*

are mostly out of this zone, and therefore it would not cause many visual discomfort problems.

Energy performance

Generated BSDF matrices in Window 6 including visible and solar transmittance information were used to calculate the systems' thermal transmittance. It was found that $U_w - value$ of both systems in all positions were around 0.9 W/m^2K, and thus there is no difference in the thermal insulation. The system in the redirecting position provides 17% more visible transmittance compared to 11% increase of the solar energy transmittance. This means that the daylight utilization can be higher while the solar gains do not increase proportionally.

Glare analysis

The main feature of the system is to redirect daylight to the ceiling which may have a side effect of increasing discomfort glare. This was limited by an optimized position of the system, however, in a situation of changing sky conditions (intermediate sky) or low altitude of the sun, some glare can occur. The glare was simulated with the dynamically positioning system, reacting on the outdoor horizontal illuminance on the roof. The system was automatically closed when the threshold of 25 klux was exceeded. As expected, the tested system had approximately in 5% higher values of the DGP. The increase mainly happened in the position closer to the façade. However, only in 1% of the cases the change was noticeable, and glare become discomfortable. This indicates that the system did not increase glare significantly by

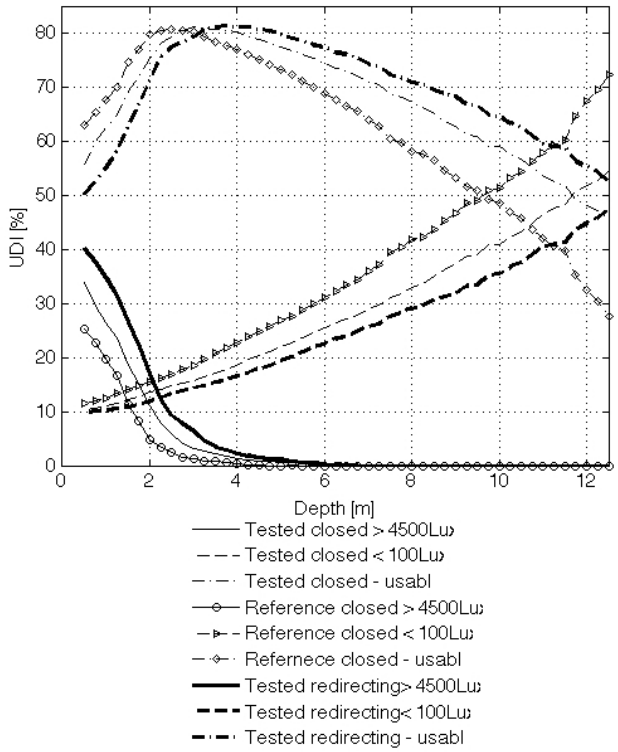

Figure 4.15*: Annual useful daylight illuminance matrix for different scenarios.*

redirecting daylight to the ceiling. The carpet plots with the DGP index are shown in figure 4.16.

Lighting energy savings

The last parameter evaluated in this study was electrical lighting energy savings by maximizing daylight. On/off, bi-level switch and continuous dimming control strategy for lighting was used. The new systems provided in all the cases higher WPI by daylight. For different light controlling systems the difference in lighting zone 1, the closest to the windows, was between 9-15%. The difference between the savings by different control strategies increased towards back of the room, and the savings with dimming systems were up to 23% compare to the situation when the light would be on all the time. For more details on the lighting energy savings, see appended paper IV.

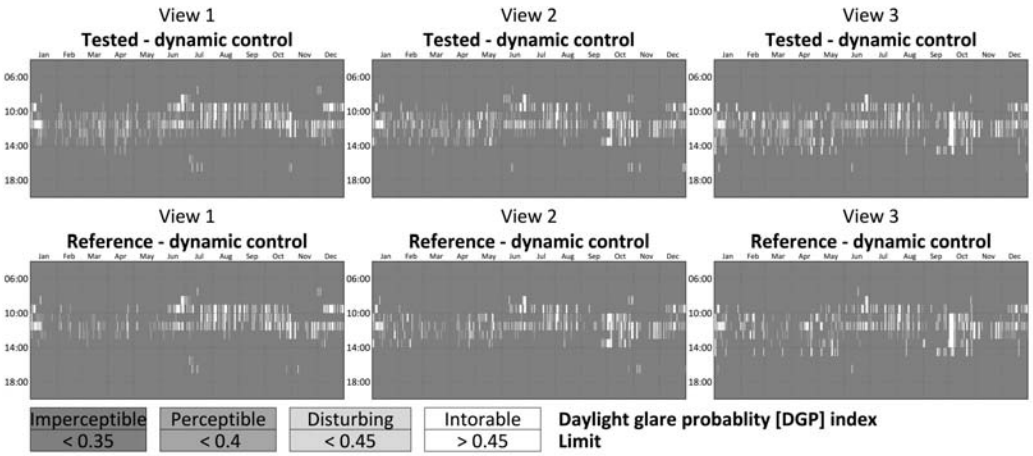

***Figure 4.16**: Annual DGP plots of glare index for tested and reference shading system under dynamically control.*

4.2.3 Conclusion

From this study it can be concluded that daylight improvement in the indoor space was achieved with the daylight redirecting lamellas shading system compared to the system made of a fritted glass. The glare analysis indicated that the redirecting system would not cause an additional glare as the positioning of the lamellas was optimized in order to reflect daylight to the ceiling. The energy for artificial lighting was reduced by utilizing daylight. Depending on the daylight-linked lighting control strategy, the savings were up to 20% compare to the reference system and up to 80% in the lighting zone closest to the windows, when compared to using the artificial light only.

4.2.4 Future work

As simulations and measurements correlated only particularly, the more extensive measurements with monitoring the entire interior and exterior conditions should be carried out. This would help to understand the redistribution of the daylight in the indoor space and would reduce high number of changing variables which are difficult to simulate.
The system directly interact with the indoor working environment by redirecting the daylight, which can influence the visual comfort of occupants, by changing light intensity or contract. Therefore it would be beneficial to carry out a study including an individual observations of occupants.

Chapter 5

Conclusion

In this chapter the main conclusions of the research work are presented. The overall conclusion is supplemented by the four sub-conclusions which conclude each individual investigation.

By experimental and simulation-based investigations it was found that it is possible to evaluate the performance of unique and innovative Complex Fenestration System (CFS). Product development methods can help to optimize the CFS as well as to facilitate the development process by identification of objectives and defining the testing procedures. CFSs combine often several functions and therefore it is important to evaluate all interconnected parameters in order to obtain reliable and overall overview about the performance. By optimal usage of a CFS it is possible to improve visual comfort by utilizing daylight, increasing transparency of windows and controlling glare. By careful design of CFSs, the energy demand of buildings can be reduced. This consist of reducing heat losses by highly insulated fenestration components, by controlling the cooling loads by integrated shading systems, and reduce electricity for lighting by better daylight utilization. Finally, it was demonstrated that it is possible to evaluate unique shading systems, which are not typically included in building performance simulation tools, by comprehensive thermal and optical performance modelling.

5.1 Slim window frame made of glass fibre reinforced polyester

This research was focused on investigating the potentials of using new innovative materials and designs of window frames to lower the energy demand of buildings. Additionally, the use of the product development method to facilitate such a development was tested.
Several designs of the window frame were suggested and the designs were based on the design objectives identified by help of the rational product development method. The rational product development method was further used to structure the testing procedure and evaluation process. The best energy performance was achieved by the slimmest frame which combined low $U_f - value$ of the frame with the largest glazed area. This provided a higher solar gains, while the load capacity was maintained with glass fibre reinforced polyester (GFRP) as the frame material. Savings of 6.5 $kWh/m^2/year$ were reached in the office building with this frame, compare to the window with traditional aluminium frame. Moreover, it can be seen from the investigation, that the frame is also suitable for a renovation as the same window opening size was used and the energy savings were still obtained.
It can be concluded that the GFRP is a suitable material for window frame, can reduce energy demand of buildings and is a serious competitor to other window frame materials. Furthermore, the rational product development method helped to smooth the transition from the problem definition to the solution by a structured process and showed that it is feasible to use such a method to stimulate the innovation in the window industry.

5.2 Energy performance of a ventilated window

The second investigation dealt with the idea of using the window as a heat recovery system. The thermal performance of a ventilated window was compared to the thermal performance of a traditional window combined with an exhaust ventilation. By an experimental testing in a Guarded Hot Box, several airflows through the window were tested, ranging between 1.3 l/s and 8 l/s. The experiment revealed that the ventilated air can be partly preheated and some of the heat loss recovered. The heat exchange takes place in a glazing and in ventilated valves in a frame. However, the heat exchange in the frame also introduced a higher heat loss through the frame and consequently caused an increase of the total window thermal transmittance. The

heat recovery efficiency is strongly dependent on the volume of airflow, and the critical airflow is around 6 l/s, when the efficiency started to decrease. The airflows higher than that further increased the heat transmittance of the window which reduced the heat recovery efficiency of the window. For the investigated case the total energy demand savings were more than 10%.
The efficiency drops with higher airflows, therefore the ventilated windows are more suitable for buildings where a small ventilation rate is required. In addition to the experimental work, the article formed and unified methodology for the assessment of an energy performance of ventilated windows. The heat balance for the window-room-ventilation system was defined and can be used for comparing traditional windows with ventilated windows.

5.3 Modelling of micro structural perforated shading screen

The comparison of four Complex Fenestration System (CFS) was carried out and the performance was evaluated by several interrelated parameters to provide an overall image about the performance. The main focus was put on the evaluation an integrated micro-structural perforated shading screen (MSPSS). This case was also used for validation of the simulations. The results from the measurements and calculations showed good correlation.
It was found that the angular dependent shading systems are beneficial all-year-round in providing daylight, heating load reduction by solar gains while decreasing the risk of overheating during summer when the sun's altitude is high. The visual comfort was evaluated by the Daylight Glare Probability (DGP) index, and it was demonstrated that the visual comfort depends on the blocking direct light as well as optimal positioning of the view direction. Furthermore, by using bi-directional information about the angularly selective CFS it was possible to reveal and accurately depict the shading system. The results were provided in the context of the incidence angle and location. The MSPSS performed well compared to the rest of the tested fenestration systems, mainly by its angular shading properties, and unobstructed view to the outside.

5.4 Redirecting daylight glass shading system

In this research study the multifunctional dynamic integrated shading and light redirecting system was investigated. The performance evaluation methodology is linked to the previous investigation as both evaluated shading system

and visual comfort. The simulation results were compared with the measurements and the results correlated with some discrepancies. Daylight improvement was achieved with the redirecting lamellas shading system compared to the original system. The glare analysis indicated that the tested redirecting system would not cause an additional glare.
It can be concluded that the visual comfort was maintained and the daylight conditions in the office were improved. By introducing higher penetration of daylight into the back of the office, the artificial lighting electricity use was decreased. Depending on the daylight-linked lighting control strategy, the savings were up to 20% compare to the reference system and up to 80% in the lighting zone closest to the windows, when compared to using the artificial light only. The thermal insulation of the façade was same for all tested systems. The solar energy transmittance increased; however, the increase is small and thus it is not expected to increase significantly the cooling demand.

Bibliography

[1] BR10. Danish Building Regulations, 2010.

[2] Directive. 2010/31/EU of the european parliament and of the council. Technical report, 2010.

[3] IEA. Energy Performance Certification of Buildings. Technical report, 2010.

[4] IEA. Energy technology perspectives. Technical Report 1, 2010.

[5] IEA. 25 Energy Efficiency Policy. Technical report, 2011.

[6] Pyonchan Ihm, Abderrezek Nemri, and Moncef Krarti. Estimation of lighting energy savings from daylighting. *Building and Environment*, 44(3):509–514, March 2009.

[7] Carlos Ernesto Ochoa and Isaac Guedi Capeluto. Advice tool for early design stages of intelligent facades based on energy and visual comfort approach. *Energy and Buildings*, 41(5):480–488, May 2009.

[8] Eleanor Lee, Stephen E. Selkowitz, Vladimir Bazjanac, and Christian Kohler. High-Performance Commercial Building Façades. *LBNL*, 2002.

[9] Marco Sala. The intelligent envelope: the current state of the art. *Renewable energy*, 5(5-8):1039–1046, 1994.

[10] J. Carmody, Stephen E. Selkowitz, Eleanor Lee, Dariush Arasteh, and T. Willmert. *Window systems for high-performance buildings*. WW Norton, 2004.

[11] R Sullivan, L Beltran, Eleanor Lee, Michael Rubin, and Stephen E. Selkowitz. Energy and daylight performance of angular selective glazings. In *Proceedings of the ASHRAE/DOE/BTECC Conference*, number December, pages 7–11, 1998.

[12] Toke Rammer Nielsen, Karsten Duer, and Svend Svendsen. Energy performance of glazings and windows. *Solar Energy*, 69(1):137–143, July 2001.

[13] S. Hubalek, M. Brink, and C. Schierz. Office workers' daily exposure to light and its influence on sleep quality and mood. *Lighting Research and Technology*, 42(1):33–50, January 2010.

[14] Moncef Krarti, Paul M. Erickson, and Timothy C. Hillman. A simplified method to estimate energy savings of artificial lighting use from daylighting. *Building and Environment*, 40(6):747–754, June 2005.

[15] David Appelfeld, Christian Skodborg Hansen, and Svend Svendsen. Development of a slim window frame made of glass fibre reinforced polyester. *Energy and Buildings*, 42(10):1918–1925, October 2010.

[16] Arild Gustavsen, B. P. Jelle, and Dariush Arasteh. State-of-the-art highly insulating window frames-Research and market review. 2007.

[17] DS/EN 15603. Energy performance of buildings - Overall energy use and definition of energy ratings. 2008.

[18] David Appelfeld and Svend Svendsen. Experimental analysis of energy performance f a ventilated window for heat recovery under controlled conditions. *Energy and Buildings*, 43(11):3200–3207, November 2011.

[19] P.H. Baker and M.E. McEvoy. An investigation into the use of a supply air window as a heat reclaim device. *Building Services Engineering Research and Technology*, 20(3):105–112, January 1999.

[20] JR Gosselin. A dual airflow window for indoor air quality improvement and energy conservation in buildings. *HVAC&Research*, 14(3):359–372, 2008.

[21] David Appelfeld, Andrew McNeil, and Svend Svendsen. An hourly based performance comparison of an integrated micro-structural perforated shading screen with standard shading systems. *Energy and Buildings*, 2012.

[22] David Appelfeld and Svend Svendsen. Performance of a daylight redirecting glass shading system demonstration in an office building. In *Building simulation 2011*, page 8, Sydney, Australia, 2011.

[23] Eleanor Lee. Advanced High-Performance Commercial Building Facades Research. In *LBNL*, 2009.

[24] J. Clarke. Energy Simulation in Buiding Design, 2001.

[25] TRNSYS. The Transient Energy System Simulation Tool, 2011.

[26] EnergyPlus. EnergyPlus Energy Simulation Software, 2011.

[27] Andrew McNeil, Jacob Jonsson, David Appelfeld, Greg Ward, and Eleanor Lee. A validation of a ray-tracing tool used to generate bi-directional scattering distribution functions for complex fenestration systems. *Solar Energy*, submitted, 2012.

[28] F. Frontini, Tilmann E Kuhn, S. Herkel, Paul Strachan, and G. Kokogiannakis. IMPLEMENTATION AND APPLICATION OF A NEW BI-DIRECTIONAL SOLAR MODELLING METHOD FOR COMPLEX FACADES WITHIN THE ESP-R BUILDING SIMULATION PROGRAM - Annex. In *Building simulation 2009*, page 75, 2009.

[29] EN ISO. EN ISO 10077-2 Thermal performance of windows, doors and shutters - Calculation of thermal transmittance - Part 2: Numerical method for frames, 2003.

[30] Robin Mitchell, Christian Kohler, Ling Zhu, and Dariush Arasteh. THERM 6.3 / WINDOW 6.3 NFRC Simulation Manual. *LBNL*, (January), 2011.

[31] Sommer Informatik GmbH. WinIso2D Professional, 2011.

[32] Www.buildingphysics.com. HEAT2, A PC-program for heat transfer in two dimensions Update manual, 2011.

[33] EN ISO. ISO 15099_Thermal performance of windows, doors and shading devices - Detailed calculations, 2003.

[34] Natural resources Canada. *Consumer' s Guide To Buying Energy-Efficient Windows and Doors*.

[35] Svend Svendsen, Jacob Birck Laustsen, and Jesper Kragh. Linear thermal transmittance of the assembly of the glazing and the frame in windows. In *Proceedings of the 7th Symposium on Building Physics in the Nordic Countries*, pages 995–1002, Raykjavik, Iceland, 2005.

[36] D Saelens, S Roels, and H Hens. Strategies to improve the energy performance of multiple-skin facades. *Building and Environment*, 43(4):638–650, April 2008.

[37] Heinrich Manz, A Schaelin, and H Simmler. Airflow patterns and thermal behavior of mechanically ventilated glass double façades. *Building and Environment*, 39(9):1023–1033, September 2004.

[38] M.J. Holmes. Optimisation of the thermal performance of mechanically and naturally ventilated glazed facades. *Renewable Energy*, 5:1091–1098, 1994.

[39] Jun Tanimoto and Ken-ichi Kimura. Simulation study on an air flow window system with an integrated roll screen. *Energy and buildings*, 26(3):317–325, 1997.

[40] D Saelens, S Roels, and H Hens. The inlet temperature as a boundary condition for multiple-skin facade modelling. *Energy and Buildings*, 36(8):825–835, August 2004.

[41] EN ISO. EN ISO 673, Glass in building - Determination of thermal transmittance (U value) - Calculation method, 1997.

[42] Arild Gustavsen, Dariush Arasteh, B. P. Jelle, C. Curcija, and Christian Kohler. Developing Low-conductance Window Frames: Capabilities and Limitations of Current Window Heat Transfer Design Tools – State-of-the-Art Review. *Journal of Building Physics*, 32(2):131–153, October 2008.

[43] Jacob Birck Laustsen and Svend Svendsen. Improved windows for cold climates. In *7th Symposium on Building Physics in the Nordic Countries*, pages 987–994, 2005.

[44] Toke Rammer Nielsen, A.C. Hviid, and S. Petersen. iDbuild, BuildingCalc and LightCalc User Guide - Version 3.2.2, 2008.

[45] Aalborg University Research, Danish Building Institute. The Calculation Programme Be06, 2005.

[46] ESPR. ESP-r energy modelling tool, 2012.

[47] Tilmann E Kuhn. Evaluation of overheating protection with sunshading systems. *Solar Energy*, 69:59–74, 2001.

[48] Tilmann E Kuhn, Sebastian Herkel, Francesco Frontini, Paul Strachan, and Georgios Kokogiannakis. Solar control: A general method for modelling of solar gains through complex facades in building simulation programs. *Energy and Buildings*, 43(1):19–27, January 2011.

[49] Tilmann E Kuhn. Solar control : A general evaluation method for facades with venetian blinds or other solar control systems. *Energy and Buildings*, 38:648–660, 2006.

[50] Greg Ward and R.A. Shakespeare. *Rendering with Radiance: The Art and Science of Lighting Visualization*. Morgan Kaufmann, California, USA, 1998.

[51] John Mardaljevic. Validation of a lighting simulation program under real sky conditions. *Lighting Research and Technology*, 27(4):181–188, 1995.

[52] Christoph F. Reinhart and Jan Wienold. The daylighting dashboard - A simulation-based design analysis for daylit spaces. *Building and Environment*, 46(2):386–396, February 2011.

[53] H.A.L. van Dijk and H. Oversloot. WIS, the European tool to calculate thermal and solar properties of windows and window components. In *Proceedings of Building Simulation*, volume 3, pages 259–266, 2003.

[54] Saint Gobain Glass. Columen II, http://exprover.saint-gobain-glass.com/b2c/default.asp?nav1=act&id=13922, 2012.

[55] Pilkington. Pilkington Spectrum, http://spectrum.pilkington.com /Main.aspx?country=GB, 2012.

[56] Swisspacer. Caluwin, http://www.swisspacer.com/en/ service/caluwin.html, 2012.

[57] John Mardaljevic, Lisa Heschong, and Eleanor Lee. Daylight metrics and energy savings. *Lighting Research and Technology*, 41(3):261–283, September 2009.

[58] A Webb. Considerations for lighting in the built environment: Non-visual effects of light. *Energy and Buildings*, 38(7):721–727, July 2006.

[59] R Compagnon. Solar and daylight availability in the urban fabric. *Energy and Buildings*, 36:321–328, 2004.

[60] United States Department of Energy. Weather data - Copenhagen.

[61] Anne Iversen, Svend Svendsen, and Toke Rammer Nielsen. The effect of different weather data sets and their resolution in climate-based daylight modelling. *Lighting Research and Technology*, pages 1477153512440545–, March 2012.

[62] Axel Jacobs. Understanding rtcontrib. Technical report, London, UK, 2010.

[63] Greg Ward. Simulating the Daylight Performance of Complex Fenestration Systems Using Bidirectional Scattering Distribution Functions within Radiance. *Journal of the Illuminating Engineering Society*, (January), 2011.

[64] John Mardaljevic. Simulation of annual daylighting profiles for internal illuminance. *Lighting Research and Technology*, 32(3):111–118, January 2000.

[65] F. Cantin and M.-C. Dubois. Daylighting metrics based on illuminance, distribution, glare and directivity. *Lighting Research and Technology*, 43(3):291–307, February 2011.

[66] A Nabil and John Mardaljevic. Useful daylight illuminance: a new paradigm for assessing daylight in buildings. *Lighting Research and Technology*, 37(1):41–59, January 2005.

[67] Andrew McNeil and Eleanor Lee. Annual Assessment of an Optically-Complex Daylighting System Using Bidirectional Scattering Distribution Functions with Radiance. *LBNL*, pages 1–29, 2010.

[68] Christoph F. Reinhart. Validation of dynamic RADIANCE-based daylight simulations for a test office with external blinds. *Energy and Buildings*, 33:683–697, 2001.

[69] John Mardaljevic. *Daylight simulation: validation, sky models and daylight coeffcients*. Phd thesis, De Montfort University, UK, 2000.

[70] CEN EN 15251. Indoor environment input for design and assessment of energy performance of buildings addressing indoor air quality, thermal environment, lightning and acoustics, 2007.

[71] Jan Wienold. *Daylight Glare in Offices*. Phd thesis, 2009.

[72] P.R. Tregenza and I.M. Waters. Daylight coefficients. *Lighting Research and Technology*, 15(2):65–71, January 1983.

[73] Andrew McNeil. The Three-Phase Daylight Coefficient Method for Simulating Complex Fenestration with Radiance. Technical report, 2011.

[74] Marilyne Andersen and Jan de Boer. Goniophotometry and assessment of bidirectional photometric properties of complex fenestration systems. *Energy and Buildings*, 38(7):836–848, July 2006.

[75] Marilyne Andersen. *Innovative bidirectional video-goniophotometer for advanced fenestration systems*. PhD thesis, 2004.

[76] J.H. Klems. A new method for predicting the solar heat gain of complex fenestration systems - I Overview and Derivation of the Matrix Layer Calculation. *LBNL*, 1994.

[77] Greg Ward. Complex Fenestration and Annual Simulation. In *8th International Radiance workshop*, Boston, USA, 2009.

[78] N Tuaycharoen and P.R. Tregenza. View and discomfort glare from windows. *Lighting Research and Technology*, 39(2):185–200, June 2007.

[79] L Roche, E Dewey, and P Littlefair. Occupant reactions to daylight in offices. *Lighting Research and Technology*, 32(3):119–126, January 2000.

[80] J. Jakubiec and Christoph F. Reinhart. The 'adaptive zone' - A concept for assessing discomfort glare throughout daylit spaces. *Lighting Research and Technology*, October 2011.

[81] Jan Wienold. Dynamic daylight glare evaluation. In *Building simulation 2009*, pages 944–951. Citeseer, 2009.

[82] Jan Wienold and Jens Christoffersen. Evaluation methods and development of a new glare prediction model for daylight environments with the use of CCD cameras. *Energy and Buildings*, 38(7):743–757, July 2006.

[83] IESNA. *Lighting Handbook, Illuminating Engineering, 9th edition,*.

[84] DS/EN 15193. Energy performance of buildings - Energy requirements for lighting, 2007.

[85] CIE 38 (TC-2.3). Commission Internationale de l'Eclairage. Radiometric and photometric characteristics of materials and their measurement, 1977.

[86] J.H. Klems. A new method for predicting the solar heat gain of complex fenestration systems - II Detailed description of the matrix layer calculation.pdf. *LBNL*, 1994.

[87] P.R. Tregenza. Subdivision of the sky hemisphere for luminance measurements. *Lighting Research and Technology*, 19(1):13–14, January 1987.

[88] International Energy Agency. Daylight in Buildings - A source book on daylighting systems and components. IEA SHC Task 21/ECBCS Annex 29.

[89] Marilyne Andersen, Michael Rubin, and Jean-louis Scartezzini. Comparison between ray-tracing simulations and bi-directional transmission measurements on prismatic glazing. *Solar Energy*, 74(2):157–173, 2003.

[90] Stefan Lechtenböhmer and Andreas Schüring. The potential for large-scale savings from insulating residential buildings in the EU. *Energy Efficiency*, 4(2):257–270, September 2010.

[91] EN ISO. prEN ISO 12567-1_Thermal performance of windows and doors - Determination of thermal transmittance by the hot-box method - Part 1: Complete windows and doors, 2009.

[92] EN ISO. EN ISO 8990 - Thermal insulation - Determination of steady-state thermal transmission properties - Calibrated and guarded hot box, 1997.

[93] IEA TASK 27. Performance of Solar Facade Components. Technical report, 2005.

[94] Nigel Cross. *Engineering Design Methods: Strategies for Product Design*, volume 58. Wiley, 2008.

[95] Jingshu Wei, Jianing Zhao, and Qingyan Chen. Optimal design for a dual-airflow window for different climate regions in China. *Energy and Buildings*, 42(11):2200–2205, November 2010.

[96] WinDat. Window Information System software (WIS), WinDatThematic Network, 2006.

[97] H A L Van Dijk and Richard Versluis. Definitions of U- and g-value in case of double skin facades or vented windows. Technical report, 2004.

[98] Lau Markussen Raffnsoe. *Master Thesis Thermal Performance of Air Flow Windows*. PhD thesis, 2007.

[99] Jacob Birck Laustsen, Ines D.P. Santos, Svend Svendsen, Steen Traberg-Borup, and Kjeld Johnsen. Solar Shading System Based on Daylight Directing Glass Lamellas. In *Building Physics 2008 - 8th Nordic Symposium*, pages 111–119, 2008.

[100] Anne Iversen and Jacob Birck Laustsen. Udvikling af nye typer solafskærmnings- systemer baseret pådagslysdirigerende solafskærmende glaslameller. Technical report, 2009.

Part II

Appended Papers

Paper I

"Development of a slim window frame made of glass fibre reinforced polyester"

D. Appelfeld, C.S. Hansen & S. Svendsen

Published in: *Energy & Buildings, 2010*

Energy and Buildings 42 (2010) 1918–1925

Contents lists available at ScienceDirect

Energy and Buildings

journal homepage: www.elsevier.com/locate/enbuild

Development of a slim window frame made of glass fibre reinforced polyester

David Appelfeld*, Christian S. Hansen, Svend Svendsen

Department of Civil Engineering, Technical University of Denmark, Brovej, Building 118, DK-2800 Kgs. Lyngby, Denmark

ARTICLE INFO

Article history:
Received 30 March 2010
Received in revised form 13 May 2010
Accepted 26 May 2010

Keywords:
Product development
Energy performance
Efficient window
Composite material

ABSTRACT

This paper presents the development of an energy efficient window frame made of a glass fibre reinforced polyester (GFRP) material. Three frame proposals were considered. The energy and structural performances of the frames were calculated and compared with wooden and aluminium reference frames. In order to estimate performances, detailed thermal calculations were performed in four successive steps including solar energy and light transmittance in addition to heat loss and supplemented with a simplified structural calculation of frame load capacity and deflection. Based on these calculations, we carried out an analysis of the potential energy savings of the frame. The calculations for a reference office building showed that the heating demand was considerably lower with a window made of GFRP than with the reference frames. It was found that GFRP is suitable for window frames, and windows made of this material are highly competitive in their contribution to the energy savings. A rational product development method was followed, and the process clearly identified the objectives of the investigation and set out the appropriate way to attain them. Using simple rational development methods, a well-defined and effective window was achieved smoothly and quickly, as is illustrated in the case study.

1. Introduction

The basis of this article is the development of window frames made of glass fibre reinforced polyester (GFRP) facilitated by rational product development methods. GFRP is rarely used as a window frame material at the moment and very few window manufactures use it as an alternative to traditional materials [1]. So the article describes an investigation to illustrate the potential benefits of using GFRP for window frames. The investigation focused only on the frame made of GFRP, so the windows all contain the same triple glazing with a warm edge and argon for easy comparison with the reference frames.

Today, a window is considered energy efficient if it has a low thermal transmittance (*U*-value), but this is not sufficient to describe a window's energy performance. Windows are one of the most crucial elements in the building façade, so a more detailed evaluation of the interactions between window performances, energy demands and the indoor environment needs to be carried out. The factors to consider include thermal transmittance, solar energy transmittance, visual transmittance and the durability of the window as well as its influence on a building's energy consumption, artificial light savings by use of daylight, and the visual comfort of occupants.

The energy consumption of buildings is responsible for approximately 40% of energy used in the developed countries. The energy requirements of buildings are defined in the building codes and the Energy Performance of Buildings Directive (EPBD) [2–4] introduces tighter requirements. Windows are typically responsible for a large fraction of the heat loss in buildings, because the *U*-value of the window, including the frame, is much higher than the *U*-value of the other parts of the building envelope. However, windows can also contribute to heating by the solar energy transmitted through the glazing. This contribution is called the solar gain, which depends on the total solar energy transmittance of a window [5]. The window frame generally covers 20–30% of the overall window area and typically has a negative impact on the energy performance with a higher thermal transmittance than the glazing and no solar transmittance. A larger glazed area created by a reduced frame width can improve both the thermal transmittance and the solar gains of the window. These aspects of a window energy performance can be simply evaluated by net energy gains (NEG) [5,6].

Over the last two decades, the energy performance of windows has been greatly improved by introducing low-emissivity coatings, inert gasses with low conductivity in the glazing cavities, and a glazing with a warm edge. In contrast, very few changes have been made in the design of window frames and the selection of suitable materials [7]. Therefore, the greater part of the heat losses can now be assigned to the poor design of the window frame [8]. The most common window frames today are made of either materials with high conductivity, such as aluminium for office buildings and materials with low conductivity, such as wood and polyvinylchloride

* Corresponding author. Tel.: +45 45251856; fax: +45 45883282.
E-mail address: dava@byg.dtu.dk (D. Appelfeld).

0378-7788/$ – see front matter © 2010 Elsevier B.V. All rights reserved.
doi:10.1016/j.enbuild.2010.05.028

Nomenclature

A_f	projected frame area [m^2]
A_g	projected visible glazing area [m^2]
A_w	projected window area [m^2]
U_f	thermal transmittance of a window frame [W/m^2 K]
U_g	thermal transmittance of a glazing [W/m^2 K]
U_w	thermal transmittance of a single window [W/m^2 K]
l_Ψ	visible perimeter of glazing [m]
Ψ	linear thermal transmittance due to combination of thermal effect of glazing, spacer and frame [W/m K]
τ_S	total solar energy transmittance of a single window
τ_g	solar energy transmittance of a glazing
τ_f	solar energy transmittance of a frame
NEG	net energy gain [kWh/m^2 year]
I	coefficient for solar gains [kWh/m^2]
D	coefficient for heat loss [kKh]

(PVC). Frames made of materials with low conductivity usually also have low strength, which requires wide frame profiles that reduce the total solar transmittance of the window.

The program iDbuild [9] was used to compare the annual energy consumption for an office building for different windows, and the program Be06 [10] was used to do the same for a domestic building. The thermal transmittance of the GFRP window frames was calculated using the finite element modelling (FEM) program THERM [11].

The article shows that it is possible to use rational product development methods to simulate the development of new windows and that window frames made of GFRP have a positive effect on the building energy performance. Besides the energy saving effect of the reduced frame size, the GFRP frame material contributes to the energy efficiency of the window with a low thermal conductivity of 0.32 W/m K [12], yet still has high strength and durability and requires minimal maintenance.

2. Methods

2.1. Rational product development method

One of our aims was to investigate the feasibility of using a product development strategy to develop a more energy efficient window. Nigel Cross's rational method of product development [13] was selected for this investigation, because of method suitability for purpose of the window development. The main and general principle of the rational method is shown in Fig. 1.

The possibilities in the project have to be identified at the beginning. Next comes the objective and problem specification, which defines the overall problem and by establishing its requirements defines its sub-problems. Furthermore, several design alternatives are generated as sub-solutions, and they are evaluated by quantitative performance calculations. We used the thermal performance and mechanical properties of the window as the performance criteria. This evaluation allowed us to select the final and most appropriate solution of a window frame. Throughout, the principle of the rational method was followed and adjusted to the purposes of window frame development.

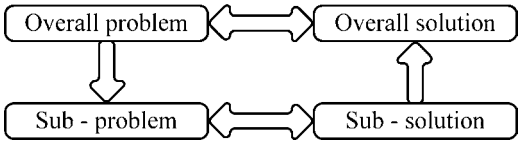

Fig. 1. Skeleton of the rational product development method [13].

2.2. Calculation of thermal performance

Calculation of thermal properties and energy performance was used to evaluate each design alternative. The energy performance evaluation was divided into four steps starting with a calculation of the heat loss coefficient of the frame and ending with a study of a window's effect on the building energy consumption.

As the first step, we calculated the *U*-value of the frames and, from this, the *U*-value of the whole window as a second step. The *U*-values were obtained by fine element method (FEM) in the simulation program Therm [11]. The third step was to use the net energy gains method to make a more complex calculation of the effect of the windows [5], taking into account the contribution of the solar gains minus heat losses of the window. The last step in the energy performance assessment was the comprehensive evaluation of the effect of the window on the energy consumption of the building. Here we took two cases, first an office building evaluated in the program iDbuild [9], and second a domestic building evaluated in the program Be06 [10]. All the proposed window frames were compared with the reference frames which were typical wooden and aluminium frames.

2.2.1. U-value of the frame

The *U*-values of all the frames were calculated based on the prescribed method in ISO 10077-2 [14]. The method is based on using a highly insulated panel which substitutes the glazing and eliminates the effect of thermal bridge by the glazing spacer.

The simulation program Therm [11] uses heat transfer coefficients prescribed by ISO 15099 [15] to solve the conductive heat transfer equations. The geometry of the profiles was drawn using computer-aided design (CAD) files as underlay. When the geometry is redrawn in Therm, the calculated geometry may contain some minor differences from the real shape.

2.2.2. Linear thermal transmittance and spacer

The thermal transmittance of the frame was calculated in the absence of the glazing and the thermal transmittance of the glazing does not include the effect of the spacer and the edge effect. The effect of the assembly edge and spacer is described by the linear thermal transmittance Ψ [14]. For the calculation of Ψ of the edge, the spacer is replaced with a simplified shape with equivalent thermal conductivity [16].

2.2.3. U-value of the window

The standard calculation of *U*-value for a window is prescribed by 10077-2 [14] as mentioned earlier, and it has to include the linear thermal transmittance (Ψ-value) of the assembly of the frame/spacer/glazing and the *U*-value of the frame and glazing [16,17]. The Ψ-value was obtained by simulation of the window frame with glazing in Therm. The *U*-value of the whole window was obtained by the following Eq. (1).

$$U_w = \frac{U_g A_g + U_f A_f + \Psi l_\Psi}{A_w} \quad (1)$$

2.2.4. Total solar energy transmittance

The total solar energy transmittance τ_S of a window is defined as the solar energy transmittance value of the glazing area and the frame area together [15]. It has to be emphasized that windows are evaluated by the total solar energy transmittance of a window including the effect of the frame as described in the formula (2).

$$\tau_S = \frac{\sum \tau_g A_g + \sum \tau_f A_f}{A_w} \quad (2)$$

Table 1
Material properties for materials used in the Therm model.

Material	Conductivity ($W m^{-1} k^{-1}$)	Material	Equivalent thermal conductivity ($W m^{-1} k^{-1}$)
Soft wood	0.13	Spacer	0.243
Glass	1	Glazing cavity	0.022
Ethylene propylene diene monomer (EPDM)	0.25		
Silicon (glue)	0.35		
GFRP[a]	0.32		
Polysulphide	0.4		
Aluminium	160		
Insulated panel	0.035		

[a] Ref. [12].

2.2.5. Net energy gains

There are various ways of assessing the energy performance of a window. But it is clearly not sufficient just to evaluate the window *U*-value. The net energy gain (NEG) includes not only the thermal performance of the window, but also the contribution of its solar gains. The NEG method is based on a window's solar gain minus its heat loss in a standard period defined as the heating season depending on the outdoor air temperature. This takes into account the tilt and relative orientation of windows in a reference building [5]. NEG can reveal that a window with a very low *U*-value has a lower NEG than another window with a higher *U*-value.

For example a window with a *U*-value of 1.27 W/m^2 K (frame *U*-value 1.33 W/m^2 K) can have a higher NEG than a window with *U*-value 0.79 W/m^2 K (frame *U*-value 0.75 W/m^2 K) [18]. This would result from the greater area of glazing in the window with a higher *U*-value, which means that the heat loss can be compensated by a higher solar gain. NEG is described by below Eq. (3).

$$E = g\,I - U\,D \tag{3}$$

where *D* is the coefficient for heat loss and *I* is the coefficient for solar gains. Both coefficients are dependent on the location and window orientation. For Denmark, *I* is 196.4 kWh/m^2 and *D* is 90.36 kKh [5]. This approach to energy performance evaluation allows an easy and quick comparison of various windows.

2.2.6. Calculation of energy use of building

The effect on total building energy consumption was evaluated using iDbuild and Be06 [9,10]. iDbuild is a building simulation tool for an evaluation of energy performance and indoor environment based on hourly weather data. The program is able to illustrate how performance parameters and combinations of parameters affect energy performance, thermal indoor environment, air quality, and daylight conditions. As a reference building, we used a low energy class office building with 60 offices and a large glazed staircase space. The office building was simulated to investigate its energy use and the effect on indoor environment with respect to temperature and daylight as Case 1 in thermal evaluation under Step 4. As Case 2 in Step 4, a domestic building was simulated by the program Be06 [10]. Be06 calculations are performed in accordance with the mandatory calculation procedure described in the EU Directive on the energy performance of buildings [2,4,19].

2.3. Mechanical properties

In addition to the energy performance of the window frames, we also made a calculation of structural load capacity and deflections. We investigated three design criteria which affect durability: no air leakage due to frame deformation, no breakage of glass due to frame deformation, and the strength of frame profiles. By ensuring that these three requirements are met, we can ensure that the window will perform well mechanically. The structural calculation establishes maximal dimensions for a window in respect of these requirements.

3. Material properties

Table 1 describes the material properties used in the numerical simulations. Note that the emissivity of all the solid materials was 0.9. It should be mentioned that the equivalent thermal conductivity λ_{eq} for the spacer and glass cavity is based on the individual case. The gas in the cavity was replaced with a solid material which provided the same total thermal transmittance of the glazing, including gas properties and radiation. The equivalent thermal conductivity of a spacer, boundary conditions and surface heat transfer coefficients are in accordance with standard 10077-2 [14] and described in Table 2.

There are several advantages in using GFRP for window frames rather than common window frame materials, such as aluminium, PVC and wood. Table 3 shows that GFRP is eight times stronger than PVC and three and half times stronger than wood, which means that GFRP frames can be slimmer and do not require additional reinforcement. Moreover, the thermal conductivity is several times lower than for aluminium and similar to wood and PVC. According to a correspondence with Fiberline [12], the thermal conductivity of GFRP is 0.32 W/m K. The low thermal conductivity reduces thermal bridges and thus the risk of condensation and the growth of mould on window frames. Furthermore, GFRP does not absorb moisture, corrode or degrade in UV-radiation, so the durability of the material is greater and profiles do not require expensive maintenance. Last but not least, the thermal expansion of GFRP is almost identical to that of glass, which means that gaskets, water striping, glazing and window frame will not be exposed to additional stresses. All the relevant mechanical properties of GFRP and other materials used for windows are listed in Table 3.

4. Product development process

4.1. Problem specification

First of all, the opportunities in developing an energy efficient window using GFRP were identified. This meant that we had to investigate how to use innovative window frame design to reduce the energy demand of buildings, and how to evaluate those effects correctly in comprehensive and detailed calculations taking solar energy into account. The limitations were to use a triple glazing and GFRP material for the frame.

Table 2
Boundary condition of the models.

Name	Temperature (°C)	Heat transfer coefficient ($W m^{-2} K^{-1}$)
Outdoor boundary condition	0	25
Indoor boundary condition	20	7.69
Reduced boundary condition	20	5

Table 3
Mechanical properties of typical materials for window frames.

	E-modulus (GPa)	Tensile strength (MPa)	Thermal conductivity (W/K m)	Thermal expansion (10^{-6}/K)	Density (kg/m^3)
Softwood	7	14	0.13	4.5	500
Aluminium	72	300	160	23	2800
Steel	210	360	50	12	7800
PVC	3	-	0.17	6.1	1390
GFRP[a]	23	240	0.32	9	450
Glass	70	30–90	237	8–9	2700

[a] Ref. [12].

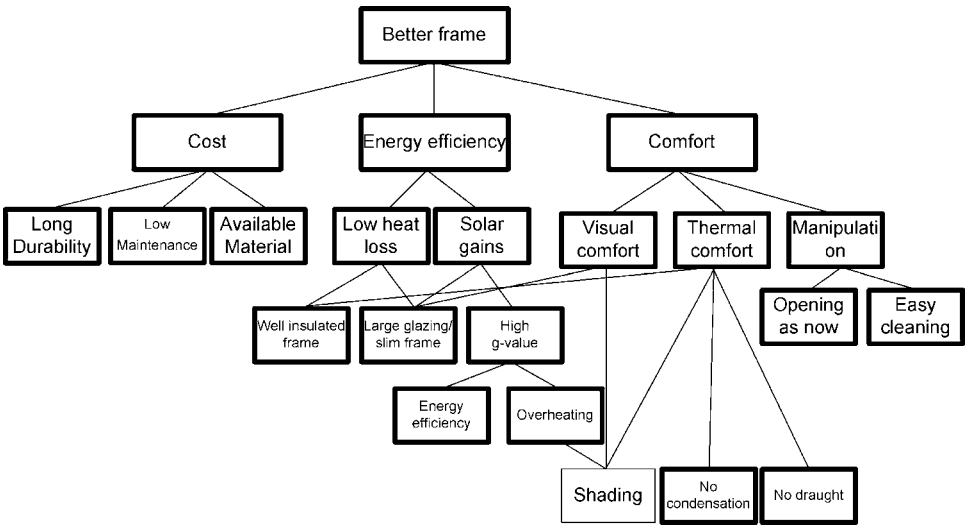

Fig. 2. Hierarchical diagram of relationships between objectives for improved window frame.

4.2. Objective clarification

From the specified opportunities, the problem objectives were explored together with their relationship and connections between levels. The newly developed window frame can serve several purposes and most of them are shown on the objective tree in Fig. 2. This figure shows how the objectives for a frame are clarified from top to low level by asking the question "HOW" and the individual sub-objectives are fulfilled from the lower level to the top by asking the question "WHY".

4.3. Requirements and limitations

All the clarified objectives for such a frame had to fulfill the specifications of a customer, user requirements, and production and technical requirements for producing and usage of the frame as listed in Table 4.

4.4. Designed alternatives

The most important and critical parameters for creating frames are width and thermal resistance of a frame, window solar gains, operability and possibility of cleaning the outside surface of a window from the inside, and the gasket tightness.

Three different alternative frames made of GFRP material were designed and are illustrated in Fig. 3. As the reference, a traditional wooden frame for a family house and a typical aluminium office window frame were used for comparison. To show the effect of the frame, all alternatives, including the reference frames, contain a triple glazing with same properties.

The Reference Frame 1 in Fig. 3(a) is a traditional wooden window used in Danish houses with a single side-hung casement opening outwards. A typical aluminium window, which is mostly used in office buildings but also in domestic buildings, is shown in Fig. 3(b). Alternative 1 of a window frame in GFRP in Fig. 3(c) is a sliding projecting window with top-hung casement and open-

Table 4
List of technical specifications for the frame.

Specification—Window frame from GFRP		
Number	R or W[a]	Requirements
1	R	Using standard double or triple glazing
2	R	Glued glazing into the frame by silicon or epoxy resin
3	W	Frame visible high at the most 50 mm
4	R	Sides of the frame connected by mechanical connections in the corners
5	W	Use same profiles for both triple and double glazed window
6	R	Wooden appearance from inside
7	W	The finishing of the frame has to be available in several colours
8	R	Manipulation by one hand
9	R	Easy operable and easy to clean
10	R	Slim hinges for placement into the frame
11	R	Hinges screwed directly into the wall
12	R	Water and air tight gasket between sash and frame—2 mm
13	R	Maximal deformation 1/300 or max 8 mm of a window side length
14	R	Minimal strength of frame 300 MPa
15	R	Net energy gain minimally of window −20 kWh/m^2 per year for double glazing
16	R	Net energy gain minimally of window 0 kWh/m^2 per year for triple glazing
17	R	Insulation in the wall has to be covered water-tight by the frame
18	R	Minimal thickness of profile wall 1.5 mm

[a] R, requirements; W, wishes.

ing outside. This kind of window is characteristic for the Danish market and allows turning the outer surface to the interior for easy cleaning. Alternatives 2a and 2b in Fig. 3(d) and (e) are tilt and turn windows with openings inward and are the most common window type in Europe. These two alternatives are different in the hinge and the width of the frames. Alternative 2a is equipped with a standard tilt and turn hinge which requires a certain amount of space for mounting and so the frame is larger. The alternative 2b is equipped

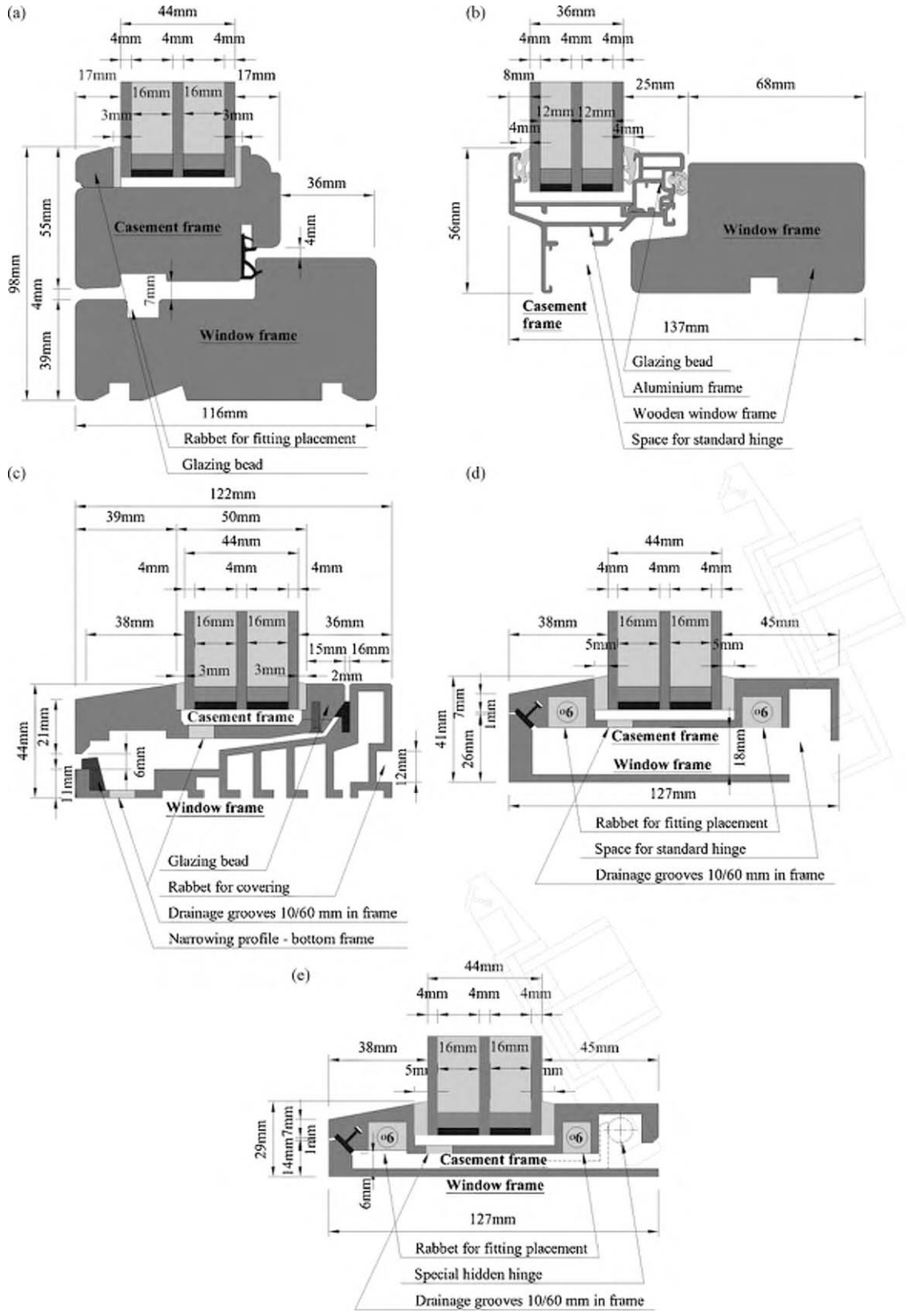

Fig. 3. (a) Reference 1—wooden frame, (b) Reference 2—aluminium frame, (c) Alternative 1, (d) Alternative 2a, (e) Alternative 2b.

Table 5
Window and frame properties of the alternatives evaluated.

Window characteristics	Reference 1	Reference 2	Alternative 1	Alternative 2a	Alternative 2b
Width of frame (mm)	98	56	44	41	29
Linear transmittance—ψ (W/m K)	0.034	0.045	0.032	0.031	0.032
g-Value glazing/window (−)	0.51/0.37	0.51/0.43	0.51/0.45	0.51/0.45	0.51/0.45
Light transmittance of glazing/window (−)	0.7/0.61	0.7/9.59	0.7/0.62	0.7/0.64	0.7/0.51
Frame area of window (%)	27	16.1	12.7	11.8	8.4

Table 6
Thermal and energy properties of evaluated frame alternatives.

	Window characteristics	Reference 1	Reference 2	Alternative 1	Alternative 2a	Alternative 2b
1	Frame U-value (W/m^2 K)	1.22	3.19	1.43	2.00	1.9
2	Window U-value (W/m^2 K)	0.85	1.24	0.79	0.85	0.8
3	NEG (kWh/m^2)	−3.9	−28.4	15.7	11.2	19.3
4	Building energy demand/heating					
	Case 1 (kWh/m^2)	29.5/11	34.5/15	28/9	29/10	28/9
	Case 2 (kWh/m^2)	67.7/61.1	74.9/67.4	66.9/58.1	67.8/58.9	66.9/57.6

with a special hinge that can be hidden in the casement frame and reduces the frame width compared to alternative 2a by 12 mm.

The alternatives were evaluated thermally in four successive steps, which were U-value of frame, U-value of window, net energy gains, and building energy consumption. Furthermore, the load capacity and deformation of the frames were assessed against the wind load.

5. The evaluation of the frames

As one of the last steps in the rational product development method, the proposed alternatives were evaluated. Thermal properties for all the frames were calculated in the program Therm [11]. Table 5 lists the characteristics of the frame alternatives and windows, including visible width of frame, linear transmittance through the glazing/frame/spacer assembly, solar energy and light transmittance of glazing/window and frame area of the window. Table 6 shows frame U-values (Step 1), the U-value of the window (Step 2), NEG (Step 3), and the energy consumption of the reference buildings (Step 4).

5.1. Thermal properties

Considering the U-value of the frames alone shows the best insulated frame to be the Reference Frame 1 with a U-value of 1.22 W/m^2 K. This is due to the fact that the thermal conductivity of wood is lower than that of GFRP. The reference aluminium frame has the highest U-value because of the high thermal conductivity of aluminium. Alternatives 2a and 2b have the highest frame U-values of the proposed frames, which are 2 W/m^2 K and 1.9 W/m^2 K, respectively. The reason is that the air cavity in the frame is large and almost connected to the exterior. Moreover the frame profiles are straight along a heat flux flow, which allows conduction of the heat. One consequence of this could be lower interior frame temperatures with a risk of condensation. However, the frames are sufficiently insulated and the surface temperature is the same or slightly lower than for the reference frames. But the U-value of the frame alone is not a sufficient description of the real energy performance of the frame and does not evaluate the overall window performance, which is required [2].

The second step in the assessment of the frames was to calculate the overall window U-value. The window U-value of the proposed windows was significantly reduced by the slimmer frames because of the larger glazing area. The U-values of all the windows are between 0.85 W/m^2 K and 0.79 W/m^2 K, except for Reference Frame 2, which has a U-value of 1.24 W/m^2 K for a window size of 1230 mm × 1480 mm. The reduction of the window U-value for Alternative 2b compared to 2a is 0.05 W/m^2 K, and this was achieved by hiding the hinge in the casement frame and narrowing the frame. The percentage of the frame area in the total window area was lowered significantly. The frame area compared to the total area of the window with dimensions 1230 mm × 1480 mm was calculated and is presented in Table 5.

The next step in accordance with the methodology was to calculate the NEG [5]. The NEG was negative only for the reference windows; otherwise it was positive for all the proposed frame alternatives. This means that the reference windows have a larger heat loss than their solar energy gain, and the proposed alternatives contributed positively to the heating of the building—firstly, because the heat loss through the window was reduced, and secondly, the energy consumption for heating the space was partially replaced by the solar energy which penetrated the room. Moreover, the partial substitution of the frame area by low U-value glazing also helped reach the lower window U-value. The slimmest frame, alternative 2b, provides the highest positive NEG, 19.3 kWh/m^2 per year, which is 23.2 kWh/m^2 per year better than Reference 1 and 47.9 kWh/m^2 per year better than Reference 2. Alternatives 1 and 2a also provide very high NEG performance: 15.7 kWh/m^2 and 11.2 kWh/m^2, respectively.

The last step of the energy performance evaluation was a simulation of a whole building energy performance in iDbuild and Be06. The results of Step 4 are shown in Table 6 and present two cases: the total energy consumption of a reference office building (Case 1) and of a reference domestic building (Case 2). The total energy consumption of buildings includes heating, cooling, ventilation, hot water and lighting [19].

Case 1 investigates primarily the impact on the energy demand of the office building with the replacement of the aluminium windows. Since the office building has the windows across the whole width of rooms, the big windows were simplified by three identical single window units coupled together. In this arrangement the different window alternatives reduced the building energy consumption from 34.5 kWh/m^2 per year to 28 kWh/m^2 per year for a building with Frame Alternatives 1 and 2b. Alternative 2b provided the biggest total energy saving of approximately 6.5 kWh/m^2 per year over the aluminium window—Reference 2. This comparison reveals the potential of using the slim frame made from GFRP, because of increasing transparent part of the window and reducing heat loss of the frame. The enlarged glazing area of all the alternatives compared to the references increased the total visual

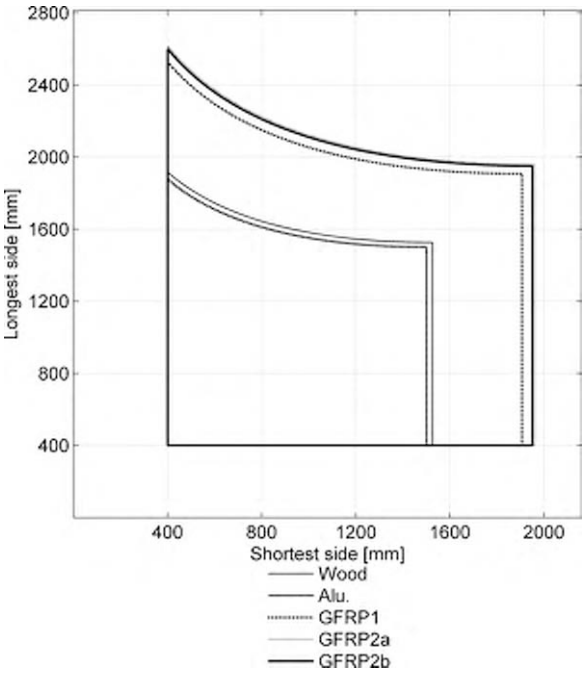

Fig. 4. Envelope of possible window sizes for different frame types.

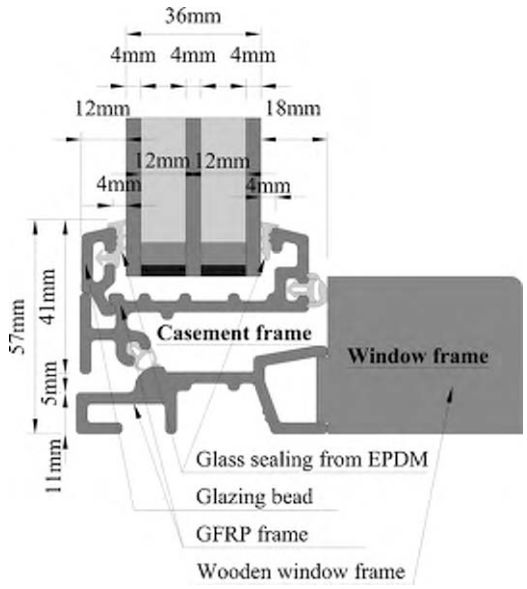

Fig. 5. Example of a real application of a GFRP window frame.

light transmittance of the window so that the daylight factor in the middle of the room increased from 5.4% (Reference 1) and 6.0% (Reference 2) to 6.3%. Moreover, the *g*-value is higher, which increases the solar gains compared to the reference window, see Table 5. Case 1 focuses on comparison with the aluminium window, but Table 6 also presents results for the wooden frame, Reference 1.

In Case 2, the focus is on the replacement of the wooden window frame by a GFRP window frame in a domestic building where wooden window frames are usual—Reference Frame 1. Table 6 shows the energy saving effect achieved when the wooden (or aluminium) window is replaced by the window made of GFRP. Using Frame Alternative 2b reduced the building energy requirement by 3.5 kWh/m^2 per year compared to the wooden frame and by 9.8 kWh/m^2 per year compared to the aluminium frame. It means that the Frame Alternative 2b performs as the best solution between all the frames. The other proposed alternatives have the smaller energy requirement reduction of 2 kWh/m^2 per year compared to Reference 1.

5.2. Structural performance

The structural performance and feasibility of the frames were evaluated and analysed. Three separate requirements were imposed on the structural performance of the windows [20]. The first requirement was a maximum deformation limit with regard to air tightness of the seal, where a serviceability state wind pressure was used. The second requirement was a maximum deformation limit with regard to failure of the glass. For this, an ultimate limit state wind load was applied to the window. The third and last requirement was load capacity. This checked that the bending stresses in the frames due to movement did not exceed the strength of the material. For a given side length it is possible to calculate the largest possible second side length using the above three requirements. The maximal possible size of the window frame is analysed in Fig. 4, which shows an envelope of the results. The lines in Fig. 4 limit the boundaries for a maximal window size. As can be seen, the alternatives proposed provide the possibility of greater window size, which means that the design and the material properties of GFRP allow bigger windows to be built without risk of wind failure.

5.3. Example of commercialized product

Up to this point, the window frames were created using the rational product development method, but one way of showing the feasibility of GRFP is to use a real example. There is a window frame comparable to the suggested frames which is already on the market and is shown in Fig. 5 [21]. This window was primarily developed for the Danish market and that is why it opens outwards. The inside surface of the frame is overlaid with wood. The width of the frame is 57 mm and the frame *U*-value is 1.42 W/m^2 K, which was achieved by optimizing the frame from previous test versions of a window of the size 1230 mm × 1480 mm. The glazing is a triple glazing, which combined with the frame provides an overall *U*-value for the window of 0.76 W/m^2 K, which is low and very similar to the windows we analysed. The NEG is calculated to be 7 kWh/m^2 per year. This is slightly lower compare to the analysed window frames and shows that the suggested frames are realistic.

6. Conclusion

The best solution for the frame is the alternative 2b, which reduced the energy consumption of the office building by 6.5 kWh/m^2 per year compared to the reference frame 2. This building energy consumption reduction and improvement was achieved using windows with slim GFRP frames which also satisfied structural criteria.

Moreover, it can be seen from the Case 1 and the Case 2 in the investigation where the window sizes were the same that this solution is suitable for renovations, requiring the simple replacement of a window [22]. The article has shown that GFRP is the suitable material for window frames and is a serious competitor to other window frame materials. As can be seen from the example of commercialized product and from some window manufactures [1,21], the potential advantages of using GFRP for window frames can be successfully implemented in real-life. The potential benefit of GFRP window frames is in saving energy by lower *U*-value of a window, increasing solar gains by reducing frame width, improving indoor comfort and meeting future energy requirements [2].

The rational product development method illustrated in the development of an energy efficient window was used and showed that it is feasible to use such a method to stimulate innovation in the window industry. The method was based on a successive and

logical chain of rational steps which transform the problem objective into a successful solution. The product development strategy helped to smooth the transition from the problem definition to the solution by a structured process.

Acknowledgements

The research was funded by the Danish Energy Agency program on research and demonstration of energy savings, EFP-2007, under the project name "Development of new types of low energy windows of composite materials", number 033001/33033-0067. The authors would like to acknowledge Fiberline Composites A/S and PRO TEC VINDUER A/S for their co-operation and contribution to this paper. The authors wish to thank Jesper Kragh for his work preceding this research project.

References

[1] S.P. Wake, Pultruded fibreglass: a window frame for the 90s, in: Proceedings of A World Conference on State-of-the-Art Window Technologies for Energy Efficiency in Buildings, Toronto, 1995.
[2] European Directive on the Energy Performance of Buildings (2002). Directive 2002/91/EC of the European Parliament and of the Council of 16 December 2002 on the Energy Performance of Buildings.
[3] Ministry of Climate and Energy, http://www.stm.dk/publikationer/UK_Regeringsgrundlag2007/index.htm.
[4] BR, The Danish Building Code, 2008, http:\\www.BR08.dk.
[5] T.R. Nielsen, K. Duer, S. Svendsen, Energy performance of glazings and windows, Solar Energy 69 (Suppl. 1–6) (2000) 137–143.
[6] A. Gustavsen, et al., Developing low-conductance window frames: capabilities and limitations of current window heat transfer design tools—state-of-the-art review, Journal of Building Physics 32 (2) (2008).
[7] http://www.swisspacer.com, 29.01.2010.
[8] N. Byars, D. Arasteh, Design options for low-conductivity window frames, Solar Energy Materials and Solar Cells 25 (1992) 143–148.
[9] T.R. Nielsen, A.C. Hviid, S. Petersen, iDbuild, BuildingCalc and LightCalc User Guide, Version 3.2.2, 2008, www.iDbuild.dk.
[10] The Calculation Programme Be06 Version 4.9.2.4, Danish Building Research Institute, Aalborg University.
[11] R. Mitchell, C. Kohler, D. Arasteh, THERM 5.2/WINDOW 5.2 NFRC Simulation Manual, Lawrence Berkeley National Laboratory, University of California, Berkeley, CA, 2006.
[12] http://www.fiberline.com, 29.01.2010.
[13] N. Cross, Engineering Design Methods: Strategies for Product Design, 4th ed., John Wiley & Sons, Chichester, 2008, ISBN 9780470519264.
[14] EN ISO 10077-2:2003, Thermal Performance of Windows, Doors and Shutters-Calculation of Thermal Transmittance, Part 2: Numerical Method for Frames, European Committee for Standardization, Brussels, Belgium, 2003.
[15] ISO 2003, ISO 15099:2003(E), Thermal Performance of Windows, Doors and Shading Devices—Detailed Calculations, International Organization for Standardization, Geneva, Switzerland, 2003.
[16] S. Svendsen, B.J. Laustsen, J. Kragh, Linear Thermal Transmittance of the assembly of the Glazing and the Frame in Windows, in: Proceedings of the 7th Symposium on Building Physics in the Nordic Countries, Technical University of Denmark, Department of Civil Engineering, 2005, ISBN 9979-9174-5-8, pp. 995–1002.
[17] Consumer's Guide To Buying Energy-Efficient Windows and Doors, Energy Publications, Office of Energy Efficiency, Natural resources Canada, 2004, ISBN 0-662-37461-4.
[18] B.J. Laustsen, S. Svendsen, Improved Windows for Cold Climates, in: Proceedings of the 7th Symposium on Building Physics in the Nordic Countries, Technical University of Denmark, Department of Civil Engineering, 2005, ISBN 9979-9174-5-8, pp. 987–994.
[19] EN 15603:2008(E), Energy Performance of Buildings—Overall Energy Use and Definition of Energy Ratings, European Committee for Standardization, Brussels, Belgium, 2008.
[20] K. Michael, Performance, durability and sustainability of advanced windows and solar components for building envelopes, in: International Energy Agency, Solar heating & cooling programme, Task 27–Performance of Solar Façade Components, October, 2007.
[21] http://protecwindows.com/da.aspx, 24.02.2010.
[22] H. Tommerup, S. Svendsen, Energy savings in Danish residential building stock, Energy and buildings 38 (2006) 618–826.

Paper II

"Experimental analysis of energy performance of a ventilated window for heat recovery under controlled conditions"

D. Appelfeld & S. Svendsen

Published in: *Energy & Buildings, 2011*

Energy and Buildings 43 (2011) 3200–3207

Contents lists available at SciVerse ScienceDirect

Energy and Buildings

journal homepage: www.elsevier.com/locate/enbuild

Experimental analysis of energy performance f a ventilated window for heat recovery under controlled conditions

David Appelfeld*, Svend Svendsen

Department of Civil Engineering, Technical University of Denmark, Brovej, Building 118 DK-2800 Kgs. Lyngby, Denmark

ARTICLE INFO

Article history:
Received 1 April 2011
Received in revised form 6 April 2011
Accepted 16 August 2011

Keywords:
Ventilated window
Active facade
Heat transfer
Guarded hot box
Thermal measurements

ABSTRACT

A ventilated window in cold climates can be considered as a passive heat recovery system. This study carried out tests to determine the thermal transmittance of ventilated windows by using the Guarded Hot Box. By testing under defined boundary conditions, the investigation described the heat balance of the ventilated window and clarified the methodology for thermal performance evaluation. Comparison between windows with and without ventilation using the window-room-ventilation heat balance revealed that a ventilated window can potentially contribute to energy savings. In addition, it was found that a significant part of preheating occurred through the window frames, which positively influenced the heat recovery of the window but increased the heat loss. Results also showed that increasing air flow decreased the recovery efficiency until the point when the additional thermal transmittance introduced by the ventilation was higher than the effect of heat recovery. Accordingly, the use of the ventilated windows might be most suitable for window unit with low ventilation rates. The results correlated with theoretical calculations in standards and software. However, the concept of a window thermal transmittance (U_w) value is not applicable for energy performance evaluation of ventilated window and requires deeper analysis.

1. Introduction

During recent decades there has been an increased national and international focus on lowering the energy demands in buildings [1,2]. Interest is growing among architects and consultants towards intelligent building components which can achieve building energy effectiveness, complying with strict energy codes and national emissions reduction goals [3,4]. Resulting initiatives with the goal of reducing transmission heat losses through building envelopes have subsequently created almost air tight buildings. However, windows still contribute in a large part to the total building heat loss, in spite of introducing coatings, sealed glazing, and tight gaskets [5]. Building envelopes have continuously improved by reducing thermal transmittance, but by preventing air leakage and air infiltration into buildings, the amount of required background ventilation had to be increased to ensure sufficient fresh air supply. Therefore, ventilation became a large part of the total building heating energy in cases when a heat exchanger cannot be used [6,7]. It is usually not an obstacle to ensure sufficient air exchange by mechanical ventilation in new buildings. However, when existing buildings, especially apartment buildings, are refurbished and air tightened it becomes expensive to build mechanical ventilation with heat recovery. In most cases, an exhaust ventilation system is used, causing an increase in energy demand for heating up the ventilated air to the required room temperature [8].

In a standard situation, a window and ventilation form two separate systems; by combining the two, it is possible to build a ventilated supply window [8]. In the ventilated window, fresh air is passed through a cavity between glass panes and some of the heat transmitted through the window is reclaimed by pre-heating the fresh air. An energy balance of ventilated windows was documented by several investigations, mainly theoretical and numerical [8–11]. The results of the investigations pointed out a potential in reducing heating demand by the air preheating. However, the supply air temperature could not reach the room air temperature [12]. It is thus necessary to further heat the supplied air to room temperature, despite the air pre-heating. Ventilated windows could be beneficial during both heating and cooling seasons; however this investigation focuses on the energy performance during the heating season [6,13].

2. Background

Ventilated windows are already available on the market, but there is little documentation available on their generic thermal energy performances under controlled and defined conditions.

* Corresponding author. Tel.: +45 45251856; fax: +45 45883282.
E-mail address: dava@byg.dtu.dk (D. Appelfeld).

0378-7788/$ – see front matter © 2011 Elsevier B.V. All rights reserved.
doi:10.1016/j.enbuild.2011.08.018

Nomenclature

$U_{w,trans,ext}$	Thermal transmittance of a ventilated window (W/m^2 K)
U_w	Thermal transmittance of a window (W/m^2 K)
$U_{w,vent}$	Ventilation heat loss of window (W/m^2 K)
$U_{w,trans}$	Total thermal transmittance of a window in a ventilated window (W/m^2 K)
T_{ni}	Interior environmental temperature (°C)
T_{ne}	Exterior environmental temperature (°C)
T_{vent}	Ventilation mean air temperature (K)
$Q_{air,vent}$	Energy flux to heat up ventilated air to room temperature (W)
ρ	Density (kg/m^3)
c_p	Specific heat capacity (J/kgK)
$Q_{w,trans}$	Energy flux from indoor environment to window (W)
$Q_{w,trans,ext}$	Energy flux from window to outdoor environment (W)
$Q_{w,vent}$	Advective energy flux (energy transported by ventilated air) (W)
A_w	Window area (m^2)
h_{ci}	Indoor convective heat transfer coefficient (W/m^2 K)
h_{ce}	Outdoor convective heat transfer coefficient (W/m^2 K)
h_{ri}	Indoor radiative heat transfer coefficient (W/m^2 K)
h_{re}	Outdoor radiative heat transfer coefficient (W/m^2 K)
Φ	Volume flow (m^3/s)
T_{si}	Indoor surface temperature of a window (°C)
T_{si}	Outdoor surface temperature of a window (°C)
$T_{gap,in}$	Air temperature in a window inlet valve (°C)
$T_{gap,out}$	Air temperature in a window outlet valve (°C)
W	Width (m)
H	High (m)
Δ	Uncertainty (by associated unit)
q_{sp}	Heat flow rate density of sample (W/m^2)
Φ_{in}	Corrected metering box heat input (W)
Φ_{sur}	Surround panel heat flow rate (W)
Φ_{edge}	Edge zone heat flow rate (W)

Several researches provided models for specific examples and ideas of how to improve the performances; however the experimental results are rarely available [9,14,15]. Impact in a real situation has to be experimentally investigated and validated with well-known boundary conditions to demonstrate the consequences of introducing ventilation through the glazing cavity. It is also important to provide the results independent of a building and HVAC set-up, therefore this investigation suggests a testing procedure which is reproducible. To build a more generic knowledge about ventilated windows, several aspects are excluded from the investigation since they are dependent on parameters such a location and orientation of a building. Therefore a "dark *U*-value", without exposing the testing sample to solar radiation, is considered because it is based only on the temperature difference across the sample which can be interpreted into any building.

This work is motivated by a current lack of available methods for evaluating ventilated window energy performance characteristics such as thermal transmittance. The aim is to determine the preheating of the air under various air flow volumes, since standardized methods of evaluating the ventilated window heat balance by measurements do not currently exist. Another objective of this work was a consolidation of the theory behind the ventilated window heat balance calculation, because presently a consistent theoretical methodology for ventilated window evaluation is missing. ISO 15099 provides notes referring to calculation of the heat balance of the ventilated window, but the ISO 15099 calculation model of thermal transmittance and ventilation heat gain for ventilated cavity windows is for information purposes only [16]. The ISO 15099 method is implemented in the computer program WIS [10]. Correlation between results in WIS and results from our analysis is discussed in this article.

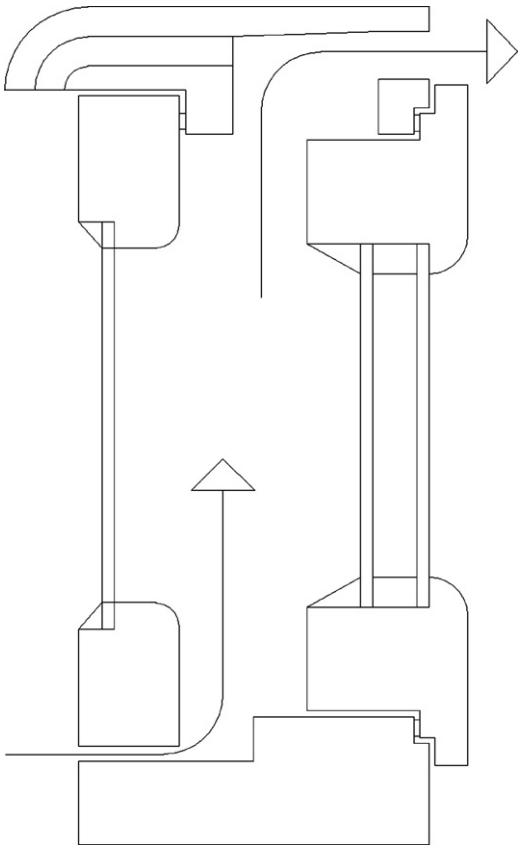

Fig. 1. Schematic picture of the used ventilated window with airflow marked.

3. Experiment

Experimental work focused on quantifying the regained heat loss from the ventilated air cavity and reducing the energy demand for heating during heating season when the temperature gradient between indoor and outdoor is 20 K. All investigations were carried out at the experimental facility at Technical University of Denmark (DTU). Specifically, the experiments utilized a Guarded Hot Box (GHB) with several adjustments compared to the standardised GHB described in ISO 12567-1 [17].

3.1. Ventilated window

The principle of the ventilated window is that the bottom and top window frames have integrated operable vents. The bottom frame connects the outside environment and the glazing air cavity. The top frame connects the air in the cavity to the interior environment. The simplified drawing of the window is shown in Fig. 1.

The tested window was a "1 + 2" coupled window with sealed double glazing on the interior side and a single uncoated glass pane on the exterior. The sealed glazing contains two low-e coatings; a soft coating on position 5 facing the sealed argon filled cavity

and a hard coating, K-glass, on position 3 facing a ventilated air cavity. All glass panes were 4 mm thick, the air gap was 83 mm, and the argon filled cavity in the double sealed glazing was 15 mm. The window frame and sash frames were made of soft wood. The inlet valve-in was positioned in the bottom frame and the air was sucked under the external sash. The valve-out was placed in the wide groove in the top frame and the valve was positioned to lead the air from the ventilated cavity via frame to the interior. The inlet valve was filled with a porous sponge to uniform the air flow.

3.2. Experimental equipment for the thermal transmittance

Thermal transmittance of the ventilated window was investigated by using the Guarded Hot Box (GHB) for measurements of the "dark U_w-value". The GHB was calibrated according to standards EN ISO 12567-1 and EN ISO 8990 [17,18]. The total heat flow through the specimen was measured based on the power input to a metering box. The heat flow through the specimen was generated by exposing the window to a temperature difference of 20 K [17]. The window was placed between a warm and a cold chamber with defined, controlled and measured environmental temperatures, T_{ni} and T_{ne}. The chamber temperatures were collected simultaneously and were based on the air temperatures and radiant temperatures of the baffle and surrounding surfaces. The air temperature in each section was measured by 9 temperature sensors. The radiant temperature was obtained from 9 T-type thermocouples and several thermopiles fixed to the surrounding surfaces, measuring temperatures over all visible surfaces of the sample. The warm chamber was placed within the guarded box to limit the heat flux through the wall of the metering box. The heat input to the metering box kept the temperature difference across the sample in steady-state conditions. The power input together with all temperatures was logged and corrected for lateral heat flow through the surround panel, its edge and the metering box wall heat loss. Both the surround panel and the edge had 8 embedded thermocouples on each side, which accounts for a total of 32 temperature sensors.

According to a method in EN ISO 12567-1 for window thermal transmittance, U_w value, measurements by the GHB, the glazing internal and external surface temperatures are not needed for determining total heat flow over a sample after the calibration. However, temperatures of the accessible window surfaces in the "1 + 2" window were measured to record a temperature gradient over the sample. Measurements were made on surfaces on position 1 (most external), 2, 3, and 6 (most internal). The surfaces in the ventilated cavity were measured in three vertical levels and each level was measured by two temperature sensors. In addition to the surface temperatures, the air in middle of the ventilated air cavity was measured at the same vertical position as on the surfaces in the cavity.

The measurements of the ventilated window were carried out in an adjusted GHB, where the air was sucked by a fan, which had a variable transformer in order to control the ventilated air mass volume. To avoid errors due to insufficient air mixing and to prevent uneven temperature distribution, the ventilated air did not enter the metering box. The air was instead directly returned through a vent to the cold chamber. This solution allowed separating the heat flow belonging to the temperature difference across the window from the amount of recovered heat and the additional energy for heating up the ventilated air to room temperature. The conditions on the cold and warm sides of window remain constant, independent of whether or not the window is ventilated. This allowed comparing the heat loss of the window with and without ventilation. Fig. 1 shows the set-up of the adjusted GHB (Fig. 2).

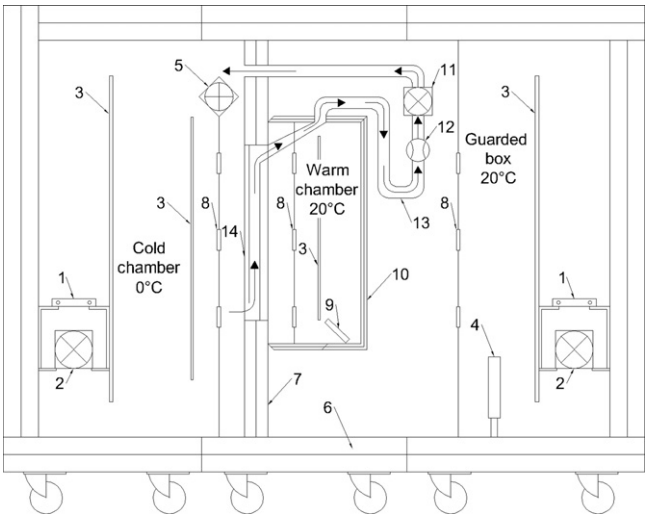

Fig. 2. Set-up of the GHB with air flow, and micro manometer. 1, cooling element; 2, fan; 3, baffle; 4, guarded box electrical heater; 5, cold side wind simulator; 6, sandwich element with polyurethane core; 7, surround panel wall from polystyrene foam (XPS) – 170 mm; 8, air temperature sensors; 9, electrical heater in metering box; 10, metering box wall from polystyrene; 11, fan with variable transformer; 12, micro manometer; 13, flexible sucking duct; 14, measured sample of size 1230 mm × 1480 mm ($w \times h$).

3.3. Experiment – set-up and procedure

During the measurements the temperature in the metering and guarded box were kept same and constant. The tests were influenced by the thermal properties of the window, especially by temperature differences and heat surface coefficients, and hence the temperature on both sides had to be controlled to allow investigation and allocation of different heat flows.

All the data were collected by a data acquisition system and directly processed by controlling software. The controlling software additionally controlled the closed loop to ensure correct electrical heater input into the metering box. Results and unprocessed data were logged for further calculations. The GHB was equipped with temperature sensors made from copper-thermocouples and thermopiles to measure temperatures. Environmental temperatures, air temperatures in the chambers, air temperature in the ventilated air cavity, temperatures in the inlet and outlet ventilated valves, and temperatures of the four window surfaces were measured.

The required air flow rate was defined according to international and national standards [1,19]. The variation of air flow through standard size windows of 1.23 m × 1.48 m was tested for a ventilation flow rate between 1l/s to 8l/s per window to ensure the required air change of 0.5 h^{-1}.

Special attention was paid to measuring the temperature of the ventilated air. Unshielded thermocouples made from stripped wire with a thickness of 0.1 mm were used to measure air temperature in the venting valves. Since the valves were relatively small, approximately 30 mm × 15 mm in a cross section, they did not allow the use of sensors with a different shielding technique. A series of these unshielded thermocouples were placed in the ventilation valves in the top and bottom vent of the window to avoid absorbance of radiation into the thermocouples and subsequently to avoid influence of the air temperature on the measurements [20].

3.4. Boundary conditions

The window thermal transmission properties depend on the specimen itself, boundary conditions, specimen dimensions, direction of heat flux, temperature differences, and air velocity on

outdoor and indoor surfaces as well as in the ventilated cavity. The test conditions replicated the standards EN ISO 12567-1, and the values influencing the results were monitored [17]. The actual air flow provided by the fan was read by a micro-manometer. This ensured that the flow was uniform and corresponded to the actual situation. The heat flow from the glazing surface to the ventilated air was conditioned by the laminar flow when the heat surface transfer coefficient can be effectively used. The convectional heat surface transfer coefficient was dependent on the air flow velocity in the cavity and increased with the air flow.

4. Evaluation model

4.1. Principle of the $U_{w,trans}$ value air flow

The principle of a U_w value of window is not applicable in this situation because the heat loss through the window is increased by introducing an air flow and partly reclaimed by the air flow. Therefore during the experiment the heat loss of the ventilated window was separated from heat loss of ventilation. Regained heat was considered as additional heat loss through the window. Instead of U_w, a total $U_{w,trans}$ value was used to describe the performance of the ventilated window. $U_{w,trans}$ consists of the heat loss by the ventilated window $U_{w,trans,ext}$ and heat loss by the ventilation, $U_{w,vent}$, which was needed to preheat the supplied air. Using $U_{w,trans}$, window energy performance could be defined for a window with and without ventilation. The theory behind the experiment and calculation of the heat balances for a ventilated window, was based on the calculations in the program WIS [21,22], standard ISO EN 15099 [16] and work performed by Lau Markussen Raffnsøe [23].

It was possible to derive the total heat loss for a ventilated window based on detailed calculation of the window heat balance. To obtain the $U_{w,trans}$ value as defined above, the heat balances for the window-room and the window itself has to be combined. The value is compounded from three heat transfer parameters: between interior and window, between window and exterior, and ventilation through the window. [16,22,23]. Furthermore, in order to provide comparable values for evaluation of the ventilated window concept, the energy flux to heat up the preheated fresh air to room temperature, $Q_{air,vent}$, has to be added. The thermal energy balance of the window is generally given as an Eq. (1). Energy flux from the indoor environment to the window $Q_{w,trans}$, energy flux from the window to the outdoor environment $Q_{w,trans,ext}$, and energy carried by the ventilated air $Q_{w,vent}$ are depicted in Eqs. (2–4). By a combination of those equations, total energy flux $Q_{w,trans}$ and total heat transmittance of the window could be defined as in Eq. (5) where $Q_{w,trans}$ is defined on the energy fluxes, the area of the sample, and the environmental temperature difference. This concept is applicable for both windows with and without ventilation.

$$Q_{w,trans} = Q_{w,trans,ext} + Q_{w,vent} \quad (1)$$

$$Q_{w,trans} = (h_{ci} + h_{ri}) \times A_w \times (T_{ni} - T_{si}) \quad (2)$$

$$Q_{w,trans,ext} = (h_{ce} + h_{re}) \times A_w \times (T_{se} - T_{ne}) \quad (3)$$

$$Q_{w,vent} = \rho \times c_p \times \varphi \times (T_{gap,out} - T_{gap,in}) \quad (4)$$

$$U_{w,trans} = \frac{Q_{w,trans,ext} + Q_{w,vent}}{A_w} \times (T_{ni} - T_{ne}) \quad (5)$$

Density, ρ, and heat capacity, c_p, are dependent on the actual mean air temperature in the ventilated air cavity. The energy flux to heat up the ventilated air to the room temperature $Q_{air,vent}$, has to be added to the total energy flux through the window in order to quantify the energy consumption of the room-window.

4.2. Pre-heating energy evaluation

Since ventilation changes the heat balance of the window/building and generates heat loss by ventilation, a different evaluation process had to be considered for defining the heat balance. The energy performance of the airflow window is assessed and compared against that of a traditional window, which is exactly the same but without the ventilation applied. Instead, the traditional window is combined with an exhaust ventilation without heat recovery, and the principle of $U_{w,trans}$ is applied. We evaluated the increase of the ventilated air temperature compared to the standard exhaust ventilation without preheating of fresh air. The comparison reflected the decrease in energy for heating the ventilated air.

The ventilation rate was defined for a room of 60 m^3 in a renovated apartment building, which was used for a case study. It was assumed that large apartments have a larger wall-to-window ratio than small flats and thus a low airflow rate was suitable for large apartments and a higher airflow rate for small apartments. The air velocity in the exhaust valve was between 0.08 m/s and 0.5 m/s, which were derived from the size of the valve opening and the airflow volume through the window. The recommended velocity to prevent draught is 0.15 m/s [1,24]. However, lower airflow rates are preferable, because in most of the cases several windows could be used to ventilate the space and therefore they do not operate under the maximum air flow rate. High ventilation rates were used for experimental purposes.

To illustrate the magnitude of decreased energy for heating the ventilated air, a case study was used. In total, nine cases were evaluated by using three different room set-up scenarios. The first scenario depicted the energy for heating a room in the building before the renovation with 1, 2, and 3 windows installed. The second scenario evaluated the room after renovation with 1, 2, and 3 standard windows installed. Scenario three was same as scenario two but with 1, 2, and 3 ventilated windows installed. Depending on the number of windows in the facade, the airflow rates were defined as well as the energy needed to preheat the fresh air to the room temperature. The scenario with one window represented 8l/s of the airflow through the window, with two windows 4l/s and with three windows 2.5l/s.

5. Performance analysis

5.1. Uncertainty analysis

The measured data were subjected to uncertainty analyses in search of measurement errors. The accuracy of measurements in the GHB depended on many factors such as apparatus, operating test conditions, specimen properties, and sensor precision [17]. The uncertainty could be split into two categories. First was the noise and deviation of the individual measurement readings and second was the systematic deviation which was introduced by the measurement equipment precision. The uncertainty was estimated by the law of propagation based on root-sum square (RSS) formulas [17,25]. All thermocouples and power input to the metering box heater were directly adjusted according to the calibration information from manufactures by the control software.

The heat flow rate density of sample q_{sp}, the thermal transmittance of the sample, and the regained energy were functions of several independent variables, u_i, which had known uncertainty Δu_i. For example, the global uncertainty for the density of heat flow rate was defined as a general equation (6).

$$\Delta q_{sp} = \sqrt{\sum_{i=1}^{n} \left[\frac{\partial q_{sp}(u_i)}{\partial u_i} \times \Delta u_i \right]^2} \quad (6)$$

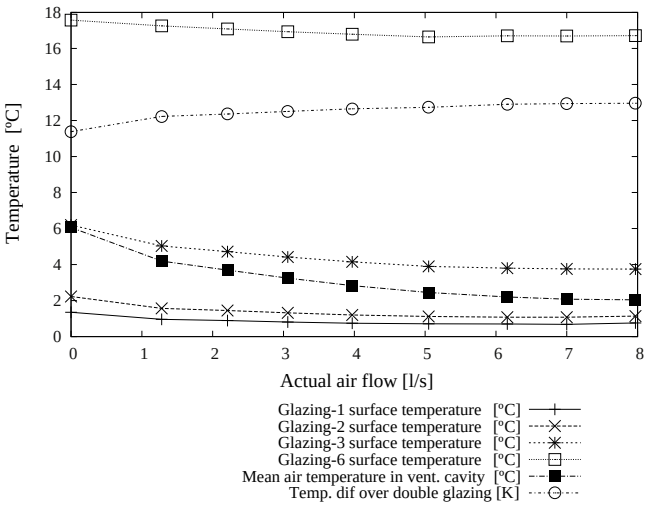

Fig. 3. Surface temperatures of glass on position 1, 2, 3 and 6 and air temperature in the ventilated cavity between the glass panes.

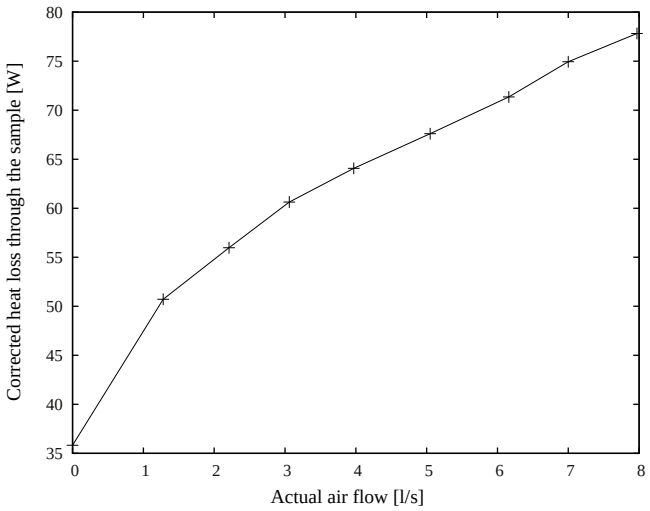

Fig. 4. Total heat loss through the sample, $Q_{w,trans}$.

Δq_{sp} was calculated from the measured total uncertainties of the heat flow rates through the surrounding panel, around the specimen edge, and into the metering box which was corrected for the heat flow through the metering box, and the area of sample by RSS, Eq. (7).

$$\Delta q_{sp} = \sqrt{\Delta \Phi_{in}^2 + \Delta \Phi_{sur}^2 + \Delta \Phi_{edge}^2 + \Delta A_W^2} \quad (7)$$

Uncertainty $\Delta U_{w,trans}$, of the measured $U_{w,trans}$ value was based on same principle. It was found that measurement itself had minimal uncertainty and therefore it could be neglected. The heat flow through the sample uncertainty varied between 0.02% and 0.3%. However the systematic deviation of the temperature measurements was relevant since the thermocouples precision was in the range ±0.5 K.

5.2. Measured temperatures

The environmental temperature in the cold side was 0 °C and steady during all measurement under different airflows. The environmental temperature in the warm side was nearly uniform and varied from 19.5 °C to 19 °C. The average surface temperatures and the average air temperature in the cavity are shown in Fig. 3. The temperatures decreased with the increase of the airflow through the air cavity. The cold air from outside, around 0 °C, entered the air cavity and cooled down the glazing and frames with the ventilation valves. By increasing the air velocity, the surface heat resistance decreased, which raised the surface heat transfer coefficient. The velocity over the surfaces was derived from the actual airflow rate and was between 0.015 m/s (1.3l/s) to 0.091 m/s (8l/s).

The mean air temperature in the cavity decreased steeper than the surface temperatures in the cavity because the volume of the ventilated air increased and the surface heat flux could not compensate for the higher volume of the ventilated cold air. Thus, the mean air temperature was approximating the mean temperature of the cavity surface closer to the exterior. In this situation, the heat transfer through the exterior glass pane was increased by applying an outdoor cold air on the surface. The temperature gradient of all surfaces was similar and indicates that the heat flow through the glass panes was dependent on the volume of the supplied air. By increasing the temperature difference over the glazing as shown in Fig. 3, it was validated that the airflow rate affects the increase of the heat flux through the double glazing. Furthermore, it was observed that the temperature on the surface 3 was relatively low and the ventilated air could not be preheated to the higher temperature. This was caused by using highly insulted double glazing with two low-emissivity coatings which on one side provided good insulating properties but on the other side did not allow air preheating.

5.3. Sample heat loss

The input from the electrical heater into the measuring box was corrected for heat loss through surround panel of the GHB, a linear thermal transmittance of an edge between the sample and the surround panel, and for a heat flow from the warm chamber to the guarded box. During the measurements, the guarded box was warmer than the metering box, which provided an extra input into the metering box. The extra heat input contribution to the metering box was between 0.35 W and 1.71 W in total, depending on the airflow. However, the additional heat input to the metering box was due to the set-up of the GHB and not due to an increase in the airflow. The total heat flux of the measured sample included heat loss of frames, heat loss of the glazing, and energy needed to preheat the air. The total heat flux was between 35.8 W and 77.8 W which corresponded respectively to the window without airflow and the window with maximum airflow. Fig. 4 shows the changes of the heat flux through the sample depending on airflow through the ventilated cavity. The correction for the surround panel and edge between the surround panel and sample was based on the calibration data and the actual temperatures. The temperature gradient at all the sensor positions was the same as for the environmental temperatures in each chamber, which described that the conditions on the both sides of the sample were steady.

5.4. Recovered heat loss and air preheating

As mentioned, the ventilated supply window works as a passive heat recovery system for preheating the ventilated fresh air. During the experiment, the heat loss of the window through a glazing and frames was partly regained by the ventilated air, $Q_{w,vent}$. The regained energy was defined based on the actual airflow volume, the air specific heat capacity, and the temperature difference between the exterior air and the exhaust window air temperature. It was detected that the air was preheated in the bottom frame before entering the glazing cavity, as it is shown by the “Valve In” line in Fig. 5. Based on the fact that air was preheated in the bottom frame, it was also assumed that the ventilated air was further preheated in the top frame. The air temperature after mixing in

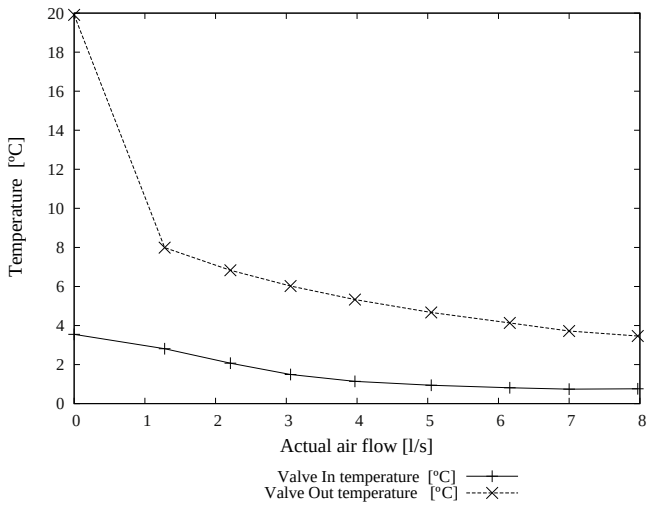

Fig. 5. Air temperatures in the inlet and outlet valves.

the top frame was used to define preheated air temperature, and is shown in Fig. 5 as "Valve Out". The thermal transmittance of the frames without ventilation was calculated based on THERM models [26] and it was estimated that the thermal transmittance of bottom frame was approximately 1.8 W/m^2 K, top frame 2.3 W/m^2 K, while the side frames was 1.7 W/m^2 K. The airflow increased the heat energy transmittance of the frames by introducing a temperature difference. The transmitted energy was partly regained but also transmitted to the exterior. Fig. 5 shows that preheating in the bottom frame varied approximately between 3 °C and 1 °C for airflow between 1.3l/s and 8l/s. From the preheating in frames could be concluded that the frames significantly increase the heat loss of the window under the airflow. The temperatures in valves were monitored by six thermocouples in the window outlet valve and six thermocouples in the window inlet valve. The temperatures in the valves differentiate ±1 °C, most likely due to the off-position from the centre of the valve and incomplete mixing of the air. The average temperatures were also examined by the uncertainty analysis. Assuming that the air was preheated from 0 °C then the air temperature was raised at the outlet by 8 °C for the airflow of 1.3l/s and 3.3 °C for the airflow of 8l/s, respectively. Fig. 6 shows that the regained heat energy varied between 12.9 W (7 W/m^2) and 34.2 W (18.2 W/m^2) for the actual ventilation flow rates between 1.3l/s and 8l/s. The decreasing gradient of the regained energy, dependent on

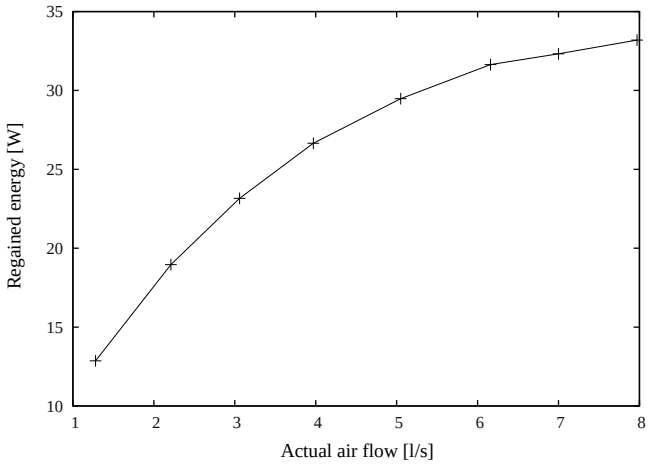

Fig. 6. Amount of recovered heat by ventilated window.

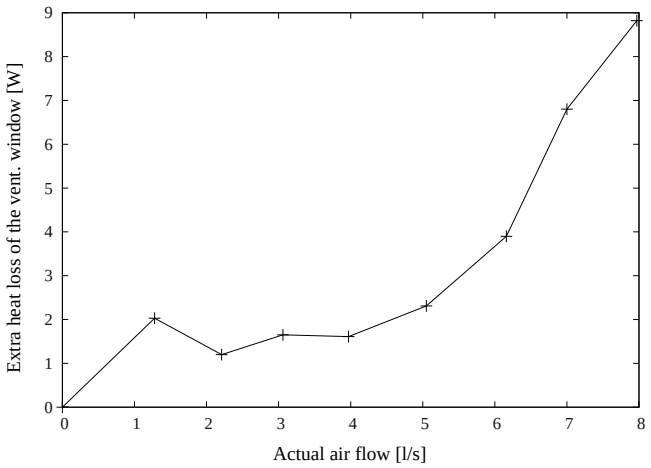

Fig. 7. Extra heat loss of a ventilated window as compared to a traditional window.

the airflow volumes, indicated that lower airflow rates were more efficient.

However, not all transmitted heat was regained by the preheating the ventilated air. Fig. 7 shows that the thermal transmittance, $U_{w,trans,ext}$, of the ventilated window ranged from 1.2 W to 8.8 W greater than the traditional window. The extra heat loss was found from an accumulation of an increased heat loss through the glazing and frames by increasing both the temperature difference and the convection surface heat transfer. Further errors in the measurements were attributed to the uncertainties discussed in paragraph 0. The peak at airflow rate of 1.3l/s was most likely caused by a relative error in the measurement point since the absolute measurements were corrected for all of the extra heat loss. The increase in the extra heat loss indicated that the heat loss through the window correlated with the change in temperature difference across the sample and furthermore with the increase of the convection heat transfer coefficient. This relationship shows that it is not worthwhile to increase the airflow rate because it increases the extra heat loss through the window, which cannot be regained. The surface temperature difference over the sealed double glazing, which corresponds to the temperature difference over the glazing, increased between 7% and 14%, which showed the reasons behind the extra heat loss. The regained energy could be increased by using less insulated double glazing, which provides a larger temperature difference over the glazing. However, double glazing will increase the extra heat loss which will not be regained and will not be beneficial because of the increased ventilated window total heat loss.

Fig. 8 shows a combination of the regained energy and the window extra heat loss, which is not regained. The energy recovery by the ventilated window lost its effect at an airflow around 6l/s. Furthermore, the results were compared to the output of the program WIS and it was found that they are correlating. The experimental results followed the increasing tendencies of the thermal transmittance of the window and higher heating energy demand for heating up the ventilated air. However, WIS did not provide the comparable data between the traditional and ventilated window. Furthermore, it was not clear how the total heat balance was defined in WIS, because the total heating load to warm up the ventilation air was accounted in the standard Uw value, while a window without ventilation misses this part of the heat loss.

5.5. Energy savings

To assess the energy performance of the ventilated window, a comparison case study was calculated. It was based on evaluation

Table 1
Heat energy savings comparison for room with and without the ventilated window.

	Before renovation			After renovation			After renovation + VW		
	1 win	2 win	3 win	1 win	2 win	3 win	1 win	2 win	3 win
Heat loss by ventilation (W)		201.7			201.7		166.4	148.2	136.1
Heat loss by infiltration (W)		201.7			28.2			28.2	
Heat loss by external wall (W)	263.6	227.2	190.8	131.8	113.6	95.4	131.8	113.6	95.4
Heat loss by window (W)	91.0	182.0	273.1	40.0	80.1	120.1	40.0	87.4	142.0
Total heat loss (W)	757.9	812.6	867.2	401.7	423.6	445.4	366.5	377.4	401.7
Ventilation vs. total (%)	26.6	24.8	23.3	50.2	47.6	45.3	45.4	39.3	33.9
Energy decrease by VW (%)		–			0.0		8.8	10.9	9.8

VW, ventilated window.

of energy needed for heating while the required ventilation had to be fulfilled in a room. Calculated energy savings were determined by using a ventilation exchange rate for rooms of 0.5 h^{-1}. It was assumed that air infiltration in the dwelling building was 0.5 h^{-1} before renovation and 0.07 h^{-1} after renovation when the building was air tightened and windows replaced. As representation of the different dwellings in the apartment building, a simplified mid-size room of 4 m × 5 m × 3 m, with floor area of 20 m^2, external walls of 15 m^2 and total volume of 60 m^3 has been selected for assessment of the ventilated window in different scenarios. The room was evaluated with windows with standardized size of 1.48 m × 1.23 m installed. As mentioned previously, three scenarios, each with 1, 2 or 3 windows illustrate preheating of the air under different airflows through the windows. Other parameters were constant over the scenarios to focus only on the evaluation of the effects of the ventilation window on the energy demand for heating. It was assumed that the room did not have any heat loss through the ceiling, floor and interior walls. Scenarios 1 and 2 illustrated how the ventilation heat loss became a more significant part of total energy demand of the heating after the renovation when 10 cm of thermal insulation was added to the 70 cm brick wall. By tightening the building, insulating external walls and changing the windows, the total energy consumption was significantly reduced. The energy needed for heating of the ventilation air changed from 26.6% to 50.2%, from 24.8% to 47.6% and from 23.3% to 45.3% of the total energy demand for the room with one, two and three windows installed. The air temperature difference to preheat was 20 K for scenario 1 and 2, and 16.5 K, 14.7 K and 13.5 K for scenario 3 with 1, 2 and 3 windows. The window's thermal transmittance varied with the ventilation airflow between 1.1 W/m^2 K and 1.3 W/m^2 K compared to the 1 W/m^2 K for the traditional windows and 2.5 W/m^2 K for the windows before the renovation. The increase of ventilation heat loss compared to the situation before renovation is approximately doubled, which shows increasing importance for reducing energy needed to heat the ventilated air. By preheating the air in the ventilated windows, the decrease of the heat load for ventilation reduced the total heating demand for the room by 8.8%, 10.9% and 9.8% for the scenarios with 1, 2 and 3 windows installed. This shows that a higher benefit occurs in the scenario with two windows installed, indicating that high ventilation rates are not feasible for energy savings. Table 1 shows the room set-up parameters for the individual scenario and indicates the potential heating energy saving in each scenario.

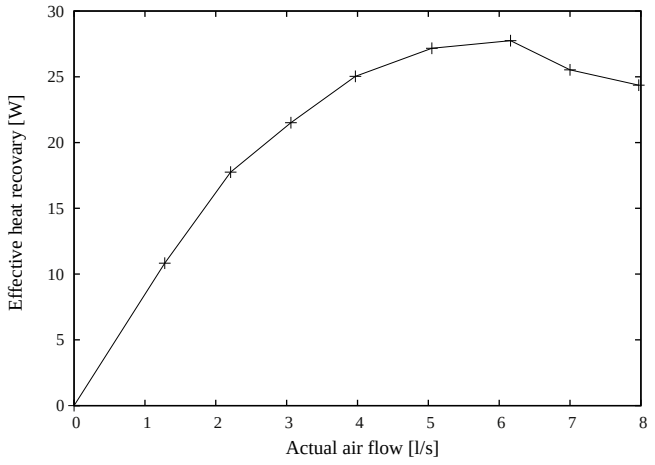

Fig. 8. Effective heat recovery of the window.

6. Conclusion

In this article, the thermal performance of a ventilated window is compared to the thermal performance of a traditional window by experimental testing in a Guarded Hot Box. The window was exposed to eight different airflow rates varying between 1.3l/s and 8 l/s under a constant temperature difference of 20 K across the test sample. Experiments confirmed that fresh air could be preheated by ventilating the fresh air through the window, regaining some of the window heat loss. The recovery efficiency depended on the airflow rate, decreasing with higher ventilation rates. The window investigated in this article was no longer energy-beneficial at airflow rates larger than 6l/s, at which point the increased heat losses due to increased window thermal transmittance became larger than the amount of energy regained by preheating. The investigation revealed that a part of the preheating of the air happened in the frames and was between 3 °C and 1 °C, depending on the airflow rate. However, the preheating of the ventilated air in the frames caused higher heat loss through the window frames with the ventilation valves and consequently caused an increase of the total window thermal transmittance. The case study calculations compared a room in an apartment building with windows with and without ventilation and showed that the total heating demand including the heat loss by ventilation can be reduced by more than 10%. The case with the ventilated window was compared to a room with combination of a traditional window and exhaust ventilation. The ventilated windows can be useful in situations where installation of ventilation with heat recovery is not possible and/or cost effective. However, it is not feasible to use ventilated windows in buildings with high required ventilation rates and a small number of windows because the regaining energy efficiency of ventilated windows decreased with the increasing airflow rates. In addition to the experimental work, the article formed a unified methodology for the assessment of the energy performance of ventilated windows. The heat balance for window-room-ventilation was defined and can be used for comparing a traditional window to a ventilated window.

Acknowledgements

The research performed in this article was funded by the Danish Energy Agency programme on research and development of energy

efficiency, F&U–2008, under the project name "ProVent: Design Knowledge for Ventilation Windows in Low Energy Buildings without Electricity Consuming Mechanical Ventilation with Heat Recovery", number 340-035. The authors would like to acknowledge project partners Niras A/S and Horn aps for their co-operation and contribution to this paper. The authors also wish to thank colleagues at DTU.BYG for their useful feedback and advice.

References

[1] BR, the Danish Building Code, 2010. http://www.ebst.dk/.
[2] European Directive on the Energy Performance of Buildings, Directive 2002/91/EC of the European Parliament and of the Council of 16 December 2002 on the Energy Performance of Buildings, 2002.
[3] C.E. Ochoa, I.G. Capeluto, Strategic decision-making for intelligent buildings: comparative impact of passive design strategies and active features in a hot climate, Building and Environment 43 (2008) 1829–1839.
[4] E. Lee, et al., High-Performance Commercial Building Facades. Building Technologies Program, Lawrence Berkeley National Laboratory, 2002.
[5] D. Appelfeld, C.S. Hansen, S. Svendsen, Development of a slim window frame made of glass fibre reinforced polyester, Energy and Buildings vol. 42 (2010) 1918–1925.
[6] J. Wei, J. Zhao, Q. Chen, Optimal design for a dual-airflow window for different climate regions in China, Energy and Buildings 42 (2010) 2200–2205.
[7] P.H. Bakert, M.E. McEvey, An investigation into the use of a supply air window as a heat reclaim device, Building Services Engineering Research and Technology 20 (3) (1999) 105–112.
[8] J.R. Gosselin, Q. Chen, A dual airflow window for indoor air quality improvement and energy conservation in buildings, HVAC&R Research 14 (3) (2008) 359–372.
[9] D. Saelens, S. Roels, H. Hens, Strategies to improve the energy performance of multiple-skin facades, Building and Environment 43 (2008) 638–650.
[10] J. Tanimoto, K. Kimura, Simulation study on an air flow window system with an integrated roll screen, Energy and Buildings 26 (1997) 317–325.
[11] (a) D. Saelens, S. Roels, H. Hens, The inlet temperature as a boundary condition for multiple-skin facade modelling, Energy and Buildings vol. 36 (2004) 825–835;
(b) EN 673, Glass in Building – Determination of Thermal Transmittance (*U* value) – Calculation Method, European Committee for Standardization, Brussels, Belgium, 1997.
[12] J.S. Carlos, H. Corvacho, P.D. Silva, J.P. Castro-Gomes, Real climate experimental study of two double window systems with preheating of ventilation air, Energy and Buildings 42 (2010) 928–934.
[13] T.T. Chow, Z. Lin, K.F. Fong, L.S. Chan, M.M. He, Thermal performance of natural airflow window in subtropical and temperate climate zones – A comparative study, Energy Conversion and Management 50 (2009) 1884–1890.
[14] H. Manz, A. Schaelin, H. Simmler, Air of patterns and thermal behaviour of mechanically ventilated glass double facades, Building and Environment 39 (2004) 1023–1033.
[15] M.J. Holmes, Optimisation of the thermal performances of mechanically and naturally ventilated glazed facades, Renewable Energy 5 (1994) 1091–1098, Part II.
[16] ISO 2003, ISO 15099:2003(E), Thermal Performance of Windows, Doors and Shading Devices – Detailed Calculations, International Organization for Standardization, Geneva, Switzerland, 2003.
[17] EN ISO 12567-1, Thermal Performance of Windows and Doors – Determination of Thermal Transmittance by the Hot-Box Method. Part 1. Complete Windows and Doors (ISO/FDIS 12567-1:2010), European Committee for Standardization, Brussels, Belgium, 2010.
[18] EN ISO 8990, Thermal Insulation. Determination of Steady-State Thermal Transmission Properties – Calibrated and Guarded Hot Box, European Committee for Standardization, Brussels, Belgium, 1996.
[19] DS/EN 15242, Ventilation for Buildings – Calculation Methods for the Determination of Air Flow Rates in Buildings Including Infiltration, European Committee for Standardization, Brussels, Belgium, 2007.
[20] K. Duer, Characterisation of advanced windows, in: Determination of Thermal Properties by Measurements, Technical University of Denmark, 2001, ISBN 8778770629.
[21] WinDat, Window Information System software (WIS), WinDatThematic Network, TNO Bouw, Netherlands, 2006. http://www.windat.ucd.ie.
[22] D. van Dijk, R. Versluis, Definitions of *U*- and *g*-value in case of double skin facades or vented windows, WinDat document N3.08 – Public, 2004.
[23] L.M. Raffnsøe, Thermal Performance of Air Flow Windows – Master thesis, Technical University of Denmark, Department of Civil Engineering, 2007.
[24] J. Toftum, R. Nielsen, Draught sensitivity is influenced by general thermal sensation, International Journal of Industrial Ergonomics 18 (1996) 295–305.
[25] S. Yuan, G.A. Russell, W.P. Goss, Uncertainty analysis of a calibrated hot box, insulation materials: testing and applications, in: A.O. Desjarlais, R.R. Zarr (Eds.), ASTM STP 1426, vol. 4, ASTM International, West Conshohocken, PA, 2002, ISBN 978-0803128989.
[26] R. Mitchell, C. Kohler, D. Arasteh, THERM 5.2/WINDOW 5.2 NFRC Simulation Manual, Lawrence Berkeley National Laboratory, University of California, Berkeley, CA, 2006.

Paper III

"An hourly-based performance comparison of an integrated micro-structural perforated shading screen with standard shading systems"

D. Appelfeld, A. McNeil & S. Svendsen

Published in: *Energy & Buildings, 2012*

Energy and Buildings 50 (2012) 166–176

Contents lists available at SciVerse ScienceDirect

Energy and Buildings

journal homepage: www.elsevier.com/locate/enbuild

An hourly based performance comparison of an integrated micro-structural perforated shading screen with standard shading systems

David Appelfeld[a,*], Andrew McNeil[b], Svend Svendsen[a]

[a] Department of Civil Engineering, Technical University of Denmark, Brovej, Building 118 DK-2800 Kgs. Lyngby, Denmark
[b] Building Technologies, Lawrence Berkeley National Laboratory, 1 Cyclotron Road, Berkeley, CA 94720, United States

ARTICLE INFO

Article history:
Received 24 February 2012
Received in revised form 8 March 2012
Accepted 16 March 2012

Keywords:
Shading
Complex fenestration system
Solar gains
Daylight
Building performance modelling

ABSTRACT

This article evaluates the performance of an integrated micro structural perforated shading screen (MSPSS). Such a system maintains a visual connection with the outdoors while imitating the shading functionality of a venetian blind. Building energy consumption is strongly influenced by the solar gains and heat transfer through the transparent parts of the fenestration systems. MSPSS is angular-dependent shading device that provides an effective strategy in the control of daylight, solar gains and overheating through windows. The study focuses on using direct experimental methods to determine bi-directional transmittance properties of shading systems that are not included as standard shading options in readily available building performance simulation tools. The impact on the indoor environment, particularly temperature and daylight were investigated and compared to three other static complex fenestration systems. The bi-directional description of the systems was used throughout the article. The simulations were validated against outdoor measurements of solar and light transmittance.

1. Introduction

Buildings are responsible for usage of significant amount of the energy and account for 40% energy consumption in Europe and the USA. Energy reduction by buildings has become an important part of energy policy and is reflected in building regulations, which require decreased total building energy demand [1,2]. The largest energy usage is attributed to heating, cooling and electrical lighting.

Optimization of window elements can reduce energy consumed for heating, cooling and electric lighting. Optimization strategies consider heating by increasing solar gains, cooling by providing solar protection and lighting by utilizing daylight [3]. All the functions cannot be addressed by a standard window and the traditional windows have to be combined with shading systems, which then can be described as complex fenestration system (CFS). The challenge is to evaluate those parameters in an interconnected context for CFS performance, since some of the functions are contradicting for static systems, e.g. increasing solar gains in winter while providing shading in the summer [4].

In recent decades, new and renovated buildings have become increasingly insulated and air tight. These steps lower building heating loads but they also increase risk of overheating by capturing excess solar gains, especially in office buildings. Removing overheating by mechanically cooling is expensive and can negate the savings from solar gains in the winter, and thus cooling loads are growing in importance. Contemporary commercial and institutional buildings typically have a low heating and high cooling loads as they have high internally generated loads by people/lights/equipment and have well-insulated envelopes. Residential buildings have relatively low internal loads vs. their envelope loads [4]. Solar shading is an effective strategy to reduce overheating and diffuse direct sunlight thus reducing energy consumption [3]. There are many options available for shading systems and it is difficult to precisely describe the energy performance impact of a non-standardized solution [5,6]. Many of the CFSs have angularly dependent solar and light energy properties but use normal-incidence glazing values of the performance indicators, e.g. total solar energy transmittance. The normal-incidence value description is not an accurate indicator for angularly dependant systems, which need to be described with bi-directional data [7]. The limitations of the available simulation tools and testing methods can be overcome by performing state-of-the-art simulation and its validation with measurements [8].

The main motivation for this research is to establish a procedure for generating information, which can be used during product development of CFSs or an initial phase of building design. This paper focuses on the performance modelling of CFSs and comparison between types. The results of the simulations were compared against measurements taken outdoors and in a laboratory. The

* Corresponding author. Tel.: +45 45251856; fax: +45 45883282.
E-mail address: dava@byg.dtu.dk (D. Appelfeld).

0378-7788/$ – see front matter © 2012 Elsevier B.V. All rights reserved.
doi:10.1016/j.enbuild.2012.03.038

aim is to determine the performance criteria of the tested CFSs to indicate impact on the energy and indoor climate in the occupied spaces.

2. Method

Performance is simulated for several shading systems and a comparison is based on the evaluation of various aspects. The bi-directional transmittance simulation results compared to measurements. The performance evaluation is performed with several steps, starting with the shading layer and ending with shading system impact onto a reference room. The design criteria for widows and CFS in modern buildings are:

- Energy use – heating, cooling, electrical lighting
- Thermal comfort – overheating
- Visual comfort – daylight, glare, view to outside

These criteria are interdependent, in this study they are addressed in the context of the following aspects: facade orientation, building location, time of day and year, window size, window position on facade, shading strategy, and human factors (view, comfort and temperature).

The building location determines the climate, including the sun position and sky luminance distribution, which is further dependent on the actual time/date. The central criteria for this article is angular dependant light transmittance (T_{vis}) and solar transmittance (T_{sol}) of the CFS. With these parameters the solar heat gain coefficient (SHGC) could be described, which is also referred as the total solar transmittance (g-value) and is central in determining cooling loads of buildings. The thermal transmittance of windows (U_w-value) is one of the major energy performance characteristics controlling heat loss. Transmittance refers to both T_{vis} and T_{sol} further in the paper if not specified otherwise.

In this paper, the interconnections of the above parameters are illustrated in case examples presented throughout the paper. Annual performance simulations are carried out when possible.

2.1. Complex fenestration systems

This study focused on a micro structural perforated shading screen (MSPSS) which is made of an insulated double glazed unit with low-e coating on surface 3 and the MSPSS on surface 2. The MSPSS is made from a stainless steel sheet with elliptical holes smaller than 1 mm. The holes are cut in a downward direction (when viewed from the inside) to reduce transmission from sources above the horizon and increase transmission from below the horizon. MSPSS was selected because the angular dependence is not symmetrical about the normal making it difficult or impossible to evaluate with standard simulation tools. The MSPSS combines solar and glare protection, provides direct view out and is not included in any standard testing software. Fig. 1 shows a side-by-side view through the MSPSS with an unobstructed view. From observations the view appears less obstructed when viewed at a greater distance. The picture is slightly blurry as it was necessary to focus on the shading layer and the background was in the distance.

In order to have a complete understanding of performance, the tested CFS is compared to references systems. MSPSS was compared to clear double glazed windows, without shading, with horizontal venetian blinds, and with a semi-transparent roller shade. The clear glazing reference case was studied to demonstrate the effect of the shading and glazing separately. Venetian blinds were used as a comparison because they are a conventional system that also provides shade and permits view. A roller shade was also used as a reference because it blocks solar gains and glare more efficiently then the semi-opened system, however, unlike MSPS and Venetian blind, it blocks the view to outside.

Fig. 1. View through MSPSS (left), unobstructed view (right).

All the shading systems were simulated with the same glazing. In all cases, the shading was located between the glass panes to limit the variations in the energy performance of the individual systems.

2.2. Determining bi-directional transmission characteristics

T_{sol} and T_{vis} are the fundamental performance indicators for CFS and all the following calculations were based on them. The calculations are carried out in several sequential steps with increasing level of information.

2.2.1. BSDF generation via simulation

Radiance was used to generate a bi-directional scattering distribution function (BSDF). Radiance is an accurate backward ray-tracing Unix-based programme that has been validated for such purposes [9]. The new software development allows generating a BSDF, which describes transmittance dependent on incident angle (IA). A model of the MSPSS was created using detailed geometric drawings from the manufacturer and reflectance measurements of an un-perforated sample also provided by the manufacturer. Radiance's programme genBSDF was used to generate a BSDF matrix [10]. The genBSDF programme generates blocks of values which describe 145 Klem's incidence angles for one of 145 oppositely placed outgoing directions [11]. This data was validated against goniophotometer measurements for a few incident angles [12]. The validated BSDF was used to calculate T_{sol} and T_{vis} of the glazing unit with the shading screen.

2.2.2. Comparing measurement with simulations

Measurements were taken of the MSPSS taken to ensure that daylight simulations using BSDFs would reliably reproduce real-world results. Measurements were taken outdoors in order to include direct light from the sun and diffuse light from the sky reproducing the type of environments experienced by a real building. Both components of daylight are important because together they determine indoor daylight conditions, unlike cooling loads which are highly dependent on the direct sunlight [3]. Measurements were taken on clear days in June and July because clear skies are the most reliably reproduced of the CIE sky types (and clear skies are commonly occur in the summer in Denmark, where the measurements were taken) [9]. The sample was rotated to imitate different incident azimuth and altitude angles so that many

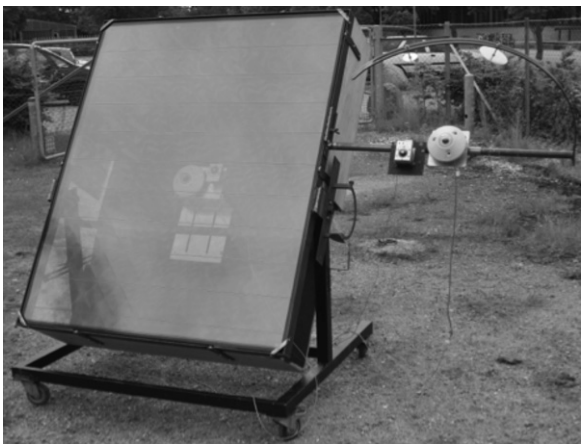

Fig. 2. Movable measurement test rig with sample mounted.

IAs could be tested in a short time. The dynamic sample positioning introduced inconsistent ratios of exposure to sky and ground for the sample. To counteract this, the sample was positioned in the simulation to match the position of the sample during each measurement, and thus the measurements and simulations were analogous.

To quickly rotate samples, a movable rig was used, that safely held the test sample and allowed to adjust the sample with respect to the sun. Due to the size of the sample, only IAs up to 60° could be measured, as accuracy could not be ensured with higher IAs. Transmittances for higher IAs were derived from simulations. The test rig, shown in Fig. 2, consisted of a mounted sample and two sets of illuminance and irradiance meters, which were aligned to the surface of the sample. One illuminance and irradiance sensor was placed behind the sample, close to the glass surface, to measure the light transmitted by the sample. The other illuminance and irradiance sensors were placed on the side of the measurement rig to measure light incident on the sample. Relative transmittance of the sample was calculated by dividing the transmitted measurement by the incident measurement. Using relative measurements accommodates surrounding with obstacles without introducing large error to the results.

A solar pointer, shown in Fig. 3, was used to accurately align the sample for each IA. The pointer, of known length, was positioned perpendicular to the surface of the glazing and a measuring. The measuring grid is marked with shadow points for each incident angle. The sample can be moved until the shadow from the pointer aligns with the shadow point for the desired incident angle. The process allows for accurate sample alignment, reducing errors in IA. Every IA was measured with and without the sensors shaded from the direct light to determine diffuse and direct radiation. Each measurement was repeated at least twice to reduce measurement error.

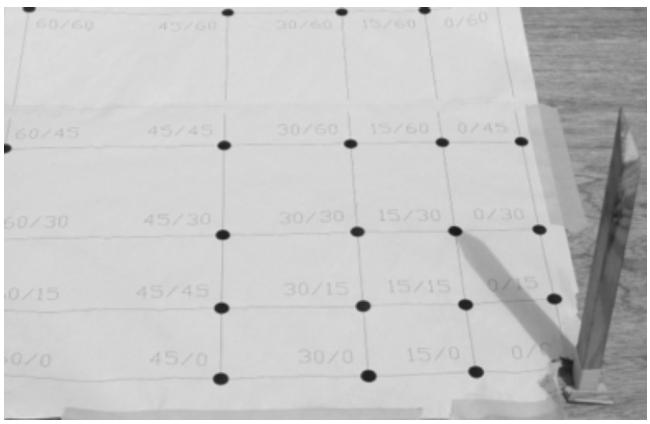

Fig. 3. Solar pointer and measurement grid, the current IA is azimuth of 15° and altitude 30°.

Table 1
Model's surface properties.

	Wall	Ceiling	Floor
Reflectance	0.5	0.8	0.3

By recording the time, sun position, total horizontal hemispherical diffuse illuminance and direct normal illuminance, it was possible to reproduce sky conditions in the simulations. Clear glazing with known properties was tested in the same manner to validate the both the measurement and simulation procedures. The sensors were calibrated before the measurements to minimize the sensor precision error.

The first preliminary test was carried out without a sample to determine how much the test rig shades the sensors. The test verified that this error was smaller than the accuracy of the sensors and therefore could be neglected. The rig was equipped with a shading box behind the sample to shade specular reflections from the sample's back surface and the ambient environment.

2.3. System performance simulations

2.3.1. Model description

The simulated model was a single office for three occupants with dimension of 3.5 m wide, 5.4 m deep, and 2.7 m high. The room model is based on the test office in IEA task 27 in order to have standardized model [13]. The window varies from the test office and is modelled as one large window of 1.2 m × 2.5 m with a 1 m sill. The surface properties of the room are listed in Table 1. The plan view of the room with the furniture is shown in Fig. 4, including view directions. The view height is 1.2 m above the floor, which corresponds to eye-level for a sitting person.

The thermal model of the office was built with an assumption that all adjacent offices have the same temperature, except the exterior wall and window, which were exposed to the outdoors. Thermal transmittance of the external wall was 0.5 W/m^2 K and the infiltration was set to 0.5 AC/h.

2.3.2. Annual daylight simulations

Radiance was also used to simulate of the daylight conditions in the reference office. Work plane illuminance was simulated throughout a year and daylight autonomy was used to evaluate the annual results. The heating and cooling loads of the tested office

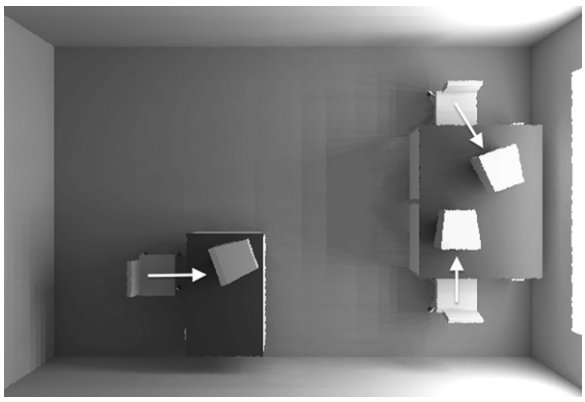

Fig. 4. The plane view of the office with view directions.

were calculated in ESP-r, which allows use bi-directional information about solar energy transmittance of CFS.

The Radiance three phase method (TPM) allows users to calculate the annual daylight performance of CFS using bi-directional information without a significant increase of the computational time. The TPM is based on the multiplication of four matrices describing light through an interior (view matrix), fenestration (transmittance matrix), exterior (daylighting matrix), and sky distribution (sky vector). This process allows for a relatively quick dynamic light and solar radiation simulation over a year. Additionally, by changing only one of the matrixes various aspects could be effectively investigated: different orientations by changing the daylighting matrix, location by changing sky vector, and different CFS by using different BSDF [5].

2.3.3. Electrical light savings and daylight

The electrical light energy was computed for all four scenarios, when no daylight is utilized to fulfil required illuminance criteria. Two work plane illuminance criteria for offices were used: 500 lx according to standard CEN-EN 15251 [14] and 300 lx according to IESNA [15,16]. The office was divided into three 1.8 m deep and 3.5 m wide lighting zones, with zone 1 closest to the window and zone 3 furthest from the window. Each zone was separately controlled. The relatively small zones were used mainly for investigational purposes to show the potential lighting energy savings.

Two control strategies were considered: on/off switching and bi-level switching. For on/off control the electric lighting in a zone was switched off when daylight alone provided the required work plane illuminance. With bi-level switching the electric lighting could be switched to half output (by switching off half of the lamps in the zone) when the daylight illuminance met half of the work plane illuminance criteria and could be switched off entirely when daylight illuminance met the full work plane illuminance criteria.

The lighting power density (LPD) for the working plane illuminance (WPI) of 500 lx of 15 W/m^2 was derived from standard EN 15193 [17]. Electric lighting savings were based on the linear substitution of electrical lighting by daylight and thus are idealized. For the WPI of 300 lx an equivalent LPD of 9 W/m^2 was used.

Daylight was evaluated using daylight autonomy (DA), which is the percentage of hours satisfying the minimal design WPI in the total number of working hours in a year [18].

2.3.4. Glare

Glare was evaluated because visual comfort of the CFS is an important aspect of the CFS performance. Daylight Glare Probability (DGP) was selected as a glare index because it is based on an extensive human evaluation study [19,20]. Glare analysis was performed for all three working positions in the office. Glare was assessed on an annual basis focusing on the working hours between 8:00 and 18:00.

2.3.5. Net energy gains

The glazing unit properties were used to calculate net energy gains (NEG). The NEG calculation method is based on a window's solar gain minus its heat loss based on outdoor temperature during the standard heating season [21,22]. NEG is a simplified method that describes the relationship between a window and a building, in kW h/m^2. The formula for NEG is:

$$E_{\text{ref}} = g \cdot I - U \cdot D$$

where I is the coefficient for solar gains and D is coefficient for heat loss. For Denmark the total coefficient for solar gain is 280.6 kW h/m^2, for north 105 kW h/m^2, for south 431 kW h/m^2 and for east/west 232 kW h/m^2. The solar gain coefficients are further multiplied by an assumed shading factor 0.7 [23]. The assigned contribution from south is 41%, north 26% and east/west 33%. The heat loss coefficient D for the heating season in Denmark is 90.36 kKh [21].

2.3.6. Energy performance

Kuhn et al. found that heating demand in the cold climates calculated using standard evaluation techniques was overestimated up to 23% and that cooling demand was underestimated up to 99% [24,25]. This study aims to determine if bi-directional information, especially angle dependant g-value, provides more accurate results for heating and cooling loads [26]. The evaluated location, Copenhagen, Denmark, is located in a Nordic climate, which could be considered as a moderate climate zone, however the cooling loads have to also be taken into account, as they are a significant part of the energy consumption in modern buildings [27]. Furthermore energy performance was calculated for Prague, Czech Republic, and Rome, Italy, to illustrate the performance based on the location.

The ESP-r model for using bi-directional information about solar energy transmittance is called Black-Box-Model and was validated [6,24,26]. The model 5° resolution for azimuth and altitude incident angles on the surface of the CFS.

3. Results

3.1. Outdoor measurements vs. Radiance simulation

The comparison of Radiance simulation results against outdoor measurements of Tvis and Tsol is shown in Fig. 5. The difference in the corresponding curves is between 0% and 4%, except for visible transmittance at the IA of 60° where the relative error is around 18%. This error was caused by comparing the relatively small values and in absolute numbers would not be significant and/or by slightly off-position of the measuring rig. The Radiance simulation results were generated using the TPM.

3.2. BSDF

BSDF's are generated by programmes genBSDF and Window6 to provide a more comprehensive description of the shading properties dependency on the azimuth and altitude of the sun. These BSDFs were validated by McNeil et al. in a connected study [10]. Fig. 6 contains visualizations of results for the front T_{vis} of the four shading systems, independent of window orientation and location.

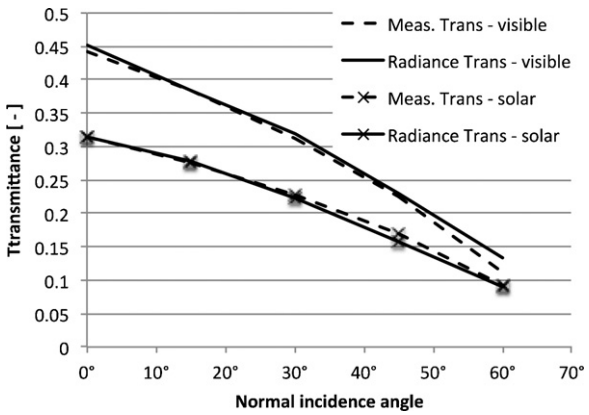

Fig. 5. Comparison of measured and simulated T_{vis} and T_{sol}.

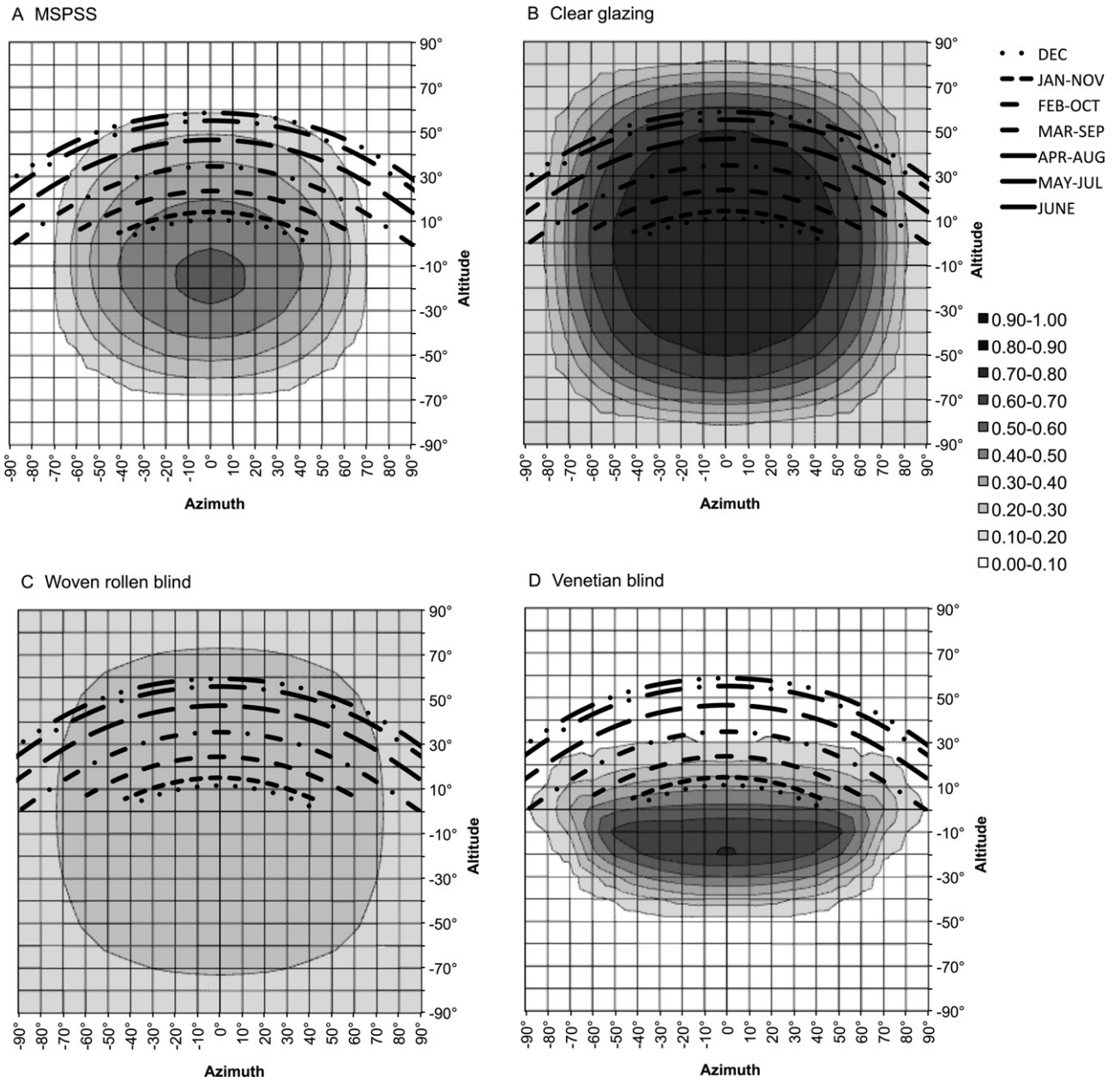

Fig. 6. Visible transmittance of CFSs with solar path of Copenhagen.

For a better understanding of the relation between the transmittance and IA the annual sun path for Copenhagen is added to the charts.

As expected the solar transmittance is the highest for the clear glazing and is symmetrical around the centre. The woven roller shade has the lowest transmittance, as it evenly reduces the transmittance and blocks view to the outside. The MSPSS and venetian blinds are more IA dependent and allow higher transmittance for the negative altitude. In other words, the light is blocked more effectively from sky. Both shadings have their highest transmittance around -15° of altitude.

For the locations of Prague and Rome the shading efficiency will be higher because the sun altitude is also higher. The solar gains can be utilized by angularly dependent systems during the winter months when the sun is low and transmittance is higher. Additionally, effective shading occurs during the summer when the sun altitude is higher. The maximum light transmittance of the MSPSS and venetian blinds was between 0.5 and 0.6, while for clear glazing it was up to 0.8. The glazing with roller shade had high shading effects and the transmittance was as low as 0.2.

3.3. Daylight autonomy

Fig. 7 contains daylight autonomy (DA) results for all four systems on south facing facades. The shaded bands illustrate the percentage when a certain level is reached. For example, for a glazing with MSPSS, 80% of working hours have an exposure of at least to 216 lx at a distance of 0.5 m from facade.

A logarithmic scale was used to provide better visibility of smaller values because the clear glazing provided high illuminance closer to the window and far exceeded other values in the chart, which were still valuable and fulfil the requirements. As expected, DA was higher close to the window and DA was lower in the back of the room. At the back of the room DA did not satisfy the lighting

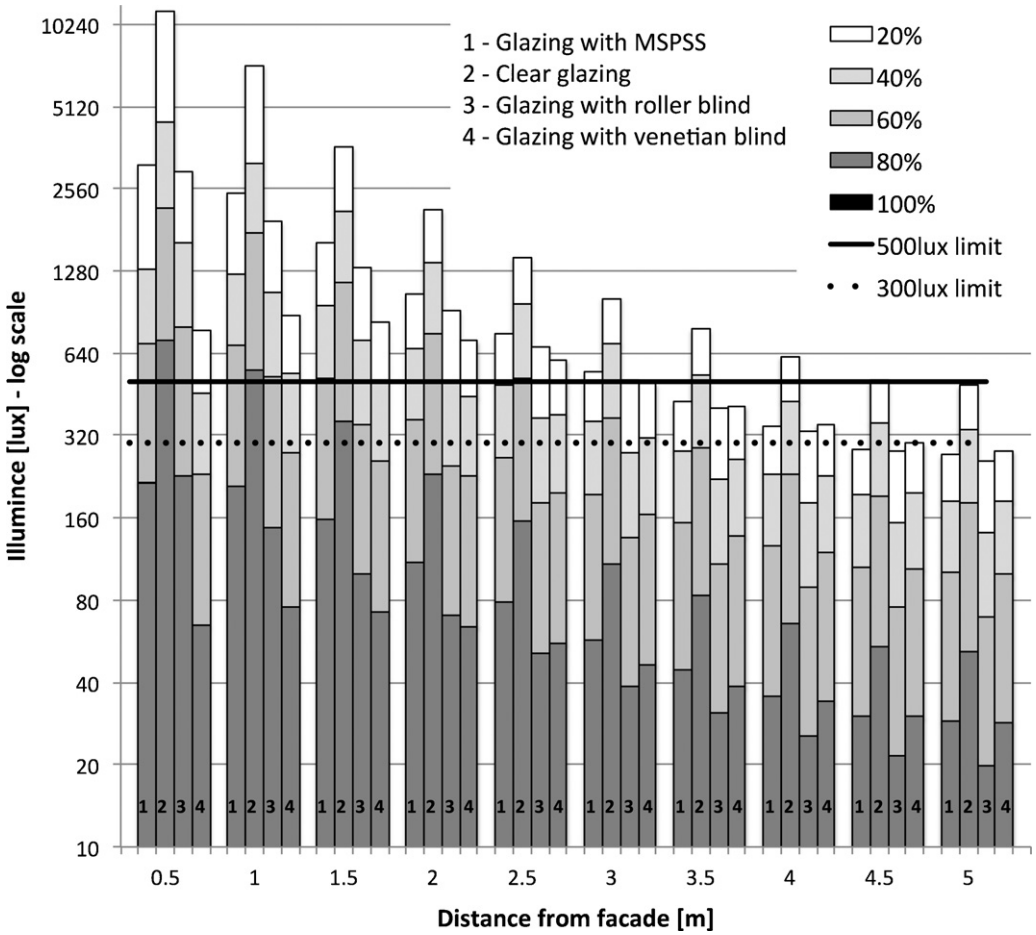

Fig. 7. Daylight autonomy.

requirements. The highest illuminance was provided with the clear glazing with WPI 10 klx close to the facade, which far exceeds WPI criteria thus the energy cannot be fully utilized and may indirectly cause a glare and overheating. The solutions with lower relative WPI can still serve purpose without the risk of a glare and overheating. While there is not a direct correlation between a WPI and glare, values above 4500 lx are generally not desirable [16,19,28]. The illuminance levels for systems with shading systems were similar with slightly better performance for MSPSS.

3.4. Electrical light savings

The analysis assumed that the light in a zone was switched off when the daylight illuminance fulfilled the WPI criteria (on/off control). In addition, bi-level switching was considered, which allows the LPD to reduce by 50% when half the WPI criteria were met by daylight illuminance (i.e. switching off half the lamps in a zone). In Figs. 8 and 9 the savings were split by on/off and bi-level lighting control. The on/off savings mean fulfilment of the criteria 300 lx or 500 lx, and bi-level were the additional savings by introducing bi-level control strategy.

The largest savings generally occurred in zone one, which was commonly saturated by daylight. Zone 3 is less exposed to daylight and thus the savings were smaller.

By illustrating the difference when the light was either fully or 50% switched off it was possible to see that in the front of the room daylight reached higher illuminance and the light was completely off, while in the back off the room the major power savings were because the bi-level lighting control system. Therefore the savings were influenced by the light control strategy. Furthermore, the savings followed illuminance levels in Fig. 7. This indicated that it was possible to shade excessive illuminance, while providing the savings of the lighting energy, as the clear glazing did not produced significantly higher savings. Additionally there was not significant difference between scenario with 500 lx and 300 lx.

The savings in zone 3 were mainly during the winter period when the sun is low and the penetrated light could reach the back of the room.

3.5. Glare assessment

Fig. 10 shows Daylight Glare Probability (DGP) for the four systems and three views. The graphs display the glare rating for every hour during the whole year. All three evaluated views are marked and illustrated in Fig. 4. View 1 was parallel along the window pointing to east and thus the higher DGP values occurred before noon. View 2 faced to southeast and higher DGP values were during afternoon. View 3 was oriented to the window, south, and higher DGP index was at noon.

The most glare occurs with clear glazing, as no direct sunlight was blocked. Conversely, the least glare occurs with the roller shade, particularly for view 1 and view 3 which experience no glare. An expected result would be that the roller shade would also prevent glare for view 2, however the position was close to the source and the roller shade was partially transparent, therefore glare occurred.

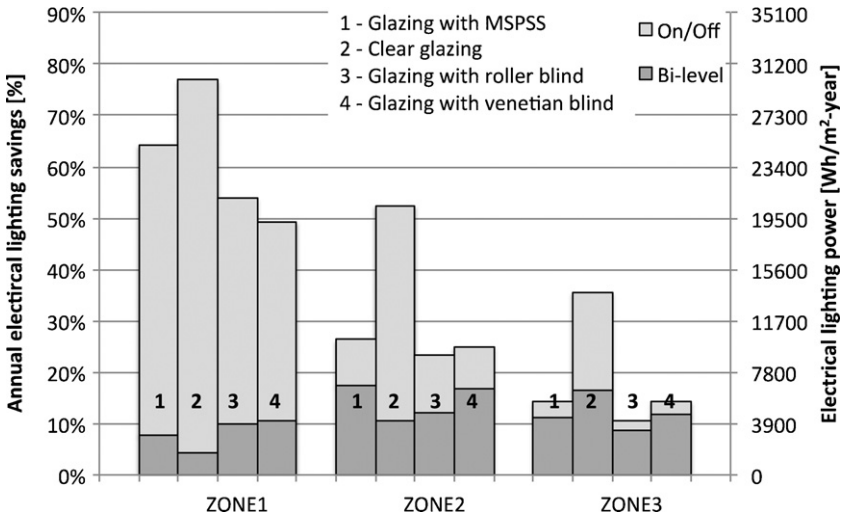

Fig. 8. Electrical light saving for work plane illuminance of 500 lx.

Of the three views studied, view 2 experiences the most glare. Glare occurs year round with clear glazing, while glare occurs only seasonally with the shading systems.

The venetian blinds block slightly more glare than MSPSS in all views, which was caused by more selective transmittance of the venetian blinds, with the lower transmittance under higher IAs. This was also possible to assume from the carpet plots in Fig. 6 and later in Fig. 12, describing angularly dependent transmittance. The observation would not be possible by considering transmission at normal-incidence only.

3.6. Net energy gain

The total solar energy transmittance (*g*-value) is the fraction of the actual solar energy that passes through the window. The CFSs were modelled in Window6 with shading located between the glass panes to avoid favouring internal or external shadings. Table 2 contains the centre pane *U*-values and normal incidence *g*-values. The results in Table 2 for individual sides do not include assigned percentage of the distribution to the individual orientation. The result of NEG for all four shading solution in the respect of the facade orientation is in Fig. 11.

MSPSS had the lowest NEG, which is mainly caused by a negative contribution from a north facade and low solar gains contribution from south. Nevertheless, shading should be used primary for the south facade and considered for the east and west facade. The MSPSS results show that the MSPSS reduces overeating, thus the MSPSS is considered to perform well with regards to shading. The north facade is not typically equipped with shading, so the negative performance of shading solutions on the north can be overlooked. The main focus was on the south orientation values since the simulation model was south facing. Fig. 11 illustrates NEG in a relation to the variable *g*-value. In the case of the large south window the rest of the CFSs generated large solar gains and would cause the space overheating. NEG does not penalize the overheating causing the cooling loads. Therefore the energy performance of the room dependent on the angular properties of the shading including cooling loads which is discussed in the next section.

The clear glazing and the glazing with roller shade had relatively constant NEG up to the normal surface IA of 40°, while the MSPSS' and venetian blinds' NEG decreased sharply from IA of 0°. The sharp drop in *g*-value is a result of the inclined structure of both shades. The solar altitude in northern Europe (Denmark) is mostly below 40° with the maximum below 60°. For shading purposes, a

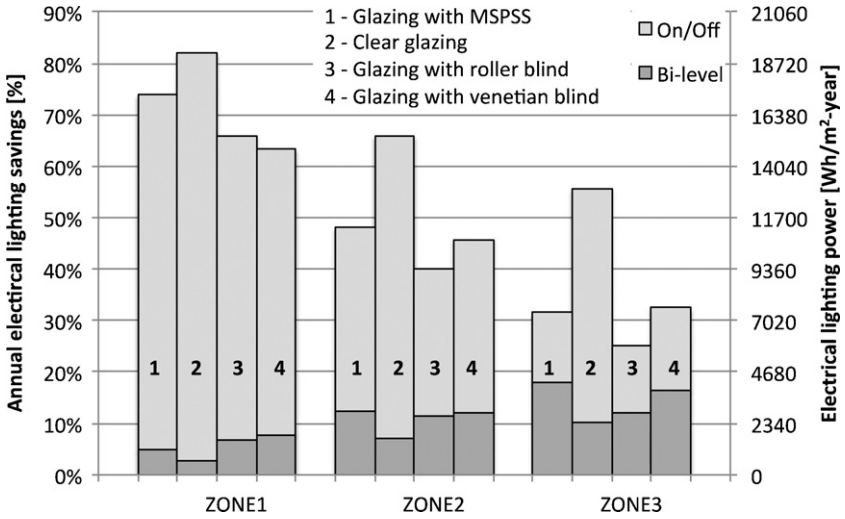

Fig. 9. Electrical light saving for work plane illuminance of 300 lx.

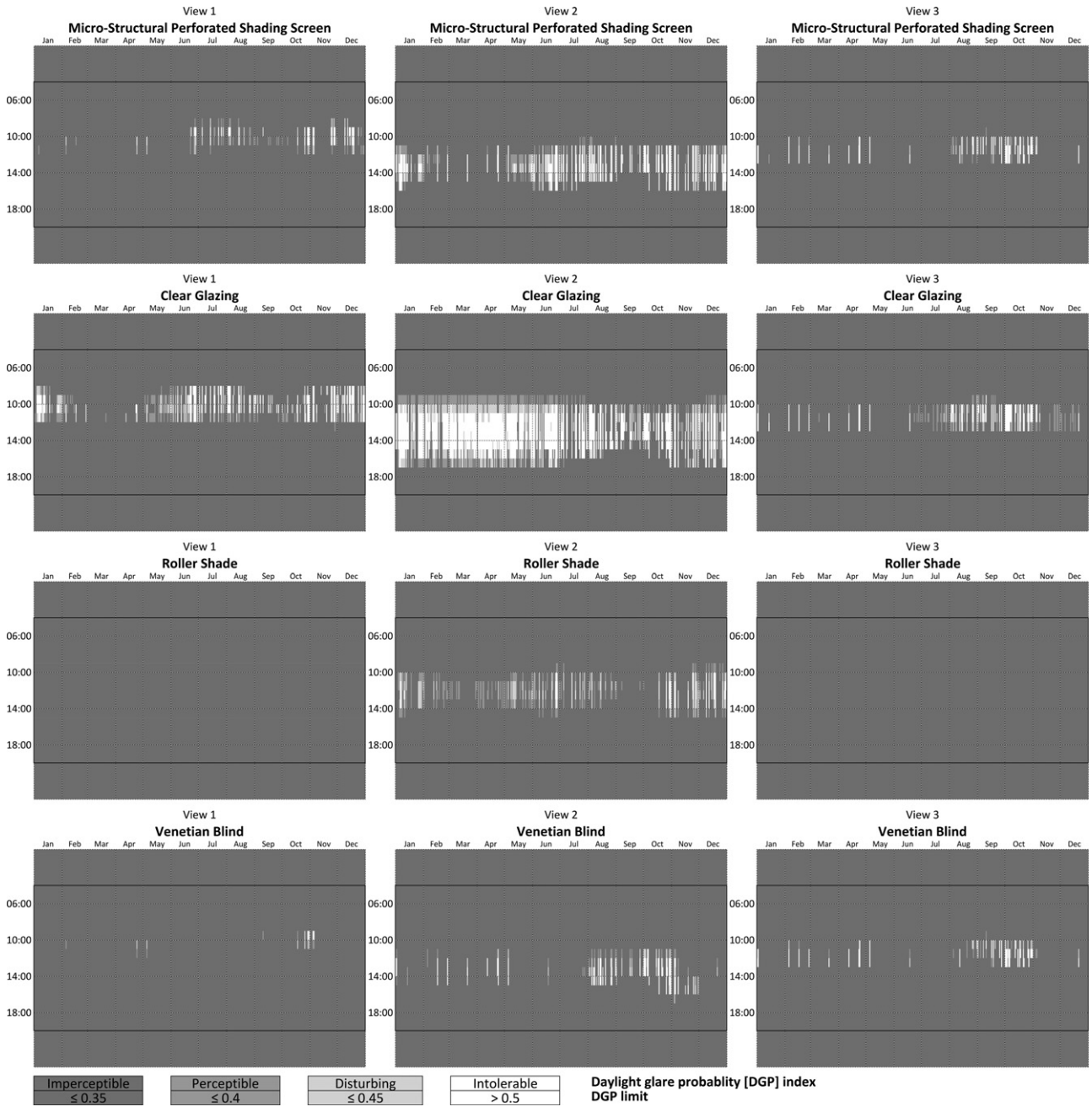

Fig. 10. Annual plots of the DGP for three views and all CFS in the location of Copenhagen.

progressive *g*-value is efficient because it provides the most shading in summer when direct solar radiation is most intense and least desirable. The *g*-value of all tested solutions, shown in Fig. 12, is similar to the front visible transmittance in Fig. 6. The total solar transmittance is less concentrated and the energy is transmitted through wider range of IAs compared to the visible transmittance.

3.7. Energy loads

Heating and cooling loads were evaluated based on the ESP-r simulation model. The model allowed testing different shading systems with the detailed bi-directional transmittance properties. The large sources of energy for heating and cooling were assigned to the

Table 2
Energy performance indicators of selected CFS and NEG.

	Centre *Ug* (W/m^{2}K)	Normal-incidence *g*-value	NEG (W/m^2 K)			
			All	North	South	East/west
MSPSS	1.23	0.37	−38.8	−84.1	0.1	−51.3
Clear glazing	1.25	0.62	7.8	−67.9	72.6	−13.2
Woven rollen shade	1.16	0.35	−37.4	−79.8	−1.1	−49.2
Venetian blind	1.10	0.49	−3.5	−63.5	47.8	−20.1

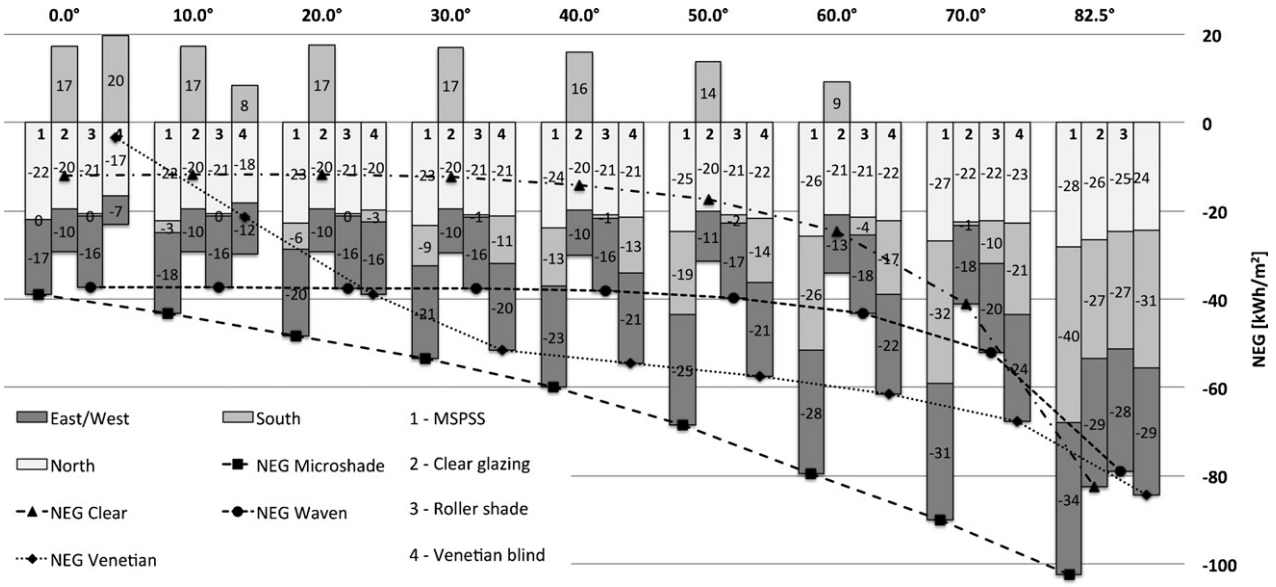

Fig. 11. NEG for four different CFSs, split for different orientation and dependent on IA.

model in the way that they were never exhausted. Table 3 contains the results for the heating and cooling loads. Heating loads excluded solar gains and considered only the energy needed to maintain the set point for heating of 20 °C, during working hours, and 15 °C outside the working hours. Heating loads were relatively low since the building was well insulated. The cooling loads were calculated using the energy needed to cool the space when the air temperature was above 26 °C. The largest cooling loads occurred with clear glazing, which did not provide any shading. All shading solutions provided similar shading protection and reduced cooling loads by 20–30% compared to the window without the shading. The larger heating loads for Prague compare to Copenhagen were caused by a fact that in Prague the temperatures in the winter months are lower as well as there are more extreme temperatures.

4. Discussion

The results describe overall performance of all four CFSs and the complexity is addressed by interconnected evaluation parameters. It was important to validate the simulation results for bi-directional transmittance against measurements since the study is dependent on the bi-directional transmittance data. The measurements and simulations correlate reasonably and thus the results are trustful and the model of the MSPSS is described accordingly to its geometry and properties.

As modern buildings are thermally well-insulated, the importance of shading solar gains for transparent elements becomes more important, especially on the southern and east/west facades, even at higher geographical latitudes. NEG illustrates that even double-glazing provides significant heating gains and has an influence on the overall performance of the building. This conclusion is supported by the results from the energy calculations in ESP-r where the southern climates require more solar protection. When the clear glazing is excluded, all three tested shadings systems provide similar energy performances, however the roller shade reduces visibility and therefore the usage potential is limited because users would likely prefer the other systems. Furthermore, the roller shade system limits daylight penetration and reduces the light energy savings by daylight compared to the more open venetian blind and the MSPSS. On the other hand, shading systems also reduce beneficial heat gains in cold months.

These two aspects are contradictory, as shading would be used during summer and solar heating gains during the winter. The bi-directional description of the performances of the individual systems provides accurate results and is clear description of the properties. By such information, together with knowledge of the local conditions, the building design can be accordingly adjusted to maximise the performance utilization of the particular shading system. From the combination of the results it is possible to see that angularly selective shading systems are the key to energy indicators for cooling and heating. Information about the variable *g*-value is valuable for northern locations where the higher *g*-value is useful during winter when the sun is low.

The transmittance of the system is directly linked to the level of daylight. From the combination of bi-directional transmittance and daylight autonomy it could be justified that more daylight be transmitted in during winter months when the daylight levels are generally lower. Higher solar and light energy protection in summer is desirable, as the light intensity is greater. This is the reason for blocking incoming radiation to protect space from overheating and excessive levels of the WPI. The shading systems provide glare protection in addition to shading extensive solar gains. The glare evaluation was performed with the actual sun position at the time of the evaluation, meaning that the light transmittance varied at each time step. In the case of the visual comfort, blocking direct light is necessary, however even the completely closed roller shade caused visual discomfort and glare. The glare is not dependent only on the shading solution, but mainly on the position of a view to the light source, and therefore optimal view direction is critical. As

Table 3
Energy loads for heating and cooling for all CFSs and investigated locations.

Location	Energy performance (kW h/m²/year)							
	MSPSS		Clear		Roller shade		Venetian blind	
	HL	CL	HL	CL	HL	CL	HL	CL
Copenhagen	8.5	22.5	6.6	30.4	9.0	22.8	9.3	20.3
Prague	12.3	24.4	10.5	30.4	12.7	24.3	13.2	23.2
Rome	0.0	63.5	0.0	78.1	0.0	63.9	0.1	59.4

Note: HL – heating loads; CL – cooling loads; MSPSS – micro structural perforated shading screen.

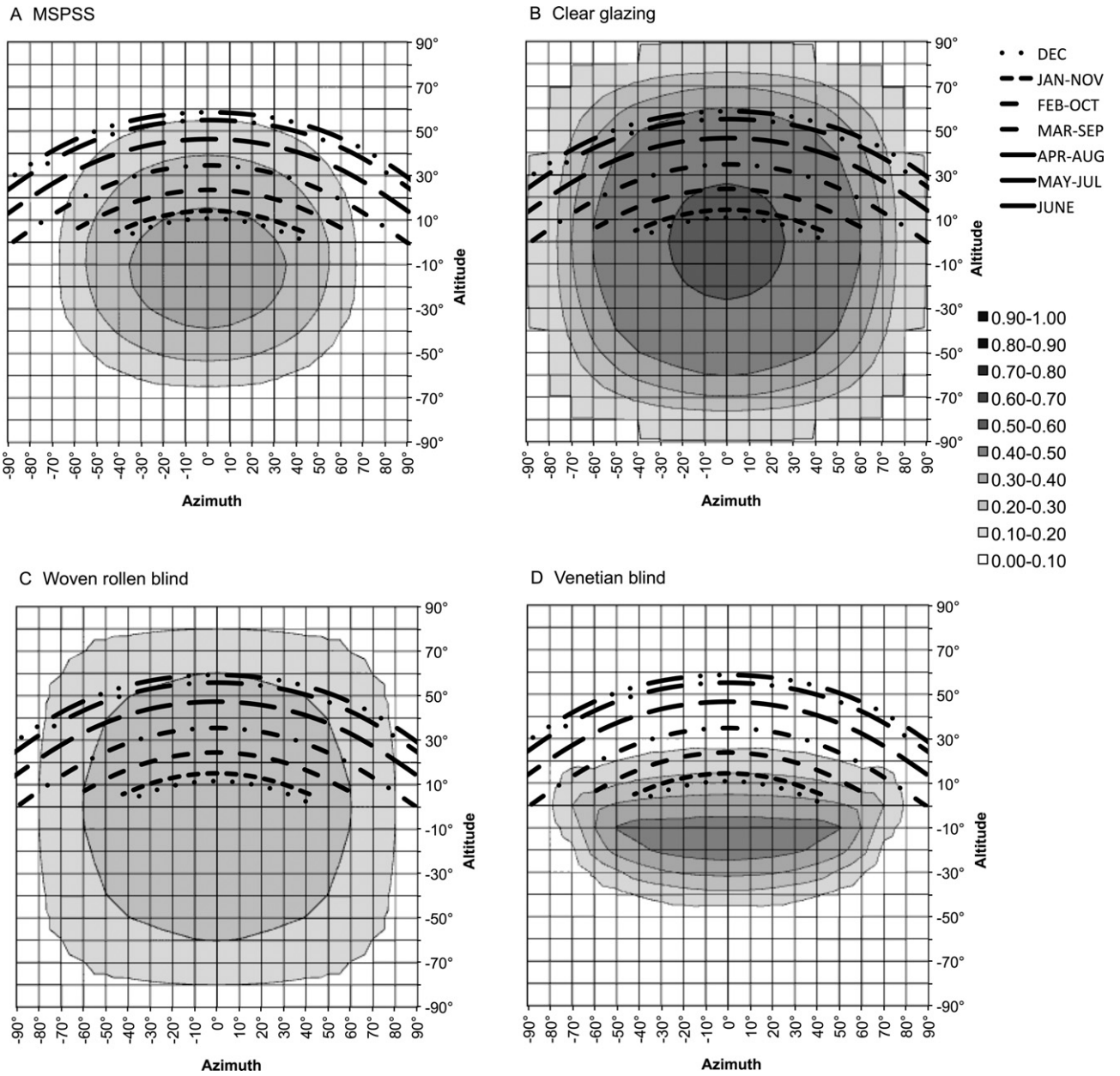

Fig. 12. BSDFs for total solar energy transmittance of the CFSs with sun path of Copenhagen.

such, it is not fully possible to say that the roller shade performs better or worse than the MSPSS or venetian blinds.

When the focus is on the view out, clear glazing would perform the best, however when the glare is included then it can become the worst. The difference between the MSPSS and venetian blind were minimal regarding the visual performance. However the MSPSS is almost invisible and does not disturb the view as venetian blind does.

The optical and thermal performances of the MSPSS could be improved by placing the layer to the external surface, if a durability of the layer allows exposing the MSPSS to the outdoor environment. An indirect shading efficiency would be increased as an absorbed energy in the glass would be reduced with the shading layer on the external surface. Thermally the glazing with the external MSPSS layer would perform better as the emissivity of the coating is lower than the normal emissivity of glass.

Such system would be suitable for renovations by attaching the shading layer onto the glazing surface of an existing window. However, placing the MSPSS layer on either internal or external surface of the glazing would make cleaning and maintenance complicated as dust would deposit in the microstructure.

5. Conclusion

A comparison of several performance indicators was carried out for four different CFSs and benchmarked against each other. The bi-directional transmittance simulations were first validated with outdoor measurements prior to using the data in further. There was a strong correlation between the measurements and simulations. To provide an overview of the CFS performance it was necessary to use several interrelated parameters. By using bi-directional information describing CFS it was possible to accurately depict the shading with a high level of understanding in the context of the IA and location. It was found that the angular dependent shading systems provided improvement all year round in providing daylight,

heating load reduction by controlling solar gains and decreasing risk of overheating during summer days when the sun altitude is high. The visual comfort depended on blocking direct light by optimal positioning of the shading and the direction of the view. This paper demonstrates that it is possible to evaluate unique shading systems, which are not typically included in the building performance simulation tools. However it has to be noted that the process needs to be automated and included in widely used simulation tools in order to shorten the time of the complete performance evaluation with all consequences.

It can be concluded that the MSPSS performed well compare to the rest of the solutions. The layer provided similar shading effect as the venetian blind. Unobstructed view to outdoor through the MSPSS did not generate extensive glare and the utilization of daylight was kept high.

Acknowledgements

The research was co-funded by the Danish Energy Agency program on research and demonstration of energy savings. The authors would like to acknowledge PhotoSolar A/S for providing the test samples and their co-operation and contribution to this paper. This work was also supported by the Assistant Secretary for Energy Efficiency and Renewable Energy, Office of Building Technology, State and Community Programs, Office of Building Research and Standards of the U.S. Department of Energy under Contract No. DE-AC02-05CH11231 and by the California Energy Commission through its Public Interest Energy Research (PIER) Program on behalf of the citizens of California.

References

[1] EU, EPBD recast, Directive 2010/31/EU of the European Parliament and of the Council of 19 May 2010 on the energy performance of buildings (recast), Official Journal of the European Union (July 2010).
[2] US DOE Office of Energy Efficiency and Renewable Energy, Buildings Energy Databook, US Department of Energy, Office of Energy Efficiency and Renewable Energy, 2005.
[3] J. Carmody, S. Selkowitz, E.S. Lee, D. Arasteh, Window Systems for High-Performance Buildings, W.W. Norton & Company, December 2003, ISBN-13:978-0393731217.
[4] M. Sala, The intelligent envelope: the current state of the art, Renewable Energy 5 (1994) 1039–1046.
[5] G. Ward, R. Mistrick, E. Lee, A. McNeil, J. Jonsson, Simulating the daylight performance of complex fenestration systems using bidirectional scattering distribution functions within radiance, Journal of the Illuminating Engineering Society (2011).
[6] F. Frontini, T.E. Kuhn, S. Herkel, P. Strachan, G. Kokogiannakis, Implementation and application of a new bi-directional soar modelling method for complex facades within the ESP-r building simulation program, in: Building Simulation 2011, Sydney, Australia, 2011.
[7] R. Sullivan, L. Beltran, E.S. Lee, M. Rubin, S.E. Selkowitz, Energy and daylight performance of angular selective glazings, in: Proceedings of the ASHRAE/DOE/BTECC Conference, Thermal Performance of the Exterior Envelopes of Buildings VII, Clearwater Beach, FL, December 7–11, 1998, 1998.
[8] A. McNeil, E.S. Lee, Annual Assessment of an Optically-Complex Daylighting System Using Bidirectional Scattering Distribution Functions with Radiance, DOE/LBNL FY10 Technical Report Deliverable.
[9] G. Ward Larson, R. Shakespeare, Rendering with Radiance: The Art and Science of Lighting Visualization, Morgan Kaufmann, San Francisco, 1998.
[10] A. McNeil, C.J. Jonsson, G. Ward, D. Appelfeld, E.S. Lee, Validation of a ray-tracing tool used to generate bi-directional scattering distribution functions for complex fenestration systems, Solar Energy, submitted for publication.
[11] J.H. Klems, A new method for predicting the solar heat gain of complex fenestration systems: I. Overview and derivation of the matrix layer calculation, ASHRAE Transactions 100 (1) (1994) 1065–1072.
[12] M. Andersen, M. Rubin, J.L. Scartezzini, Comparison between ray-tracing simulations and bi-directional transmission measurements on prismatic glazing, Solar Energy 74 (2003) 157–173.
[13] IEA TASK 27, Performance of Solar Facade Components, 2005.
[14] CEN –EN 15251, Indoor Environment Input for Design and Assessment of Energy Performance of Buildings Addressing Indoor Air Quality, Thermal Environment, Lightning and Acoustics, European Committee for Standardization, Brussels, Belgium, 2007.
[15] IESNA Lighting Handbook, Illuminating Engineering, 9th edition, July 2000, ISBN-13:978-0879951504.
[16] J. Mardaljevic, L. Heschong, E. Lee, Daylight metrics and energy savings, Lighting Research and Technology 41 (2009) 261–283.
[17] EN 15193, Energy Performance of Buildings—Energy Requirements for Lighting, European Committee for Standardization, Brussels, Belgium, 2007.
[18] C.F. Reinhart, O. Walkenhorst, Dynamic RADIANCE-based daylight simulations for a full-scale test office with outer venetian blinds, Energy and Buildings 33 (7) (2001) 683–697.
[19] J. Wienold, Dynamic daylight glare evaluation, in: Building Simulation 2009, Glasgow, Scotland, 2009.
[20] J. Wienold, J. Christoffersen, Evaluation methods and development of a new glare prediction method for daylight environments with the use of CCD cameras, Energy and Buildings 38 (7) (2006) 743–757.
[21] T.R. Nielsen, K. Duer, S. Svendsen, Energy performance of glazings and windows, Solar Energy 69 (Suppl. 1–6) (2000) 137–143.
[22] D. Appelfeld, C.S. Hansen, S. Svendsen, Development of a slim window frame made of glass fibre reinforced polyester, Energy and Buildings 42 (2010) 1918–1925.
[23] EN832, Thermal Performance of Buildings — Calculation of Energy Use for Heating — Residential Buildings, CEN, 1998.
[24] T.E. Kuhn, S. Herkel, F. Frontini, P. Strachan, G. Kokogiannakis, Solar control: a general method for modelling of solar gains through complex facades in building simulation programs, Energy and Buildings 43 (2011) 19–27.
[25] T.E. Kuhn, Solar control: a general evaluation method for facades with venetian blinds or other solar control systems to be used 'stand-alone' or within building simulation programs, Energy and Buildings 38 (6) (2006) 648–660.
[26] T.E. Kuhn, C. Buhler, W.J. Platzer, Evaluation of overheating protection with sun-shading systems, Solar Energy 69 (Suppl. 1–6) (2000) 59–74.
[27] S. Lechtenböhmer, A. Schüring, The potential for large-scale savings from insulating residential buildings in the EU, Energy Efficiency 4 (2010) 257–270.
[28] D. Appelfeld, S. Svendsen, S.T. Borup, Performance of a daylight redirecting glass shading system demonstration in an office building, in: Building Simulation 2011, Sydney, Australia, 2011.

Paper IV

"Performance of a daylight redirecting glass shading system"

D. Appelfeld, S. Svendsen

Submitted to: *Lighting Research and technology, 2012*

Performance of a daylight redirecting glass shading system

David Appelfeld*, Svend Svendsen
Technical University of Denmark, Department of Civil Engineering, Section of Building Physics and Services, Brovej, Building 118, DK-2800 Kgs. Lyngby, Denmark

Keywords: *Shading system, daylight, redirecting light, indoor climate, visual comfort*

****Corresponding author:***
Email: dava@byg.dtu.dk

Abstract

This paper evaluates the daylighting performance of a prototype external dynamic shading and light redirecting system. The demonstration project was carried out on a building with an open-space office. The prototype and original façades had the same orientation and surroundings. The research employs available simulation tools for the performance evaluation of the shading system. This was accompanied by measurements of the daylight conditions in the investigated space. The prototype system improved the daylighting conditions compared to the existing system. The visual aspects were kept, as the redirected daylight did not cause discomfort glare. By utilizing higher illuminance, it was possible to save 20% of the lighting energy. The thermal insulation of the fenestration was maintained, with slightly increased solar gains, without producing an excessive overheating.

Introduction

The growing demand for energy savings and seeking new innovative technologies is the motivation of this research. Therefore cutting the energy used by buildings is of an interest in this study. Available simulation programs cannot easily evaluate unique complex fenestration systems using standardized methods, since they are mostly created to evaluate specific solutions, such as venetian blinds. The complexity of the assessment can be seen from many perspectives such as energy impact, shape, material, cost and operating cost. Therefore, more generic and versatile state-of-the-art simulation programs and techniques have to be used to evaluate an impact of a unique shading system [1]. Consequently, by the obtained knowledge it is possible to do an evaluation on more standardized level for future solution development. Additionally, the need to cut down energy consumption of buildings has led to buildings that are increasingly insulated against heat losses. It has been emphasized in many publications and studies that buildings consume large part of overall energy used globally [2]. The glazed areas in the new office buildings are often large, which increases solar gains during the cold periods of year and increases working plane illuminance (WPI). During the warmer season, the over-glazed areas can cause overheating and glare, and thus solar shading is necessary. Using energy to remove excessive heat is costly and may eliminate the energy saving effect of utilizing solar energy. In addition, the solar gains in newly built buildings are considered as a significant contributor to heating. Commercial buildings have traditionally combination of high internal gains generated by people/light/equipment, and well-insulated envelopes, resulting in low heating and high cooling loads. Therefore, the solar gains have to be

included in the total energy balance of buildings, as they may positivity contribute to heating but can produce overheatings [3]. Transparent parts of the building envelopes serve several functions. First, they must provide enough light transmittance, or daylight utilization. Second, they should provide sufficient solar energy transmittance during cold months. Third, they should prevent indoor space from overheating during warmer months by shading excessive solar radiation. Fourth, the view to outside is desired and should be unobstructed and maintained. Since a significant portion of energy in buildings is devoted to lighting and ventilation, daylight and cooling have a large energy saving potential for advanced solar shading systems [4].

Light redirecting glass lamellas shading system Background

Based on previous studies, a shading system with light redirecting glass lamellas with a solar control surface was built[5, 6]. The shading system removes the drawback of the current systems, and provides view out, while shades excessive solar gains and redirect daylight into the back of an office room where daylight is desirable. The investigation is based on the full-scale demonstration in the office building and is accompanied by computer modelling. The simulation model can be used for various buildings, since it is not feasible to build a demonstration for all possible buildings and shading scenarios. The evaluation of the performance of the shading system by simulations is the objective and the central point of the research. The focus is to evaluate the performance of the demonstrated system, based on the simulations and measurements and comparing it with the reference system. Lighting energy can be reduced by offsetting artificial light by daylight, which is explicitly dependent on a daylight-linked lighting control strategy and is investigated here. Furthermore, evaluation of glare and visual comfort is important aspect of the system performance as the redirected direct sunlight can cause an uncomfortable glare. Additionally, a thermal performance had to be analysed as the system increases the solar energy penetration of the transparent envelope. It is important to evaluate all the parameters as the evaluation based on the illuminance distribution, glare and directivity is useful in characterising quality of (day)lighting conditions in a room [7].

Table 1: *Surface reflectance values.*

Surface	Visible reflectance (R_{vis})
Floor	20.5%
White walls	89.3%
Wooden partitions	32.6%
Ceiling	89.9%
Wooden furniture	40.0%

Experiment

Demonstration building

The demonstration building equipped with a prototype of an external dynamic integrated shading and light redirecting system is located in Humlebaek 30 km north of Copenhagen, Denmark (55.96°North - 12.49°East). The building was refurbished from a production facility to an open-space office, which created a deep office space with working places far away from the façade. The building is one floor high with 2.26 m high windows. The whole building has dimensions of 66 m 28 m with the longer façade oriented 11°west by south. The surrounded landscape is relatively flat without big trees and high buildings that might shade the investigated façade. However, the opposite building blocks the open horizon. The office has a room depth of 14 m. The floor plan of building is in Figure 1. The buildings and façades layout allows preservation of a reference office space with the same orientation and similar layout as the tested space. The two spaces were fitted with same set of illuminance sensors to monitor the actual conditions. The open-space office is divided by small meeting rooms, which are separated by partitions. The partitions are made of wood and glass. The glazed part allows better penetration of light into the office. The test and reference areas are both approximately 9.5 m wide and 14 m deep with the ceiling height of 3.45 m. The building has windows on the south and west façades with 20 cm wide columns between individual windows. The window openings are 1.98 m wide and 2.26 m high with windowsill 0.75 m above the floor. The reflectance of the surfaces in the building and outdoors were measured by illuminance meter in order to have identical surface properties for the measurements and simulation model. The visible reflectance measurements were averaged from three values measured on different places of the surface, and the values are presented in Table 1. The roughness and specularity of the surfaces for the model were neglected.

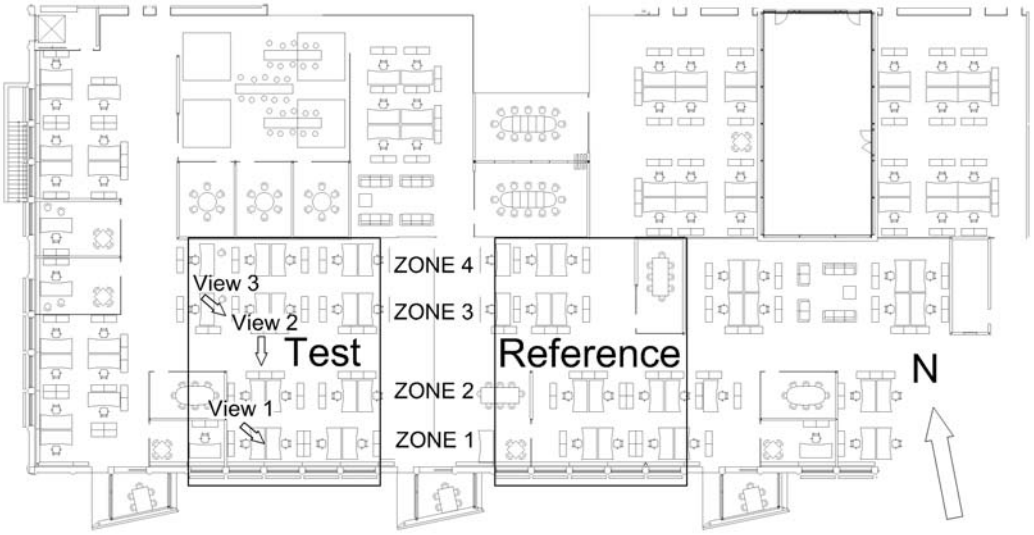

Figure 1: *The layout of the building with open- space office and marked view directions and lighting zones position.*

The shading system

The major difference between the tested (new) and reference (original) shading system is that newly installed lamellas rotate in an opposite direction, compared to a conventional shading system. The outer edge moves upwards and the upper surface goes towards the façade when the system is closing. Each window consists of eight horizontal 330 mm wide lamellas. The rotation directions of the lamellas are demonstrated in Figure 2. In the tested system, the four uppermost lamellas rotate toward the façade and the rest of the lamellas rotate in the opposite direction (same as the original system). This strategy allows the upper part of the system to redirect and shade in closed position, while the lower part acts as a traditional shading system which allows to see to outside. The tested system was made of highly reflective solar control coated glass to redirect daylight into the back of the office. Tested lamellas were produced by Saint Gobain Glass (SGG) and the used glass was Antelio Silver 10 mm, with light reflectance of 31%. The original lamellas were made of Parasol Green 8 mm with light reflection of 6%, made by SGG, with white frit covering 55% of the surface. The properties of the shading glass, glazing and glass partitions are listed in Table 2. The exterior shading system is supplemented by internal venetian blinds and curtains.

Table 2: *Centre-of-glass properties of glass used in the model.*

Glass	Visible transmittance (T_{vis})
Glazing	73%
Glass partitions	88%
Tested glass lam.	66%
Ref. glass lam.	68% (without frit)

**lam = lamellas*

Shading control strategy

The shading strategy of the system is based on results from the previous investigation, the location, and the sun position. The most effective daylight redirecting position is when the four uppermost lamellas are in the position of 30°towards the façade.5, 6 The lamellas stay in this position when the sky is overcast or the total horizontal illuminance is lower than the threshold of 25 klux for longer than 10 min. The time delay prevents frequent opening and closing of the shading system, which could disturb the occupants. The threshold for moving lamellas back to the redirecting position was set to 17.5 klux with time offset of at least 20min. The redirecting position was 30°all year around, except May and June when the position was set to 25°to avoid direct reflection from the lamellas surfaces to the occupants faces. The system was controlled automatically according to predefined pattern, both in the reality and simulations. The

system had three possible positions:

- Redirecting position 30°(25°) only for tested system and four upper lamellas;
- Open position 0° tested and reference system;
- Close position 90° tested and reference system.

Mainly closed and redirecting positions were used for the investigation, as the opened position would be randomly dependent on behaviour of the office occupants. The redirecting position was designed to avoid reflection of the direct sunlight from the lamellas surfaces when the sun is partially behind clouds. Hence, the space occupants are not exposed to the reflections from and between lamellas. The lowest redirecting lamella (fourth from top) was approximately 2 m above the floor and therefore it did not interface directly with view out when in redirecting position.

Simulation models

To overcome the lack of standardized simulation tools to test the performance of the shading and redirecting system, the state-of-the-art software Radiance was used [8]. It is generally complicated to simulate effect of reflective surfaces. Therefore, Radiance was used for the investigation to depict the transparent properties of the façade and its effect on the indoor environment. Radiance is capable of simulating illuminance and luminance distribution in complex spaces with diffuse, specular and transparent materials. Throughout the study, several Radiance simulation techniques were used, as it was suitable to us some technique in one cases and different technique in other situation. The techniques are in detail explained further in the text. Program Window 6 was used to assess basic thermal and solar energy properties of the system [9]. The g-values of each system in different position were obtained and completed with visual light transmittance of the system.

Working plane illuminance

The comparison between two cases was based on a horizontal working plane illuminance (WPI). There are several thresholds, standards, and design recommendations described in literature. The simulated WPI was derived for tested and reference system to find the performance of the system. Several thresholds for WPI were observed and cumulated over the whole year, and evaluated by daylight autonomy (DA) and useful daylight illuminance (UDI). [10, 11, 12, 13, 14, 15, 16]

- 100 lux Is considered as insufficient for performing tasks under daylighting conditions and it is a lower limit for UDI.
- 500 lux Is described as minimal WPI for the office work and it is used as threshold for DA analysis.
- 4500 lux Many people find illuminance above the level too high and uncomfortable.

The placement of windows on the façade creates an almost-continuous band of windows. Therefore, sensors equidistant from the façade were considered to have same WPI. The study investigated a row of illuminance sensors perpendicular to the façade with spacing of 0.25 m starting at 0.5 m from the façade in the high of the working plan of 0.85 m. Other sensors were located at the same position as the physical illuminance sensors used for the measurements. These were located on the working plane and under the ceiling, facing the floor, to monitor reflected light to the ceiling. The spacing of the physical sensors on the working plane was 0.5 m, 3.6 m and 8.5 m from the façade and 1.5 m, 3.3 m, 5.1 m and 6.9 m from the façade under the ceiling.

Annual daylight simulation

To calculate an annual WPI a three-phase method (TPM) using Radiance was used [17]. This method uses a Radiance tool rtcontrib to calculate results in the form of matrix, generated from the transmission of fenestration system matrix (XML), exterior daylighting matrix (DMX) and interior view matrix (VMX). This approach quickly generates different situations for various fenestration systems, locations and sky conditions by replacing only one-matrix [18]. The Radiance simulation parameters for generating VMX, XML, DMX matrixes are listed in Table 3. This approach is suitable for annual simulation as the sky for every hour is unique and the combinations can be repeatedly generated without performing the whole simulations. The last information needed for multiplication of matrixes is a sky vector, which describes the sky distributions. The sky vector was derived from test reference year (TRY) for Copenhagen, Denmark[19]. The sky model uses the Perez sky, which is generated from the direct normal irradiance and horizontal diffuse irradiance [10, 20]. The sky was divided into 2305 patches according to a Reinharts subdivision for detailed results [21]. By multiplying matrixes, the total illuminance at the sensors from all sources in the model was calculated. The transmission matrix was generated by

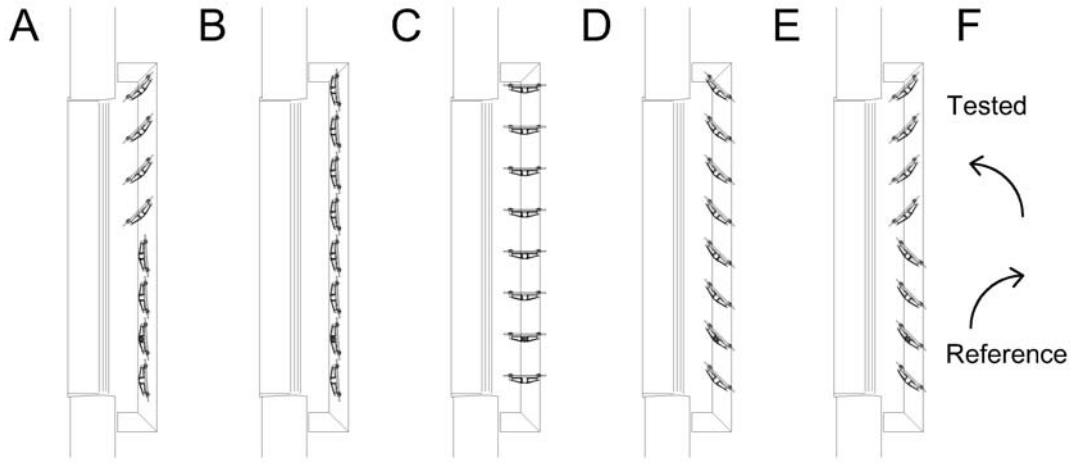

Figure 2: *Illustration of the positions and rotations of the shading system. A) Tested system in redirecting position with closed lower 4 lamellas; B) Whole shading system in the closed position; C) Whole shading system in the opened position; D) Reference shading system in the rotation of 45°; E) Tested shading system in redirecting position with lower for lamellas in the rotation of 45°; F) Rotation direction of tested and reference system from the opened position to the closed position.*

the Radiance program genBSDF which generates a bidirectional scattering distribution function (BSDF) for a given complex fenestration geometry [22]. Annual daylight simulation is in several resources referred to as dynamic daylighting simulation, which is conducted in steps in agreement with TPM.[17, 23] The annual illuminance matrix provides information needed to evaluate the daylight conditions in the interior. The commonly used daylight performance matrixes nowadays are daylight factor (DF), useful daylight illuminance (UDI) and daylight autonomy (DA). [7, 10, 11, 13, 15]. Daylight factor (DF) was not used in this investigation because it does not quantify the redistribution of the direct beam of the radiation to provide diffuse illuminance in the indoor space. DA is the percentage of hours satisfying the minimal designed WPI from the total number of working hours in a year. The criterion for minimal WPI according to ISO standard is 500 lux [14]. The commonly used design WPI is between 300500 lux. The UDI matrix quantifies when the daylight is perceived as useful for occupants of a space. It is calculated as percentage of the occupied working hours when WPI is between the lower and upper thresholds. 100 lux is considered as the lower illuminace level. The upper level is not clearly defined and differs between publications. As the upper threshold, when the occupants may feel uncomfortable, 4500 lux was used. According to Wienold [16] 30% of people find horizontal illuminance above 4500 dissatisfying. Midrange between 100 lux and 4500 lux may be considered as usable for most of the occupants. Some subjects may consider the values in this range as uncomfortable, however values should not be considered as not useful since every subject perceive the illuminance levels differently [15, 16].

Glare

The visual comfort is a major criterion in the performance of the daylight redirecting shading system. The glare analysis has to be carried out, as the view out is provided [24]. However, the perception of glare is often reduced, even under high glare index values, when working under daylighting conditions [25]. Daylight glare probability (DGP) was selected as a glare index because it is based on an extensive human evaluation study. [26, 27]. The annual DGP analysis was facilited by an enhanced simplified DGP calculation method in order to include the direct sunlight in the analysis [26]. The glare assessment was performed for working hours between 8:00 and 18:00 over the whole year, with three different views as the glare is dependent on the visual zone and view direction [16, 28]. The views are marked in Figure 1.

Table 3: *Radiance parameters for TPM.*

Radiance simulation parameters	VMX	XML	DMX
Ambient bounces (-ab)	6	3	6
Ambient divisions (-ad)	2048	350	10000
Limit weight (-lw)	$1.00e^{-12}$	0.0001 (-st)	$1.00e^{-3}$
Direct source subdivisions (-ds)	0.1	0.2	0.1

Glare was read from rendered images by Radiance, because it is not possible to evaluate the discomfort glare just by the horizontal illuminance [15].

Lighting energy savings

Lighting energy savings were calculated for three lighting control systems. The WPI criteria were based upon CEN-EN 15251 [14] for open-space office with WPI of 500 lux. The lighting power density of 15 W/m2 is derived from EN 15193 [29]. A percentage of the working hours satisfying the daylighting conditions annually was accounted. When the minimum light threshold is not reached artificial light could be added and the artificial light energy saving is equal to the amount of daylight. The lighting control strategies were linked to daylight and were as follows: on/off control, bi-level control, and continuous control. For on/off control the electric lighting within a zone was switched off when the WPI was sufficient by daylight. With bi-level switching, half of the lamps in the zone were switched off when daylight fulfilled half of the required WPI and were switched off when the WPI criteria was fully met. By continuous control the electrical lighting was linearly dimmed by amount equal to the available daylight, until minimal supplied output of 20% and then switched off when the criteria was met. The lighting energy savings were idealized because they were based on the WPI level. The office space was divided into 4 zones. Each zone consisting of one row of tables paralel along the façade, see Figure 1. Each zone was approximately 33.25 m2 of the floor area. The WPI level had to be fulfilling in the back of each zone, which means that the whole zone was lit sufficiently.

Results and discussion

Validation and comparison of daylight simulations and measurements The measurement sensors were placed to be minimally blocked by surroundings. The space was modelled without furniture for daylight simulations, which was comparable with the measurements as the sensors had free view to the façade.

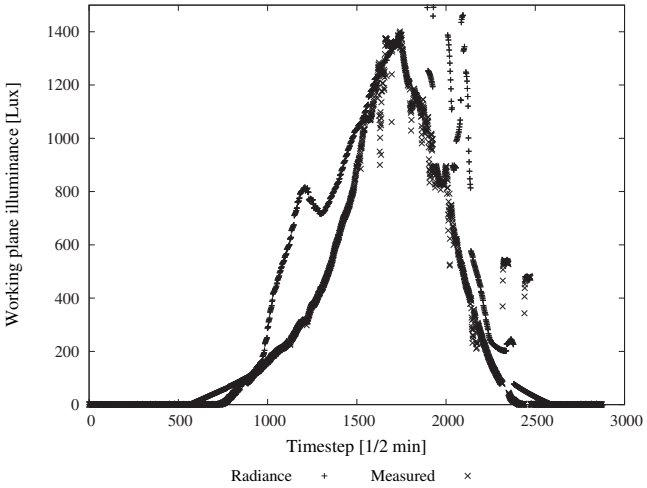

Figure 3: *Comparison of measured and Radiance illuminance on the sensor.*

The reason for removing the furniture from simulations was that in reality, the furniture was not fixed and it was hard to assume where it would be at the time of the measurements. However the measurements results were influenced in several cases by immediate surroundings in the office and therefore not all the results correlated. Additionally it was not possible to observe position of the lamellas during whole period of measurements as well as the position of an interior shading, curtains and venetian blinds. For those reasons, errors between simulation and measurements occurred. The compared illuminance sensor for measurements and simulations was placed in the distance of 3.6 m from the window, which is approximately in the position where the daylighting conditions could be improved. Sensors closer to the window were exposed to the high level of illuminance and could have high errors. Furthermore, the sensors deeper in the room had higher probability of being shaded. The two curves in Figure 3 present the results from the Radiance simulation and measurements. To have conditions similar as possible, a day without occupancy was selected. This limited shading of the sensors during the simulated period as well it was ensured that the artificial light was turned off. Additionally a sunny day was selected for

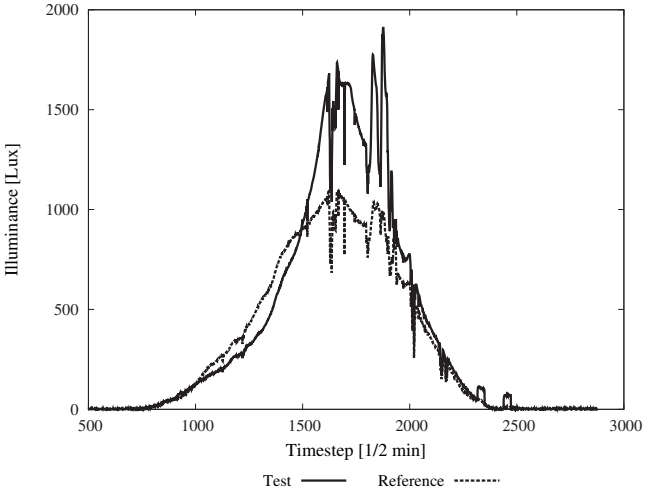

Figure 4: *Comparison of measured illuminance under ceiling for test and reference area.*

validation of the results, since the sky distribution for the sunny sky can be generated accurately with the Radiance program gensky. Chosen day was Sunday, September 5, 2010, during which the shading system was closed. The light coming through the building from the west façade caused the scattered data, between time step 2000 and 2500 , with an half minute intervals, (approximately between 16:30 and 21:00), in Figure 3. This is common for both measurements and simulations and indicates that the simulated model provides comparable data to the measurements. The peak in the morning in the simulations is not common with measured data and was probably caused by the unknown position of the internal shades or by blocking of the direct light coming from the side of the sensor. Another reasons for this discrepancy might be imprecise cosine-correction of the illuminance sensor or the uncertainty of the tilt of the sensor. At low solar altitudes, these two factors might have an impact on the measured results. The comparison of the illuminance level in the tested and reference area are shown in Figure 4. The data were measured by a sensor placed under the ceiling in the distance of 3.4 m from the façade. From the figure, it is visible that daylight was redirected to the ceiling and further reflected into the room. The difference between the sensor in the tested and reference area is up to 500 lux, which demonstrated the effect of the light redirecting properties of the shadings system.

Daylight autonomy

Figure 5 shows DA for whole year for the shading system under the dynamic control, which is a combination of closed and redirecting position. The reference system cannot technically be placed in the redirecting position, therefore the reference system is presented in the closed position in Figure 6. The differences between the results of the tested and reference system are by type of the glass used and the control strategy. The illuminance threshold for DA was reached more often and in a larger distance from the façade with the tested façade. The threshold of 500 lux was reached in 50% of the time at a distance of 4.5 m from the façade for the tested system, compared to 3.2 m for the reference system. For the tested system, in the distance of 4 m from the façade, 60% of the occupied hours had at least 500 lux on the working plane, whilst for the reference shading it was around 43%. The improvement of the daylight conditions is visible all over the depth of the investigated space. Furthermore, the room depth with at least 300 lux in 20% of time was moved from 7.8 m to 10.2 m from the façade and covers most of the working area in the office. The primary purpose of the shading system is to block the radiation penetrating the indoor space. The tested system still blocks the light neat the façade but increases the horizontal illuminance deeper in the office. Furthermore, DA does not penalize excessive illuminance and therefore UDI matrix was calculated to illustrate illuminance levels throughout the office.

Useful daylight illuminance

The excessive WPI is presented for both cases and for every investigated position of the shading system in closed and redirecting position. Figure 7 shows horizontal illuminance for closed and redirecting position of the tested and reference shading. The results were split to show the performance of the systems in each position. The depth of the room with illuminance level higher than 4500 lux shifted in average approximately 1 m into the room, which is not a significant downgrade, because the working places are not directly placed in this zone. In the case of exceeding the upper limit, occupants can close the internal shading system manually in the same way, as they would do it with the original system. More importantly, the situation with insufficiently low daylighting condition in the evaluated space was limited, especially in the back of the office space. The illuminated zone with horizontal illuminance between 100 lux and 4500 lux is larger with tested system than with the reference shading system. The daylight redirecting position of the lamellas further increase the zone lit by daylight. The tested system

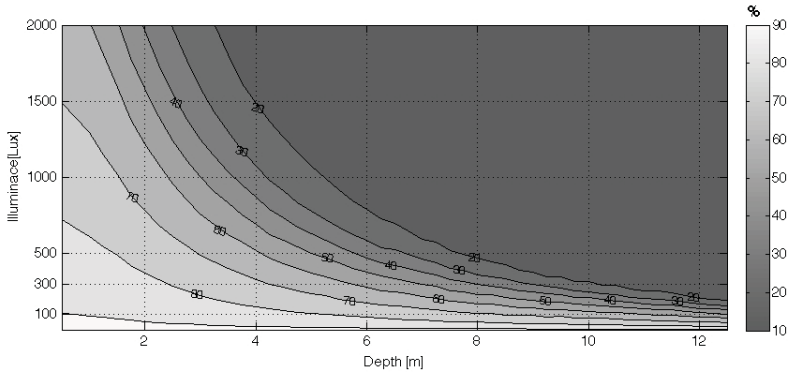

Figure 5: *Daylight autonomy of the tested shading system with dynamically controlled position.*

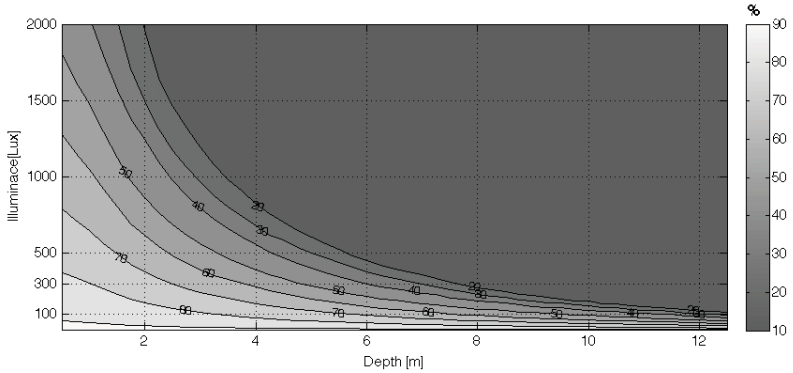

Figure 6: *Daylight autonomy of the reference shading system in the closed position.*

provides usable UDI for more than 20% of hours of occupancy in the back of the room compare to the reference system. The percentage of UDI was improved throughout the whole depth of the room starting approximately 3 m from the façade. The zone with the minimal horizontal illuminance of 100 lux is reduced with tested system, which indicates that the daylight conditions were satisfied in the higher percentage of the working hours.

Glare analysis

When the direct sunlight is redirected to the ceiling, the risk of a discomfort glare can increase. By introduction the dynamic control of the lamellas, the risk of glare from the reflection was reduced by optimizing the position of the lamellas in order to remove the first and second reflection from the glass surface to the occupants faces. However, in cases when the sun had low altitude or under conditions of intermediate sky the discomfort glare could occur. A horizontal roof illuminance for the simulated weather conditions was calculated and in 17% of the working hours, the threshold was above 25 klux, which defines when the shading system was in closed or redirecting position. The Table 4 shows number of hours when the system was closed, opened and when there was darkness. Figure 8 shows annual DGP plots for both systems. The control of the lamellas position was dynamic, reacting on the sun intensity. The tested system generated more glare, however the changes are minimal from the temporal plots in Figure 8. Under the view 1 there was most of glare, as the position was the closest to the façade. In 5% of the time, view 1, there was deterioration of the visual comfort on DGP scale; however, most of 5% was within range of imperceptible glare. This means that the shading capabilities of the tested system are similar to the original reference system and do not generated significant increase of glare. From those results could be concluded that while increasing light penetration into the office, the risk of the glare was not increased by redirecting and reflecting the daylight. The cumulative DGP curves for dynamically controlled system in Figure 9 shows that both systems perform likewise and most detected glare was in the range of imperceptible. In Figure 10, the original shading system shades slightly more, with most of the glare in the range of imperceptible glare. This observation shows that it is effective to redirect daylight into the ceiling instead only shading in the days with outdoor illuminance under 25 klux.

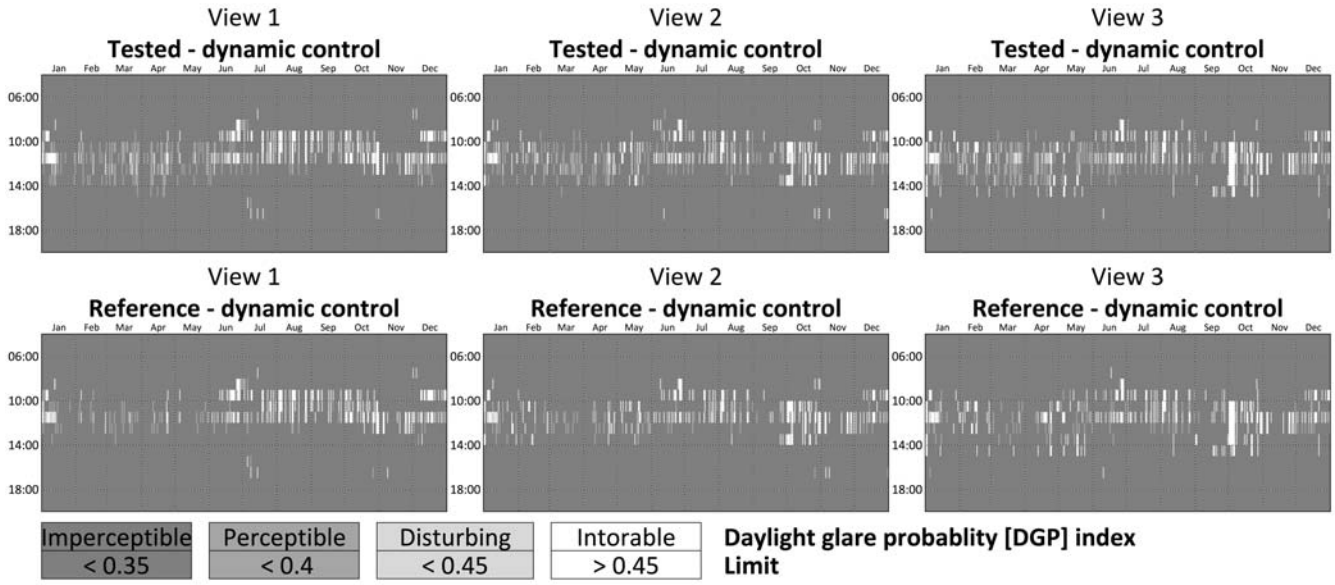

Figure 8: *Annual DGP plots of glare index for tested and reference shading system under dynamically control.*

Artificial light savings

The analysis considered all the savings by utilizing daylight instead of artificial light only. As the lighting control strategy was not predefined, three lighting controls were investigated. The tested system was dynamically controlled while the reference was in closed position for shading and daylight was used when the criterion were met. In Figure 11 each zones savings are shown for each lighting control as well as for the tested and reference system. In all cases, the tested system provides higher savings of different magnitude. Near to the façade (zone 1) the difference between the tested and reference system as well as between different lighting control strategies are between 9-15% as the daylight penetration was higher closer to the windows. The difference between tested and reference case increase towards back of the room (zone 4), which was caused by redirecting daylight into the room. Lighting control strategy influences the savings increasingly further from the façade. On/off control does not provide almost any savings in zone 4, while bi-level switching control strategy is approximately 7% of the lighting power and the continuous dimming reaches 23% of the savings compare to the situation when the light will be all the time on. The improvement of the tested system compare to the reference is between 10-15% in zone 1 through zone 4 for the continuous dimming and bi-level control.

Solar gains and energy performance

The system at different position provides different thermal and optical properties. Using generated BSDF matrixes for each system, the g-value and vis were calculated for each position and shading system. The thermal transmittance of all the systems, U-value, was 0.9 W/m2K for all the scenarios. The genBSDF model included all the surrounding edges, such as windowsill and frames as well actual size of the window. From the investigation in Window 6, the system in the redirecting position provides 17% more visible transmittance compared to 11% increase in solar energy transmittance. Using this strategy, daylight utilization increases while the solar gains do not increase proportionally. Those values are valid for the centre properties of the fenestration system. The bi-directional information would provide more detailed and accurate information about the performance, however it is out of the paper scope[30]. Thermally there is no difference and any system would not thermally insulate more than other.

Conclusion

This paper evaluated a prototype dynamic integrated shading and light redirecting system designed to optimize daylight conditions in an office building whilst a quality of the indoor environment and view out was preserved and improved. Part of an existing façade with glass lamellas in Humlebaek, Denmark was rebuilt to test and further develop the prototype of the concept. The tested and reference façade had

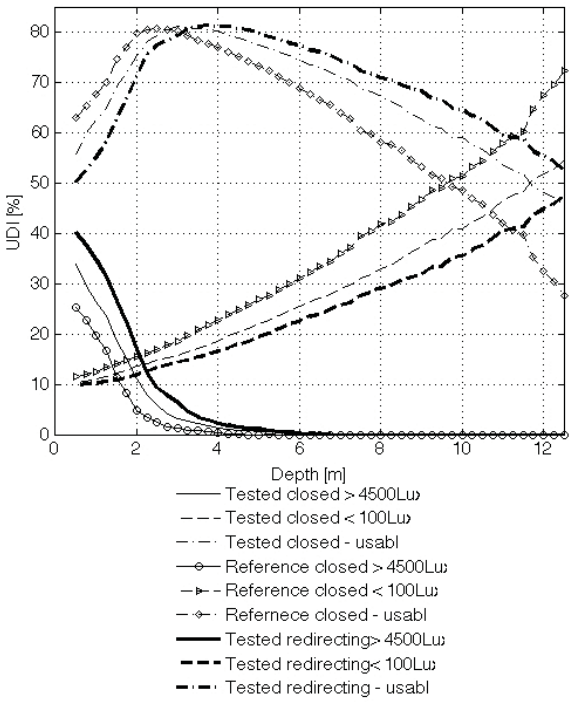

Figure 7: *Annual useful daylight illuminance matrix for different scenarios.*

the same orientation and layout and thus it was possible to compare the investigated parameters. The automated external redirecting glass lamellas system was synchronized with the actual sun position and sky distribution to expand the zone with the designed working plane illuminance lit by daylight and maximized the view out. In this study, the lighting conditions were simulated and measured during summer and autumn. The simulation results were compared with the measurements and the results correlated. Daylight improvement was achieved with the redirecting glass lamellas shading system compared to the original system. Glare analysis indicated that the tested redirecting system would not cause additional glare compared to the reference shading system. However, it is recommended to use an internal manual shading system, to block the excessive glare. It can be concluded that the visual comfort was maintained and the daylight conditions in the office were improved. By introducing higher penetration of daylight into the back of the office, the artificial lighting electricity use was decreased. Depending on the daylight-linked lighting control, the savings were up to 20% compare to the reference system and up to 80% in zone 1, when compared to using the artificial light only. Thermal insulation

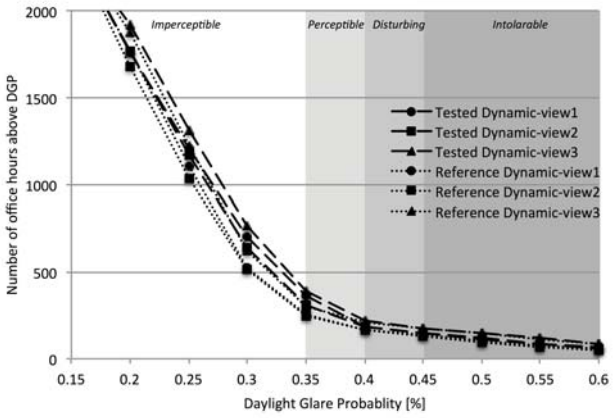

Figure 9: *Annual working hours DGP profile for view 1, 2, 3; for the tested and reference system in dynamically controlled system, which switch between closed and redirecting position.*

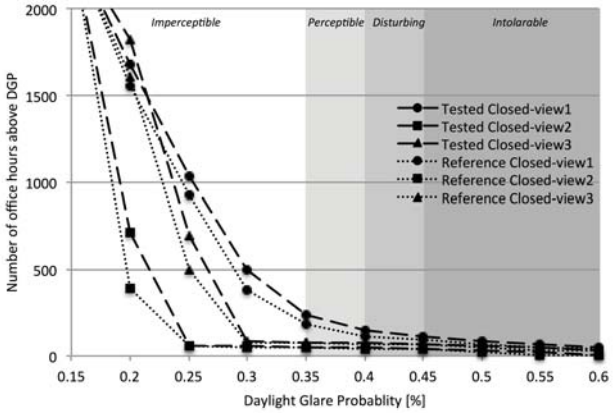

Figure 10: *Annual working hours DGP profile for view 1, 2, 3 for the tested and reference system in closed (shading) position.*

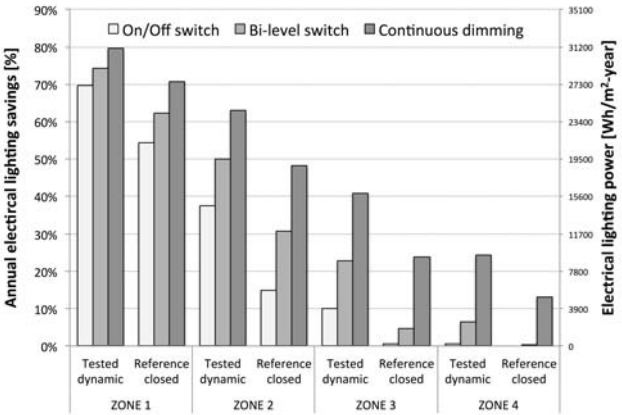

Figure 11: *Electrical light savings for WPI of 500 lux and different daylight linked lighting control strategies.*

of the façade was not influenced by the tested shading solution. The solar energy transmittance was increased; however, the increase is small and thus it is not expected to increase the cooling demand.

Acknowledgements

The research performed in this study was funded by the Danish Energy Agency programme for research and development of energy efficiency, PSO - F&U 2008.

References

[1] a. Laouadi and A. Parekh. Optical models of complex fenestration systems. *Lighting Research and Technology*, 39(2):123–145, June 2007.

[2] Directive 2002/91/EC. DIRECTIVE 2010/31/EU OF THE EUROPEAN PARLIAMENT AND OF THE COUNCIL. Technical report, 2010.

[3] DS/EN 15603. Energy performance of buildings - Overall energy use and definition of energy ratings. 2008.

[4] Eleanor Lee. Advanced High-Performance Commercial Building Facades Research. In *LBNL*, 2009.

[5] Jacob Birck Laustsen, Ines D.P. Santos, Svend Svendsen, Steen Traberg-Borup, and Kjeld Johnsen. Solar Shading System Based on Daylight Directing Glass Lamellas. In *Building Physics 2008 - 8th Nordic Symposium*, pages 111–119, 2008.

[6] Anne Iversen and Jacob Birck Laustsen. Udvikling af nye typer solafskærmnings- systemer baseret pådagslysdirigerende solafskærmende glaslameller. Technical report, 2009.

[7] F. Cantin and M.-C. Dubois. Daylighting metrics based on illuminance, distribution, glare and directivity. *Lighting Research and Technology*, 43(3):291–307, February 2011.

[8] G. Ward and R.A. Shakespeare. *Rendering with Radiance*. Space & Light, Davis, California, USA, 1998.

[9] Robin Mitchell, Christian Kohler, Arasteh, and Dariush. *THERM 5.2 / WINDOW 5.2 NFRC Simulation Manual*. Number July. Lawrence Berkeley National Laboratory, University of California, Berkeley, 2006.

[10] A Nabil and J Mardaljevic. Useful daylight illuminance: a new paradigm for assessing daylight in buildings. *Lighting Research and Technology*, 37(1):41–59, January 2005.

[11] Christoph F. Reinhart and Jan Wienold. The daylighting dashboard A simulation-based design analysis for daylit spaces. *Building and Environment*, 46(2):386–396, February 2011.

[12] John Mardaljevic. *Daylight simulation: validation, sky models and daylight coeffcients*. Phd thesis, De Montfort University, UK, 2000.

[13] A Mcneil and E S Lee. Annual Assessment of an Optically-Complex Daylighting System Using Bidirectional Scattering Distribution Functions with Radiance. *LBNL*, pages 1–29, 2010.

[14] CEN EN 15251. Indoor environment input for design and assessment of energy performance of buildings addressing indoor air quality, thermal environment, lightning and acoustics, 2007.

[15] J Mardaljevic, L Heschong, and E Lee. Daylight metrics and energy savings. *Lighting Research and Technology*, 41(3):261–283, September 2009.

[16] Jan Wienold. *Daylight Glare in Offices*. Phd thesis, 2009.

[17] G. Ward. Simulating the Daylight Performance of Complex Fenestration Systems Using Bidirectional Scattering Distribution Functions within Radiance. *Journal of the Illuminating Engineering Society*, (January), 2011.

[18] Greg Ward. The Radiance rtcontrib Program. In *Radiance workshop 2005*, Montreol, Canada, 2005.

[19] United States Department of Energy. Weather data.

[20] R Perez and R Seals. All-weather model for sky luminance distribution-preliminary configuration and validation. *Solar energy*, 50:235–245, 1993.

[21] Greg Ward. Complex Fenestration and Annual Simulation. In *8th International Radiance workshop*, Boston, USA, 2009.

[22] A Mcneil, C J Jonsson, D Appelfeld, G Ward, and E S Lee. A validation of a ray-tracing tool used to generate bi-directional scattering distribution functions for complex fenestration systems. *Solar Energy*, submitted, 2012.

[23] Axel Jacobs. Understanding rtcontrib. Technical report, London, UK, 2010.

[24] N Tuaycharoen and P.R. Tregenza. View and discomfort glare from windows. *Lighting Research and Technology*, 39(2):185–200, June 2007.

[25] L Roche, E Dewey, and P Littlefair. Occupant reactions to daylight in offices. *Lighting Research and Technology*, 32(3):119–126, January 2000.

[26] Jan Wienold. Dynamic daylight glare evaluation. In *Building simulation 2009*, pages 944–951. Citeseer, 2009.

[27] J WIENOLD and J CHRISTOFFERSEN. Evaluation methods and development of a new glare prediction model for daylight environments with the use of CCD cameras. *Energy and Buildings*, 38(7):743–757, July 2006.

[28] J. a. Jakubiec and C. F. Reinhart. The 'adaptive zone' - A concept for assessing discomfort glare throughout daylit spaces. *Lighting Research and Technology*, October 2011.

[29] DS/EN 15193. Energy performance of buildings - Energy requirements for lighting, 2007.

[30] David Appelfeld, Andrew Mcneil, and Svend Svendsen. An hourly based performance comparison of an integrated micro-structural perforated shading screen with standard shading systems. *Energy & Buildings*, 2012.

Part III

Appendix-supplementary papers

Paper V

"A validation of a ray-tracing tool used to generate bi-directional scattering distribution functions for complex fenestration systems"

A. McNeil, C.J. Jonsson, D. Appelfeld, G. Ward, & E.S. Lee

Submitted to: *Solar Energy, 2012*

A validation of a ray-tracing tool used to generate bi-directional scattering distribution functions for complex fenestration systems

***A. McNeil*[1], *C.J. Jonsson*[1], *D. Appelfeld*[2], *G. Ward*[3], *E.S. Lee*[1]**

[1] *Building Technologies Program, Environmental Energy Technologies Division, Lawrence Berkeley National Laboratory, Mailstop 90-3111, 1 Cyclotron Road, Berkeley, CA 94720 USA*

[2] *Technical University of Denmark, Department of Civil Engineering, Section of Building Physics and Services, Brovej, Building 118, DK-2800 Kgs. Lyngby, Denmark*

[3] *Anyhere Software, 950 Creston Road, Berkeley, CA, 94708 USA*

Keywords: *Daylight, Complex fenestration systems, Bi-directional scattering distribution function, Illuminance, Shading devices, Daylight simulations.*

Abstract

A new Radiance ray-tracing simulation tool, genBSDF, enables users to generate bi-directional scattering distribution functions (BSDF) for an optically complex fenestration system (CFS). Prior to genBSDF, BSDF data for arbitrary fenestration systems could only be produced using either expensive commercially available forward ray tracing software or by measurement (with a goniophotometer or imaging sphere). genBSDF outputs CFS data in the Window 6 XML file format and so can be used with that software to model any arbitrary window system composed of glazing and shading layers. This study explains the basis of the genBSDF tool, its use, then validates the tool by comparing its output for four different CFS to BSDF data produced through alternate means. Like Radiance, genBSDF is free and open source.

1 Introduction

Until recently there has been little support for complex fenestration systems technologies in simulation programs like Radiance and EnergyPlus. This disconnect made it difficult for manufacturers to predict performance of their products and for designers or owners to evaluate technologies for their buildings. Designers typically made overly conservative assumptions and simplifications when evaluating the performance of optically complex fenestration systems (CFS), such as conventional venetian blinds, roller shades, or more innovative systems such as daylight-redirecting shading systems. The inability to accurately predict energy performance has hindered the adoption of promising technologies. New capabilities have been added to Radiance, Window 6, and are in progress for EnergyPlus that enable users to simulate the daylighting and solar heat gain performance of optically complex fenestration systems. These new capabilities use bi-directional scattering distribution functions (BSDF) to characterize the way light transmits and is reflected by CFS. To generate BSDF data, a manufacturer needs to take measurements with a goniophotometer and/or

simulate CFS properties using a forward ray tracing program like TracePro. Currently there are few goniophotometers in existence and the most popular forward ray tracing application is rather expensive. A new addition to Radiance, called genBSDF, allows users to generate a BSDF for arbitrary systems via simulation. The genBSDF program operates like a forward ray tracer, using the ray tracing capabilities of Radiance and switching the convention of source and receiver. genBSDF also uses the source tracking capabilities of rtcontrib. Radiance and the new genBSDF are free, open-source software enabling designers and manufacturers to generate BSDFs without expensive equipment or software.

1.1 Background

A BSDF characterizes the way light interacts with a material or system. Outgoing light distributions (transmitted and reflected) are characterized for many incident directions. Klems proposed a method to model solar gains for CFS using BSDF data [1] and described a means to derive a single BSDF for a multi-layer window system by multiplying the BSDF matrix for each layer [2]. The software program Window 6 [3] implemented Klems matrix multiplication algorithm to generate a BSDF for a complete multilayer window system.

The Window coordinate system, called the Klems angle basis, was designed specifically to simplify the matrix multiplication. The Klems angle basis has 145 input and output directions in nine concentric theta bands (Figure 1). The number of phi divisions of each theta band and the width of the theta band are modulated to so that all divisions have roughly the same cosine-weighted solid angle. Angular divisions are indexed starting from the normal patch working outwards. The incident hemisphere uses a right-handed coordinate system and the transmitted hemisphere uses a left-handed coordinate system. This coordinate systems are shown in figure 1. Light incident at theta 40°and phi 90°are in the Klems incident patch 64. If this light is transmitted specularly it leaves at a theta angle of 40°but phi angle of 270°, however it is still in patch 64 on the outgoing Klems's coordinate system. The switching of the coordinate systems convention allows the incident and specular transmission patches to have the same index, simplifying BSDF multiplication for layered systems.

Window 6 uses an XML file specification to organize data in a BSDF file. The XML file contains data blocks describing reflection on front and back surfaces and transmission on front and back surfaces (transmission data for front a back are the same due to reciprocity). Each data block contains 21,025 values made up of 145 outgoing directions for each 145 of incoming directions (145x145). Radiance and EnergyPlus support BSDFs using Window 6 XML specification and the Klems angle basis.

Current methods for creating a BSDF varies based on the CFS to be characterized. Measurement can be used to characterize homogeneous or micro structure samples. An integrating sphere spectrophotometer can be used to measure total specular and diffuse transmission for one incident direction. Using angled sample holders allow testing at non-normal incident angles in an integrating sphere spectrophotometer. Polynomial functions can be used to modify the distribution of diffuse transmission for some CFS. A goniophotometer provides high-resolution spatial transmission data. For non-isotropic systems, the overhead of adjusting sample orientation limits the number of incident angles measured on a goniophotometer. Macro-scaled CFS often require ray tracing simulations to generate a BSDF because the incident light source of measurement devices can't cover the CFS variation adequately.

There are two types of illuminating sources that can be used when generating a BSDF: 1) a collimated source, or 2) an area source that fills the Klems patch. With a collimated source, all light arriving has the same incident angle corresponding to the center of the Klems patch. With the area source, the outgoing BSDF distribution is integrated over all angles within the incident patch. In a simulation, the same output distribution is used for energy arriving at any angle within the patch, regardless of incident direction with in the patch. For this reason, it is better for a BSDF to be produced using an area source that characterizes optical properties integrated of the incident patch. Generating BSDFs using area sources or collimated sources is not difficult through simulation, but to do so with measurements is a challenge.

Raytracing has been compared with other methods to produce BSDFs before [4, 5] and it is clear that a raytracer must be set up to replicate the conditions of the other method as close as possible to get good agreement. Poor agreement does not necessarily indicate that one method is incorrect. Whenever a BSDF value is measured at an angle where the function has a non-zero derivative, be it with a physical detector or a virtual detector in a raytracer, the result can depend on the solid angle the detector. The measured value is an average over the solid angle of the detector, a limitation of trying to measure a per solid

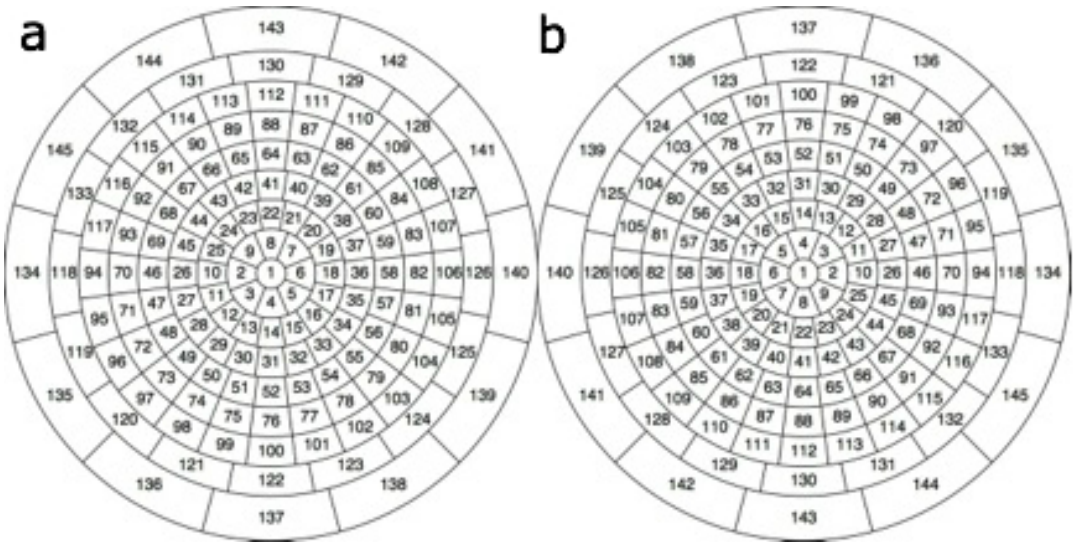

Figure 1: *Angular projection of Klems angle basis viewed from the incident side for (a) incident and (b) transmitted hemispheres.*

angle property using a finite area sensor. This is not only a concern when comparing raytracers with goniophotometers, but also when comparing different raytracing configurations.

2 Overview of genBSDF

2.1 Description of genBSDF function

The genBSDF tool is a PERL program that uses other Radiance programs to act like a forward ray tracer. The program uses the radiance source primitive to create two infinitely distant hemispheres (one for transmission and one for reflection) to receive emitted rays. These receiving hemispheres are combined with CFS geometry into an octree model. An imaginary rectangular emitting box (or bounding box) on the outdoor side of the CFS sample is used to generate rays to sample the system. Ray origins are randomly distributed over the emitting surface and ray directions are randomly distributed over each Klems patch (within the range of angles defined by the conical direction of the Klems patch). By default, genBSDF emits 1000 samples per Klems patch, 145,000 sample rays in total. Distributing the sample ray directions over the Klems patch, genBSDF is using the patch illuminating source method for generating a BSDF.

The rays emitted navigate through the CFS model until they hit the receiving surface. When a ray strikes a surface, additional rays are spawned to simulate both diffuse and specular reflection. As multiple interreflections occur, an ever expanding ray tree is produced. When rays finally hit the receiving surface, they are binned into Klems patches using the ray's vector. The weight of rays accumulated in a Klems patch are summed to generate the contribution coefficient. Rays that do not reach the receiving surface are not included in the contribution. The contribution coefficients for all the emitted rays in a Klems patch are averaged. To get to BSDF values, the averaged coefficients are divided by the solid angle and average cosine theta of the *emitting* patch. A full BSDF contains data for front and back transmission and front and back reflection.

You may have noticed in the previous paragraphs the quotes used for *receiving* hemisphere and *emitting* surface. The reason for the quotes is because while Radiance is a backwards ray tracing program [6], genBSDF uses Radiance as though it were a forward ray tracer. The rays emitted by genBSDF by standard radiance convention are not light rays but detector rays that are looking for light sources and the *receiving* hemispheres are actually light sources in typical Radiance. The actual value returned from rtcontrib is the accumulated contribution coefficients from the Klems patches on the receiving surface. However, whether a ray tracer is backwards or forwards depends on what is defined as a source and receiver. The flexibility of Radiance and in particular the program rtcontrib allows for sources and receivers to be reversed by genBSDF. The physics of light support this role reversal.

2.2 Using genBSDF

Since genBSDF is written in PERL, it can be run on any operating system capable of running PERL

Table 1: *Command line options for generating Klems basis BSDFs with genBSDF*

Command Line Option	Description
-c Nsamp	Sets the number of sample rays per Klems division. The default is 1000 samples per Klems division.
-n Nproc	Sets the number rtrace processes to run. This option allows users to make use of multiple processors to reduce computation time. The default is 1.
-r 'rtcontrib opts...'	Set simulation options for rtcontrib (-ab, -ad, -ss, -lw etc.)
+b (-b)	Create a BTDF and BRDF for back (indoor) surface of CFS.
+f (-f)	Create a BTDF and BRDF for front (outdoor) surface of CFS.
{+|−} mgf	Specifies the input model format. The default for input model format is Radiance (-mgf). MGF can be used with +mgf.
{+|−}geom unit	Geometry will be included in the resulting XML file if +geom is set (this is the default). Geometry is excluded with -geom. The length unit must be given in either case, and must be one of meter, foot, inch, centimeter, or millimeter. Output geometry is MGF regardless of input format.
-dim Xmin Xmax Ymin Ymax Zmin Zmax	Normally, "emitting" rectangles are positioned according to the bounding box of the model. This option allows the user to specify a different bounding box.

(including MS Windows, Mac and Linux), though currently genBSDF uses some system commands that need to be rewritten for use on MS Windows. To run genBSDF a working installation of Radiance is required since genBSDF uses system commands to run the Radiance programs rtcontrib, rtrace, cnt, rcalc, oconv, rad2mgf, and mgf2rad.

The first step for using genBSDF is to create a model of the system. The model can be in either MGF [7] format or Radiance format. There are various converters available to convert geometry from other formats to Radiance format, however Radiance material descriptions must be added by hand. Using a Radiance input model permits measured BSDF materials to be incorporated via the new BSDF primitive. The genBSDF tool uses the Klems coordinate system, so the model must be oriented accordingly. The positive Z direction points inside and positive Y is up for the fenestration. The model should be entirely in the -Z half-space. Geometry that protrudes into the +Z half-space may cause unexpected errors in subsequent simulations using the BSDF. Since Radiance defines the emitting planes (plane just above and below the CFS) as rectangular, genBSDF expects that the CFS is contained within a rectangular profile. For CFS not contained within the profile, output will be produced but some sample rays will be generated outside of the system model and taint the resulting BSDF. We can override this behavior using the dim option to specify a subregion for sampling.

The genBSDF program is run from a command prompt. Table 1 contains the command-line options recognized by genBSDF.

3 Validation

Four test cases were used to validate genBSDF (Table 2). A BSDF was created using genBSDF for all four cases. The resulting front transmission data from genBSDF was compared against analytically derived values, TracePro simulation data, or goniophotometer measurements.

3.1 Validation Case 1: Air (100% specular transmission)

The BSDF matrix for air (and other specularly transmitting materials) is a diagonal matrix. The diagonal values of the matrix are the specular transmission times cosine theta integrated over the discrete patch divided by the solid angle of the patch. To test this case, we used a polygon with no material specified (void):

We ran genBSDF using this polygon description and set the number of sample rays per Klems patch to 10,000. The result is a diagonal matrix as expected. The results for theta bands 1-9 were all identical to the expected value to six significant digits. Table 3 contains the expected BSDF value and mean genBSDF result for each theta band.

Table 2: *CTest cases for validation.*

Test Case	Validated Against
Air (100% specular transmission)	Analytically derived values
50% Lambertian transmission	Analytically derived values
Mirrored blinds with flat slats	TracePro simulation
Micro-perforated shading film	Goniophotometer measurements

Table 3: *CTest cases for validation.*

Theta band	Patch numbers	Theta range	Solid angle	Average cosine theta	BSDF value for specular patch	genBSDF result (mean for theta band)	Percent difference
1	1	0-5°	0.0239	0.9981	41.9043	41.9043	0.00%
2	2-9	5-15°	0.0238	0.9811	42.8864	42.8764	0.02%
3	10-25	15-25°	0.0234	0.9361	45.6281	45.6281	0.00%
4	26-45	25-35°	0.0274	0.8627	42.3330	42.3330	0.00%
5	46-69	35-45°	0.0293	0.7631	44.6724	44.6724	0.00%
6	70-93	45-55°	0.0350	0.6403	44.6724	44.6724	0.00%
7	94-117	55-65°	0.0395	0.4981	50.7996	50.7996	0.00%
8	118-133	65-75°	0.0643	0.3407	45.6281	45.6281	0.00%
9	134-145	75-90°	0.1355	0.1294	57.0215	57.0215	0.00%

```
### void.rad ###
void polygon plane
0
0
12  0   0   0
    0   10  0
    10  10  0
    10  0   0

genBSDF void.rad ≻ void.xml
```

```
### diffuse50.rad ###
void trans diffuse50
0
0
7   0.5  0.5  0.5  0  0  1  0

diffuse50 polygon bottom
0
0
12  0   0   0
    0   1   0
    1   1   0
    1   0   0
```

3.2 Validation Case 2: Lambertian diffuser with 50% transmission

The BSDF for a Lambertian transmitter equals the total transmission divided by π. The Radiance trans material provides the ability to model diffuse transmission. The input model for genBSDF was as follows:

The BSDF for this model was generated using genBSDF with the default number of samples per Klems division (1000). The resulting BSDF was comprised of values ranging between 96-104% of the anticipated result. For most simulations, this is likely within acceptable limits. To satisfy our curiosity, we also generated a BSDF using 10,000 samples per Klems division and generated a BSDF by changing the default -ad parameter from 700 to 7000. The ad parameter sends out more ambient samples, which reduces noise in the inter-reflected component. Table 4 contains statistical analysis of the BSDF values from the 1000 and 10,000 sample genBSDF runs.

3.3 4.3. Validation Case 3: Mirrored blinds

A flat slat blind system with specular upper and matte lower finishes was modeled in Radiance and TracePro to compare BSDF output. The blind slats are 80 mm deep, 0.4 mm thick and spaced 72 mm apart. The width of the blinds were 2 m. The upper surface had a purely specular reflectance of 91.7%. The lower slat surface had a Lambertian reflectance

Table 4: *Distribution of values in generated BSDF.*

genBSDF settings	-c 1,000	-c 10,000	-c 1000 -r '-ad 7000'
mean	0.15916	0.15915	0.15915
maximum BSDF value	0.16507	0.16265	0.16231
maximum relative error	3.7%	2.2%	2.0%
minimum BSDF value	0.1525	0.15660	0.15915
minimum relative error	-4.2%	-1.6%	-1.0%
mean bias error	0.00058%	-0.000071%	0.000034%
RMS Error	0.89%	0.56%	0.53%

of 29%.

TracePro and genBSDF have different methods for sampling a model. In TracePro, the sample rays are generated along the centerline between to blind slats, and are collimated they all have the same direction. In genBSDF sample origins are distributed randomly over the inside plane of the blinds and sample ray directions are not collimate, but are distributed randomly over the Klems patch.

Figure 2 illustrates the percent difference between the two results with the incident patch number on the x-axis and outgoing patch number on the y-axis. Agreement between genBSDF and TracePro results vary and mostly depend on incident patch (shown as columns in Figure 2). Results for some incident patches are not consistent between programs: for example, the Klems patch 1 (normal incidence) shows 100% disagreement for all outgoing angles (the leftmost column in Figure 2). Since the incident light in TracePro is collimated and Klems patch 1 is perpendicular to the blind, most of the flux is transmitted directly while the 0.4 mm face of the slat blocks just some of the light. In Radiance, the incident light is spread over the patch, so some light reflects off the matte and specular surfaces. The flux reflecting off the matte surface is evident in many patches, registering a larger percent error. None of the flux in TracePro strikes the matte or specular surfaces of the slat, therefore the percentage difference is large up to 100%. Results for some incident patches are consistent between programs. In the case of Klems patch 76 where percent differences are less than 10%, the incident flux strikes the matte surface (underside) of the slat. The diffuse reflection is evident in results from both TracePro and genBSDF simulations.

To verify that the difference between results from genBSDF and TracePro is attributable to the difference in simulation procedure, we created a modified version of genBSDF that mimics the simulation procedure of TracePro. First, the illuminating source was changed from an area source to a collimated source originating from the center of each patch by removing the random variables in ray direction. Second, since the TracePro model emits rays from a thin strip, the genBSDF emitting surface was reduced from the 2 m square covering the entire system to the section of the CFS modeled in TracePro: a 2 mm wide and 72 mm tall strip aligned with one period of the blind system (the TracePro model was sufficient to characterize the system and kept the calculation time to a minimum). Finally, since TracePro cannot model infinitely distant receivers, the genBSDF infinitely distant receiving hemisphere was changed to a 20 m disk, which is the size of the hemisphere used in TracePro. This final change mimics the hemisphere used in TracePro to collect and bin outgoing flux.

Figure 3 shows the percent difference of BSDF values between the modified version of genBSDF and TracePro. Overall, the percent error is low. However, exiting patches 50-54 exhibit high percent error over many incident patches. These errors are not alarming because the magnitude of error is small. The reason that these errors appear is the flux reaching these patches arrives by a specular reflection of a very small sliver of the matte surface. The probability of an ambient sample ray from the sliver of matte surface goning in to an equally small sliver of the specular surface to reflect in the direction of patches 50-54 is low and thus the Monte-Carlo simulation results are noisy. Figure 4 shows detailed BSDF values for outgoing patch 54.

3.4 Validation Case 4: Micro-perforated shade

The final validation case involves a micro-perforated shading system measured with a goniophotometer and modeled in Radiance with genBSDF. The micro-perforated metal screen is a thin sheed of metal with elliptical holes less than 1 mm in width and less than 0.5 mm in height (Figure 5). The holes are

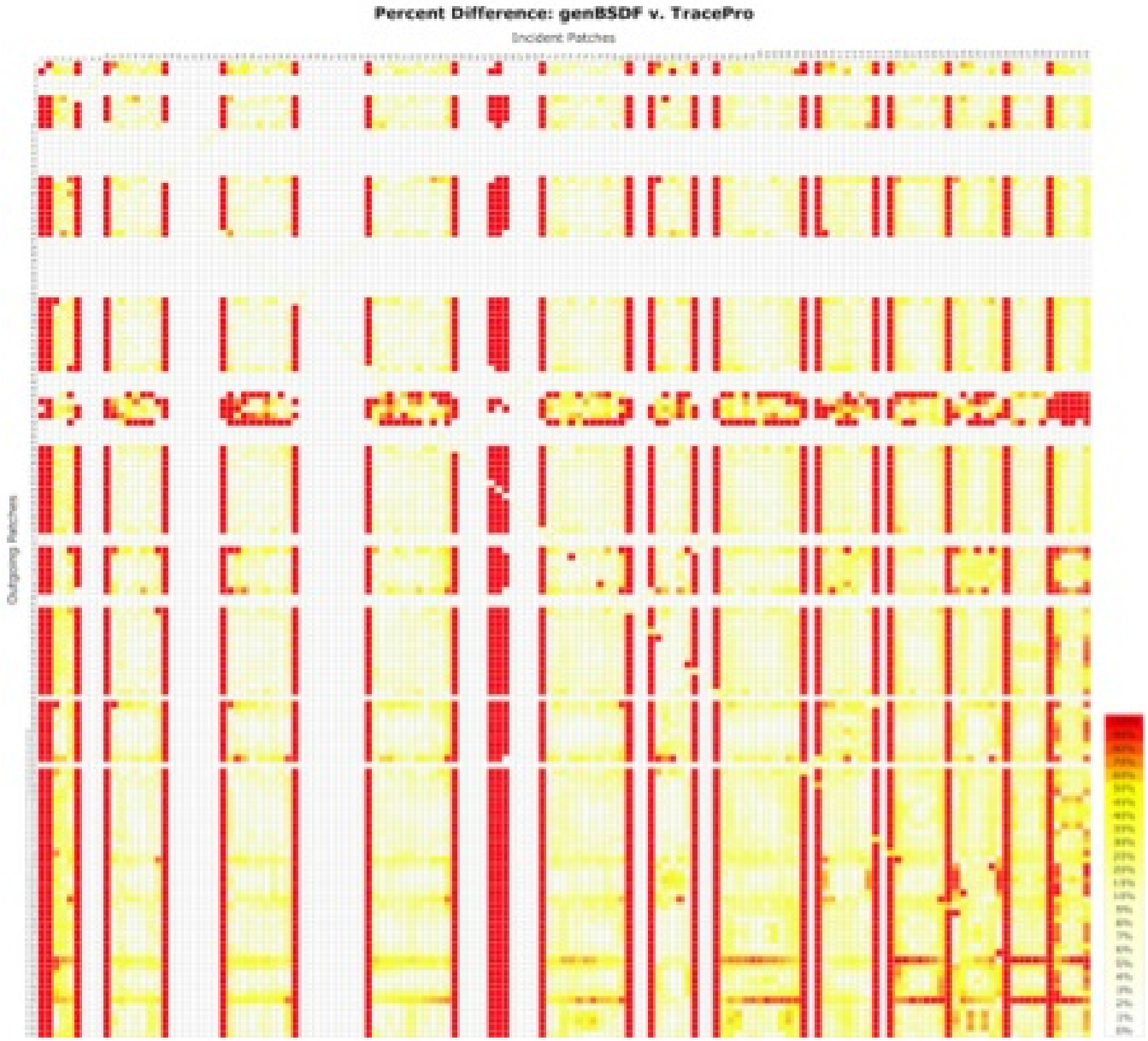

Figure 2: *Percent difference between genBSDF and TracePro generated BSDF's for flat specular blinds.*

cut in a downward direction (when viewed from the inside). Maximum transmission of the perforated shade occurs when looking from inside to outside in a downward direction about 10°below horizontal. A CAD model of the micro-perforated shade was created using a dimensioned drawing provided by the manufacturer. An un-cut sample of metal provided by the manufacturer was measured in a spectrophotometer to obtain the reflectance of the material. The BSDF for the shading system was then determined using the geometry and measured reflectance in the modified version of genBSDF, where the source is collimated. The collimated source in the simulation was used to more closely resemble the source used by the goniophotometer.

Figure 6 compares the genBSDF results to the goniophotometer measurements for one incident angle (Klems incident patch #88). The most striking difference between the measured and simulated BSDFs occurs at outgoing directions corresponding to patches #64 and #112. There are peaks measured in these directions that are not replicated in the simulations. Patches #64 and #112 are adjacent to the specular patch (#88) and are in the scattering plane defined by the surface normal and the incident ray. The pattern continues out to patch 41 and patch 130 as well, though these peaks are much lower. The Y-axis in Figure 6 uses logarithmic scale to show those differences, otherwise the direct direct transmittance through patch #88 would dominate and the chart would not illustrate the energy transmitted to the other directions. The non-specular patches contain

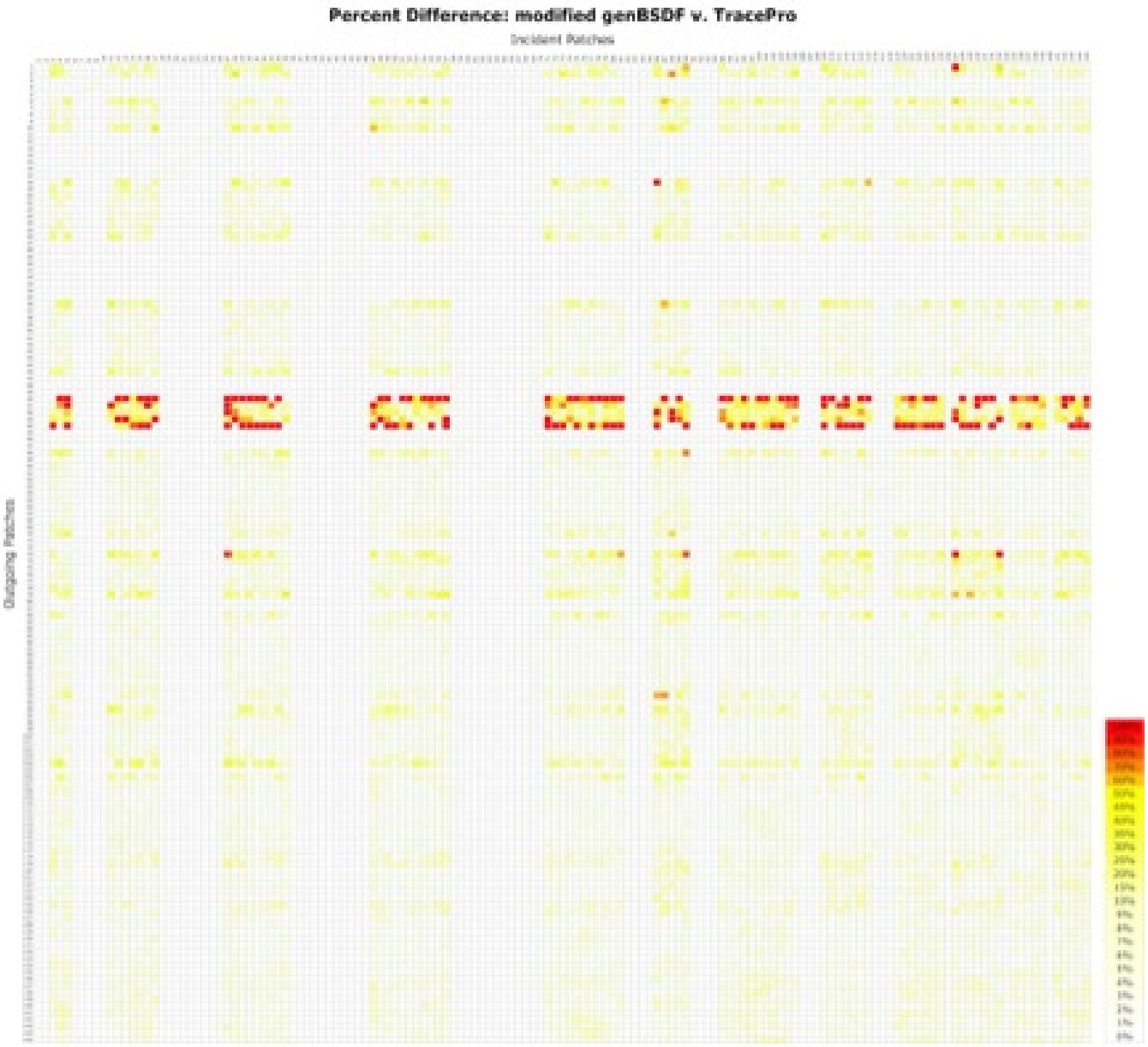

Figure 3: *Percent difference between genBSDF and TracePro generated BSDF's for flat specular blinds.*

2-5 orders of magnitude less energy than the direct transmission in the specular patch (patch #88).
The difference between the measured and simulated values is caused by diffraction. Radiance only simulates ray optics and does not reproduce wave optic phenomenon including diffraction. The ellipse diameter is larger than would typically be considered to cause diffraction, but the effect is so small (1000x smaller than the peak) that diffraction could indeed be the cause.
Figure 7 contains charts of transmission for incident theta angles ranging from 0°to 70°. The phi angle is 90°(azimuthal angle 0°) and above the horizon. Simulation tracks the goniophotometer measurements for both direct-hemispherical and direct-direct with perturbations occurring at 0°and 30°incident angles. These charts illustrate that BSDF generated via simulation provides reasonably accurate transmission values.

4 Discussion

Over the course of validating genBSDF, critical differences in assumptions were identified that resulted in differences in BSDF values generated by genBSDF and other simulation or measurement methods. Ensuring that the sampled area of the CFS system is representative of the system as a whole is relatively easy to remedy. To characterize optical properties using the Klems angle basis, it is more appropriate to use an solid-angle source matching the Klems patch

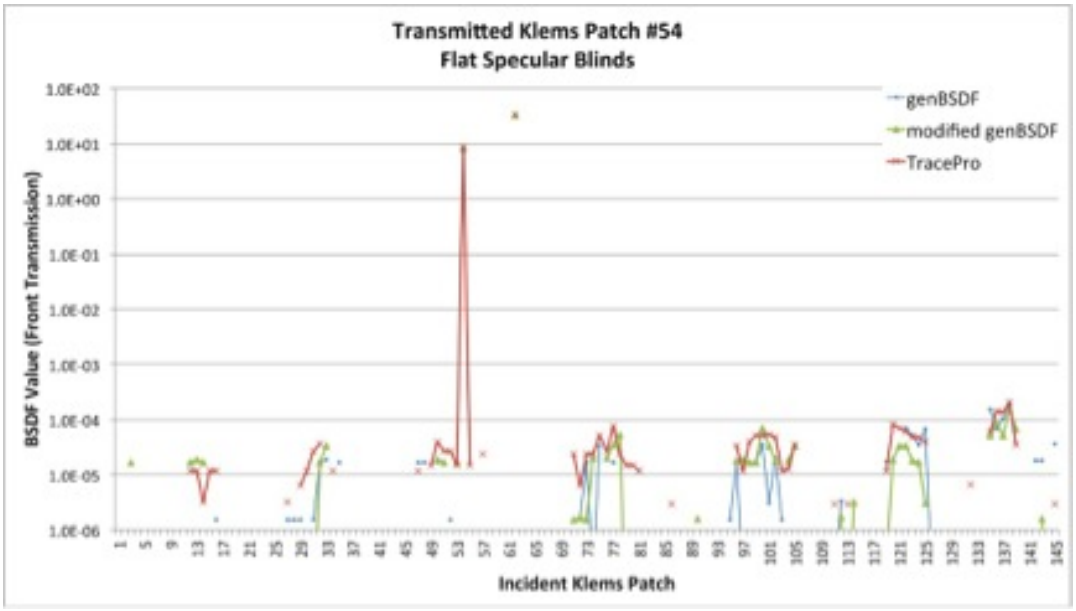

Figure 4: *Plot of BSDF values for transmitted patch 54 from genBSDF, the modified version of genBSDF, and TracePro.*

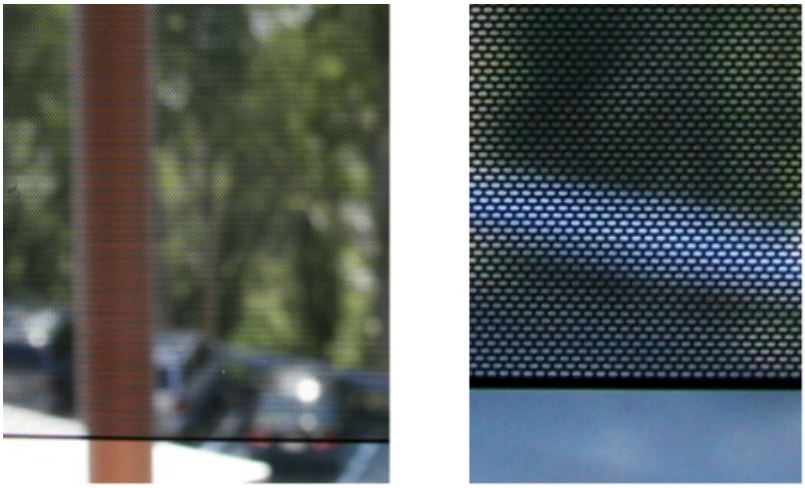

Figure 5: *View through the micro-perforated shade held at arms length (left), and a closeup view of the micro-perforated shade (right).*

rather than a collimated source. The genBSDF tool uses a solid angle source, and this can be done in TracePro with some effort. However it is unlikely that an area source can be used with the goniophotometer since the source would need to be both large and focused and is further complicated by the fact that area source size and shape is different for each theta ring in the Klems basis.

By modifying genBSDF to match the assumptions used to model the system in TracePro software, we were able to demonstrate that genBSDF produces the same BSDF data as TracePro for nearly all input and output angles, with the exception of a few exiting patches that could be explained by inadequate Monte-Carlo sampling (Case 3). Comparisons against measured data showed more variation in Case 4 some of which can be explained by diffraction . However, the overall transmission in Case 4 was determined to be reasonably accurate.

Generating BSDF datasets for daylight and energy simulation is a challenge. Direct measurement of bidirectional scattering properties with a goniophotometer is only possible for systems with small scale, homogeneous structures. These measurements are also time consuming, for non-symmetric systems with anisotropic transmission, obtaining measured data for 145 incident angles can currently take up to a month for a single sample. For macro-geometric systems, like specular blinds, the systems are too large to be practically measured in a scanning goniopho-

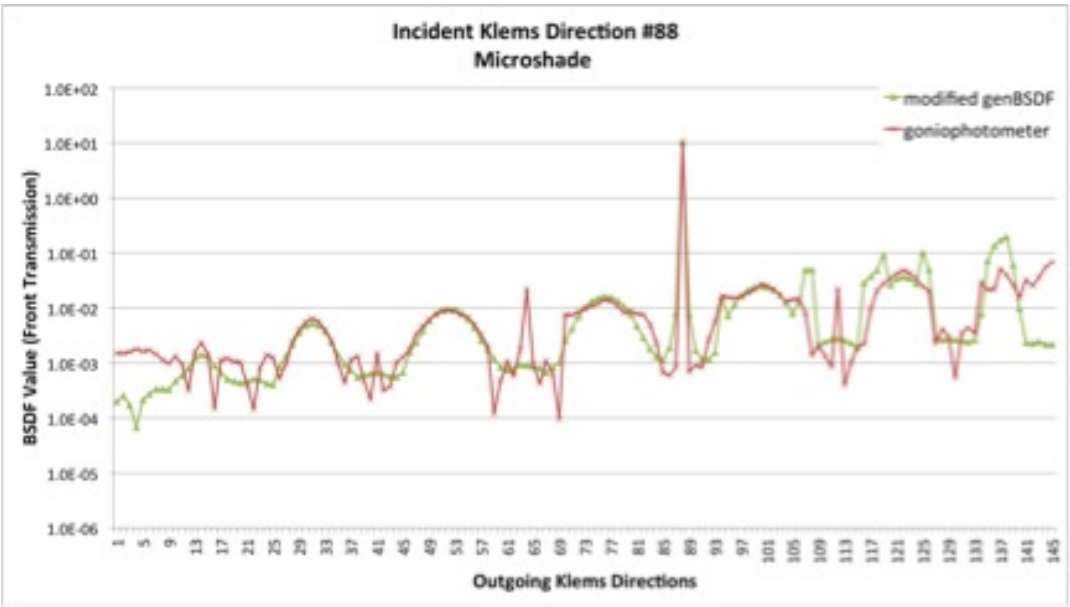

Figure 6: *Chart of measured and simulated BSDF values for Klems incident patch number 88.*

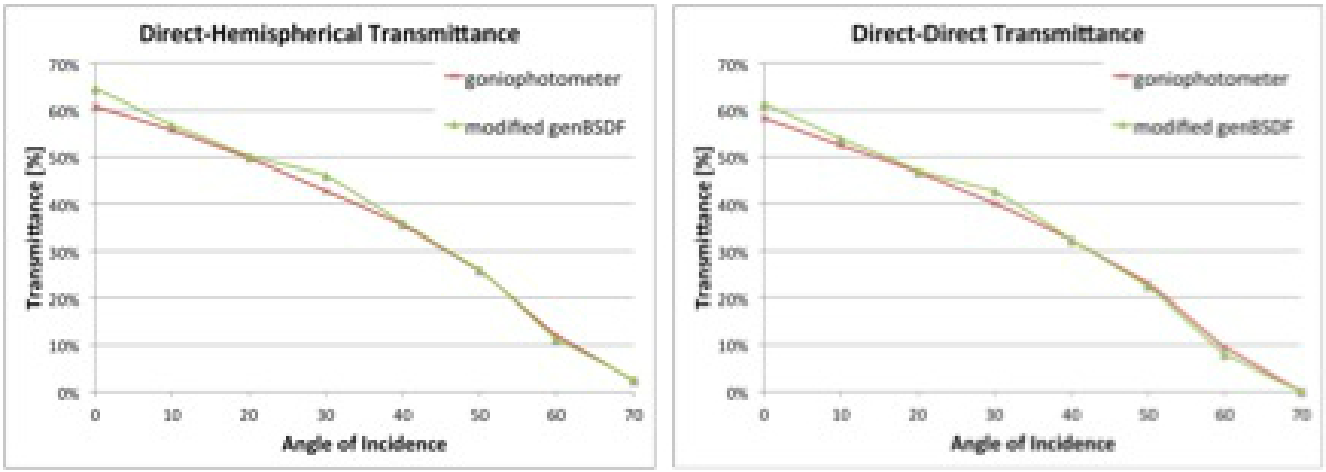

Figure 7: *Charts of (a) direct-hemispherical transmittance, (b) direct-direct transmittance for measured and simulated BSDFs.*

tometer and so BSDF datasets can only be produced using BSDF material data assigned to surfaces in a ray-tracing simulation.

The Window 6 BSDF XML schema is currently the only standardized format to describe directionally dependent window optical properties. Users of simulation programs will use BSDF data in to improve the accuracy of solar optical modeling in their simulations. When BSDF capabilities of Radiance and Energy plus are fully functional, users will need a convenient and trusted means to obtain BSDF data for commercially available fenestration systems. To address this need the NFRC and LBNL are in the process of developing a complex glazing database (CGDB) that will contain BSDFs for optically complex fenestration systems. The CGDB submittal process may be similar to the international glazing database (IGDB) where products are tested by independent labs and submitted for review and inclusion in the database.

The genBSDF tool may offer a pathway for product data to be included in the CGDB. Currently, genBSDF only generates data for the visible spectrum, but my modifying the material reflectance values in the RADIANCE it may be possible to produce data for the NIR spectrum or many wavelength bands. This is done by changing the material properties and re-running genBSDF. The results must then be manually assembled using the many output files from genBSDF runs. This would be cumbersome for many wavelength bands, but could perhaps be automated.

5 Conclusion

As part of the Radiance simulation suite of tools, a new ray-tracing tool was developed to generate bidirectional scattering distribution function datasets for shading and daylighting systems. The genBSDF tool is free, open source, and has been validated against TracePro and measured data. The output BSDF data produced by this tool follows the BSDF file format defined by the Window 6 program, by the daylighting simulation tools in Radiance (mkillum, rtcontrib), and by EnergyPlus. The tool provides end users with the ability to create BSDF data for macroscopic scale complex fenestration systems (CFS) of any arbitrary geometry and then evaluate the performance of these systems using building simulation tools. System geometry and material bidirectional reflectance properties are needed to model CFS accurately.
The ability to model the performance of CFS using BSDF data is a relatively new capability. There is still significant work to be done to build and validate tools that address the broad range of available optically complex fenestration systems. Measurement systems need significant improvements to enable more routine data collection. Quality control is needed to ensure that the methods used to create BSDF data by different parties are generated using consistent protocols.

6 Acknowledgements

We thank PhotoSolar for providing samples of the micro-perforated shade screen for testing.
This work was supported by the Assistant Secretary for Energy Efficiency and Renewable Energy, Office of Building Technology, State and Community Programs, Office of Building Research and Standards of the U.S. Department of Energy under Contract No. DE-AC02-05CH11231 and by the California Energy Commission through its Public Interest Energy Research (PIER) Program on behalf of the citizens of California.

References

[1] J.H. Klems. A new method for predicting the solar heat gain of complex fenestration systems - I Overview and Derivation of the Matrix Layer Calculation. *LBNL*, 1994.

[2] J.H. Klems. A new method for predicting the solar heat gain of complex fenestration systems - II Detailed description of the matrix layer calculation.pdf. *LBNL*, 1994.

[3] Robin Mitchell, Christian Kohler, Ling Zhu, and Dariush Arasteh. THERM 6.3 / WINDOW 6.3 NFRC Simulation Manual. *LBNL*, (January), 2011.

[4] Marilyne Andersen, Michael Rubin, and Jean-louis Scartezzini. Comparison between ray-tracing simulations and bi-directional transmission measurements on prismatic glazing. *Solar Energy*, 74(2):157–173, 2003.

[5] Marilyne Andersen, Michael Rubin, R Powles, and Jean-louis Scartezzini. Bidirectional transmission properties of venetian blinds : experimental assessment compared to ray-tracing calculations. *Solar energy*, (June 2004), 2004.

[6] G. Ward and R.A. Shakespeare. *Rendering with Radiance: The Art and Science of Lighting Visualization*. Morgan Kaufmann, California, USA, 1998.

[7] Greg Ward. The Materials and Geometry Format. Available from: radsite.lbl.gov/mgf/mgfdoc.pdf, 1996.

Paper VI

"Performance of a daylight redirecting glass shading system demonstration in and office building"

D. Appelfeld, S. Svendsen & S. Traberg-Borup

Published in: *Procceadings of Buildings Simulation, 2011*

PERFORMANCE OF A DAYLIGHT REDIRECTING GLASS SHADING SYSTEM DEMONSTRATION IN AN OFFICE BUILDING

David Appelfeld[1,*], Svend Svendsen[1] and Steen Traberg-Borup[2]
[1]Technical University of Denmark, Department of Civil Engineering, Section of Building Physics and Services
[2] SBi, Danish Building Research Institute, Denmark
[*]Corresponding Author: dava@byg.dtu.dk

ABSTRACT

This paper evaluates the daylighting performance of a prototype external dynamic integrated shading and light redirecting system. The demonstration project was carried out on a building with an open-plan office. The prototype and original façades were placed on the same floor with the same orientation and similar surroundings. The existing façade was used as the reference for measurements and simulations. The focus of this research project was to employ available simulation tools for the system performance evaluation. This was accompanied by measurements of the daylight conditions in the investigated space. The prototype system improved daylighting conditions compared to the existing shading system.

INTRODUCTION

The growing demand for energy savings, money savings, and seeking new innovative technologies is the motivation of the research. Available simulation programs cannot easily evaluate unique complex fenestration systems using standardized methods, since they are mostly created to evaluate specific solutions. The complexity of the assessment can be seen from many perspectives such as energy impact, shape, material, cost and operating cost. Therefore, we have to use more generic and versatile simulation programs and techniques to have the possibility to evaluate the performance impact. Consequently, by the obtained knowledge it is possible to do an evaluation on more standardized level for future solution development.

Additionally, the need to cut down energy consumption of buildings has led to buildings that are increasingly insulated against heat losses. It has been emphasized in many publications and studies that buildings consume around 40% of overall energy used globally (EU, 2010). Therefore cutting the energy used by buildings is of major interest in this study. The solar gains in the buildings are twofold. The glazed areas in the new office buildings are getting larger, which increases solar gains during the cold periods of year and increase working plane illuminance, however during the warmer season the over-glazed areas can cause overheating problems or cause glare. Using energy to remove excessive heat is costly and may completely wash out the energy saving effect of utilizing solar energy for space heating. In addition, the solar gains in newly built buildings are considered as significant source of heating. Therefore, the solar gains have to be included in the total energy demand of a building (EN 15603, 2008). Hence, transparent parts of the building envelopes serve several functions. First, they must provide enough light transmittance, or daylight utilization, which is also the main purpose behind this article. Second, they should provide sufficient solar energy transmittance during cold months. Third, they should prevent indoor space from overheating during warmer months by shading excessive solar gains without blocking the view and the solar energy gains, as has been a pitfall of current shading systems. Since a significant portion of energy in the buildings is devoted to lighting and ventilation, daylight and cooling have a large energy saving potential for advanced solar shading systems (Lee, 2009).

BACKGROUND

Based on previous studies, a shading system with light redirecting glass lamellas with a solar control surface was built as demonstration (Laustsen et al., 2008; Iversen et al., 2009). The shading system removes the drawback of the current systems, which partly block views, while shade excessive solar gains and redirect daylight into the back of deep office rooms where daylight is desirable. The investigation was based on the full-scale demonstration project and is accompanied by computer modelling. The simulation model can be used for various buildings, since it is not feasible to build a demonstration for all possible buildings and shading scenarios. The evaluation of the performance of the shading system by simulations is the objective and the central point of the research. The main focuses are to evaluate the daylighting performance of the demonstrated system, based on simulations and measurements of illuminance readings at working plane and comparing it with the reference system. The scope of this study is therefore not to evaluate the visual comfort aspects like glare, that might be caused by the shading system.

EXPERIMENT

Demonstration building

The demonstration building equipped with a prototype of an external dynamic integrated shading and light redirecting system is located in Humlebaek 30km north of Copenhagen, Denmark (55.96N - 12.49E). The building was refurbished from a production facility to an open space office, which caused deep open office space with working spaces far away from the façade. The building is one floor high and the open façade with 2.26m high windows is oriented 11° west by south. The whole building has dimensions of 66m x 28m with the longer side oriented south. The surrounded landscape is relatively flat without any big trees or high buildings that might shade the investigated façade. However, the opposite building blocks the open horizon. The open space office has a room depth up to 14m. The floor plan of building is on Figure 1. The building/façade layout allows preservation of a reference office space with the same orientation and similar layout as the investigated space for comparison of daylighting conditions. The two spaces were fitted with same set of illuminance sensors to monitor the actual conditions. The open space is divided by small meeting rooms, which are separated by the partitions. The partitions are partially from wood and glass, which allow better penetration of light into the space. The test and reference areas are both approximately 9.5m wide and 14m deep with ceiling height of 3.45m. The building has windows on the south and west façades with columns between individual windows. The window openings are 1.98m wide and 2.26m high with windowsill 0.75m above the floor. The reflectance of the surfaces in the building and outdoors were measured by illuminance meter in order to have identical surface properties for the measurements and simulation model. The visible reflectance measurements were averaged from three values measured on different places of the surface, values are presented in Table 1. The roughness and specularity of surfaces for the model were neglected.

Table 1
Building model surface reflectance values

SURFACE	VISIBLE REFLECTANCE (R_{vis})
Floor	20.5%
White walls	89.3%
Wooden partitions	32.6%
Ceiling	89.9%

The shading system

The major difference between the new and original shading system is that newly installed lamellas rotate in an opposite direction, compared to the conventional shading system. The outer edge moves upwards and the upper surface goes towards the façade when the system is closing.

Each window consists of eight horizontal 330mm wide lamellas. The rotation directions of the lamellas are demonstrated on Figure 2. Four uppermost lamellas rotated in toward the façade and the rest of lamellas rotate in opposite direction out of the facade. This strategy allows the upper part of the system to redirect and shade while the lower part acts as a traditional shading system which allows to see outside. The new system is made from highly reflective solar control coated glass to redirect daylight into the back of the room. New lamellas were produced by Saint Gobain Glass (SGG) and the used glass was Antelio Silver 10mm, with light reflectance of 31%. The original lamellas were made from Parasol Green 8mm with light reflection of 6%, made by SGG, with white frit covering 55% of the surface. The properties of shading glass, glazing and glass partitions are listed in Table 2.

Table 2
Centre-of-glass properties of glass used in the model

GLASS	VIS. TRANSMITTANCE (T_{vis})
Glazing	73%
Glass partitions	88%
New glass lamellas	66%
Old glass lamellas	68% (without frit)

Shading control strategy

The shading strategy of the system was based on results from the previous investigation, location and sun position. The most effective daylight redirecting position is when the lamellas are in the position of 30° towards the façade (Laustsen et al., 2008). The lamellas stay in this position when the sky is overcast or the total horizontal illuminance is lower than threshold of 25 klux for longer than 10min. The time delay prevents excessive opening and closing the shading system, which could irritate office occupants. The threshold for moving lamellas back to the redirecting stage, in the case that the daylighting conditions are poor, was set to 17.5 klux with time offset of at least 20min. This assumption was based on the illuminance under clear, overcast and intermediate sky. The redirecting position was 30° all year around expect May and June when the position was set to 25° down towards the façade to avoid direct reflection from the lamellas' surfaces to the occupants' faces. The system had three possible positions:

- Redirecting position 30° (25°)
- Open position 0°
- Close position 90°

In addition, the redirecting position was designed to avoid reflection of direct sunlight from the lamellas surfaces when the sun is partially behind clouds.

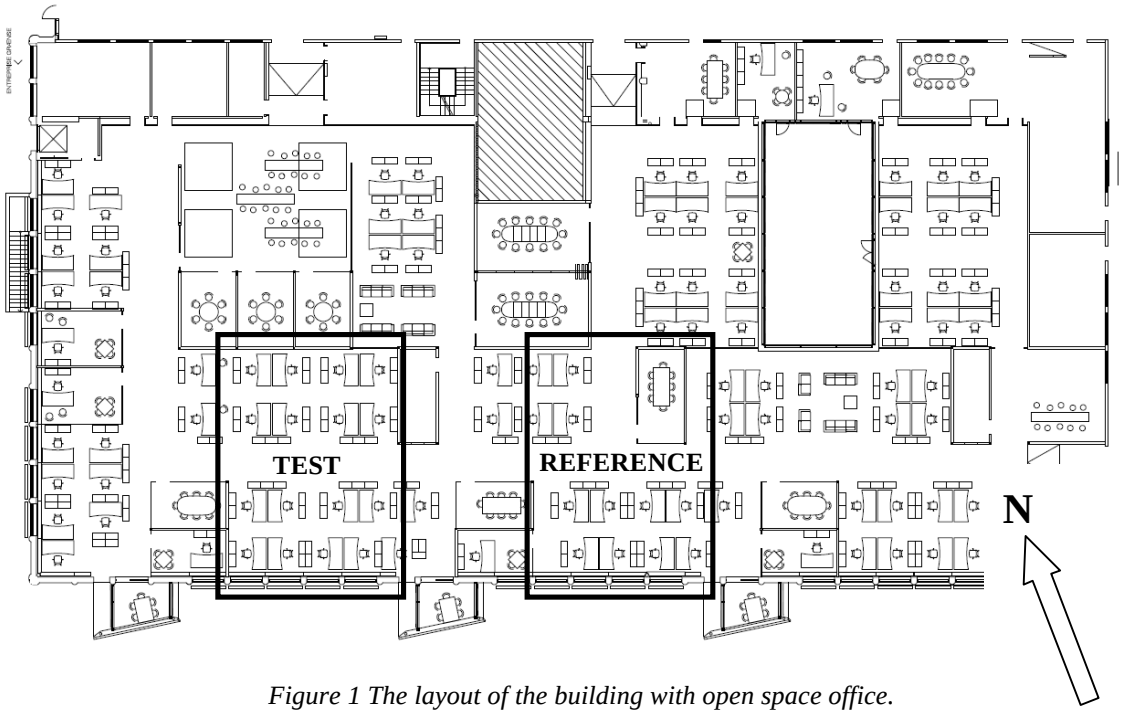

Figure 1 The layout of the building with open space office.

Hence the space occupants were not exposed to the reflections from and between lamellas. The lowest rotating lamella (fourth from top) was approximately 2m above the floor and therefore it did not interface directly with view out when in redirecting position.

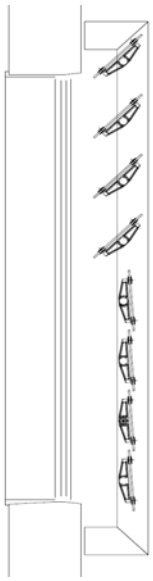

Figure 2 Illustration of the position and rotation angle range for the shading system, outside on the right.

Modelling

To overcome the lack of standardized simulation tools to test the performance of unique shading and redirecting system the state-of-the-art software Radiance was used (Ward et al., 1998). It is generally complicated to simulate effect of reflective surfaces. Therefore, Radiance was utilized for the investigation to depict the transparent properties of the façade and its effect on the indoor environment. Radiance is an accurate backward ray-tracing program which has been extensively validated over past two decades by comparison with measurements and calculation tools. Radiance is capable of simulating illuminance and luminance distribution in complex spaces with diffuse, specular and transparent materials.
Furthermore, to illustrate the potential advantages and disadvantages the tested system was compared with reference case, which is an identical building with the original shading system.

Annual simulations

The comparison between two cases was based on horizontal illuminance on a working plane. There are several thresholds, standards, and design recommendations described in literature. The simulated working plane illuminance was derived from test and reference case to find the impact of the new system. Several thresholds for working plane illuminance were observed and cumulated over the whole year and evaluated by daylight autonomy (DA) and useful daylight illuminance (UDI) matrix, which are explained in detail in next section (Nabil et al., 2005; Reinhart et al., 2011; Mardaljevic, 2000, 2009; McNeil, 2010; CEN - EN 15251, 2007; Mardaljevic et al., 2009, Wienold 2010).

- 100 lux – Are considered as insufficient for performing tasks under daylighting conditions. It is a lower limit for UDI.
- 300 lux – Illuminance around 300 lux is considered as effective for task light source with or without additional artificial light.
- 500 lux – Are described as minimal working illuminance on working space in the office. Therefore it is used as threshold for DA analysis.

- 3000 lux – many people prefer to work under illuminance lower then the level.
- 4500 lux – many people find illuminance above the level too high and uncomfortable.

The recent development of Radiance enabled annually based simulations by using the program "**rtcontrib"** (Ward, 2005). The geometric model of the building, surroundings and detailed model of the fenestration system was created using the program SketchUp and converted to the Radiance format. The placement of windows on the façade created an almost-continuous band of glazing. Therefore, sensors which are equidistant from the façade could be considered to have same illuminance. The study investigated a row of illuminance sensors perpendicular to the facade with spacing of 0.25m starting 0.5m from the facade on the working plan in height of 0.85m. Other sensors were located at the same position as the physical illuminance sensors used for the measurements. These were located on the working plane and under the ceiling facing the floor to monitor reflected light to the ceiling. The spacing of the physical sensors on the working plane was 0.5m, 3.6m and 8.5m from the facade and 1.5m, 3.3m, 5.1m and 6.9m from the facade under the ceiling.

Daylight Simulation

To calculate the annual illuminance on the working plane the three-phase method using Radiance was used (Ward et al., 2011). This method uses the Radiance tool rtcontrib to calculate results in the matrix form, generated from the transmission of fenestration system matrix (XML), exterior daylighting matrix (DMX) and interior view matrix (VMX). This approach allows us to quickly generate different situations for various fenestration systems, locations and sky conditions. The combination can be generated without repeatedly performing whole simulations. This approach is suitable for annual simulation because the sky for every hour is unique. The last information needed for multiplication of matrixes is the sky vector, which describes sky distributions. The sky vector is generated by the Radiance program gendaylit from test reference year (TRY) weather file for Copenhagen, Denmark (DOE, 2011). The sky model uses the Perez sky (Perez et al, 1993; Nabil, 2005), which is generated from the direct normal irradiance and horizontal diffuse irradiance. The sky was divided into 2305 patches according to Reinhart's subdivision for detailed results (Ward, 2009). By multiplying matrixes, the total illuminance at the sensors from all sources in the model is calculated. The transmission matrix was generated by the Radiance program genBSDF which generates a bidirectional scattering distribution function (BSDF) for given complex fenestration geometry. 145 Klems hemispherical directions were used on each of the sites of the fenestration layer to generate the transmission matrix.

A percentage of the working hours satisfying the daylighting conditions annually were accounted. When the minimum light threshold is not reached artificial light could be added and the artificial light energy saving is equal to the amount of daylight.
Annual daylight simulation is in several resources referred to as dynamic daylighting simulation, which is conducted in steps in agreement with three-phase method (Jacobs, 2010; Ward et al., 2011).

1. Sky model with irradiance/illuminance data.
2. Time steps within the working hours.
3. Radiance simulation for each time step and each sensor position or rendering, i.e. view, daylighting and transmission matrix combination.
4. Assess how many times the required designed working illuminance is satisfied (or partly satisfied).
5. Count how much artificial light is needed to add to satisfied minimal working plane illuminance.

The Radiance simulation parameters for generating VMX, XML, DMX matrix are listed in Table 3.

Table 3
Radiance parameters for matrixes

RADIANCE SIMULATIN PARAMTER	**VMX**	**XML**	**DMX**
Ambient bounces (-ab)	6	3	6
Ambient divisions (-ad)	2048	350	10000
Limit weight (-lw)	1.00E-12	0.0001 (-st)	1.00E-3
Direct source subdivisions (-ds)	0.1	0.2	0.1

Daylight factor (DF) was not used for investigating the daylight conditions in the room because it does not quantify the redistribution of the direct beam of the radiation to provide diffuse illuminance in the indoor space, which is the main feature of the daylight redirecting shading system. Furthermore, the building location and orientation is not taken into account in DF concept.

The annual illuminance matrix provides information needed to evaluate the daylight conditions in the interior. The commonly used daylight performance matrixes nowadays, except DF, are useful daylight illuminance (UDI) and daylight autonomy (DA) (Mardaljevic, 2005; Nabi et al., 2005; McNeal et al., 2010; Reinhart et al., 2011).

DA is the percentage of hours which satisfy the minimal designed working plane illuminance from the total number of working hours in a year. The criterion for minimal illuminance according to ISO standard is 500 lux (CEN - EN 15251, 2007). The

commonly used design horizontal working illuminance is between 300 – 500 lux.

The UDI matrix quantifies when the daylight is perceived as useful for occupants of the space. It is calculated as percentage of the occupied working hours when the illuminance on the working plan is between the lower and upper thresholds. 100 lux is considered as the lower illuminace level. The upper level is not clearly defined and differs between studies and publications. Therefore several levels was recorded in this study. As the threshold, when the occupants may feel uncomfortable, 4500 lux was used. According to (Wienold, 2010) 30% of people find horizontal illuminance above 4500 as dissatisfying. Midrange between 100 lux and 4500 lux may be considered as usable for most of the occupants. Some subjects may consider the values in this range as uncomfortable, however values should not be considered as not useful values since every subject perceive different illuminance levels differently (Wienold, 2010; Mardaljevic et al., 2009).

DISCUSSION AND RESULT ANALYSIS

Comparison of simulations and measurements

The placement of the measurement sensors was caused to be minimally blocked. The space was modelled without furniture which was comparable with the measurements because the sensors had free view to the façade and provided comparable results. The reason for removing the furniture from simulations was that furniture was not fixed and it was hard to assume where it would be at the time of the measurements. However the measurement results were influenced in several cases by immediate surroundings in the office and therefore not all the results correlated.

Additionally it was not possible to observe position of the lamellas during whole time of measurements as well as interior shading position, curtains and venetian blinds, which were operated manually. For those reasons errors between simulation and measurements could occur. The compared illuminance sensor for measurements and simulations was placed in the distance of 3.6m from the window, which is approximately in the position where the daylighting conditions could be improved. Sensors closer to the window were exposed to the high level of illuminance and could have a high error. Furthermore the sensors deeper in the room had higher probability of being shaded. The two curves on Figure 3 present the values for Radiance simulation and measurements for a sunny day. To have conditions similar as possible, a day without occupancy was selected for simulated. This limited shading of the sensor during the simulated period as well it was ensured that the artificial light was turned off. Additionally a sunny day was selected for validation of the results in sensor 2, since sky distributions for sunny skies can be generated accurately with the Radiance program **gensky**. Chosen day was Sunday, September 5, 2010, during which the shading system was closed. The light coming through the building from the west facade caused the scattered data, between time steps 2000-2500 (approximately between 4:30pm and 9pm), on Figure 3. This is common for both measurements and simulations and indicates that the simulated model provides comparable data to the measurements. The peak in the morning in the simulations is not common with measured data and it was probably caused by the unknown position of the internal shades or by blocking of the direct or reflected light coming from the side of sensor. This assumption is based on the fact that no furniture and internal shadings were modelled, therefore the extra illuminance contribution in simulations could occur. Another reasons for this discrepancy might be imprecise cosine-correction of the illuminance sensor or due to uncertainty of the tilt of the sensor. At low solar altitudes, these two factors might have an impact on the measured results.

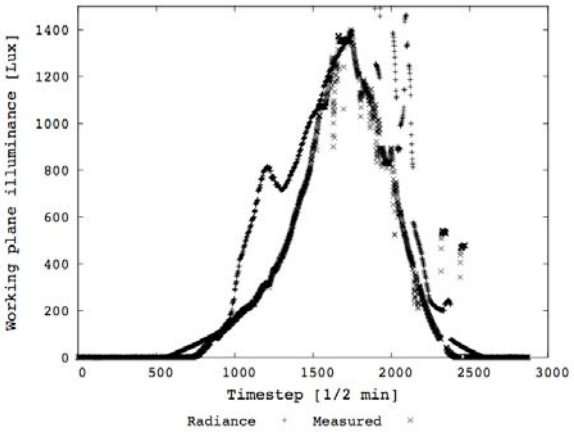

Figure 3 Comparison of measured and Radiance illuminance in sensor 2

The comparison of illuminance level in the tested and the reference area is seen on Figure 4. The sample of measured data is from the sensor placed under the ceiling in the distance of 3.4m from the façade. From the graph it is visible that light was redirected to the ceiling and further reflected into the room. The difference between the sensor in the tested and reference area is up to 500 lux, which demonstrated the effect of the light redirecting properties of the shadings system.

Daylight autonomy

Figure 5 and Figure 6 present the situation when the shading system was in the shading position, closed. This position was common for both test and reference case and therefore could be comparable. Higher percentage of the hours over the observed illuminance thresholds was reached in the deeper distance from the facade and DA was satisfied more

often. The threshold of 500 lux was reached minimum 50% of all the working hours at a distance of 4.5m from the façade for the tested system compared to approximately 3.2m for the reference system. In the distance of 4m from facade in the tested situation around 55% of time reached at least 500 lux on the working plane whilst for the reference shading it was around 45%. The improvement of the daylight conditions is visible all over the depth of the investigated space. Furthermore, the room depth where 300 lux was could be reached moved from 8m to 10m from the facade, which covers most of the working area in the office space. The primary purpose of the shading in the closed position is to block the lighting penetrating the indoor space. The tested system blocks the light closer to façade but allows to increase the horizontal illuminance deeper in the room where it is needed.

Furthermore, the system in the redirecting position, under rotation of 30°, were compared and provided very similar results with the situation when the lamellas were closed. The redirecting position was simulated for both tested and reference system to have comparable data, although the reference system does not technically allow to be in the redirecting position. The dynamic rotation of the lamellas was not simulated and is beyond the scope of the investigation, therefor the results may vary from reality when the system was automatically positioned to the closed, opened or redirecting position. Furthermore, DA does not penalize excessive illuminance and therefore UDI matrix was calculated to illustrate illuminance levels through the space.

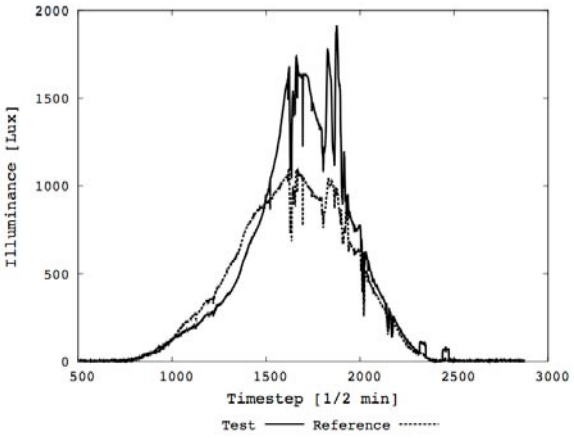

Figure 4 Comparison of measured illuminance under ceiling for test and reference area

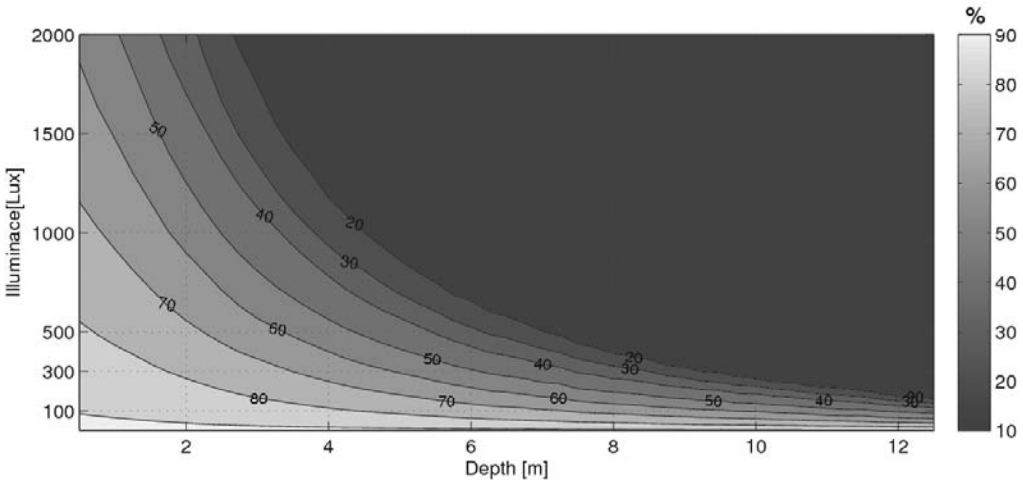

Figure 5 Daylight autonomy of the tested shading system in the closed position

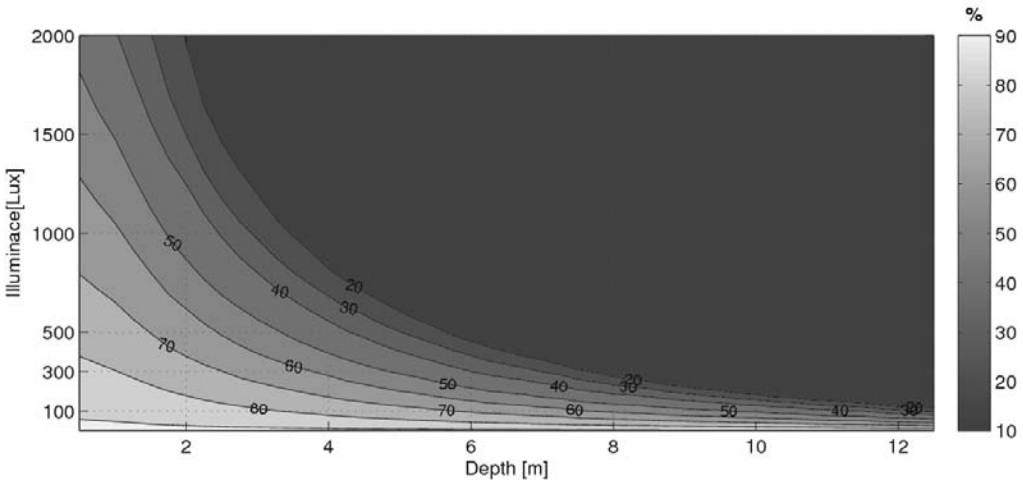

Figure 6 Daylight autonomy of the reference shading system in the closed position

Useful daylight illuminance

The excessive working plane illuminance is present for both cases and in every investigated position of the shading system in closed, open or redirecting position. Figure 7 shows horizontal illuminance for closed and redirecting position of the tested and reference shading. The depth of the room with illuminance level higher than 4500 lux shifted in average approximately 1m into the room, which is not a significant downgrade, because the working places are not directly placed in this zone. In the case of exceeding the upper limit occupants can close internal shading system manually in the same way as they would do it with the original system.

More importantly, the situation with insufficiently low daylighting condition in the evaluated space was limited, especially in the back of the office space. The illuminated zone with horizontal illuminance between 100 lux and 4500 lux is larger with tested system than with the reference shading system. The daylight redirecting position of the lamellas further increase the zone lit by daylight. The tested system provides usable UDI for more than 20% of hours of occupancy in the back of the room compare to the reference system. The percentage of UDI was improved throughout the whole depth of the room staring approximately 3m from the façade. Also the zone with the minimal horizontal illuminance of 100 lux is reduced with tested system, which indicates that the daylight conditions were satisfied in the larger percentage of the occupancy hours.

Future work

Apart from performing the daylighting analysis, the further work on the evaluation of this system should include more in depth glare analysis with focus on the visual zone of the occupants and annual evaluation (Wienold, 2010). This is necessary because discomfort glare is not possible to estimate based on the horizontal illuminance (Mardaljevic 2009). Moreover, we will evaluate the changes to the energy consumption from artificial lighting reductions. The solar gains for heating during the winter should be evaluated, since it is considered as source of energy for the low energy buildings as well as buildings in the Nordic countries. The assessment of overheating is important for overall energy consumption because the excessive overheating may remove the benefits of improved working illuminance conditions. There could be other results when taking into account glare and overheating.

CONCLUSION

This paper evaluates a prototype dynamic integrated shading and light redirecting system designed to optimize daylight conditions in an office building whilst a quality of indoor environment and view out is preserved and improved. Part of an existing façade with glass lamellas in Humlebaek, Denmark was rebuilt to test and further develop the prototype of the concept. The demonstration building façade had a reference office space with the same orientation and layout as the tested shading system for comparison of investigated parameters. The automated external glass lamellas were synchronized with the actual sky and the sun distribution to expand the zone with the designed workspace illuminance lit by daylight and maximizes view out. In this study, the lighting conditions were simulated and measured during summer and autumn. The simulation results were compared with the measurements and the results correlated. Daylight improvement was achieved with the redirecting glass lamellas shading system compared to the existing shading system in the building, which was found by both simulation and measurements.

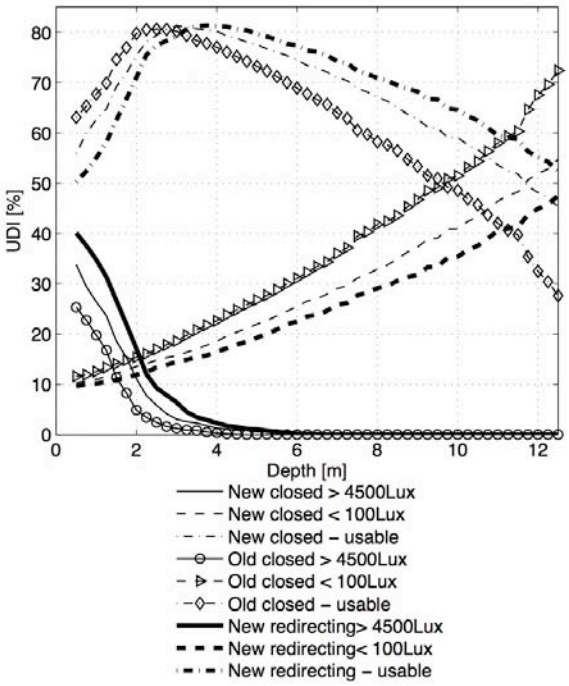

Figure 7 Annual useful daylight illuminance matrix for different scenarios.

ACKNOWLEDGEMENTS

The research performed in this study was funded by the Danish Energy Agency programme for research and development of energy efficiency, PSO - F&U 2008.

REFERENCES

CEN - EN 15251, 2007, Indoor environment input for design and assessment of energy performance of buildings addressing indoor air

quality, thermal environment, lightning and acoustics.

DOE, 2011, United States Department of Energy, Weather data, Internet, http://apps1.eere.energy.gov/buildings/energyplus/weatherdata/6_europe_wmo_region_6/DNK_Copenhagen.061800_IWEC.zip, May 2011.

EN 15603, 2008, Energy Performance of Buildings—Overall Energy Use and Definition of Energy Ratings, European Committee for Standardization, Brus- sels, Belgium.

EU, 2010, EPBD recast (2010), Directive 2010/31/EU of the European Parliament and of the Council of 19 May 2010 on the energy performance of buildings (recast), Official Journal of the European Union, 18/06/2010., EU of the European Parliament.

Iversen, A.; Laustsen J.B.; Svendsen, S.; Traberg-Borup, S.; Johnsen, J., 2009. Udvikling af nye typer solafskærmnings-systemer baseret på dagslysdirigerende solafskærmende glaslameller, Lyngby, Denmark.

Jacobs A. 2010. Understanding rtcontrib, London, UK.

Laustsen, J. B.; Santos, I. D. P.; Svendsen, S.; Traberg-Borup, S.; Johnsen, K., 2008, Solar Shading System Based on Daylight Directing Glass Lamellas, Building Physics 2008 - 8th Nordic Symposium

Lee E.; 2009. Advanced High-Performance Commercial Building Facades Research, LBNL, Berkeley, USA – presentation

Mardaljevic, J.; 2000. Daylight simulation: validation, sky models and daylight coeffcients. PhD thesis. Leicester: De Montfort University.

Mardaljevic J.; Heschong L.; Lee E.; 2009. Daylight metrics and energy savings, Lighting Res. Technol., 41 pp. 261–283

McNeil, A.; Lee, E.S. 2010. Annual Assessment of an Optically-Complex Daylighting System Using Biderectional Scattering Distribution Function with Radiance, DEO/LBNL FY10 Technical Report Deliverable, Berkeley, California, USA – under review.

Nabil, A.; Mardaljevic, J. 2005. Useful daylight illuminance: a new paradigm for assessing daylight in buildings, Lighting Res. Technol., 37 (1) pp. 41-59.

Perez R.; Seals R.; Michalsky J.; 1993.All-weather model for sky luminance distribution-preliminary configuration and validation. Solar Energy, 50(3), 235-245.

Reinhart, C.F., Wienold, J. 2011. A simulation-based analysis for daylit spaces, Building and Environment 46, pp. 386-396.

Ward G., 2005. Radiance's new rtcontrib program, 4rd Internatiol Radiance Workshop Montreal, Canada.

Ward G.; Mistrick R.; Lee E. S.; McNeil A.; Jonsson J.; 2011. Simulating the Daylight Performance of Complex Fenestration Systems Using Bidirectional Scattering Distribution Functions within Radiance, Berkeley, USA - accepted for publication in Leukos, Journal of the Illuminating

Ward G., 2005. Radiance's new rtcontrib program, 4rd International Radiance Workshop Montreal, Canada.

Ward, G.; Shakespeare, R.A., 1998. Rendering with Radiance, published by Space & Light, Davis, California, USA.

Ward G., 2009. Complex Fenestration and Annual Simulation, 8rd International Radiance Workshop Boston, USA.

Wienold J. 2009. Dynamic Daylight Glare Evaluation, Building Simulation 2009, Glasgow, Scotland.

Wienold J. 2010. Daylight Glare in Offices, ISBN 978-3-8396-0162-4, Freiburg, Germany

Windows are crucial elements of building envelopes and influence indoor comfort and energy efficiency of buildings, so they have a high potential for reducing building energy by using daylight and lowering energy demand for heating and cooling. This Ph.D. work uses comprehensive thermal and optical performance modelling to stimulate the development of advanced window systems with shading, which serve several functions, fulfil new energy regulations and form the basis for the design of low-energy buildings in the future. The evaluation of unique advanced window systems is demonstrated by simulations and measurements of several case examples..

DTU Civil Engineering
Department of Civil Engineering
Technical University of Denmark

Brovej, Building 118
2800 Kgs. Lyngby
Telephone 45 25 17 00

www.byg.dtu.dk

ISBN: 9788778773500
ISSN: 1601-2917